AD-A265 707

R-939
January 1993

NCEL

Technical Report

By: Robert M. Ebeling, PhD
and Ernest E. Morrison

Sponsored by:
Office of Navy Technology
and Department of the Army

THE SEISMIC DESIGN OF WATERFRONT RETAINING STRUCTURES

DTIC
ELECTE
JUN 11 1993
S A D

93-13063

ABSTRACT This technical report deals with the soil mechanics aspects of the design of waterfront retaining structures built to withstand the effects of earthquake loadings. It addresses the stability and movement of gravity retaining walls and anchored sheet pile walls and the dynamic forces against the walls of drydocks.

The effects of wall displacements, submergence, liquefaction potential, and excess pore water pressures, as well as inertial and hydrodynamic forces, are incorporated in the design procedures. Several new computational procedures are described.

The procedures used to calculate the dynamic earth pressures acting on retaining structures consider the magnitude of wall displacements. For example, dynamic active earth pressures are computed for walls that retain yielding backfills, i.e., backfills that undergo sufficient displacements during seismic events to mobilize fully the shear resistance of the soil. For smaller wall movements, the shear resistance of the soil is not fully mobilized and the dynamic earth pressures acting on those walls are greater because the soil comprising the backfill does not yield, i.e., a non-yielding backfill. Procedures for incorporating the effects of submergence within the earth pressure computations, including consideration of excess pore water pressure, are described.

NAVAL CIVIL ENGINEEING LABORATORY PORT HUENEME CALIFORNIA 93043-4328

Approved for public release, distribution is unlimited

93 6 10 031

METRIC CONVERSION FACTORS

Approximate Conversions to Metric Measures

Symbol	When You Know	Multiply by	To Find	Symbol
		LENGTH		
in	inches	*2.5	centimeters	cm
ft	feet	30	centimeters	cm
yd	yards	0.9	meters	m
mi	miles	1.6	kilometers	km
		AREA		
in^2	square inches	6.5	square centimeters	cm^2
ft^2	square feet	0.09	square meters	m^2
yd^2	square yards	0.8	square meters	m^2
mi^2	square miles	2.6	square kilometers	km^2
	acres	0.4	hectares	ha
		MASS (weight)		
oz	ounces	28	grams	g
lb	pounds	0.45	kilograms	kg
	short tons (2,000 lb)	0.9	tonnes	t
		VOLUME		
tsp	teaspoons	5	milliliters	ml
Tbsp	tablespoons	15	milliliters	ml
fl oz	fluid ounces	30	milliliters	ml
c	cups	0.24	liters	l
pt	pints	0.47	liters	l
qt	quarts	0.95	liters	l
gal	gallons	3.8	liters	l
ft^3	cubic feet	0.03	cubic meters	m^3
yd^3	cubic yards	0.76	cubic meters	m^3
		TEMPERATURE (exact)		
°F	Fahrenheit temperature	5/9 (after subtracting 32)	Celsius temperature	°C

*1 in = 2.54 (exactly). For other exact conversions and more detailed tables, see NBS Misc. Publ. 286, Units of Weights and Measures, Price $2.25, SD Catalog No. C13.10:286.

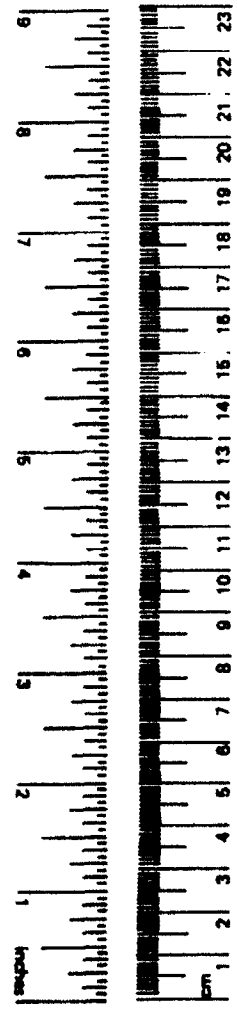

Approximate Conversions from Metric Measures

Symbol	When You Know	Multiply by	To Find	Symbol
		LENGTH		
mm	millimeters	0.04	inches	in
cm	centimeters	0.4	inches	in
m	meters	3.3	feet	ft
m	meters	1.1	yards	yd
km	kilometers	0.6	miles	mi
		AREA		
cm^2	square centimeters	0.16	square inches	in^2
m^2	square meters	1.2	square yards	yd^2
km^2	square kilometers	0.4	square miles	mi^2
ha	hectares (10,000 m^2)	2.5	acres	
		MASS (weight)		
g	grams	0.035	ounces	oz
kg	kilograms	2.2	pounds	lb
t	tonnes (1,000 kg)	1.1	short tons	
		VOLUME		
ml	milliliters	0.03	fluid ounces	fl oz
l	liters	2.1	pints	pt
l	liters	1.06	quarts	qt
l	liters	0.26	gallons	gal
m^3	cubic meters	35	cubic feet	ft^3
m^3	cubic meters	1.3	cubic yards	yd^3
		TEMPERATURE (exact)		
°C	Celsius temperature	9/5 (then add 32)	Fahrenheit temperature	°F

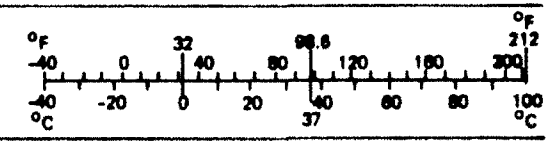

REPORT DOCUMENTATION PAGE

Form Approved
OMB No. 0704-018

Public reporting burden for this collection of information is estimated to average 1 hour per response, including the time for reviewing instructions, searching existing data sources, gathering and maintaining the data needed, and completing and reviewing the collection of information. Send comments regarding this burden estimate or any other aspect of this collection information, including suggestions for reducing this burden, to Washington Headquarters Services, Directorate for Information and Reports, 1215 Jefferson Davis Highway, Suite 1204, Arlington, VA 22202-4302, and to the Office of Management and Budget, Paperwork Reduction Project (0704-0188), Washington, DC 20503.

1. AGENCY USE ONLY *(Leave blank)*

2. REPORT DATE
January 1993

3. REPORT TYPE AND DATES COVERED
Final Report

4. TITLE AND SUBTITLE
THE SEISMIC DESIGN OF WATERFRONT RETAINING STRUCTURES

5. FUNDING NUMBERS
RM - 33F60-001-0106
WU - DN387338

6. AUTHOR(S)
Robert M. Ebeling and Ernest E. Morrison, Jr.

7. PERFORMING ORGANIZATION NAME(S) AND ADDRESS(S)
U.S. Army Waterways Experiment Station
Information Technology Laboratory
3909 Halls Ferry Road
Vicksburg, MS 39180-6199

8. PERFORMING ORGANIZATION REPORT NUMBER
Technical Report ITL-92-11
NCEL TR-939

9. SPONSORING/MONITORING AGENCY NAME(S) AND ADDRESS(S)
Chief of Naval Research / Department of the Army
Office of Naval Technology / U.S. Army Corps of Engineers
800 No. Quincy Street / Washington, DC 20314-1000
Arlington, VA 22217-5000

10. SPONSORING/MONITORING AGENCY REPORT NUMBER

11. SUPPLEMENTARY NOTES
Available from National Technical Information Service, 5285 Port Royal Road, Springfield, VA 22161

12a. DISTRIBUTION/AVAILABILITY STATEMENT
Approved for public release; distribution is unlimited.

12b. DISTRIBUTION CODE

13. ABSTRACT *(Maximum 200 words)*

This technical report deals with the soil mechanics aspects of the design of waterfront retaining structures built to withstand the effects of earthquake loadings. It addresses the stability and movement of gravity retaining walls and anchored sheet pile walls and the dynamic forces against the walls of drydocks.

The effects of wall displacements, submergence, liquefaction potential, and excess pore water pressures, as well as inertial and hydrodynamic forces, are incorporated in the design procedures. Several new computational procedures are described.

The procedures used to calculate the dynamic earth pressures acting on retaining structures consider the magnitude of wall displacements. For example, dynamic active earth pressures are computed for walls that retain yielding backfills, i.e., backfills that undergo sufficient displacements during seismic events to mobilize fully the shear resistance of the soil. For smaller wall movements, the shear resistance of the soil is not fully mobilized and the dynamic earth pressures acting on those walls are greater because the soil comprising the backfill does not yield, i.e., a non-yielding backfill. Procedures for incorporating the effects of submergence within the earth pressure computations, including consideration of excess pore water pressure, are described.

14. SUBJECT TERMS
Dynamic earth pressures, earthquake engineering, earth retaining structures, hydraulic structures, soil dynamics

15. NUMBER OF PAGES
329

16. PRICE CODE

17. SECURITY CLASSIFICATION OF REPORT
Unclassified

18. SECURITY CLASSIFICATION OF THIS PAGE
Unclassified

19. SECURITY CLASSIFICATION OF ABSTRACT
Unclassified

20. LIMITATION OF ABSTRACT
UL

PREFACE

This report describes procedures used in the seismic design of waterfront retaining structures. Funding for the preparation of this report was provided by the US Naval Civil Engineering Laboratory through the following instruments: NAVCOMPT Form N6830591WR00011, dated 24 October 1990; Amendment #1 to that form, dated 30 November 1990; NAVCOMPT Form N6830592WR00013, dated 10 October 1991; Amendment #1 to the latter, dated 3 February 1992; and the Computer-Aided Structural Engineering Program sponsored by the Directorate, Headquarters, US Army Corps of Engineers (HQUSACE), under the Structural Engineering Research Program. Supplemental support was also provided by the US Army Civil Works Guidance Update Program toward cooperative production of geotechnical seismic design guidance for the Corps of Engineers. General project management was provided by Dr. Mary Ellen Hynes and Dr. Joseph P. Koester, both of the Earthquake Engineering and Seismology Branch (EESB), Earthquake Engineering and Geosciences Division (EEGD), Geotechnical Laboratory (GL), under the general supervision of Dr. William F. Marcuson III, Director, GL. Mr. John Ferritto of the Naval Civil Engineering Laboratory, Port Hueneme, CA, was the Project Monitor.

The work was performed at the US Army Engineer Waterways Experiment Station (WES) by Dr. Robert M. Ebeling and Mr. Ernest E. Morrison, Interdisciplinary Research Group, Computer-Aided Engineering Division (CAED), Information Technology Laboratory (ITL). This report was prepared by Dr. Ebeling and Mr. Morrison with contributions provided by Professor Robert V. Whitman of Massachusetts Institute of Technology and Professor W. D. Liam Finn of University of British Columbia. Review commentary was also provided by Dr. Paul F. Hadala, Assistant Director, GL, Professor William P. Dawkins of Oklahoma State University, Dr. John Christian of Stone & Webster Engineering Corporation, and Professor Raymond B. Seed of University of California, Berkeley. The work was accomplished under the general direction of Dr. Reed L. Mosher, Acting Chief, CAED and the general supervision of Dr. N. Radhakrishnan, Director, ITL.

At the time of publication of this report, Director of WES was Dr. Robert W. Whalin. Commander was COL Leonard G. Hassell, EN.

Accesion For
NTIS CRA&I ☑
DTIC TAB ☐
Unannounced ☐
Justification
By
Distribution /
Availability Codes
Dist | Avail and / or Special
A-1

DTIC QUALITY INSPECTED 3

PROCEDURAL SUMMARY

This section summarizes the computational procedures described in this report to compute dynamic earth pressures. The procedures for computing dynamic earth pressures are grouped according to the expected displacement of the backfill and wall during seismic events. A yielding backfill displaces sufficiently (refer to the values given in Table 1, Chapter 2) to mobilize fully the shear resistance of the soil, with either dynamic active earth pressures or dynamic passive earth pressures acting on the wall, depending upon the direction of wall movement. When the displacement of the backfill (and wall) is less than one-fourth to one-half of the Table 1 values, the term non-yielding backfill is used because the shear strength of the soil is not fully mobilized.

The procedures for computing dynamic active and passive earth pressures for a wall retaining a dry yielding backfill or a submerged yielding backfill are discussed in detail in Chapter 4 and summarized in Table i and Table ii, respectively. The procedures for computing dynamic earth pressures for a wall retaining a non-yielding backfill are discussed in Chapter 5 and summarized in Table i.

The assignment of the seismic coefficient in the design procedures for walls retaining yielding backfills are discussed in detail in Chapter 6 and summarized in Table iii. The assignment of the seismic coefficient in the design procedures for walls retaining non-yielding backfills are discussed in detail in Chapter 8 and summarized in Table iii.

TABLE i

DETERMINATION OF DYNAMIC EARTH PRESSURES FOR DRY BACKFILLS

YIELDING BACKFILL

DYNAMIC ACTIVE EARTH PRESSURES

MONONOBE - OKABE

Equivalent Static Formulation (Arango)

Simplified Procedure (Seed and Whitman)
- restricted to: vertical wall and level backfills.
- approximate if: $\phi \neq 35°$, $k_v \neq 0$.

DYNAMIC PASSIVE EARTH PRESSURES

MONONOBE - OKABE
- approximate for $\delta > 0$.
- inaccurate for some wall geometries and loading conditions.

Equivalent Static Formulation
- approximate if: $K_P(\beta^*, \theta^*)$ is computed using Coulomb's equation, see above comments.
- approximate if: $K_P(\beta^*, \theta^*)$ is computed using Log-Spiral solutions.

Simplified Procedure (Towhata and Islam)
- restricted to: vertical walls and level backfills and $\delta = 0°$.
- approximate if: $\phi \neq 35°$, $k_v \neq 0$.

TABLE i - Continued

DETERMINATION OF DYNAMIC EARTH PRESSURES FOR DRY BACKFILLS

NON-YIELDING BACKFILL
LATERAL SEISMIC FORCE Wood's Simplified Procedure - restricted to: k_h constant with depth and $k_v = 0$. Soil-Structure Interaction Analysis Using the Finite Element Method

TABLE ii

DETERMINATION OF DYNAMIC EARTH PRESSURES FOR SUBMERGED OR PARTIALLY SUBMERGED BACKFILLS

Select the appropriate technique for either yielding backfill or non-yielding backfill with additional computations as specified by one of the following procedures: Restrained water case Free water case - restricted to soils of high permeability (e.g. $k > 1$ cm/sec)

TABLE iii

DESIGN PROCEDURES - ASSIGNMENT OF SEISMIC COEFFICIENT

YIELDING BACKFILL
Preselected Seismic Coefficient Method - The approximate value of horizontal displacement is related to the value of the horizontal seismic coefficient. Displacement Controlled Approach - The seismic coefficient is computed based upon an explicit choice of an allowable level of permanent horizontal wall displacement.

NON-YIELDING BACKFILL
Displacement Of The Wall Is Not Allowed The seismic coefficient is set equal to the peak horizontal acceleration coefficient, assuming acceleration within the backfill to be constant with depth. Otherwise, consider dynamic finite element method of analysis.

TABLE OF CONTENTS

	PAGE
PREFACE	i
PROCEDURAL SUMMARY	ii
TABLE i	iii
TABLE ii	iv
TABLE iii	v
CONVERSION FACTORS, NON-SI TO SI (METRIC) UNITS OF MEASUREMENT	xvi
CHAPTER 1 GENERAL DESIGN CONSIDERATIONS FOR WATERFRONT SITES	1
1.1 Scope and Applicability	1
1.2 Limit States	3
1.3 Key Role of Liquefaction Hazard Assessment	3
1.4 Choice of Design Ground Motions	5
1.4.1 Design Seismic Event	6
1.4.2 Seismic Coefficients	7
1.4.3 Vertical Ground Accelerations	9
CHAPTER 2 GENERAL DESIGN CONSIDERATIONS FOR RETAINING WALLS	11
2.1 Approaches to Design for Various Classes of Structure	11
2.2 Interdependence between Wall Deformations and Forces Acting on the Wall	11
2.2.1 Wall Deformations and Static Earth Pressure Forces	11
2.2.2 Wall Deformations and Dynamic Earth Pressure Forces	16
2.3 Comments on Analyses for Various Cases	18
2.3.1 Analysis of Failure Surfaces Passing below Wall	19
2.3.2 Analysis of Post-Seismic Condition	19
CHAPTER 3 STATIC EARTH PRESSURES - YIELDING BACKFILLS	21
3.1 Introduction	21
3.2 Rankine Theory	23

PAGE

3.2.1 Rankine Theory - Active Earth Pressures - Cohesionless Soils 23

3.2.2 Rankine Theory - Active Earth Pressures - Cohesive Soils - General Case 25

3.2.3 Rankine Theory - Passive Earth Pressures 26

3.3 Coulomb Theory 28

3.3.1 Coulomb Theory - Active Earth Pressures 28

3.3.2 Coulomb Active Pressures - Hydrostatic Water Table Within Backfill and Surcharge 30

3.3.3 Coulomb Active Pressures - Steady State Seepage Within Backfill 33

3.3.4 Coulomb Theory - Passive Earth Pressures 35

3.3.4.1 Accuracy Of Coulomb's Theory for Passive Earth Pressure Coefficients 36

3.4 Earth Pressures Computed Using the Trial Wedge Procedure . . 36

3.5 Active And Passive Earth Pressure Coefficients from Log Spiral Procedure 41

3.6 Surface Loadings 45

CHAPTER 4 DYNAMIC EARTH PRESSURES - YIELDING BACKFILLS 55

4.1 Introduction 55

4.2 Dynamic Active Earth Pressure Force 55

4.2.1 Vertical Position of P_{AE} along Back of Wall 63

4.2.2 Simplified Procedure for Dynamic Active Earth Pressures . 64

4.2.3 Limiting Value for Horizontal Acceleration 66

4.3 Effect of Submergence of the Backfill on the Mononobe-Okabe Method of Analysis 66

4.3.1 Submerged Backfill with No Excess Pore Pressures 68

4.3.2 Submerged Backfill with Excess Pore Pressure 69

4.3.3 Partial Submergence 72

4.4 Dynamic Passive Earth Pressures 72

PAGE

4.4.1 Simplified Procedure for Dynamic Passive Earth Pressures 76

4.5 Effect of Vertical Accelerations on the Values for the Dynamic Active and Passive Earth Pressures 78

4.6 Cases with Surface Loadings 79

CHAPTER 5 EARTH PRESSURES ON WALLS RETAINING NONYIELDING BACKFILLS 133

5.1 Introduction 133

5.2 Wood's Solution 133

CHAPTER 6 ANALYSIS AND DESIGN EXAMPLES FOR GRAVITY WALLS RETAINING YIELDING BACKFILLS 139

6.1 Introduction 139

6.2 Procedure Based upon Preselected Seismic Coefficient 140

6.2.1 Stability of Rigid Walls Retaining Dry Backfills which Undergo Movements during Earthquakes 142

6.2.2 Stability of Rigid Walls Retaining Submerged Backfills which Undergo Movements During Earthquakes - No Excess Pore Water Pressures 148

6.2.3 Stability of Rigid Walls Retaining Submerged Backfills which Undergo Movements During Earthquakes - Excess Pore Water Pressures 151

6.2.4 Stability of Rigid Walls Retaining Submerged Backfills which Undergo Movements During Earthquakes - Liquified Backfill 155

6.3 Displacement Controlled Approach 158

6.3.1 Displacement Controlled Design Procedure for a Wall Retaining Dry Backfill 160

6.3.2 Analysis of Earthquake Induced Displacements for a Wall Retaining Dry Backfill 163

6.3.3 Displacement Controlled Design Procedure for a Wall Retaining Submerged Backfill - No Excess Pore Water Pressures 164

6.3.4 Analysis of Earthquake Induced Displacements for a Wall Retaining Submerged Backfill - No Excess Pore Water Pressures 165

PAGE

6.3.5 Displacement Controlled Design Procedure for a Wall Retaining Submerged Backfill - Excess Pore Water Pressures 166

6.3.6 Analysis of Earthquake Induced Displacements for a Wall Retaining Submerged Backfill - Excess Pore Water Pressures 167

CHAPTER 7 ANALYSIS AND DESIGN OF ANCHORED SHEET PILE WALLS 203

7.1 Introduction 203

7.2 Background 204

7.2.1 Summary of the Japanese Code for Design of Anchored Sheet Pile Walls 205

7.2.2 Displacements of Anchored Sheet Piles during Earthquakes 206

7.3 Design of Anchored Sheet Pile Walls - Static Loadings . . . 207

7.4 Design of Anchored Sheet Pile Walls for Earthquake Loadings 210

7.4.1 Design of Anchored Sheet Pile Walls - No Excess Pore Water Pressures 217

7.4.2 Design of Anchored Sheet Pile Walls - Excess Pore Water Pressures 227

7.5 Use of Finite Element Analyses 231

CHAPTER 8 ANALYSIS AND DESIGN OF WALLS RETAINING NONYIELDING BACKFILLS 233

8.1 Introduction 233

8.2 An Example 234

REFERENCES 247

APPENDIX A: COMPUTATION OF THE DYNAMIC ACTIVE AND PASSIVE EARTH PRESSURE FORCES FOR PARTIALLY SUBMERGED BACKFILLS USING THE WEDGE METHOD A1

A.1 Introduction A1

A.2 Active Earth Pressures A2

A.2.1 Calculation of Water Pressure Forces for a Hydrostatic Water Table A2

PAGE

A.2.2 Static Water Pressure Forces Acting on the Wedge A3

A.2.3 Excess Pore Water Pressures due to Earthquake Shaking with Constant r_u A3

A.2.4 Excess Pore Water Pressure Forces Acting on the wedge . . A4

A.2.5 Equilibrium of Vertical Forces A4

A.2.6 Equilibrium of Forces in the Horizontal Direction A5

A.2.7 Surcharge Loading A6

A.2.8 Static Active Wedge Analysis A7

A.3 Passive Earth Pressures A8

A.3.1 Calculation of Water Pressure Forces for a Hydrostatic Water Table A9

A.3.2 Equilibrium of Vertical Forces A10

A.3.3 Equilibrium of Forces in the Horizontal Direction A10

A.3.4 Surcharge Loading A12

A.3.5 Static Passive Wedge Analysis A13

APPENDIX B: THE WESTERGAARD PROCEDURE FOR COMPUTING HYDRODYNAMIC WATER PRESSURES ALONG VERTICAL WALLS DURING EARTHQUAKES B1

B.1 The Westergaard Added Mass Procedure B2

APPENDIX C: DESIGN EXAMPLE FOR AN ANCHORED SHEET PILE WALL C1

C.1 Design of An Anchored Sheet Pile Wall For Static Loading . . C1

C.1.1 Active Earth Pressure Coefficients K_A C1

C.1.2 "Factored" Passive Earth Pressure Coefficient K_p C2

C.1.3 Depth of Penetration C2

C.1.4 Tie Rod Force T_{FES} C5

C.1.5 Maximum Moment M_{FES} C6

C.1.6 Design Moment M_{design} C7

PAGE

C.1.7 Selection of the Sheet Pile Section C8

C.1.8 Design Tie Rod C8

C.1.9 Design Anchorage C9

C.1.10 Site Anchorage C11

C.2 Design of An Anchored Sheet Pile Wall for Seismic Loading C12

C.2.1 Static Design (Step 1) C12

C.2.2 Horizontal Seismic Coefficient, k_h (Step 2) C12

C.2.3 Vertical Seismic Coefficient, k_v (Step 3) C12

C.2.4 Depth of Penetration (Steps 4 to 6) C12

C.2.5 Tie Rod Force T_{FES} (Step 7) C18

C.2.6 Maximum Moment M_{FES} (Step 8) C19

C.2.7 Design Moment M_{design} (Step 9) C21

C.2.8 Design Tie Rods (Step 10) C23

C.2.9 Design of Anchorage (Step 11) C24

C.2.10 Size Anchor Wall (Step 12) C24

C.2.11 Site Anchorage (Step 13) C27

APPENDIX D: COMPUTER-BASED NUMERICAL ANALYSES D1

D.1 Some Key References D2

D.2 Principal Issues D2

D.2.1 Total Versus Effective Stress Analysis D3

D.2.2 Modeling Versus Nonlinear Behavior D3

D.2.3 Time Versus Frequency Domain Analysis D3

D.2.4 1-D Versus 2-D Versus 3-D D4

D.2.5 Nature of Input Ground Motion D4

D.2.6 Effect of Free Water D4

D.3 A Final Perspective D4

APPENDIX E: NOTATION E1

LIST OF TABLES

No.		Page
1	Approximate Magnitudes of Movements Required to Reach Minimum Active and Maximum Passive Earth Pressure Conditions	16
2	Ultimate Friction Factors for Dissimilar Materials	31
3	Valves of K_A and K_p for Log-Spiral Failure Surface	44
4	Section Numbers That Outline Each of the Two Design Procedures for Yielding Walls for the Four Categories of Retaining Walls Identified in Figure 6.1	142
5	Minimum Factors of Safety When Using the Preselected Seismic Coefficient Method of Analysis	143
6	Qualitative and Quantitative Description of the Reported Degrees of Damage	207
7	Ten Stages of the Analyses in the Design of Anchored Walls for Seismic Loadings	218
C.1	Horizontal Force Components	C3
C.2	Moments About Tie Rod Due to Active Earth Pressures	C4
C.3	Moments About Tie Rod Due to Passive Earth Pressures	C4
C.4	Calculation of the Depth of Penetration	C5
C.5	Horizontal Force Components for D = 10 Feet	C5
C.6	Moment Internal to the Sheet Pile at y = 12.79 Feet Below the Water Table and About the Elevation of the Tie Rod	C6
C.7	Design Moment for Sheet Pile Wall in Dense Sand	C7
C.8	Allowable Bending Moment for Four ASTM A328 Grade Sheet Pile Sections ($\sigma_{allowable} = 0.65 \cdot \sigma_{yield}$)	C8
C.9	Five Horizontal Static Active Earth Pressure Force Components of P_{AE} with D = 20.24 Feet	C14
C.10	Summary of Depth of Penetration Calculations	C18
C.11	Tie Rod Force T_{FES}	C19
C.12	Moment of Forces Acting Above y = 15.32 Feet Below the Water Table and About the Tie Rod	C21
C.13	Design Moment for Sheet Pile Wall in Dense Sand	C22
C.14	Allowable Bending Moment for Four ASTM A328 Grade Sheet Pile Sections ($\sigma_{allowable} = 0.9 \cdot \sigma_{yield}$)	C22
C.15	Required Geometry of Tie Rod	C23
D.1	Partial Listing of Computer-Based Codes for Dynamic Analysis of Soil Systems	D1

LIST OF FIGURES

No.		Page
1.1	Overall limit states at waterfronts	4
2.1	Potential soil and structural failure modes due to earthquake shaking of an anchored sheet pile wall	12
2.2	Rigid walls retaining backfills which undergo movements during earthquakes	13
2.3	Horizontal pressure components and anchor force acting on sheet pile wall	14
2.4	Effect of wall movement on static horizontal earth pressures	15

No.		Page
2.5	Effect of wall movement on static and dynamic horizontal earth pressures	17
2.6	Effect of wall movement on static and dynamic horizontal earth pressures	18
2.7	Failure surface below wall	19
3.1	Three earth pressure theories for active and passive earth pressures	22
3.2	Computation of Rankine active and passive earth pressures for level backfills	24
3.3	Rankine active and passive earth pressures for inclined backfills	26
3.4	Coulomb active and passive earth pressures for inclined backfills and inclined walls	29
3.5	Coulomb active earth pressures for a partially submerged backfill and a uniform surcharge	32
3.6	Coulomb active earth pressures for a backfill subjected to steady state flow	34
3.7	Coulomb and log-spiral passive earth pressure coefficients with $\delta=\phi/2$ - vertical wall and level backfill	37
3.8	Coulomb and log-spiral passive earth pressure coefficients with $\delta=\phi$ - vertical wall and level backfill	37
3.9	Example of trial wedge procedure	38
3.10	Example of trial wedge procedure, hydrostatic water table	40
3.11	Active and passive earth pressure coefficients with wall friction-sloping wall	42
3.12	Active and passive earth pressure coefficients with wall friction-sloping backfill	43
3.13	Theory of elasticity equations for pressures on wall due to surcharge loads	46
3.14	Use of an imaginary load to enforce a zero-displacement condition at the soil-structure interface	47
4.1	Driving and resisting seismic wedges, no saturation	56
4.2	Variation in K_{AE} and $K_{AE} \cdot \cos \delta$ with k_h	58
4.3	Variation in $K_{AE} \cdot \cos \delta$ with k_h, ϕ, and β	58
4.4	Variation in α_{PE} with Ψ for δ equal to ϕ vertical wall and level backfill	60
4.5	Variation in α_{AE} with Ψ for δ equal to zero degrees, vertical wall and level backfill	60
4.6	Variation in dynamic active horizontal earth pressure coefficient with peak horizontal acceleration	61
4.7	Equivalent static formulation of the Mononobe-Okobe active dynamic earth pressure problem	62
4.8	Values of factor F_{AE} for determination of K_{AE}	63
4.9	Point of action of P_{AE}	65
4.10	Static active earth pressure force and incremental dynamic active earth pressure force for dry backfill	66
4.11	Limiting values for horizontal acceleration equal to $k_h^* \cdot g$	67
4.12	Modified effective friction angle	71
4.13	Effective unit weight for partially submerged backfills	73
4.14	Variation α_{PE} with Ψ for δ equal to $\phi/2$, vertical wall and level backfill	75
4.15	Variation in α_{PE} with Ψ for δ equal to zero degrees, vertical wall and level backfill	75

No.		Page
4.16	Equivalent static formulation of the Mononobe-Okabe passive dynamic earth pressure problem	76
4.17	Values of factor F_{PE}	77
4.18	Mononobe-Okabe active wedge relationships including surcharge loading	80
4.19	Static active earth pressure force including surcharge	81
4.20	Static active earth pressure force and incremental dynamic active earth pressure force including surcharge	83
5.1	Model of elastic backfill behind a rigid wall	134
5.2	Pressure distributions on smooth rigid wall for 1-g static horizontal body force	135
5.3	Resultant force and resultant moment on smooth rigid wall for 1-g static horizontal body force	136
6.1	Rigid walls retaining backfills which undergo movements during earthquakes	141
6.2	Rigid walls retaining dry backfill which undergo movements during earthquakes	144
6.3	Linear and uniform base pressure distributions	147
6.4	Rigid wall retaining submerged backfill which undergo movements during no excess pore water pressures	150
6.5	Rigid wall retaining submerged backfill which undergo movements during earthquakes, including excess pore water pressures	153
6.6	Rigid wall retaining submerged backfill which undergo movements during earthquakes-liquified backfill	156
6.7	Gravity retaining wall and failure wedge treated as a sliding block	159
6.8	Incremental displacement	159
6.9	Forces acting on a gravity wall for a limiting acceleration equal to $N^* \cdot g$	162
7.1	Decrease in failure surface slope of the active and passive sliding wedges with increasing lateral accelerations	207
7.2	Reduction in bending moments in anchored bulkhead from wall flexibility	209
7.3	Free earth support analysis distribution of earth pressures, moments and displacements, and design moment distributions	210
7.4	Two distributions for unbalanced water pressures	211
7.5	Measured distributions of bending moment in three model tests on anchored bulkhead	213
7.6	Anchored sheet pile walls retaining backfills which undergo movements during earthquakes	215
7.7	Anchored sheet pile wall with no excess pore water pressure due to earthquake shaking	217
7.8	Static and inertial horizontal force components of the Mononobe-Okabe earth pressure forces	219
7.9	Distributions of horizontal stresses corresponding to ΔP_{AE}	222
7.10	Horizontal pressure components and anchor force acting on sheet pile wall	222
7.11	Dynamic forces acting on an anchor block	224
7.12	Anchored sheet pile wall with excess pore water pressures generated during earthquake shaking	226
8.1	Simplified procedure for dynamic analysis of a wall retaining nonyielding backfill	232
8.2	Linear and uniform base pressure distributions	234

No.		Page
A.1	Dynamic active wedge analysis with excess pore water pressures	A1
A.2	Equilibrium of horizontal hydrostatic water pressure forces acting on backfill wedge	A3
A.3	Dynamic active wedge analysis including a surcharge loading	A7
A.4	Dynamic active wedge analysis including a surcharge loading	A8
A.5	Dynamic passive wedge analysis with excess pore water pressure	A9
A.6	Dynamic passive wedge analysis including a surcharge load	A12
A.7	Dynamic passive wedge analysis including a surcharge load	A13
B.1	Hydrostatic and westergaard hydrodynamic water pressures acting along vertical wall during earthquakes	B2
C.1	Anchored sheet pile wall design problem	C1
C.2	Horizontal earth pressure components in free earth support design	C3
C.3	Horizontal active and passive earth pressure components acting on a continuous slender anchor	C10
C.4	Design criteria for deadman anchorage	C11
C.5	Distribution of horizontal stresses corresponding to ΔP_{AE}	C20
C.6	Seismic design problem for a continuous anchor blast	C24
C.7	Simplified procedure for siting a continuous anchor wall	C28
D.1	Earth retaining structure, soil-structure interaction	D5

CONVERSION FACTORS, NON-SI TO SI (METRIC)
UNITS OF MEASUREMENT

Multiply	By	To Obtain
acceleration of gravity (standard)	980.665	centimeters/second/second
	32.174	feet/second/second
	386.086	inches/second/second
feet	0.3048	meters
feet/second/second	30.4838	centimeters/second/second
gal	1.0	centimeters/second/second
inches	2.54	centimeters
pounds	4.4822	newtons
tons	8.896	kilonewtons

CHAPTER 1 GENERAL DESIGN CONSIDERATIONS FOR WATERFRONT SITES

1.1 Scope and Applicability

This manual deals with the soil mechanics aspects of the seismic design of waterfront earth retaining structures. Specifically, this report addresses:

* The stability and movement of gravity retaining walls and anchored bulkheads.

* Dynamic forces against subsurface structures such as walls of dry docks and U-frame locks.

The report does not address the seismic design of structural frameworks of buildings or structures such as docks and cranes. It also does not consider the behavior or design of piles or pile groups.

The design of waterfront retaining structures against earthquakes is still an evolving art. The soils behind and beneath such structures often are cohesionless and saturated with a relatively high water table, and hence there is a strong possibility of pore pressure buildup and associated liquefaction phenomena during strong ground shaking. There have been numerous instances of failure or unsatisfactory performance. However, there has been a lack of detailed measurements and observations concerning such failures. There also are very few detailed measurements at waterfront structures that have performed well during major earthquakes. A small number of model testing programs have filled in some of the blanks in the understanding of dynamic response of such structures. Theoretical studies have been made, but with very limited opportunities to check the results of these calculations against actual, observed behavior. As a result, there are still major gaps in knowledge concerning proper methods for analysis and design.

The methods set forth in this report are hence based largely upon judgement. It is the responsibility of the reader to judge the validity of these methods, and no responsibility is assumed for the design of any structure based on the methods described herein.

The methods make use primarily of simplified procedures for evaluating forces and deformations. There is discussion of the use of finite element models, and use of the simpler finite element methods is recommended in some circumstances. The most sophisticated analyses using finite element codes and complex stress-strain relations are useful mainly for understanding patterns of behavior, but quantitative results from such analyses should be used with considerable caution.

This report is divided into eight chapters and five appendixes. The subsequent sections in Chapter 1 describe the limit states associated with the seismic stability of waterfront structures during earthquake loadings, the key role of liquefaction hazard assessment, and the choice of the design ground motion(s).

Chapter 2 describes the general design considerations for retaining structures, identifying the interdependence between wall deformations and forces acting on the wall. Additional considerations such as failure surfaces

passing below the wall, failure of anchoring systems for sheet pile walls, and analysis of the post-seismic condition are also discussed.

The procedures for calculating static earth pressures acting on walls retaining yielding backfills are described in Chapter 3. A wall retaining a yielding backfill is defined as a wall with movements greater than or equal to the values given in Table 1 (Chapter 2). These movements allow the full mobilization of the shearing resistance within the backfill. For a wall that moves away from the backfill, active earth pressures act along the soil-wall interface. In the case of a wall that moves towards the backfill, displacing the soil, passive earth pressures act along the interface.

Chapter 4 describes the procedures for calculating seismic earth pressures acting on walls retaining yielding backfills. The Mononobe-Okabe theory for calculating the dynamic active earth pressure force and dynamic passive earth pressure force is described. Two limiting cases used to incorporate the effect of submergence of the backfill in the Mononobe-Okabe method of analysis are discussed: (1) the restrained water case and (2) the free water case. These procedures include an approach for incorporating excess pore water pressures generated during earthquake shaking within each of the analyses.

The procedures for calculating dynamic earth pressures acting on walls retaining nonyielding backfills are described in Chapter 5. A wall retaining a nonyielding backfill is one that does not develop the limiting dynamic active or passive earth pressures because sufficient wall movements do not occur and the shear strength of the backfill is not fully mobilized - wall movements that are less than one-fourth to one-half of Table 1 (Chapter 2) wall movement values. The simplified analytical procedure due to Wood (1973) and a complete soil-structure interaction analysis using the finite element method are discussed.

The analysis and design of gravity walls retaining yielding backfill are described in Chapter 6. Both the preselected seismic coefficient method of analysis and the Richards and Elms (1979) procedure based on displacement control are discussed.

Chapter 7 discusses the analysis and design of anchored sheet pile walls.

The analysis and design of gravity walls retaining nonyielding backfill using the Wood (1973) simplified procedure is described in Chapter 8.

Appendix A describes the computation of the dynamic active and passive earth pressure forces for partially submerged backfills using the wedge method.

Appendix B describes the Westergaard procedure for computing hydrodynamic water pressures along vertical walls during earthquakes.

Appendix C contains a design example of an anchored sheet pile wall.

Appendix D is a brief guide to the several types of finite element methods that might be used when considered appropriate.

Appendix E summarizes the notation used in this report.

1.2 Limit States

A broad look at the problem of seismic safety of waterfront structures involves the three general limit states shown in Figure 1.1 which should be considered in design.

1) **Gross site instability**: This limit state involves lateral earth movements exceeding several feet. Such instability would be the result of liquefaction of a site, together with failure of an edge retaining structure to hold the liquefied soil mass in place. Liquefaction of backfill is a problem associated with the site, mostly independent of the type of retaining structure. Failure of the retaining structure might result from overturning, sliding, or a failure surface passing beneath the structure. Any of these modes might be triggered by liquefaction of soil beneath or behind the retaining structure. There might also be a structural failure, such as failure of an anchorage which is a common problem if there is liquefaction of the backfill.

2) **Unacceptable movement of retaining structure**: Even if a retaining structure along the waterfront edge of a site remains essentially in place, too much permanent movement of the structure may be the cause of damage to facilities immediately adjacent to the quay. Facilities of potential concern include cranes and crane rails, piping systems, warehouses, or other buildings. An earthquake-induced permanent movement of an inch will seldom be of concern. There have been several cases where movements as large as 4 inches have not seriously interrupted operations or caused material damage, and hence have not been considered failures. The level of tolerable displacement is usually specific to the planned installation.

Permanent outward movement of retaining structures may be caused by tilting and/or sliding of massive walls or excessive deformations of anchored bulkheads. Partial liquefaction of backfill will make such movements more likely, but this limit state is of concern even if there are no problems with liquefaction.

3) **Local instabilities and settlements**: If a site experiences liquefaction and yet is contained against major lateral flow, buildings and other structures founded at the site may still experience unacceptable damage. Possible modes of failure include bearing capacity failure, excessive settlements, and tearing apart via local lateral spreading. Just the occurrence of sand boils in buildings can seriously interrupt operations and lead to costly clean-up operations.

This document addresses the first two of these limit states. The third limit state is discussed in the National Research Council (1985), Seed (1987), and Tokimatsu and Seed (1987).

1.3 Key Role of Liquefaction Hazard Assessment

The foregoing discussion of general limit states has emphasized problems due to soil liquefaction. Backfills behind waterfront retaining structures often are cohesionless soils, and by their location have relatively high water tables. Cohesionless soils may also exist beneath the base or on the waterside of such structures. Waterfront sites are often developed by hydraulic filling using cohesionless soils, resulting in low density fills that are

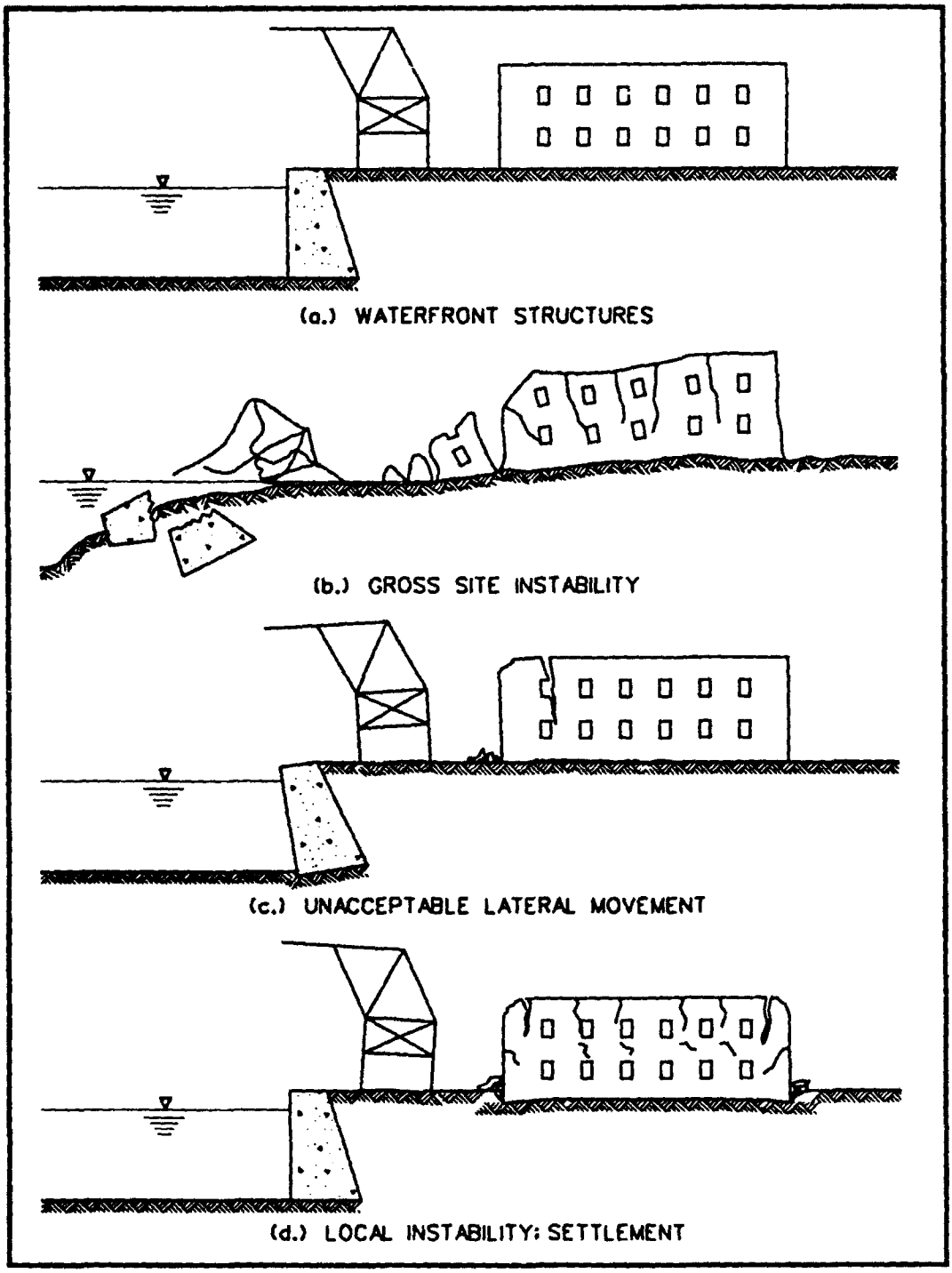

Figure 1.1 Overall limit states at waterfronts

susceptible to liquefaction. Thus, liquefaction may be a problem for buildings or other structures located well away from the actual waterfront. Hence, evaluation of potential liquefaction should be the first step in analysis of any existing or new site, and the first step in establishing criteria for control of newly-placed fill. Methods for such evaluation are set forth in numerous articles, including the National Research Council (1985) and Seed, Tokimatsu, Harder and Chung (1985).

The word "liquefaction" has been applied to different but related phenomena (National Research Council 1985). To some, it implies a flow failure of an earthen mass in the form of slope failure or lateral spreading, bearing capacity failure, etc. Others use the word to connote a number of phenomena related to the buildup of pore pressures within soil, including the appearance of sand boils and excessive movements of buildings, structures, or slopes. Situations in which there is a loss of shearing resistance, resulting in flow slides or bearing capacity failures clearly are unacceptable. However, some shaking-induced increase in pore pressure may be acceptable, provided it does not lead to excessive movements or settlements.

Application of the procedures set forth in this manual may require evaluation of: (a) residual strength for use in analyzing for flow or bearing capacity failure; or (b) buildup of excess pore pressure during shaking. As a general design principle, the predicted buildup of excess pore pressure should not exceed 30 to 40 percent of the initial vertical effective stress, except in cases where massive walls have been designed to resist larger pore pressures and where there are no nearby buildings or other structures that would be damaged by excessive settlements or bearing capacity failures. With very loose and contractive cohesionless soils, flow failures occur when the residual excess pore pressure ratio reaches about 40 percent (Vasquez and Dobry 1988, or Marcuson, Hynes, and Franklin 1990).* Even with soils less susceptible to flow failures, the actual level of pore pressure buildup becomes uncertain and difficult to predict with confidence when the excess pore pressure ratio reaches this level.

Remedial measures for improving seismic stability to resist liquefaction, the buildup of excess pore water pressures, or unacceptable movements, are beyond the scope of this report. Remedial measures are discussed in numerous publications, including Chapter 5 of the National Research Council (1985).

1.4 Choice of Design Ground Motions

A key requirement for any analysis for purposes of seismic design is a quantitative specification of the design ground motion. In this connection,

---

* The word "contractive" reflects the tendency of a soil specimen to decrease in volume during a drained shear test. During undrained shearing of a contractive soil specimen, the pore water pressure increases, in excess of the pre-sheared pore water pressure value. "Dilative" soil specimens exhibit the opposite behavior; an increase in volume during drained shear testing and negative excess pore water pressures during undrained shear testing. Loose sands and dense sands are commonly used as examples of soils exhibiting contractive and dilative behavior, respectively, during shear.

it is important to distinguish between the level of ground shaking that a structure or facility is to resist safely and a parameter, generally called a seismic coefficient that is used as input to a simplified, pseudo-static analysis.

1.4.1 Design Seismic Event

Most often a design seismic event is specified by a peak acceleration. However, more information concerning the ground motion often is necessary. Duration of shaking is an important parameter for analysis of liquefaction. Magnitude is used as an indirect measure of duration. For estimating permanent displacements, specification of either peak ground velocity or predominant period of the ground motion is essential. Both duration and predominant periods are influenced strongly by the magnitude of the causative earthquake, and hence magnitude sometimes is used as a parameter in analyses.

Unless the design event is prescribed for the site in question, peak accelerations and peak velocities may be selected using one of the following approaches:

(1) By using available maps for the contiguous 48 states. Such maps may be found in National Earthquake Hazards Reduction Program (1988). Such maps are available for several different levels of risk, expressed as probability of non-exceedance in a stated time interval or mean recurrence interval. A probability of non-exceedance of 90 percent in 50 years (mean recurrence interval of 475 years) is considered normal for ordinary buildings.

(2) By using attenuation relations giving ground motion as a function of magnitude and distance (e.g. attenuation relationships for various tectonic environments and site conditions are summarized in Joyner and Boore (1988). This approach requires a specific choice of a magnitude of the causative earthquake, requiring expertise in engineering seismology. Once this choice is made, the procedure is essentially deterministic. Generally it is necessary to consider various combinations of magnitude and distance.

(3) By a site-specific probabilistic seismic hazard assessment (e.g. National Research Council 1988). Seismic source zones must be identified and characterized, and attenuation relations must be chosen. Satisfactory accomplishment of such an analysis requires considerable expertise and experience, with input from both experienced engineers and seismologists. This approach requires selection of a level of risk.

It is of greatest importance to recognize that, for a given site, the ground motion description suitable for design of a building may not be appropriate for analysis of liquefaction.

Local soil conditions: The soil conditions at a site should be considered when selecting the design ground motion. Attenuation relations are available for several different types of ground conditions, and hence the analyses in items (2) and (3) might be made for any of these particular site conditions. However, attenuation relations applicable to the soft ground conditions often found at waterfront sites are the least reliable. The maps referred to under item (1) apply for a specific type of ground condition: soft rock. More recent maps will apply for deep, firm alluvium, after revision of the document referenced in item (1). Hence, it generally is nec-

essary to make a special analysis to establish the effects of local soil conditions.

A site-specific site response study is made using one-dimensional analyses that model the vertical propagation of shear waves through a column of soil. Available models include the computer codes SHAKE (Schnabel, Lysmer, and Seed 1972), DESRA (Lee and Finn 1975, 1978) and CHARSOL (Streeter, Wylie, and Richart 1974). These programs differ in that SHAKE and CHARSOL are formulated using the total stress procedures, while DESRA is formulated using both total and effective stress procedures. All three computer codes incorporate the nonlinear stress-strain response of the soil during shaking in their analytical formulation, which has been shown to be an essential requirement in the dynamic analysis of soil sites.

For any site-specific response study, it first will be necessary to define the ground motion at the base of the soil column. This will require an establishment of a peak acceleration for firm ground using one of the three methods enumerated above, and the selection of several representatives time histories of motion scaled to the selected peak acceleration. These time histories must be selected with considerable care, taking into account the magnitude of the causative earthquake and the distance from the epicenter. Procedures for choosing suitable time histories are set forth in Seed and Idriss (1982), Green (1992), and procedures are also under development by the US Army Corps of Engineers.

If a site response analysis is made, the peak ground motions will in general vary vertically along the soil column. Depending upon the type of analysis being made, it may be desirable to average the motions over depth to provide a single input value. At each depth, the largest motion computed in any of the several analyses using different time histories should be used.

If finite element analyses are made, it will again be necessary to select several time histories to use as input at the base of the grid, or a time history corresponding to a target spectra (refer to page 54 of Seed and Idriss 1982 or Green 1992).

1.4.2 Seismic Coefficients

A seismic coefficient (typical symbols are k_h and k_v) is a dimensionless number that, when multiplied times the weight of some body, gives a pseudo-static inertia force for use in analysis and design. The coefficients k_h and k_v are, in effect, decimal fractions of the acceleration of gravity (g). For some analyses, it is appropriate to use values of $k_h g$ or $k_v g$ smaller than the peak accelerations anticipated during the design earthquake event.

For analysis of liquefaction, it is conventional to use 0.65 times the peak acceleration. The reason is that liquefaction is controlled by the amplitude of a succession of cycles of motion, rather than just by the single largest peak. The most common, empirical methods of analysis described in the National Research Council (1985) and Seed, Tokimatsu, Harder, and Chung (1985) presume use of this reduction factor.

In design of buildings, it is common practice to base design upon a seismic coefficient corresponding to a ground motion smaller than the design ground motion. It is recognized that a building designed on this basis may

likely yield and even experience some nonlife-threatening damage if the design ground motion actually occurs. The permitted reduction depends upon the ductility of the structural system; that is, the ability of the structure to undergo yielding and yet remain intact so as to continue to support safely the normal dead and live loads. This approach represents a compromise between desirable performance and cost of earthquake resistance.

The same principle applies to earth structures, once it has been established that site instability caused by liquefaction is not a problem. If a retaining wall system yields, some permanent outward displacement will occur, which often is an acceptable alternative to significantly increased cost of construction. However, there is no generally accepted set of rules for selecting an appropriate seismic coefficient. The displacement controlled approach to design (Section 6.3) is in effect a systematic and rational method for evaluating a seismic coefficient based upon allowable permanent displacement. The AASHTO seismic design for highway bridges (1983) is an example of design guidance using the seismic coefficient method for earth retaining structures.* AASHTO recommends that a value of $k_h = 0.5A$ be used for most cases if the wall is designed to move up to 10A (in.) where A is peak ground acceleration coefficient for a site (acceleration = Ag). However, use of $k_h = 0.5A$ is not necessarily conservative for areas of high seismicity (see Whitman and Liao 1985).

Various relationships have been proposed for estimating permanent displacements, as a function of the ratio k_h/A and parameters describing the ground motion. Richards and Elms (1979) and Whitman and Liao (1985) use peak ground acceleration and velocity, while Makdisi and Seed (1979) use peak ground acceleration and magnitude. Values for the ratio V/a_{max} may be used, both for computations and to relate the several methods. Typical values for the ratio V/a_{max} are provided in numerous publications discussing ground shaking, including the 1982 Seed and Idriss, and the 1983 Newmark and Hall EERI monographs, and Sadigh (1983). Seed and Idriss (1982), Newmark and Hall (1983), and Sadigh (1973) report that values for the ratio V/a_{max} varies with geologic conditions at the site. Additionally, Sadigh (1973) reports that the values for the ratio V/a_{max} varies with earthquake magnitude, the ratio increasing in value with increasing magnitude earthquake.

Based upon simplified assumptions and using the Whitman and Liao relationship for earthquakes to magnitude 7, k_h values were computed:

	A = 0.2	A = 0.4
Displacement < 1 in.	$k_h = 0.13$	$k_h = 0.30$
Displacement < 4 in.	$k_h = 0.10$	$k_h = 0.25$

These numbers are based upon V/Ag = 50 in/sec/g (Sadigh 1983), which applies to deep stiff soil sites (geologic condition); smaller k_h would be appropriate for hard (e.g. rock) sites. The Whitman and Liao study did not directly address the special case of sites located within epicentral regions.

---

* The map in AASHTO (1983) is not accepted widely as being representative of the ground shaking hazard.

The value assigned to k_h is to be established by the seismic design team for the project considering the seismotectonic structures within the region, or as specified by the design agency.

1.4.3 Vertical Ground Accelerations

The effect of vertical ground accelerations upon response of waterfront structures is quite complex. Peak vertical accelerations can equal or exceed peak horizontal accelerations, especially in epicentral regions. However, the predominant frequencies generally differ in the vertical and horizontal components, and phasing relationships are very complicated. Where retaining structures support dry backfills, studies have shown that vertical motions have little overall influences (Whitman and Liao 1985). However, the Whitman and Liao study did not directly address the special case of sites located within epicentral regions. For cases where water is present within soils or against walls, the possible influence of vertical motions have received little study. It is very difficult to represent adequately the effect of vertical motions in pseudo-static analyses, such as those set forth in this manual.

The value assigned to k_v is to be established by the seismic design team for the project considering the seismotectonic structures within the region, or as specified by the design agency. However, pending the results of further studies and in the absence of specific guidance for the choice of k_v for waterfront structures the following guidance has been expressed in literature: A vertical seismic coefficient be used in situations where the horizontal seismic coefficient is 0.1 or greater for gravity walls and 0.05 or greater for anchored sheet pile walls. This rough guidance excludes the special case of structures located within epicentral regions for the reasons discussed previously. It is recommended that three solutions should be made: one assuming the acceleration upward, one assuming it downward, and the other assuming zero vertical acceleration. If the vertical seismic coefficient is found to have a major effect and the use of the most conservative assumption has a major cost implication, more sophisticated dynamic analyses should probably be considered.

CHAPTER 2 GENERAL DESIGN CONSIDERATIONS FOR RETAINING WALLS

2.1 Approaches to Design for Various Classes of Structure

The basic elements of seismic design of waterfront retaining structures are a set of design criteria, specification of the static and seismic forces acting on the structure in terms of magnitude, direction and point of application, and a procedure for estimating whether the structure satisfies the design criteria.

The criteria are related to the type of structure and its function. Limits of tolerable deformations may be specified, or it may be sufficient to assure the gross stability of the structure by specifying factors of safety against rotational and sliding failure and overstressing the foundation. In addition, the structural capacity of the wall to resist internal moments and shears with adequate safety margins must be assured. Structural capacity is a controlling factor in design for tied-back or anchored walls of relatively thin section such as sheet pile walls. Crib walls, or gravity walls composed of blocks of rock are examples of structures requiring a check for safety against sliding and tipping at each level of interface between structural components.

Development of design criteria begins with a clear concept of the failure modes of the retaining structure. Anchored sheet pile walls display the most varied modes of failure as shown in Figure 2.1, which illustrates both gross stability problems and potential structural failure modes. The more restricted failure modes of a gravity wall are shown in Figure 2.2. A failure surface passing below a wall can occur whenever there is weak soil in the foundation, and not just when there is a stratum of liquified soil.

Retaining structures must be designed for the static soil and water pressures existing before the earthquake and for superimposed dynamic and inertia forces generated by seismic excitation, and for post seismic conditions, since strengths of soils may be altered as a result of an earthquake. Figure 2.3 shows the various force components using an anchored sheet pile wall example from Chapter 7. With massive walls, it is especially important to include the inertia force acting on the wall itself. There are superimposed inertia forces from water as well as from soil. Chapters 3, 4, and 5 consider the evaluation of static and dynamic earth and water pressures.

2.2 Interdependence between Wall Deformations and Forces Acting on the Wall

The interdependence between wall deformations and the static and dynamic earth pressure forces acting on the wall has been demonstrated in a number of tests on model retaining walls at various scales. An understanding of this interdependence is fundamental to the proper selection of earth pressures for analysis and design of walls. The results from these testing programs are summarized in the following two sections.

2.2.1 Wall Deformations and Static Earth Pressure Forces

The relationships between the movement of the sand backfills and the measured static earth pressure forces acting on the wall are shown in Figure 2.4. The figure is based on data from the model retaining wall tests conducted by Terzaghi (1934, 1936, and 1954) at MIT and the tests by Johnson

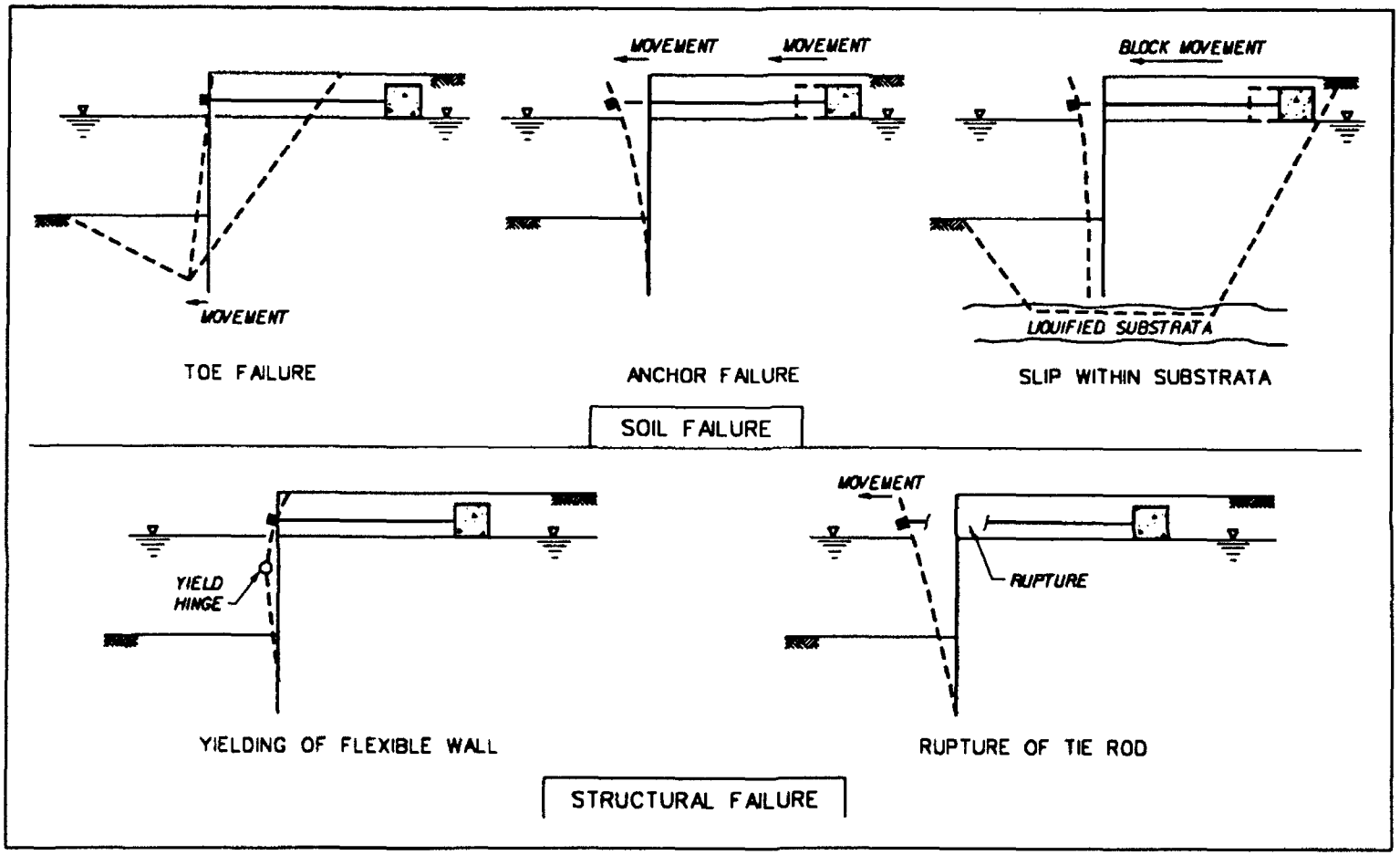

Figure 2.1 Potential soil and structural failure modes due to earthquake shaking of an anchored sheet pile wall

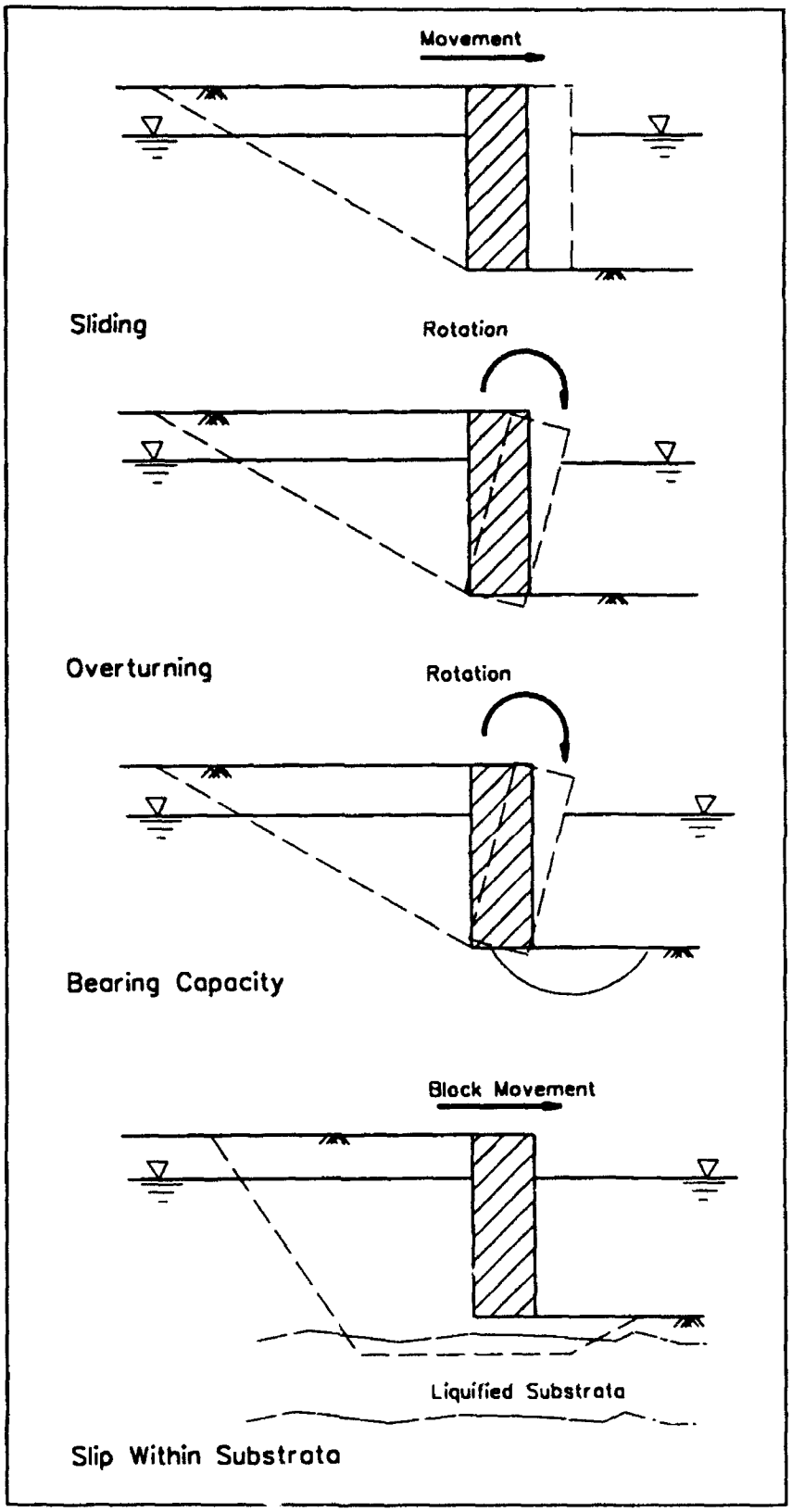

Figure 2.2 Rigid walls retaining backfills which undergo movements during earthquakes

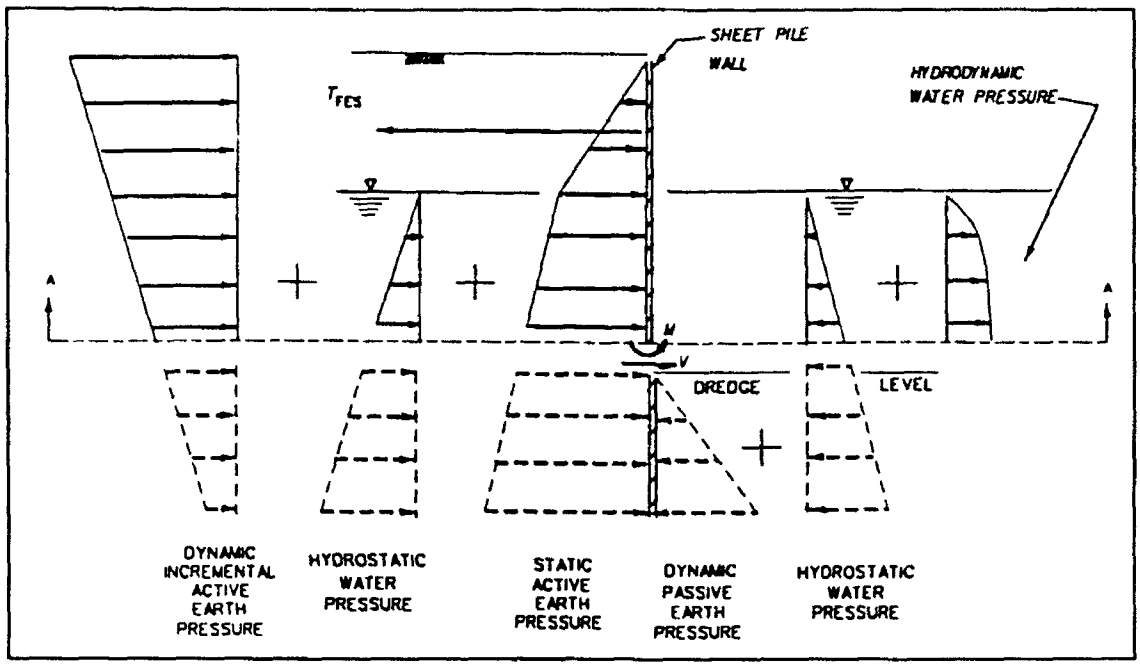

Figure 2.3 Horizontal pressure components and anchor force acting on sheet pile wall

(1953) at Princeton University, conducted under the direction of Tschebotarioff. The backfill movements are presented as the movement at the top of the wall, Y, divided by the height of the wall, H, and the earth pressure forces are expressed in terms of an equivalent horizontal earth pressure coefficient, K_h. K_h is equal to the horizontal effective stress, σ_h', divided by the vertical effective stress, σ_v'.

The test results in Figure 2.4 show that as the wall is rotated from vertical (Y = 0) and away from the backfill, the horizontal earth pressure coefficient acting on the wall decreases from the value recorded prior to movement of the wall. The zero wall movement horizontal earth pressure coefficient is equal to the at-rest value, K_o. When the backfill movements at the top of the wall, Y, attain a value equal to 0.004 times the height of the wall, H, the earth pressure force acting on the wall decreases to the limiting value of the <u>active</u> earth pressure force, P_A, and the earth pressure coefficient reduces to the active coefficient, K_A.

In a second series of tests, the wall was rotated from vertical in the opposite direction, displacing the backfill. The horizontal earth pressure coefficient acting on the wall increased from the K_o value. When the backfill movements at the top of the wall, Y, attain a value equal to 0.04 times the height of the wall, H, the earth pressure force acting on the wall increases to the other limiting value of the passive earth pressure force, P_P, with a corresponding passive earth pressure coefficient, K_P. The movements required to develop <u>passive</u> earth pressures are on the order of ten times the movements required to develop active earth pressures.

With the soil in either the active or passive state, the magnitude of the backfill displacements are sufficient to fully mobilize the shear strength

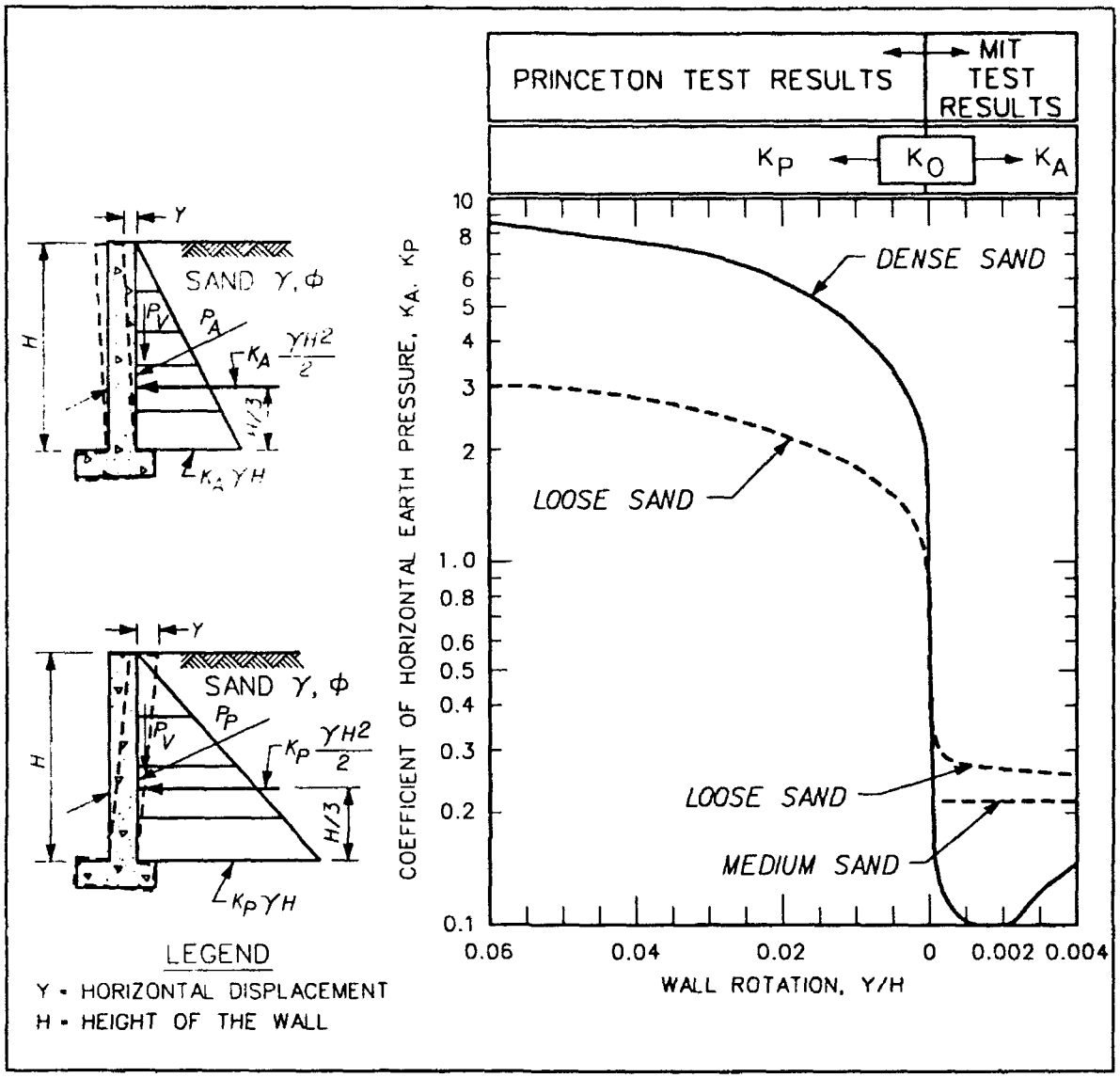

After NAVFAC DM-7.2

Figure 2.4 Effect of wall movement on static horizontal earth pressures

of soil within a wedge of backfill located directly behind the heel of the wall. With the soil wedge in a state of plastic equilibrium, P_A or P_P may be computed using either Rankine's or Coulomb's theory for earth pressures or the logarithmic spiral procedures, as described in Chapter 3. The values for K_A and K_P measured in above tests using backfills placed at a range of densities agree with the values computed using the appropriate earth pressure theories.

The test results show that the relationship between backfill displacements and earth pressures varies with the relative density of the backfill. Table 1 lists the minimum wall movements required to reach active and passive earth pressure conditions for various types of backfills. Clough and Duncan, (1991) and Duncan, Clough, and Ebeling (1990) give the following easy-to-remember guidelines for the amounts of movements required to reach the pressure extremes; for a cohesionless backfill the movement required to reach the minimum active condition is no more than about 1 inch in 20 feet ($\Delta/H = 0.004$)

and the movement required to reach the minimum passive condition is no more than about 1 inch in 2 feet ($\Delta/H = 0.04$).

Table 1

Approximate Magnitudes of Movements Required to Reach Minimum Active and Maximum Passive Earth Pressure Conditions From Clough and Duncan (1991)

Type of Backfill	Values of Y/H[a]	
	Active	Passive
Dense sand	0.001	0.01
Medium-dense sand	0.002	0.02
Loose sand	0.004	0.04

[a]Y = movement of top of wall required to reach minimum active or maximum passive pressure, by tilting or lateral translation.
H - height of wall.

2.2.2 Wall Deformations and Dynamic Earth Pressure Forces

The interdependence between wall deformations and the forces acting on the wall has been extended to problems involving dynamic earth pressures in tests on model retaining walls conducted at the University of Washington and at research laboratories in Japan. The University of Washington studies involved a series of static and dynamic tests using an instrumented model retaining wall mounted on a shaking table, as described by Sherif, Ishibashi and Lee (1982), Sherif and Fang (1984a), Sherif and Fang (1984b), and Ishibashi and Fang (1987). The shaking table used in this testing program is capable of applying a harmonic motion of constant amplitude to the base of the wall and the backfill. In each of the tests, the wall was constrained either to translate without rotation, to rotate about either the base or the top of the wall, or some combination of translation and rotation. During the course of the dynamic earth pressure tests, the wall was moved away from the backfill in a prescribed manner while the base was vibrated. Movement of the wall continued until active dynamic earth pressures acted along the back of the wall. Static tests were also carried out for comparison.

The active state during the dynamic tests occurred at almost the same wall displacement as in the static tests, at a value of wall rotation equal to 0.001 for the static and dynamic test results that are shown in Figure 2.5 on dense Ottawa sand. This was also the finding in a similar program of testing using a model wall retaining dense sand, as reported by Ichihara and Matsuzawa (1973) and shown in Figure 2.6. The magnitude of these wall movements are in general agreement with those measured in the MIT testing program shown in Figure 2.4 and those values reported in Table 1.

There has been relatively little experimental investigation of the dynamic passive case, however, the available results indicate that considerable wall movements are required to reach the full passive condition.

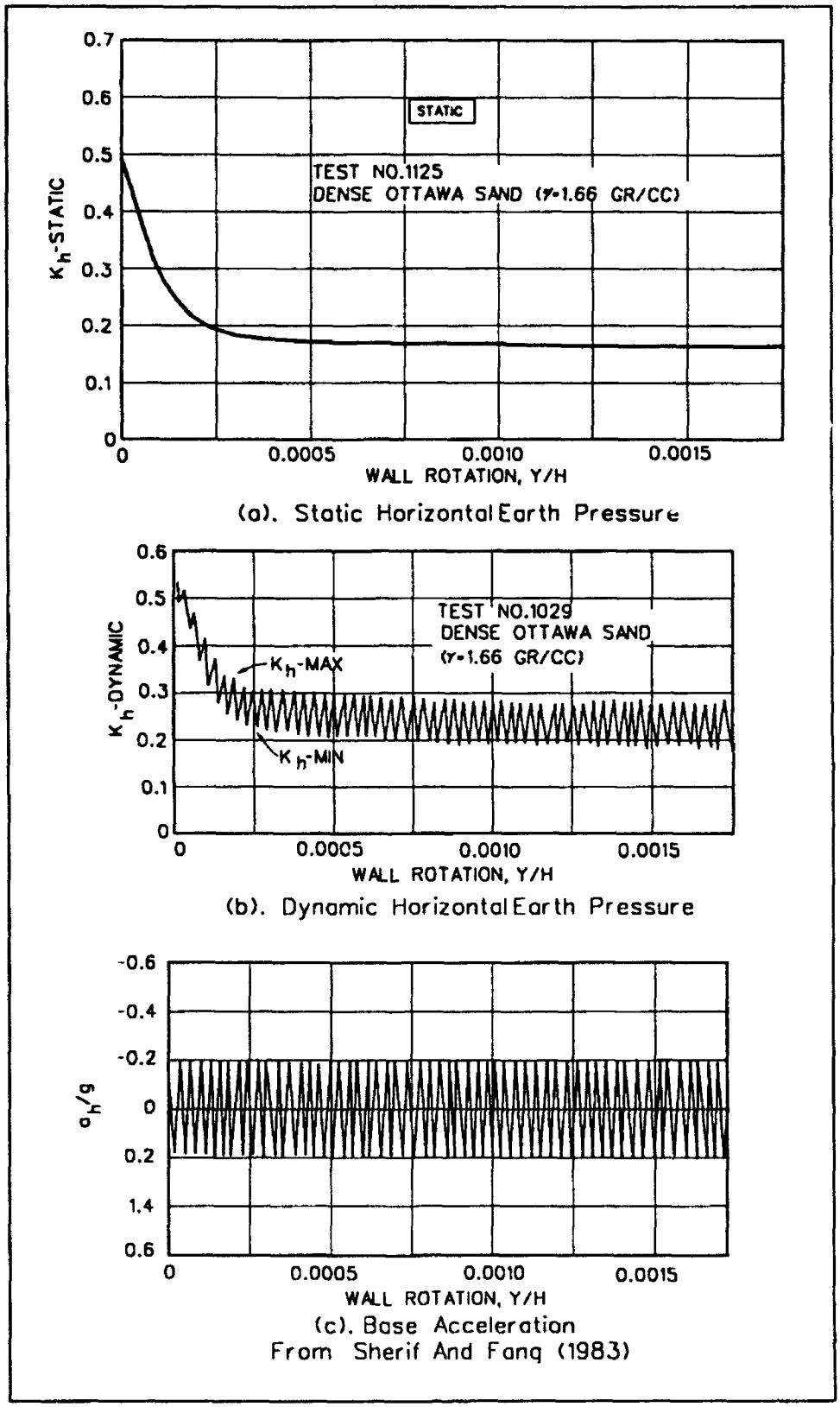

Figure 2.5 Effect of wall movement on static and dynamic horizontal earth pressures

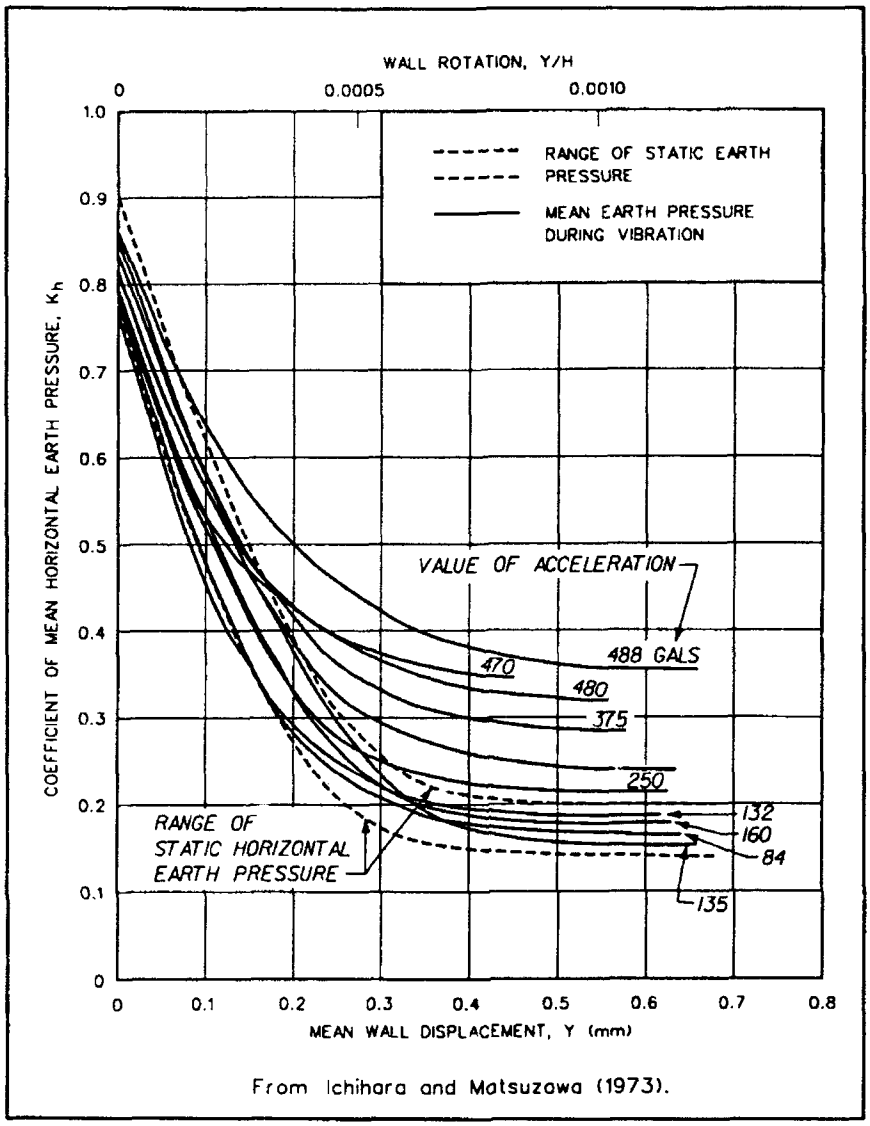

Figure 2.6 Effect of wall movement on static and dynamic horizontal earth pressures

The Table 1 values are used as rough guidance throughout this report, pending the results from additional research into the relationships between dynamic earth pressures and wall displacements.

2.3 Comments on Analyses for Various Cases

The greatest part of this report is devoted to the evaluation of static and dynamic earth and water pressures against walls, and the use of these pressures in the analysis of the equilibrium of such walls. Such analyses are presented and discussed in Chapters 6, 7, and 8. The examples and discussion generally presume uniform and cohesionless backfills.

The soil strength parameters used in the analysis must be consistent with the displacements. Large displacements, or an accumulation of smaller

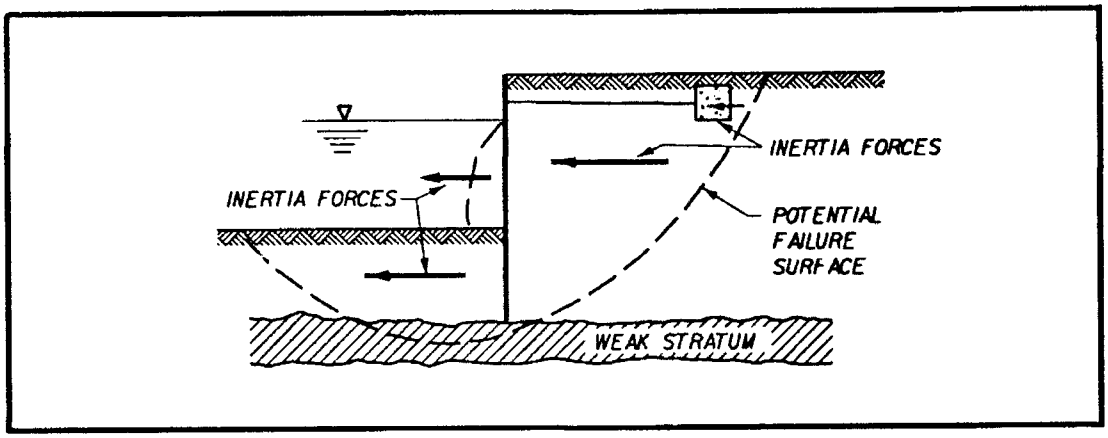

Figure 2.7 Failure surface below wall

displacements tend to support the use of residual strength parameters, as compared to peak values. Wall displacements must also be considered when assigning the foundation to structure interface strength parameters.

There are two potentially important situations that are not discussed or illustrated in detail in this manual. A brief treatment of these cases appears in the following subsections.

2.3.1 Analysis of Failure Surfaces Passing below Wall

This situation may be a problem if soils of low strength exist below a wall, either because the before-earthquake strength of this material is small or because the strength of the soil decreases as a result of earthquake shaking.

Such cases may be studied using principles from the analysis of slope stability (e.g. Edris and Wright 1987). Figure 2.7 shows again the diagram from Figure 2.1, and indicates the inertia forces that must be considered in addition to the static forces. Evaluation of suitable strengths may require careful consideration. Appropriate excess pore pressures should be applied where the failure surface passes through cohesionless soils; see Seed and Harder (1990), Marcuson, Hynes, and Franklin (1990). With cohesive soils, the possibility of degradation of strength by cyclic straining should be considered. A safety factor ranging from 1.1 to 1.2 is considered satisfactory: provided that reasonable conservative strengths and seismic coefficients have been assigned. With a smaller safety factor, permanent displacements may be estimated using the Makdisi-Seed procedure (Makdisi and Seed 1979) or the Sarma-Ambraseys procedure (Hynes-Griffin and Franklin 1984).

2.3.2 Analysis of Post-Seismic Condition

There are four circumstances that may cause the safety of a retaining structure to be less following an earthquake than prior to the earthquake.

1. Persistent excess pore pressures on the landside of the wall. Any such buildup may be evaluated using procedures described in Seed and Harder (1990) and Marcuson, Hynes, and Franklin (1990). The period of time during which such excess pressures will persist can be estimated using appropriate consolidation theory.

2. Residual earth pressures as a result of seismic straining. There is evidence that such residual pressures may reach those associated with the at-rest condition (see Whitman 1990).

3. Reduction in strength of backfill (or soils beneath or outside of toe of wall) as a result of earthquake shaking. In the extreme case, only the residual strength (see the National Research Council 1985; Seed 1987; Seed and Harder 1990; Marcuson, Hynes, and Franklin 1990; Poulos, Castro, and France 1985; and Stark and Mesri 1992) may be available in some soils. Residual strengths may be treated as cohesive shear strengths for evaluation of corresponding earth pressures.

4. Lowering of water level on waterside of wall during the falling water phase of a tsunami. Estimates of possible water level decrease during tsunamis require expert input.

The possibility that each of these situations may occur must be considered, and where appropriate the adjusted earth and fluid pressures must be introduced into an analysis of static equilibrium of the wall. Safety factors somewhat less than those for the usual static case are normally considered appropriate.

CHAPTER 3 STATIC EARTH PRESSURES - YIELDING BACKFILLS

3.1 Introduction

Methods for evaluating static earth pressures are essential for design. They also form the basis for simplified methods for determining dynamic earth pressures associated with earthquakes. This chapter describes analytical procedures for computing earth pressures for earth retaining structures with static loadings. Three methods are described: the classical earth pressure theories of Rankine and Coulomb and the results of logarithmic spiral failure surface analyses. The three failure mechanisms are illustrated in Figure 3.1.

The Rankine theory of active and passive earth pressures (Rankine 1857) determines the state of stress within a semi-infinite (soil) mass that, because of expansion or compression of the (soil) mass, is transformed from an elastic state to a state of plastic equilibrium. The orientation of the linear slip lines within the (soil mass) are also determined in the analysis. The shear stress at failure within the soil is defined by a Mohr-Coulomb shear strength relationship. The resulting failure surfaces within the soil mass and the corresponding Rankine active and passive earth pressures are shown in Figure 3.1 for a cohesionless soil.

The wedge theory, as developed by Coulomb (1776), looks at the equilibrium of forces acting upon a soil wedge without regard to the state of stress within the soil mass. This wedge theory assumes a linear slip plane within the backfill and the full mobilization of the shear strength of the soil along this plane. Interface friction between the wall and the backfill may be considered in the analysis.

Numerous authors have developed relationships for active and passive earth pressure coefficients based upon an assumption of a logarithmic failure surface, as illustrated in Figure 3.1. One of the most commonly used sets of coefficients was tabulated by Caquot and Kerisel (1948). Representative K_A and K_P values from that effort are illustrated in Table 3 and discussed in Section 3.5. NAVFAC developed nomographs from the Caquot and Kerisel efforts, and are also included in this chapter (Figures 3.11 and 3.12).

Rankine's theory, Coulomb's wedge theory, and the logarithmic spiral procedure result in similar values for active and passive thrust when the interface friction between the wall and the backfill is equal to zero. For interface friction angles greater than zero, the wedge method and the logarithmic spiral procedure result in nearly the same values for active thrust. The logarithmic spiral procedure results in accurate values for passive thrust for all values of interface friction between the wall and the backfill. The accuracy of the passive thrust values computed using the wedge method diminishes with increasing values of interface friction because the boundary of the failure block becomes increasingly curved.

This procedure is illustrated in example 1 at the end of this chapter.

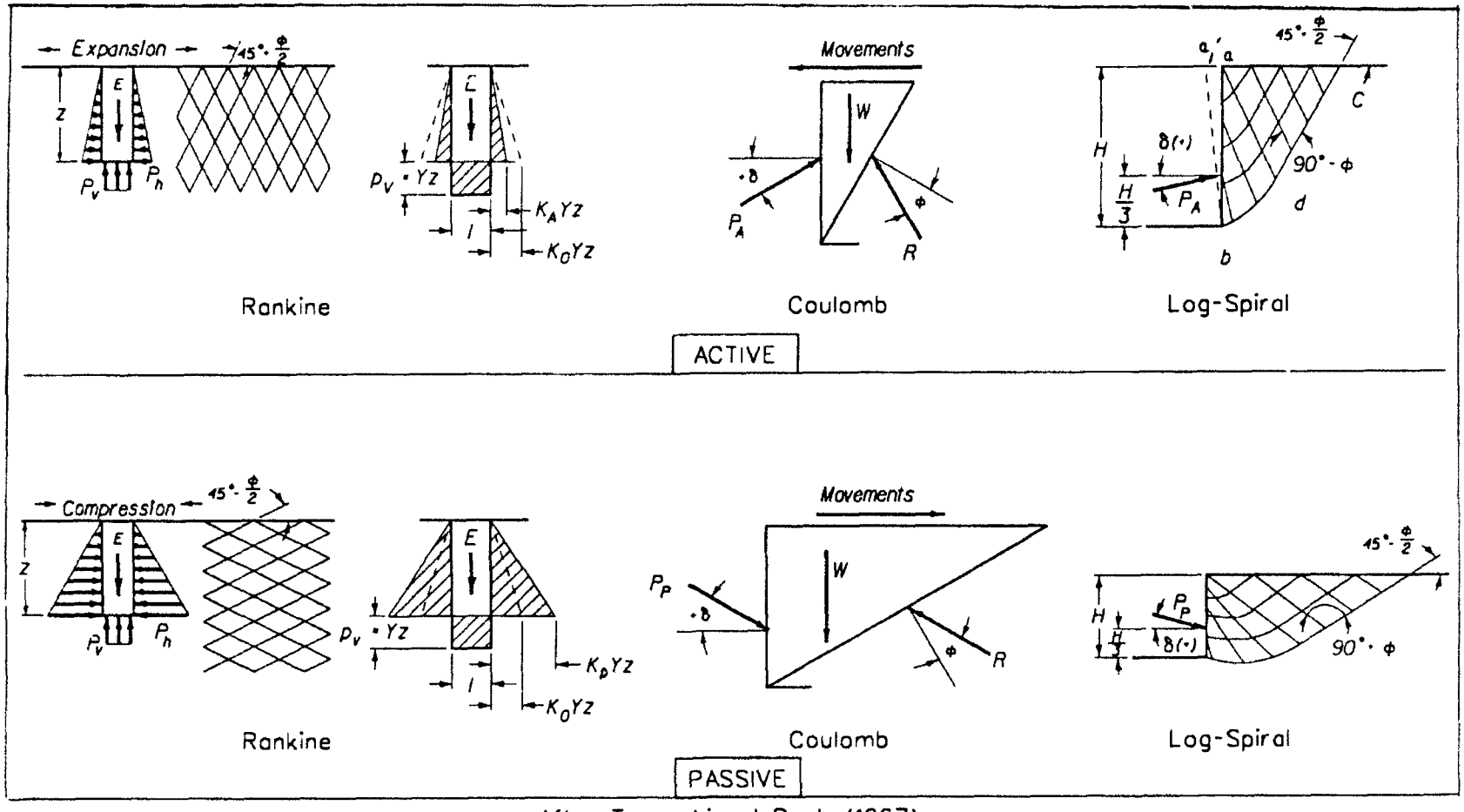

After Terzaghi and Peck (1967).

Figure 3.1. Three earth pressure theories for active and passive earth pressures

3.2 Rankine Theory

The Rankine theory of active and passive earth pressures is the simplest of the earth pressure theories. It is assumed that the vertical stress at any depth is equal to the depth times the unit weight of the overlying soil plus any surcharge on the surface of the ground. Horizontal stresses are then found assuming that shear resistance is fully mobilized within the soil. The forces and stresses corresponding to these two limiting states are shown in Figure 3.2 for a vertical retaining wall of height H. The effects of surcharge and groundwater pressures may be incorporated into the theory.

The backfill in Figure 3.2 is categorized as one of three types, according to the strength parameters assigned for the soil: frictional ($c = 0$, $\phi > 0$), cohesive ($c = S_u$, $\phi = 0$) or a combination of the two ($c > 0$, $\phi > 0$). Both effective and total stress methods are used in stability analyses of earth retaining structures. In an effective stress analysis the Mohr-Coulomb shear strength relationship defines the ultimate shearing resistance, τ_f, of the backfill as

$$\tau_f = c + \sigma_n' \tan\phi \tag{1}$$

where c is the effective cohesion, σ_n' is the effective normal stress on the failure plane, and ϕ is the effective angle of internal friction. The effective stress, σ', is equal to the difference between the total stress, σ, and the pore water pressure, u.

$$\sigma' = \sigma - u \tag{2}$$

The effective stress is the portion of total stress that is carried by the soil skeleton. The internal pore water pressures, as governed by seepage conditions, are considered explicitly in the effective stress analysis. For the total stress methods of analysis, the strength of the soil is equal to the undrained strength of the soil, S_u.

$$\tau_f = S_u \tag{3}$$

The internal pore water pressures are not considered explicitly in the total stress analysis, but the effects of the pore water are reflected in the value of S_u.

3.2.1 Rankine Theory - Active Earth Pressures - Cohesionless Soils

Active earth pressures result when the wall movements away from the backfill are sufficient to mobilize fully the shearing resistance within the soil mass behind the wall.

If the soil is frictional and dry, the horizontal effective stress at any depth is obtained from the vertical effective stress, γZ, using the active coefficient K_A:

$$\sigma_A = K_A \gamma z \tag{4}$$

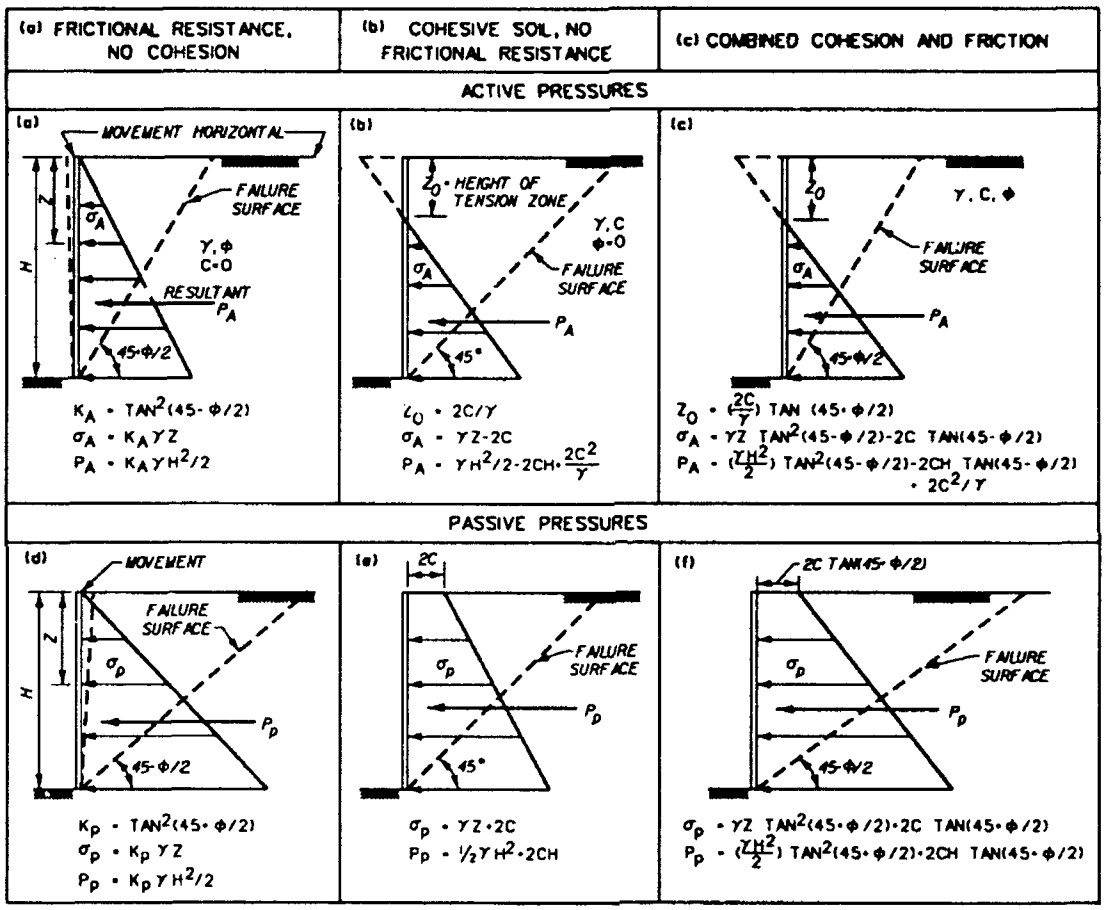

After NAVFAC DM-7.2

Figure 3.2 Computation of Rankine active and passive earth pressures for level backfills

If there are zero shear stresses on vertical and horizontal planes, the Rankine active earth pressure coefficient, K_A, is equal to

$$K_A = \tan^2(45 - \phi/2). \tag{5}$$

The variation in the active earth pressure is linear with z, as shown in Figure 3.2 (a). A planar slip surface extends upwards from the heel of the wall through the backfill, inclined at an angle α_A from horizontal. For frictional backfills, α_A is equal to

$$\alpha_A = 45 + \phi/2. \tag{6}$$

P_A is the resultant force of the σ_a distribution and is equal to

$$P_A = K_A \frac{1}{2}\gamma H^2 \tag{7}$$

acting normal to the back of the wall at one-third H above the heel of wall. In these expressions, γ is the dry unit weight.

If the soil is saturated with water table at the surface, the foregoing equations still apply but γ is replaced by γ_b, the buoyant unit weight. Equations 4 and 7 give the effective stresses and the active thrust from the mineral skeleton, and water pressures must be added.

The Rankine active earth pressure coefficient for a dry frictional backfill inclined at an angle β from horizontal is determined by computing the resultant forces acting on vertical planes within an infinite slope verging on instability, as described by Terzaghi (1943) and Taylor (1948). K_A is equal to

$$K_A = \cos\beta \frac{\cos\beta - \sqrt{\cos^2\beta - \cos^2\phi}}{\cos\beta + \sqrt{\cos^2\beta - \cos^2\phi}} \tag{8}$$

with the limitation that β is less than or equal to ϕ. Equation 4 still applies but is inclined at the backfill slope angle β, as shown in Figure 3.3. The distribution of σ_a is linear with depth along the back of the wall. Thus, there are shear stresses on vertical (and hence horizontal) planes. P_A is computed using Equation 7. It is inclined at an angle β from the normal to the back of the wall, and acts at one-third H above the heel of the wall.

3.2.2 Rankine Theory - Active Earth Pressures - Cohesive Soils - General Case

For the cases shown in Figure 3.2 (b) and (c), the active earth pressure, σ_a, normal to the back of the wall at depth z is equal to

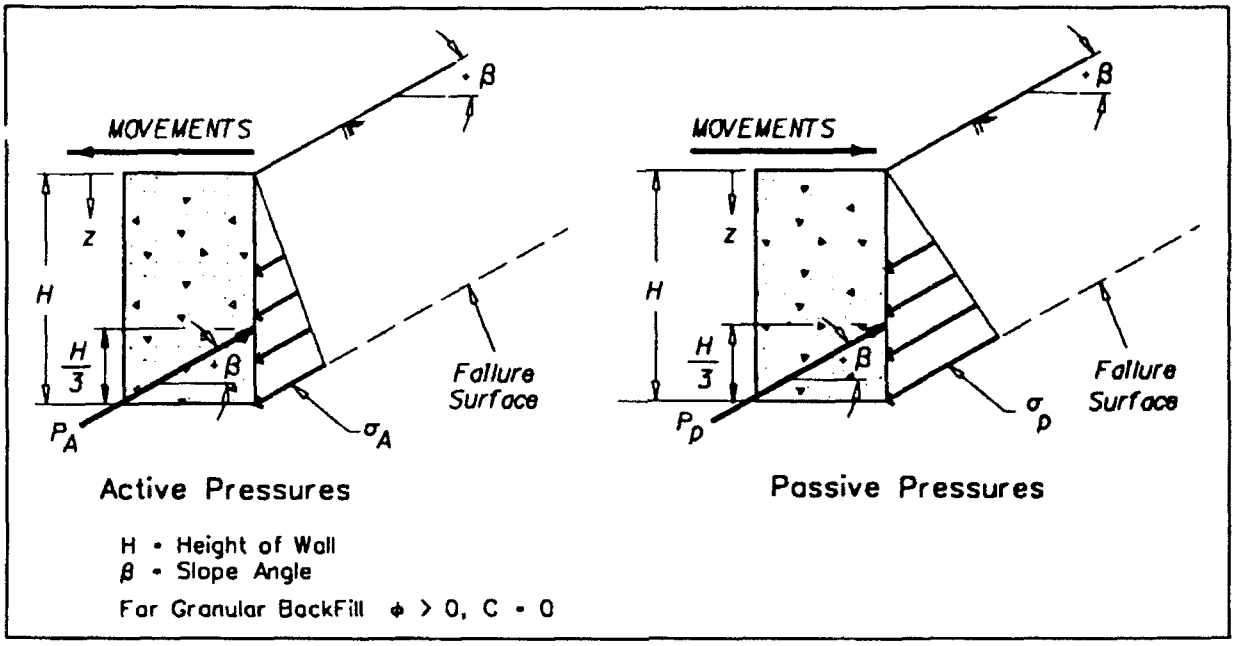

Figure 3.3 Rankine active and passive earth pressures for inclined backfills

$$\sigma_a = \gamma_t z K_A - 2c\sqrt{K_A} \tag{9}$$

The P_A and α_A relationships for backfills whose strengths are defined using S_u or an effective cohesion and effective angle of internal friction are given in the figure.

According to Equation 9, tensile stresses develop to a depth Z_o at the top of the backfill to wall interface in a backfill whose shear strength is either fully or partially attributed to the cohesion or undrained strength. A gap may form within this region over time. During rainstorms, these gaps will fill with water, resulting in hydrostatic water pressures along the back of the wall to depth Z_o. Tensile stresses are set equal to zero over the depth Z_o when applying this theory to long term wall designs because c' goes to zero with time for clayey soils due to changes in water content. For clayey backfills, retaining walls are designed using Terzaghi and Peck's (1967) equivalent fluid pressure values rather than active earth pressures because earth pressure theories do not account for the effects of creep in clayey backfills (Clough and Duncan 1991).

3.2.3 Rankine Theory - Passive Earth Pressures

The derivation of the Rankine theory of passive earth pressures follows the same steps as were used in the derivation of the active earth pressure relationships. The forces and stresses corresponding to this limiting state are shown in Figure 3.2 (d), (e), and (f) for a vertical wall retaining the three types of soil backfill. The effects of surcharge and groundwater pressures are not included in this figure. To develop passive earth pressures, the wall moves towards the backfill, with the resulting displacements sufficient to fully mobilize the shear resistance within the

soil mass (Section 2.2.1). The passive earth pressure, σ_p, normal to the back of the wall at depth z is equal to

$$\sigma_p = \gamma_t z K_p + 2c\sqrt{K_p} \tag{10}$$

and the Rankine passive earth pressure coefficient, K_p, for level backfill is equal to

$$K_p = \tan^2(45 + \phi/2). \tag{11}$$

A planar slip surface extends upwards from the heel of the wall through the backfill and is inclined at an angle α_p from horizontal, where α_p is equal to

$$\alpha_p = 45 - \phi/2. \tag{12}$$

P_p is the resultant force of the σ_p distribution and is equal to

$$P_p = K_p \frac{1}{2}\gamma_t H^2 \tag{13}$$

for dry frictional backfills and is normal to the back of the wall at one-third H above the heel of the wall. The P_p and α_p relationships for backfills whose strengths are defined using S_u or an effective cohesion and effective angle of internal friction are given in Figure 3.2.

This procedure is illustrated in example 2 at the end of this chapter.

K_p for a frictional backfill inclined at an angle β from horizontal is equal to

$$K_p = \cos\beta \frac{\cos\beta + \sqrt{\cos^2\beta - \cos^2\phi}}{\cos\beta - \sqrt{\cos^2\beta - \cos^2\phi}} \tag{14}$$

with the limitation that β is less than or equal to ϕ. P_p is computed using Equation 13. It is inclined at an angle β from the normal to the back of the vertical wall, and acts at one-third H above the back of the wall as shown in Figure 3.3. With c = 0, σ_p from Equation 10 becomes

$$\sigma_p = \gamma_t z K_p. \tag{15}$$

The distribution of σ_p is linear with depth along the back of the wall and is inclined at the backfill slope angle β, as shown in Figure 3.3.

3.3 Coulomb Theory

The Coulomb theory of active and passive earth pressures looks at the equilibrium of the forces acting on a soil wedge, assuming that the wall movements are sufficient to fully mobilize the shear resistance along a planar surface that extends from the heel of the wall into the backfill as shown in Figure 3.4. Coulomb's wedge theory allows for shear stresses along the wall to backfill interface. The forces corresponding to the active and passive states of stress are shown in Figure 3.4 for a wall with a face inclined at angle $+\theta$ from vertical, retaining a frictional backfill inclined at angle $+\beta$. The effects of surcharge and groundwater pressures are not included in this figure.

3.3.1 Coulomb Theory - Active Earth Pressures

In the active case the wall movements away from the backfill are sufficient to fully mobilize the shear resistance within a soil wedge. Coulomb's theory assumes that the presence of the wall introduces shearing stress along the interface, due to the downward movement of the backfill along the back of the wall as the wall moves away from the backfill. The active earth pressure force P_A is computed using Equation 7 and is oriented at an angle δ to the normal along the back of the wall at a height equal to H/3 above the heel, as shown in Figure 3.4. The shear component of P_A acts upward on the soil wedge due to the downward movement of the soil wedge along the face of the wall. K_A is equal to

$$K_A = \frac{\cos^2(\phi - \theta)}{\cos^2\theta \cos(\theta + \delta)\left[1 + \sqrt{\frac{\sin(\phi + \delta)\sin(\phi - \beta)}{\cos(\delta + \theta)\cos(\beta - \theta)}}\right]^2} \tag{16}$$

for frictional backfills. The active earth pressure, σ_a, along the back of the wall at depth z is computed using Equation 4 and oriented at an angle δ to the normal along the back of the wall. The variation in σ_a is assumed linear with depth for a dry backfill, as shown in Figure 3.4.

The planar slip surface extends upwards from the heel of the wall through the backfill and is inclined at an angle α_A from horizontal. α_A is equal to

$$\alpha_A = \phi + \tan^{-1}\left[\frac{-\tan(\phi - \beta) + c_1}{c_2}\right] \tag{17}$$

where

$$c_1 = \sqrt{[\tan(\phi - \beta)][\tan(\phi - \beta) + \cot(\phi - \theta)][1 + \tan(\delta + \theta)\cot(\phi - \theta)]}$$

and

$$c_2 = 1 + \left[[\tan(\delta + \theta)] \cdot [\tan(\phi - \beta) + \cot(\phi - \theta)]\right].$$

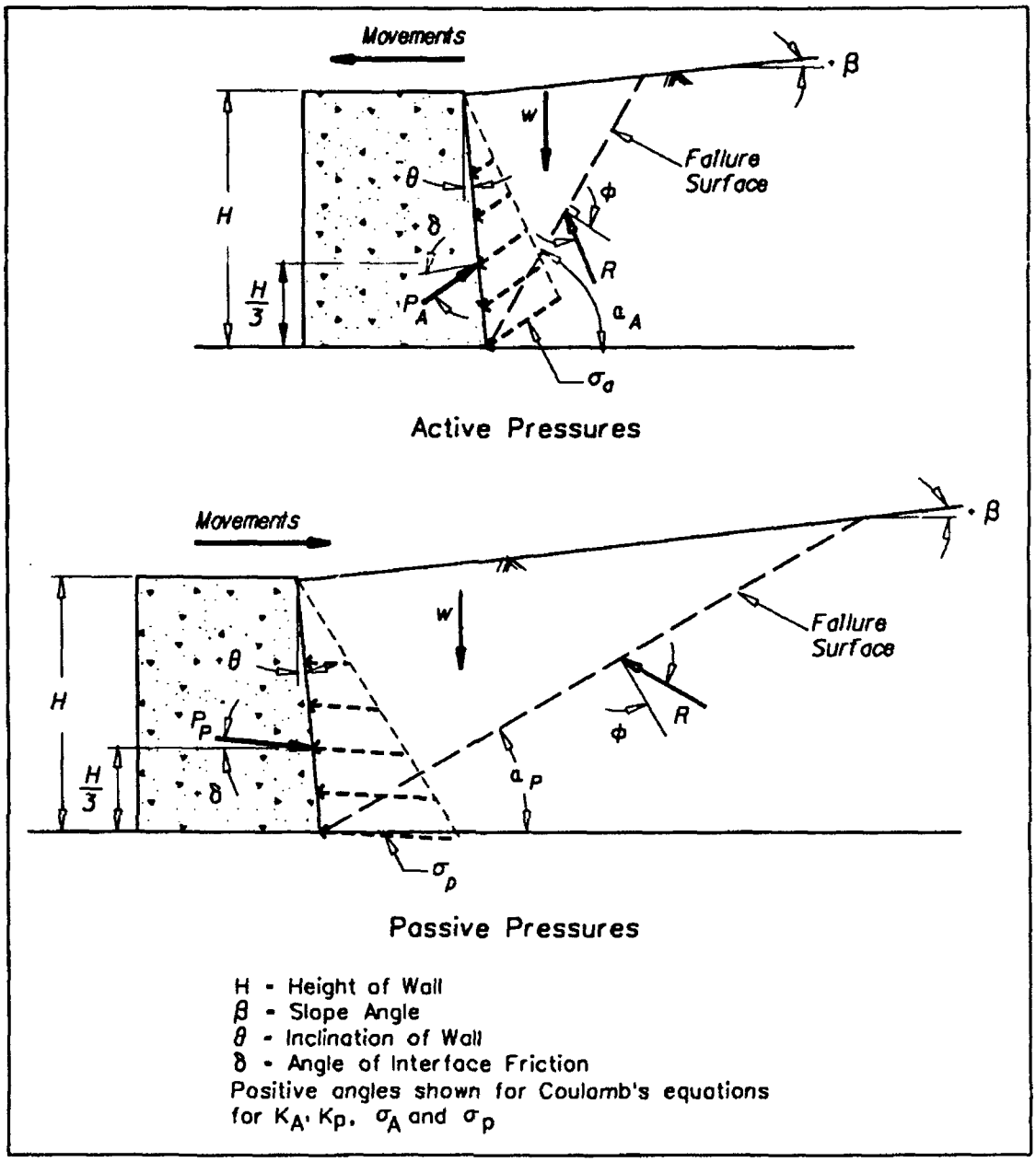

Figure 3.4 Coulomb active and passive earth pressures for inclined backfills and inclined walls

One widely quoted reference for effective angles of friction along interfaces between various types of materials, δ, is Table 2. Potyondy (1961) and Peterson et. al. (1976) also provide recommendations for δ values from static direct shear test results.

This procedure is illustrated in example 3 at the end of this chapter.

3.3.2 Coulomb Active Pressures - Hydrostatic Water Table Within Backfill and Surcharge

The distribution of Coulomb active earth pressures for a partially submerged wall retaining a frictional backfill and supporting a uniform surcharge, q, is shown in Figure 3.5. With a hydrostatic water table at height H_w above the base of the wall, the resulting pressures acting along the back of the wall are equal to the sum of (1) the thrust of the soil skeleton as a result of its unit weight, (2) the thrust of the soil skeleton as a result of the surcharge, q, and (3) the thrust of the pore water. The effective weight of the backfill, σ'_{wt}, above the water table is equal to

$$\sigma'_{wt} = \gamma_t \cdot z \tag{18}$$

and below the water table, σ'_{wt} is equal to

$$\sigma'_{wt} = \gamma_t \cdot (H - H_w) + \gamma' \cdot [z - (H - H_w)]. \tag{19}$$

where γ' is the effective unit weight at depth z. For hydrostatic pore water pressures, γ' is equal to the buoyant unit weight, γ_b.
The buoyant unit weight, γ_b, is equal to

$$\gamma_b = \gamma_t - \gamma_w. \tag{20}$$

σ_a is equal to the sum of the thrust of the soil skeleton as a result of its unit weight and the thrust of the soil skeleton as a result of the surcharge,

$$\sigma_a = (\sigma'_{wt} + q) \cdot K_A \tag{21}$$

and is inclined at an angle δ from the normal to the back of the wall. K_A is computed using Equation 16 for a level backfill ($\beta = 0$) and a vertical wall face ($\theta = 0$). The hydrostatic water pressures are equal to

$$u = \gamma_w \cdot [z - (H - H_w)] \tag{22}$$

and is normal to the back of the wall. The total thrust on the wall, P, is equal to the sum of the equivalent forces for the three pressure distributions. Due to the shape of the three pressure distributions, its point of action is higher up the back of the wall than one-third H above the heel. The orientation of the failure surface is not affected by the hydrostatic water pressures and is calculated using Equation 17.

Table 2. Ultimate Friction Factors for Dissimilar Materials
From NAVFAC DM-7.2

Interface Materials	Friction Factor, tan δ	Friction angle, δ degrees
Mass concrete on the following foundation materials:		
Clean sound rock.....	0.70	35
Clean gravel, gravel-sand mixtures, coarse sand...	0.55 to 0.60	29 to 31
Clean fine to medium sand, silty medium to coarse sand, silty or clayey gravel.....	0.45 to 0.55	24 to 29
Clean fine sand, silty or clayey fine to medium sand.....	0.35 to 0.45	19 to 24
Fine sandy silt, nonplastic silt.....	0.30 to 0.35	17 to 19
Very stiff and hard residual or preconsolidated clay.....	0.40 to 0.50	22 to 26
Medium stiff and stiff clay and silty clay.....	0.30 to 0.35	17 to 19
(Masonry on foundation materials has same friction factors.)		
Steel sheet piles against the following soils:		
Clean gravel, gravel-sand mixtures, well-graded rock fill with spalls.....	0.40	22
Clean sand, silty sand-gravel mixture, single size hard rock fill.....	0.30	17
Silty sand, gravel or sand mixed with silt or clay	0.25	14
Fine sandy silt, nonplastic silt.....	0.20	11
Formed concrete or concrete sheet piling against the following soils:		
Clean gravel, gravel-sand mixture, well-graded rock fill with spalls.....	0.40 to 0.50	22 to 26
Clean sand, silty sand-gravel mixture, single size hard rock fill.....	0.30 to 0.40	17 to 22
Silty sand, gravel or sand mixed with silt or clay	0.30	17
Fine sandy silt, nonplastic silt.....	0.25	14
Various structural materials:		
Masonry on masonry, igneous and metamorphic rocks:		
Dressed soft rock on dressed soft rock.....	0.70	35
Dressed hard rock on dressed soft rock.....	0.65	33
Dressed hard rock on dressed hard rock.....	0.55	29
Masonry on wood (cross grain).....	0.50	26
Steel on steel at sheet pile interlocks.....	0.30	17

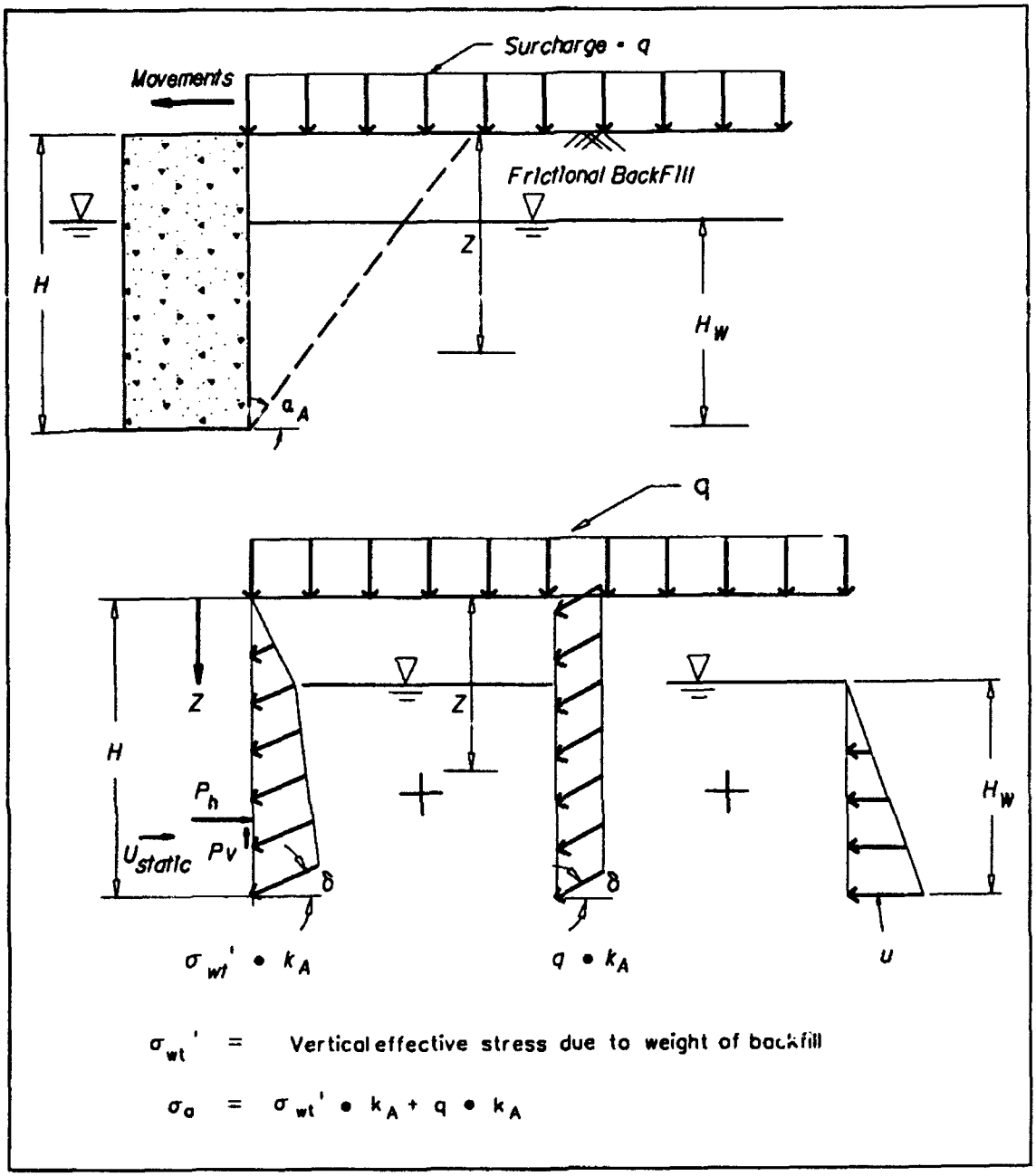

Figure 3.5 Coulomb active earth pressures for a partially submerged backfill and a uniform surcharge

The equation for σ_a of a soil whose shear strength is defined in terms of the effective strength parameters c and ϕ would be equal to

$$\sigma_a = (\sigma'_{wt} + q) \cdot K_A - 2c\sqrt{K_A} \tag{23}$$

and inclined at an angle δ from the normal to the back of the wall.

3.3.3 Coulomb Active Pressures - Steady State Seepage Within Backfill

This section summarizes the equations for determining the Coulomb active earth pressure forces and pore water pressures acting on the back of a wall retaining a drained backfill that is subjected to steady state flow. Figure 3.6 shows a wall with a vertical face retaining a level backfill, supporting a uniform surcharge load, q, and subjected to a constant water infiltration. The wall has a drainage system consisting of a gravel drain below the sand backfill, with weep holes through the wall. Steady state flow may develop during a rainstorm of sufficient intensity and duration. The resulting flownet is shown in Figure 3.6, consisting of vertical flow lines and horizontal equipotential lines, assuming the drain has sufficient permeability and thickness to be free draining (i.e. with zero pressure head within the drain). Adjacent to the back of the wall, the flow net has five head drops. With the datum at the base of the wall, the total head at the top of the backfill is equal to the height of the wall, H, and a total head is equal to zero at the weep holes. The drop in total head between each of the five equipotential lines is equal to H/5. Neglecting the velocity head, the total head, h, is equal to

$$h = h_e + h_p \tag{24}$$

where h_e is the elevation head, and h_p is the pressure head equal to

$$h_p = \frac{u}{\gamma_w}. \tag{25}$$

With the total head equal to the elevation head for each of the equipotential lines, h_p and the pore water pressure, u, are equal to zero. The seepage gradient, i, at any point in the backfill is equal to

$$i = \frac{\Delta h}{\Delta l} \tag{26}$$

where Δh is the change in total head and Δl the length of the flow path over which the incremental head drop occurs. With horizontal equipotential lines, the flow is vertical and directed downward ($i_y = +i$). For steady state seepage conditions, the effective unit weight is equal to

$$\gamma' = \gamma_b \pm \gamma_w \cdot i_y. \tag{27}$$

The seepage force is added to the buoyant unit weight when flow is downward and subtracted with upward flow. For the example shown in Figure 3.6 with i equal to positive unity and directed downward, γ' is equal to the total unit weight, γ_t. The effective weight of the backfill, σ'_{wt}, is equal to

$$\sigma'_{wt} = \gamma' \cdot z = (\gamma_b + \gamma_w) \cdot z = \gamma_t \cdot z \tag{28}$$

An alternative procedure for calculating σ'_{wt} is using the total overburden pressure, σ_{wt}, and pore water pressures, u. By Equation 7, we see that with

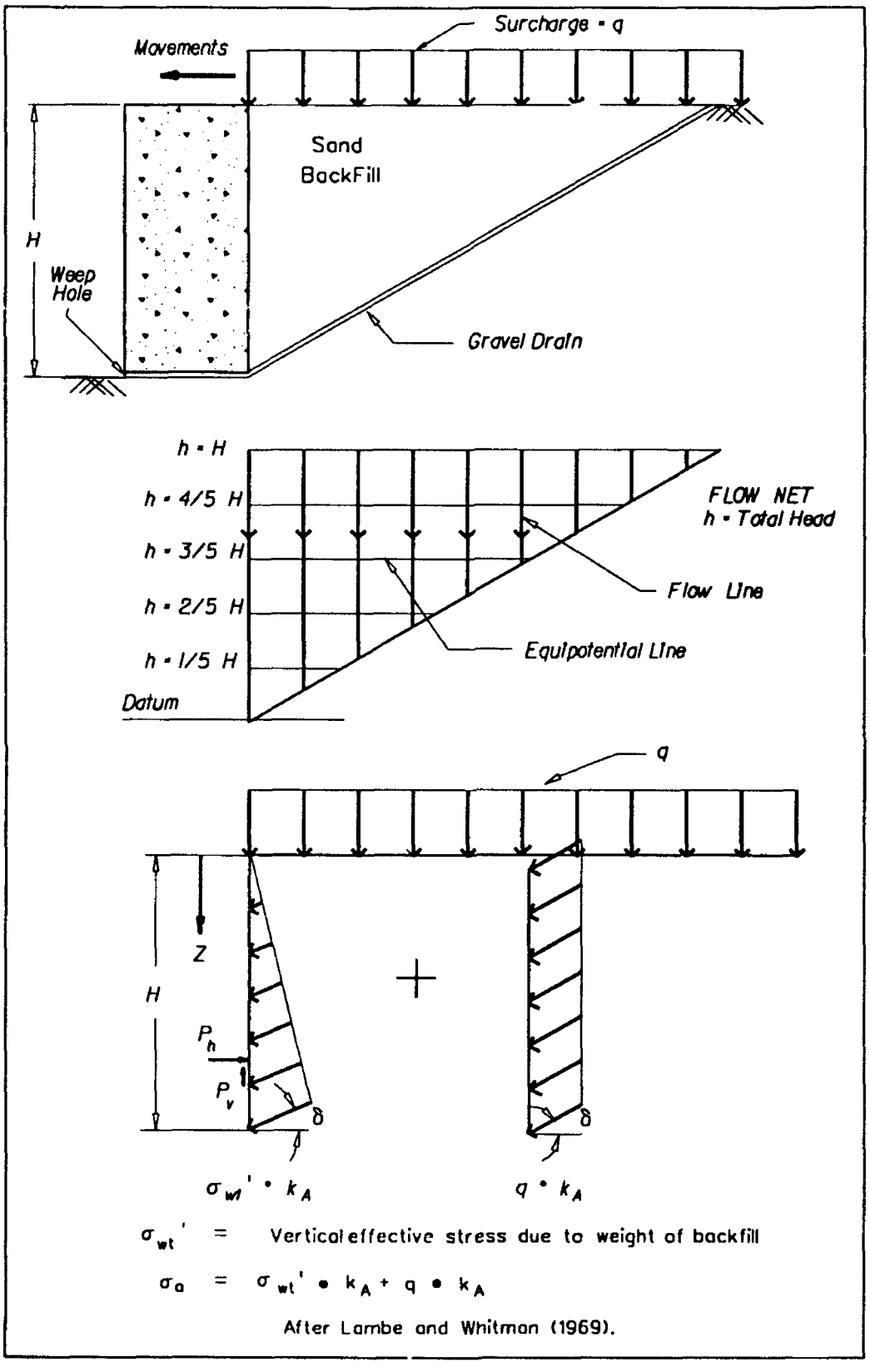

Figure 3.6 Coulomb active earth pressures for a backfill subjected to steady state flow

the pore water pressure equal to zero, this procedure also results in the Equation 28 relationship ($\gamma' = \gamma_t$).

The resulting pressures acting along the back of the wall are equal to the sum of (1) the thrust of the soil skeleton as a result of its unit weight and (2) the thrust of the soil skeleton as a result of the surcharge. The pore water pressure acting on the wall is equal to zero, with horizontal equipotential lines and the total head equal to the elevation head within the drained backfill. In this case, the effective weight is equal to the total weight. σ_a is computed using Equation 21, inclined at an angle δ from the normal to the back of the wall and equal to the sum of the pressures shown in Figure 3.6. K_A is computed using Equation 16, and α_A is computed using Equation 17. Downward vertical steady state seepage in a backfill results in nearly the same earth pressures as are computed in the case of a dry backfill.

In backfills where there is a lateral component to the seepage force or the gradients vary throughout the backfill, the trial wedge procedure, in conjunction with a flow net, must be used to compute P_A and α_A. Spacial variations in u with constant elevation will alter the location of the critical slip surface from the value given in Equation 17. The trial wedge procedure is also required to find the values for P_A and α_A when point loads or loads of finite width are placed on top of the backfill. An example using the trial wedge procedure for a retaining wall similar to that shown in Figure 3.6 but with a vertical drain along the back of the wall is described in Section 3.4.

3.3.4 Coulomb Theory - Passive Earth Pressures

The forces and stresses corresponding to the passive states of stress are shown in Figure 3.4 for a wall with a face inclined at angle $+\theta$ from vertical, and retaining a frictional backfill inclined at angle $+\beta$. The effects of surcharge and groundwater pressures are not included in this figure. To develop passive earth pressures, the wall moves towards the backfill, with the resulting displacements sufficient to mobilize fully the shear resistance along the linear slip plane. Coulomb's theory allows for a shear force along the back of the walls that is due to the upward movement of the backfill as the wall moves towards the backfill. The passive earth pressure force P_P is computed using Equation 13 and oriented at an angle δ to the normal along the back of the wall at a height equal to H/3 above the heel of the wall, as shown in Figure 3.4. The shear component of P_P acts downward on the soil wedge due to the upward movement of the soil wedge along the face of the wall. This is the reverse of the situation for the shear component of P_A. K_P is equal to

$$K_P = \frac{\cos^2(\phi + \theta)}{\cos^2\theta \cos(\delta - \theta)\left[1 - \sqrt{\frac{\sin(\phi + \delta)\sin(\phi + \beta)}{\cos(\delta - \theta)\cos(\beta - \theta)}}\right]^2} \qquad (29)$$

for frictional backfills. The passive earth pressure, σ_p, along the back of the wall at depth z is computed using Equation 15 and oriented at an angle δ to the normal along the back of the wall. The variation in σ_p is assumed linear with depth for a dry backfill, as shown in Figure 3.4. The planar slip surface extends upwards from the heel of the wall through the backfill and is inclined at an angle α_P from horizontal. α_P is equal to

$$\alpha_P = -\phi + \tan^{-1}\left[\frac{\tan(\phi + \beta) + c_3}{c_4}\right] \tag{30}$$

where

$$c_3 = \sqrt{[\tan(\phi + \beta)][\tan(\phi + \beta) + \cot(\phi + \theta)][1 + \tan(\delta - \theta)\cot(\phi + \theta)]}$$

and

$$c_4 = 1 + \left[[\tan(\delta - \theta)] \cdot [\tan(\phi + \beta) + \cot(\phi + \theta)]\right].$$

This procedure is illustrated in example 4 at the end of this chapter.

3.3.4.1 Accuracy of Coulomb's Theory for Passive Earth Pressure Coefficients

Equations 29 and 30 provide reasonable estimates for K_P and the orientation of the slip plane, α_P, so long as δ is restricted to values which are less than $\phi/2$. Coulomb's relationship overestimates the value for K_P when δ is greater than $\phi/2$. The large shear component of P_P introduces significant curvature in the failure surface. The Coulomb procedure, however, restricts the theoretical slip surface to a plane. When δ is greater than $\phi/2$, the value for K_P must be computed using a method of analysis which uses a curved failure surface to obtained valid values. Section 3.5 presents a graphical tabulation of K_P values obtained by using a log spiral failure surface. Figures 3.7 and 3.8 show the variation in the values for K_P with friction angle, computed using Coulomb's equation for K_p based on a planer failure surface versus a log spiral failure surface analysis.

3.4 Earth Pressures Computed Using the Trial Wedge Procedure

The trial wedge procedure of analysis is used to calculate the earth pressure forces acting on walls when the backfill supports point loads or loads of finite width or when there is seepage within the backfill. The procedure involves the solution of the equations of equilibrium for a series of trial wedges within the backfill for the resulting earth pressure force on the back of the wall. When applying this procedure to active earth pressure problems, the shear strength along the trial slip plane is assumed to be fully mobilized. The active earth pressure force is equal to the largest value for the earth pressure force acting on the wall obtained from the series of trial wedge solutions. The steps involved in the trial wedge procedure are described using the retaining wall problem shown in Figure 3.9, a problem originally solved by Terzaghi (1943) and described by Lambe and Whitman (1969). A 20 feet high wall retains a saturated sand backfill with ϕ equal to 30 degrees and δ equal to 30 degrees. The backfill is drained by a vertical gravel drain along the back of the wall, with weep holes along its base. In this problem, a heavy rainfall is presumed to have resulted in steady state seepage within the backfill. The solution for the active earth pressure force

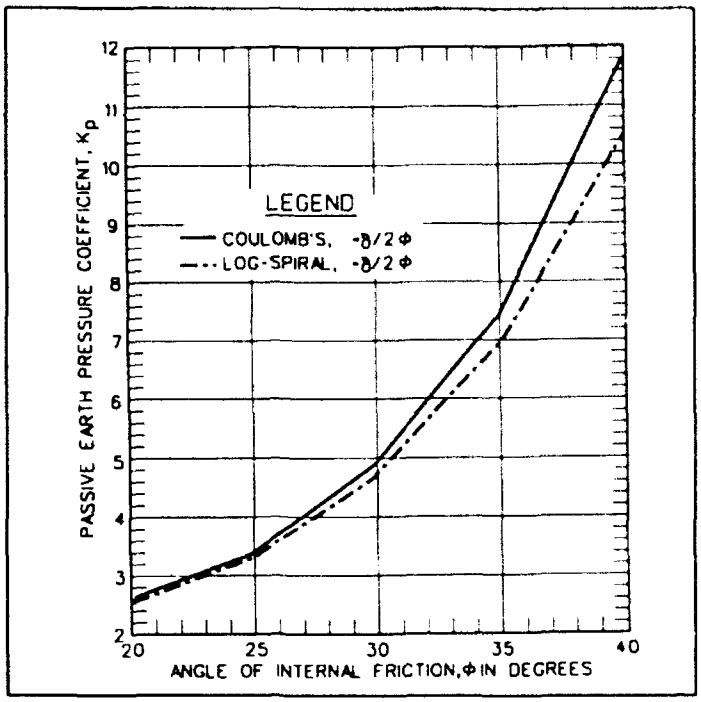

Figure 3.7 Coulomb and log-spiral passive earth pressure coefficients with $\delta = \phi/2$ - vertical wall and level backfill

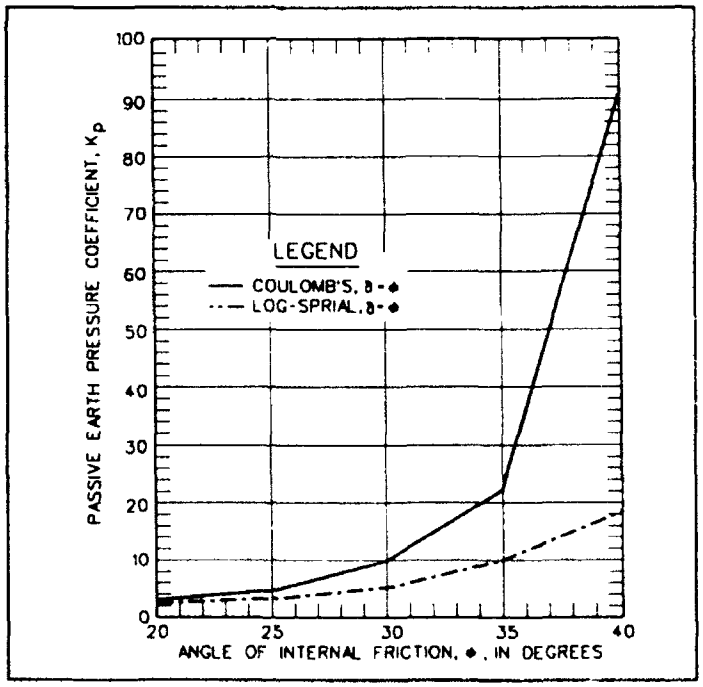

Figure 3.8 Coulomb and log-spiral passive earth pressure coefficients with $\delta = \phi$ - vertical wall and level backfill

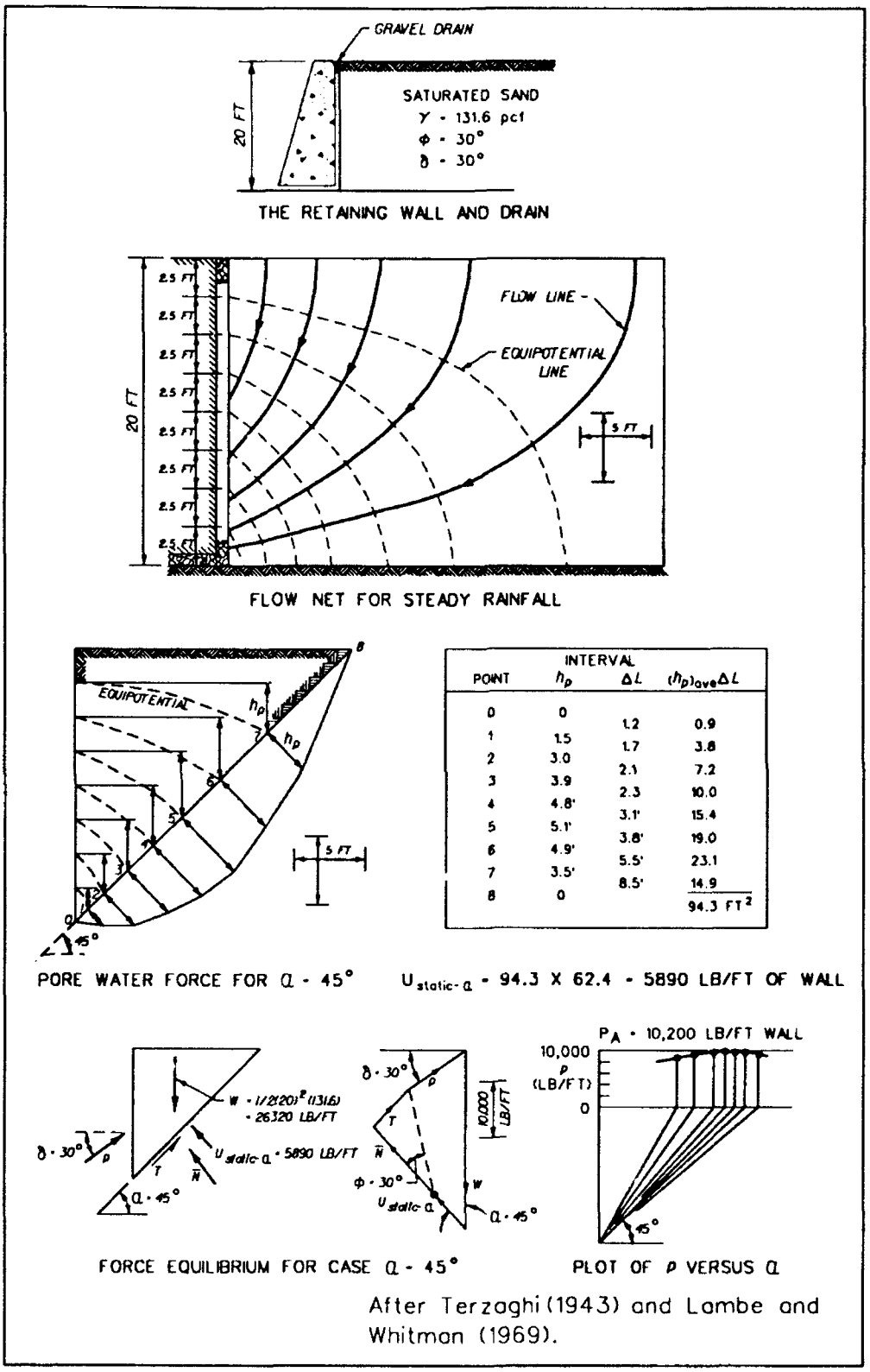

POINT	h_p	INTERVAL ΔL	$(h_p)_{ave}\Delta L$
0	0		
		1.2	0.9
1	1.5		
		1.7	3.8
2	3.0		
		2.1	7.2
3	3.9		
		2.3	10.0
4	4.8'		
		3.1'	15.4
5	5.1'		
		3.8'	19.0
6	4.9'		
		5.5'	23.1
7	3.5'		
		8.5'	14.9
8	0		
			94.3 FT²

Figure 3.9 Example of trial wedge procedure

on the back of the wall using the trial wedge procedure, is outlined in the following eight steps.

(1) Determine the variation in pore water pressures within the backfill. In this example the flow net for steady state seepage is constructed graphically and is shown in Figure 3.9.

(2) Assume an inclination for the trial slip surface, α, defining the soil wedge to be analyzed.

(3) Assume sufficient displacement so the shear strength of the sand is fully mobilized along the plane of slip, resulting in active earth pressures. For this condition, the shear force, T, required for equilibrium along the base of the soil wedge is equal to the ultimate shear strength force along the slip surface.

$$T = \bar{N} \tan\phi \tag{31}$$

(4) Calculate the total weight of the soil within the trial wedge, W.

(5) Calculate the variation in pore water pressure along the trial slip surface. Using the flow net, the pore water pressure is computed at a point by first solving for h_p, using Equation 24, and then computing u using Equation 25. An example of the distribution in u along the trial slip surface for α = 45 degrees is shown in Figure 3.9.

(6) Calculate the pore water pressure force , $U_{static-\alpha}$, acting normal to the trial slip surface, inclined at angle α to the horizontal. $U_{static-\alpha}$ is the resultant of the pore water pressures calculated in step (5).

(7) Analyze the trial wedge for the corresponding effective earth pressure force, P, acting at an angle δ = 30 degrees to the normal to the back of the wall. Using the equations of equilibrium ($\sum F_x = 0$ and $\sum F_y = 0$), the resulting equation for the unknown force P is equal to

$$P = \frac{(W - U_{static-\alpha}\cos\alpha)\tan(\alpha - \phi) + U_{static-\alpha}\sin\alpha}{\sin\delta\tan(\alpha - \phi) + \cos\delta}. \tag{32}$$

Note that because of the presence of the free flowing drain along the back of the wall in which the total head equals the elevation head, the pore water pressures are equal to zero along the back of the wall.

(8) Repeat steps 2 through 7 for other trial slip surfaces until the largest value for P is computed, as shown in Figure 3.9. The slip surface that maximizes the value for P corresponds to the critical slip surface, $\alpha_A = \alpha$ and $P_A = P$. In this case, α_A = 45 degrees, and P_A = 10,200 pounds per foot of wall and acts at δ = 30 degrees from the normal to the back of the wall.

Hydrostatic Water Pressures:

Consider the possibility is that the drain shown in Figure 3.9 does not function as intended and hydrostatic pore water pressures develop along the back of the wall as shown in Figure 3.10. For each slip surface analyzed

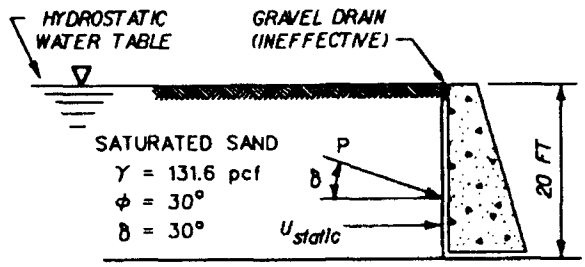

RETAINING WALL WITH HYDROSTATIC WATER TABLE AT TOP OF BACKFILL

FOR HYDROSTATIC WATER TABLE

$$U_{static} = \tfrac{1}{2}\,\gamma_{\omega}\,H^2$$

$$= \tfrac{1}{2}(62.4)(20)^2 = 12{,}480 \text{ LB/FT OF WALL}$$

NORMAL TO SLIP PLANE $\alpha = 54.3°$

(Refer to Figure A.2)

$$U_{static-\alpha} = U_{static} \cdot \frac{1}{\sin 54.3°}$$

$$U_{static-\alpha} = 15{,}368 \text{ LB/FT OF WALL}$$

PLOT OF P VERSUS α

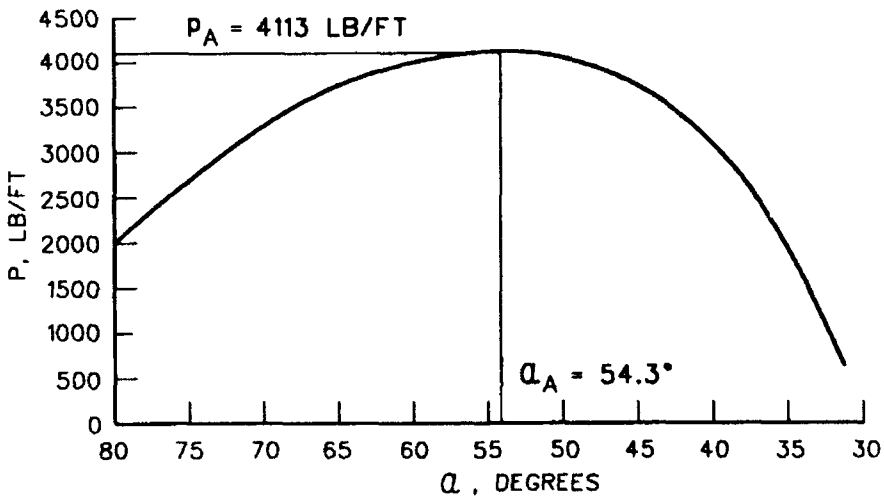

Figure 3.10 Example of trail wedge procedure, hydrostatic water table

using the trial wedge method the effective force P, acting at angle δ to the normal for the wall, is given in section A.2 of Appendix A as

$$P = \frac{[\ W - U_{static-\alpha}\cos\alpha\ ]\tan(\ \alpha - \phi'\ )}{\cos\delta + \sin\delta\tan(\ \alpha - \phi'\ )} \qquad \text{(A-21)}$$

The hydrostatic water pressure forces acting normal to the slip surface and normal to the back of the wall are $U_{static-\alpha}$ and U_{static}, respectively, and are computed following the procedures described in section A.2.1 and A.2.2 of Appendix A. Otherwise, the solution of the trial wedge analysis to compute the active earth pressure force follows the same eight steps described previously.

Using the trial wedge procedure for the problem shown in Figure 3.10, the wedge that maximizes the value for P corresponds to the critical slip surface, α_A = 54.34 degrees, and P_A = 4,113 pounds per foot of wall which acts at δ = 30 degrees from the normal to the back of the wall. Although P_A for the ineffective drain case (Figure 3.10) is 6,087 pounds per foot less than for the effective drain case (Figure 3.9), the total horizontal design load for the ineffective drain is larger by 7,208 pounds per foot of wall compared to the effective drain case due to the contribution of the water pressure force (U_{static} = 12,480 pounds per foot of wall).

A closed form solution exists for this example, as P_A may be calculated using Equation 7, with K_A computed using the Coulomb Equation 16. The corresponding critical slip surface α_A is given in Equation 17.

3.5 Active and Passive Earth Pressure Coefficients from Log Spiral Procedure

A logarithmic spiral failure surface may be used to determine the active and passive pressures against retaining structures when interface friction acts along the back of the wall.

Values for the active and passive earth pressure coefficients are presented in Figures 3.11 and 3.12 and Table 3. Figure 3.11 provides values for K_A and K_P for walls with inclined faces retaining horizontal backfills. Figure 3.12 provides values for K_A and K_P for walls with vertical faces retaining horizontal or inclined backfills. These figures and Table 3 were assembled from tables of K_A and K_P values given in Caquot and Kerisel (1948). Kerisel and Absi (1990) have also assembled tables of K_A and K_P values based on a log-spiral failure surface. The sign convention for the angles are shown in the insert figures in Figures 3.11 and 3.12. Note that the sign convention for δ is determined by the orientation of the shear stress acting on the wedge of the soil. δ is positive when the shear is acting upward on the soil wedge, the usual case for active pressures, and negative if the shear acts downward on the soil mass, the usual case for passive pressures. The values for K_A and K_P from these figures and this table are accurate for all values of δ less than or equal to ϕ.

These procedures are illustrated in examples 5 and 6 at the end of this chapter.

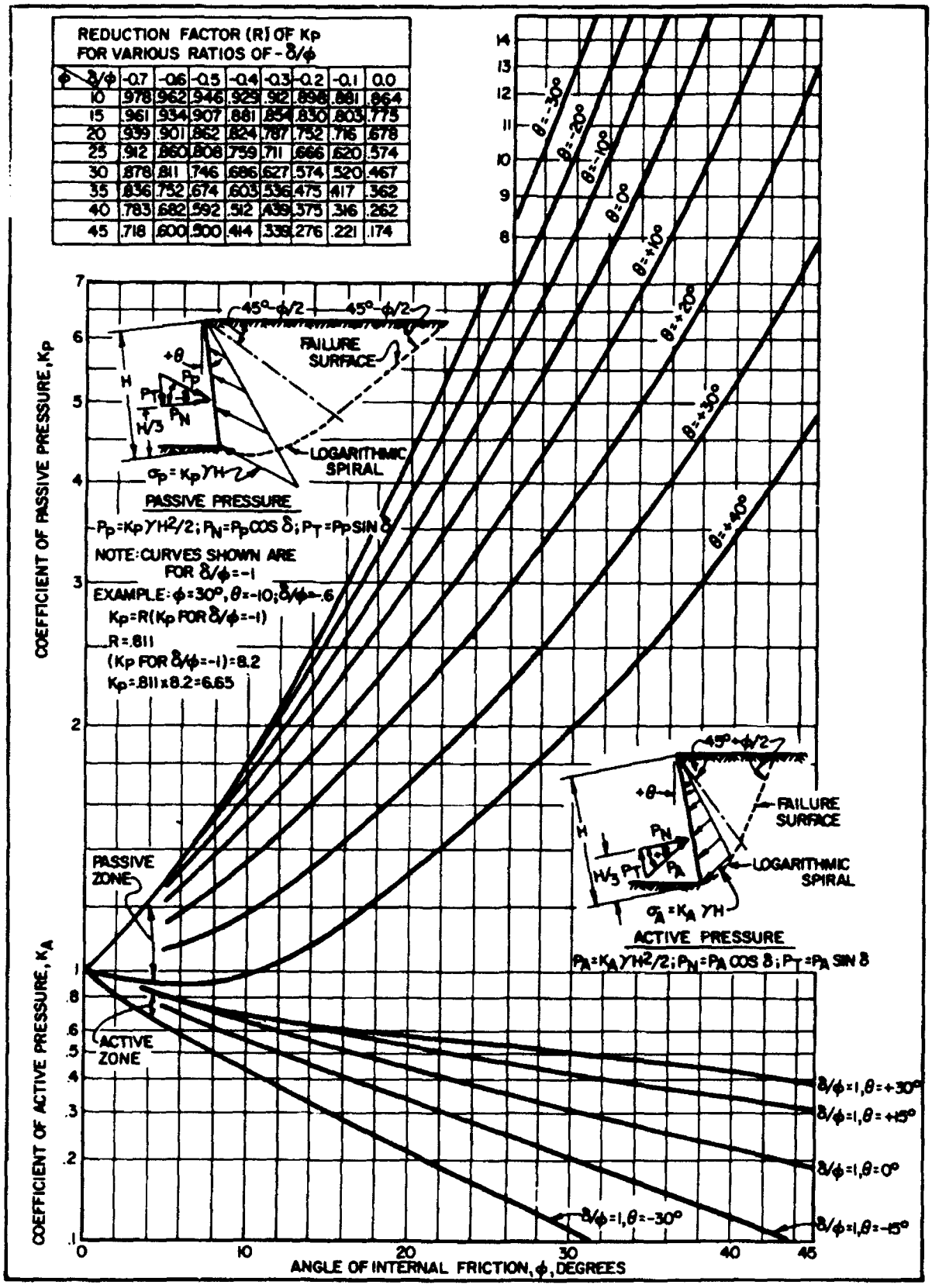

Figure 3.11 Active and passive earth pressure coefficients with wall friction - sloping wall

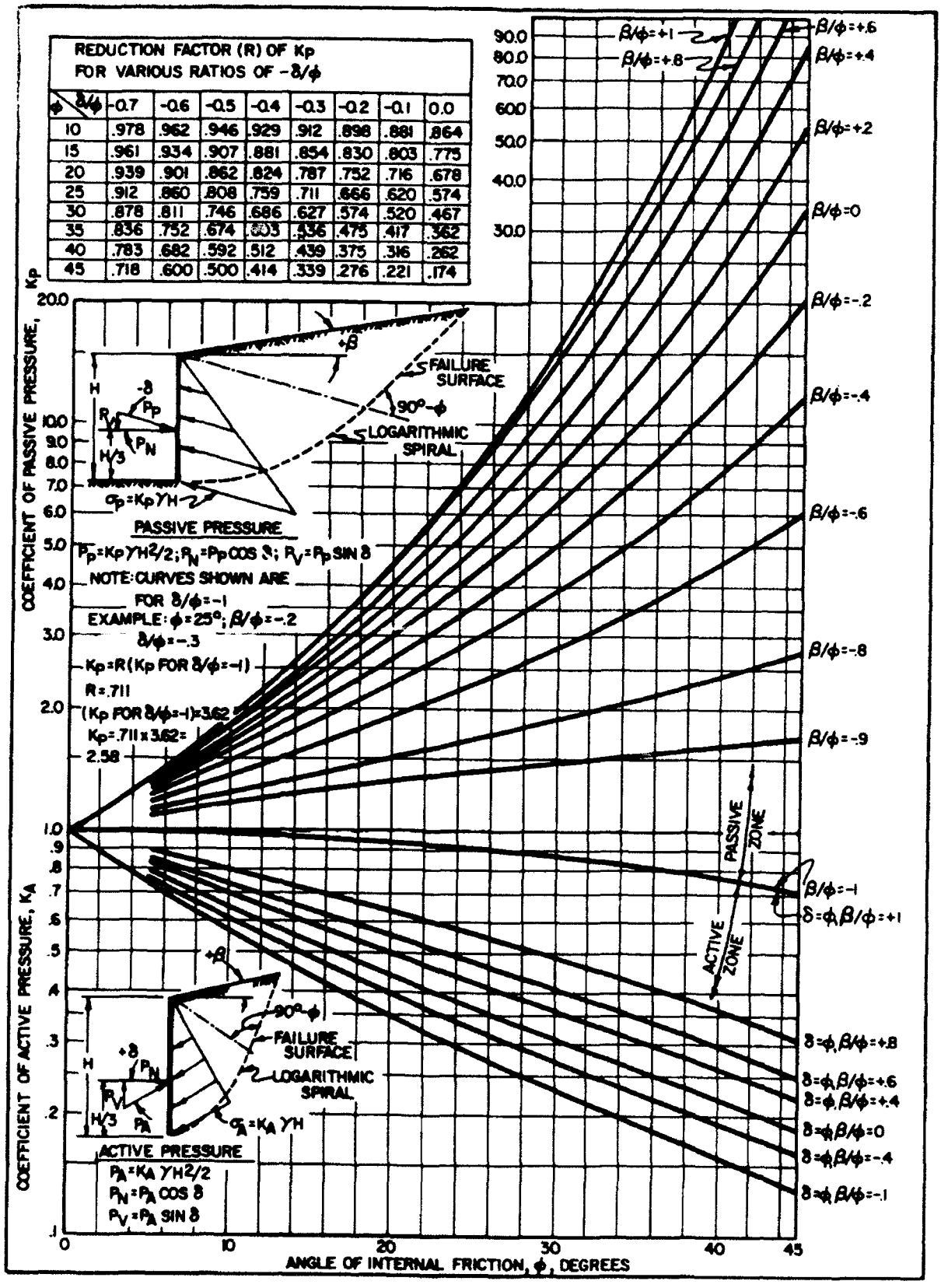

REDUCTION FACTOR (R) OF Kp FOR VARIOUS RATIOS OF $-\delta/\phi$

ϕ \ δ/ϕ	-0.7	-0.6	-0.5	-0.4	-0.3	-0.2	-0.1	0.0
10	.978	.962	.946	.929	.912	.898	.881	.864
15	.961	.934	.907	.881	.854	.830	.803	.775
20	.939	.901	.862	.824	.787	.752	.716	.678
25	.912	.860	.808	.759	.711	.666	.620	.574
30	.878	.811	.746	.686	.627	.574	.520	.467
35	.836	.752	.674	.603	.536	.475	.417	.362
40	.783	.682	.592	.512	.439	.375	.316	.262
45	.718	.600	.500	.414	.339	.276	.221	.174

Figure 3.12 Active and passive earth pressure coefficients with wall friction - sloping backfill

Table 3 Values for K_A and K_p for Log-Spiral Failure Surface
After Caquot and Kerisel (1948)

K_A								
			ϕ					
δ	β	θ	20°	25°	30°	35°	40°	45°
0°	-15°	-10°	0.37	0.30	0.24	0.19	0.14	0.11
		0°	0.42	0.35	0.29	0.24	0.19	0.16
		10°	0.45	0.39	0.34	0.29	0.24	0.21
	0°	-10°	0.42	0.34	0.27	0.21	0.16	0.12
		0°	0.49	0.41	0.33	0.27	0.22	0.17
		10°	0.55	0.47	0.40	0.34	0.28	0.24
	15°	-10°	0.55	0.41	0.32	0.23	0.17	0.13
		0°	0.65	0.51	0.41	0.32	0.25	0.20
		10°	0.75	0.60	0.49	0.41	0.34	0.28
ϕ	-15°	-10°	0.31	0.26	0.21	0.17	0.14	0.11
		0°	0.37	0.31	0.26	0.23	0.19	0.17
		10°	0.41	0.36	0.31	0.27	0.25	0.23
	0°	-10°	0.37	0.30	0.24	0.19	0.15	0.12
		0°	0.44	0.37	0.30	0.26	0.22	0.19
		10°	0.50	0.43	0.38	0.33	0.30	0.26
	15°	-10°	0.50	0.37	0.29	0.22	0.17	0.14
		0°	0.61	0.48	0.37	0.32	0.25	0.21
		10	0.72	0.58	0.46	0.42	0.35	0.31

K_p								
			ϕ					
δ	β	θ	20°	25°	30°	35°	40°	45°
0°	-15°	-10°	1.32	1.66	2.05	2.52	3.09	3.95
		0°	1.09	1.33	1.56	1.82	2.09	2.48
		10°	0.87	1.03	1.17	1.30	1.33	1.54
	0°	-10°	2.33	2.96	3.82	5.00	6.68	9.20
		0°	2.04	2.46	3.00	3.69	4.59	5.83
		10°	1.74	1.89	2.33	2.70	3.14	3.69
	15°	-10°	3.36	4.56	6.30	8.98	12.2	20.0
		0°	2.99	3.86	5.04	6.72	10.4	12.8
		10°	2.63	3.23	3.97	4.98	6.37	8.2
$-\phi$	-15°	-10°	1.95	2.90	4.39	6.97	11.8	22.7
		0°	1.62	2.31	3.35	5.04	7.99	14.3
		10°	1.29	1.79	2.50	3.58	5.09	8.86
	0°	-10°	3.45	5.17	8.17	13.8	25.5	52.9
		0°	3.01	4.29	6.42	10.2	17.5	33.5
		10°	2.57	3.50	4.98	7.47	12.0	21.2
	15°	-10°	4.95	7.95	13.5	24.8	50.4	11.5
		0°	4.42	6.72	10.8	18.6	39.6	73.6
		10	3.88	5.62	8.51	13.8	24.3	46.9

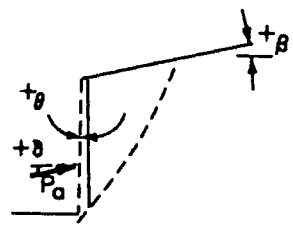

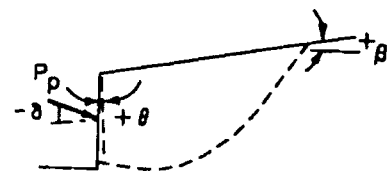

3.6 Surface Loadings

There are three approaches used to approximate the additional lateral earth pressures on walls due to surface loadings; (1) the wedge method of analysis, (2) elastic solutions, and (3) finite element analyses.

Trial wedge analyses, as described in Section 3.4, may be performed to account for uniform and irregular surface load distributions for those walls whose movements satisfy the criteria listed in Table 1. The wedge analysis described in Section 3.4 is modified by including that portion of the surface loading between the back of the wall and the intersection of the trial slip surface and the backfill surface in the force equilibrium calculation for each wedge analyzed. The resulting relationship for a vertical wall retaining a partially submerged backfill (for a hydrostatic water table) is given in section A.2.8 of Appendix A. The difficult part of the problem is to determine the point of action of this force along the back of the wall. The point of action of the resulting earth pressure force for an infinitely long line load parallel to the wall may be computed using the simplified procedure described in Article 31 of Terzaghi and Peck (1967).

Elastic solutions of the type shown in Figure 3.13 can be used to calculate the increase in the horizontal earth pressure, σ_x, using either a solution for a point load, a line load or a strip load acting on the surface of an elastic mass, i.e. the soil backfill. Most applications of elastic solutions for surface loadings to earth retaining structures assume the wall to be unyielding (i.e. zero movement horizontally) and zero shear stress induced along the soil to wall interface (Clough and Duncan 1991). To account for the zero wall movements along the soil to wall interface, the computed value for σ_x using elastic theory is doubled. This is equivalent to applying an imaginary load of equal magnitude equidistant from the soil to wall interface so as to cancel the deflections at the interface as shown in Figure 3.14. Experiments by Spangler (1938) and Terzaghi (1954) have validated this procedure of doubling the σ_x values computed using the Boussinesq solution for point loads.

The finite element method of analysis has been applied to a variety of earth retaining structures and used to calculate stresses and movements for problems involving a wide variety of boundary and loading conditions. Some key aspects of the application of the finite element method in the analysis of U-frame locks, gravity walls, and basement walls are summarized in Ebeling (1990).

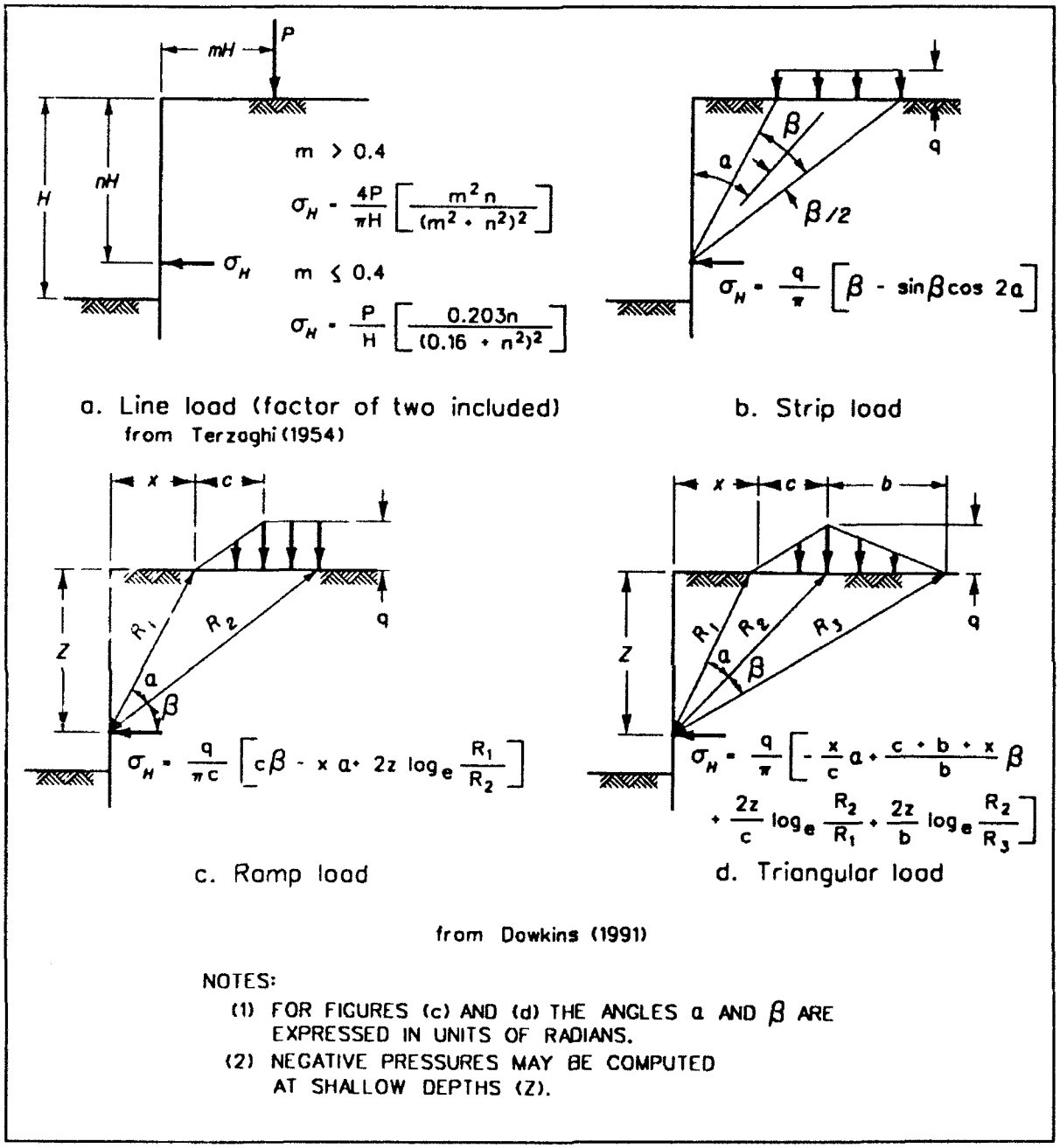

Figure 3.13 Theory of elasticity equations for pressures on wall due to surcharge loads

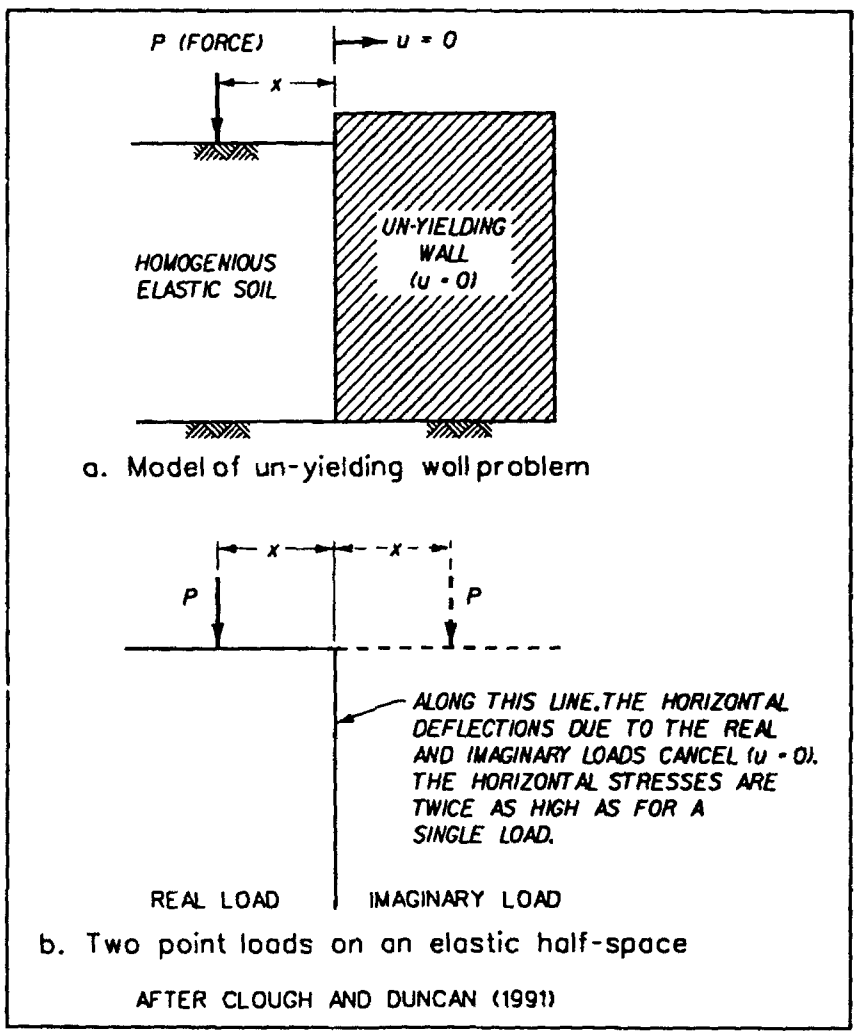

Figure 3.14 Use of an imaginary load to enforce a zero-displacement condition at the soil-structure interface

CHAPTER 3 - EXAMPLES

Contents

Example Problems 1 through 6.

Commentary

The following examples illustrate the procedures described in Chapter 3. The results of the computations shown are rounded for ease of checking calculations and not to the appropriate number of significant figures. Additionally, the values assigned to variables in these problems were selected for ease of computations.

Example No. 1 Reference Section: 3.2.1

For a wall of height H = 20 ft retaining a dry level cohesionless backfill with ϕ' = 30 degrees and δ = 0 degrees, compute K_A, α_A, and P_A.

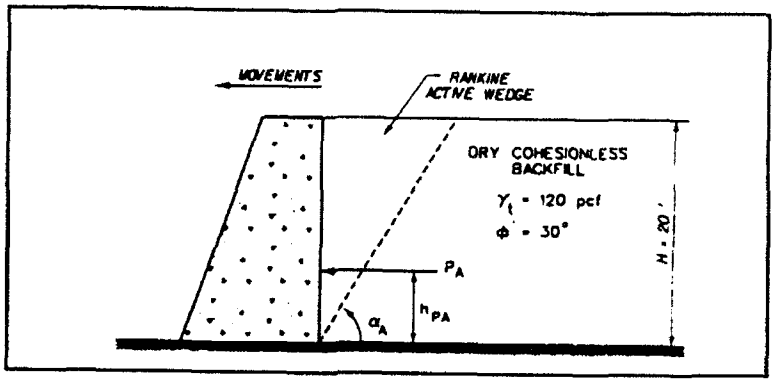

$$K_A = \tan^2(45° - 30°/2) \qquad \text{(by eq 5)}$$

$K_A = 1/3$

$$P_A = \frac{1}{3} \cdot \frac{1}{2}(120 \text{ pcf})(20 \text{ ft})^2 \qquad \text{(by eq 7)}$$

P_A = 8,000 lb per ft of wall

$$\alpha_A = 45° + 30°/2 \qquad \text{(by eq 6)}$$

α_A = 60° from the horizontal

h_{PA} = H/3 = 6.67 ft

Example No. 2 Reference Section: 3.2.2

For a wall of height H = 20 ft retaining a dry level cohesionless backfill with ϕ' = 30 degrees and δ = 0 degrees, compute K_P, α_P, and P_P.

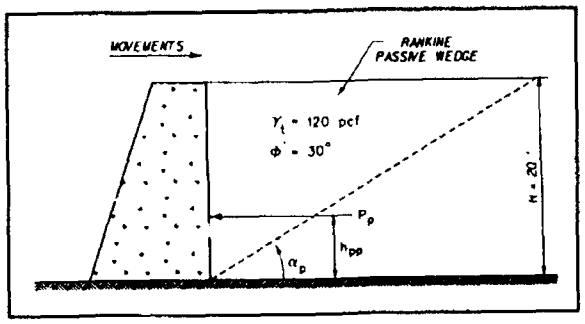

$$K_p = \tan^2(45° + 30°/2) \qquad \text{(by eq 11)}$$

K_P = 3.0

$$P_P = 3.0 \cdot \frac{1}{2}(120 \text{ pcf})(20')^2 \qquad \text{(by eq 13)}$$

P_P = 72,000 lb per ft of wall

$$\alpha_P = 45° - 30°/2 \qquad \text{(by eq 12)}$$

α_P = 30° from the horizontal

h_{PP} = H/3 = 6.67 ft

Example No. 3 Reference Section: 3.3.1

For a wall of height H = 20′ retaining a dry cohesionless backfill with ϕ' = 30 degrees, δ = 3 degrees, β = 6 degrees, and θ = 0 degrees, compute K_A, α_A, and P_A.

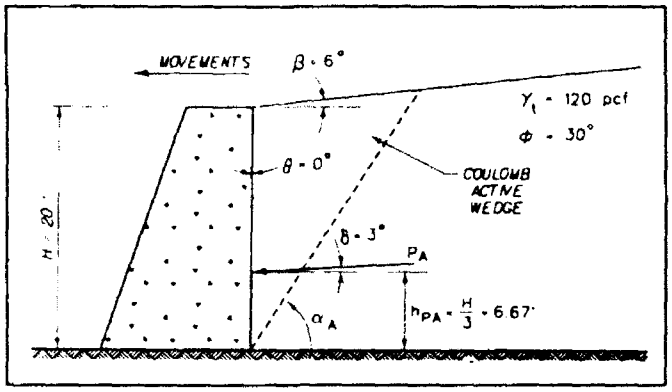

$$K_A = \frac{\cos^2(30-0)}{\cos^2(0)\cos(0+3)\left[1+\sqrt{\frac{\sin(30+3)\sin(30-6)}{\cos(3+0)\cos(6-0)}}\right]^2} \qquad \text{(by eq 16)}$$

$K_A = 0.3465$

$$P_A = 0.3465 \cdot \frac{1}{2}(120\ \text{pcf})(20')^2 \qquad \text{(by eq 7)}$$

P_A = 8316 lb per ft of wall

$$c_1 = \sqrt{[\tan(30-6)][\tan(30-6)+\cot(30)][1+\tan(3)\cot(30)]}$$

$c_1 = 1.0283$

$$c_2 = 1 + [[\tan(3)] \cdot [\tan(30-6)+\cot(30)]]$$

$c_2 = 1.11411$

$$\alpha_A = 30 + \tan^{-1}\left[\frac{-\tan(30-6)+1.0283}{1.11411}\right] \qquad \text{(by eq 17)}$$

α_A = 57.6° from the horizontal

Example No. 4 Reference Section: 3.3.4

For wall of height H = 20 ft retaining a dry cohesionless backfill with ϕ' = 30 degrees, δ = 3 degrees, β = 6 degrees, and θ = 0 degrees, compute K_P, α_P, and P_P.

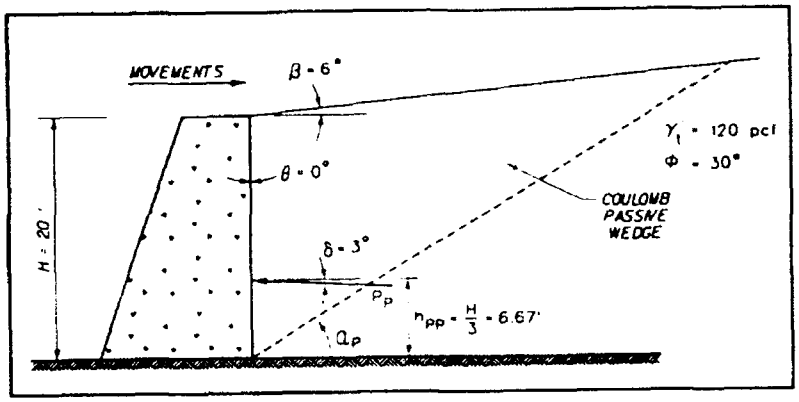

$$K_P = \frac{\cos^2(30+0)}{\cos^2(0)\cos(3-0)\left[1 - \sqrt{\frac{\sin(30+3)\ \sin(30+6)}{\cos(3-0)\ \cos(6-0)}}\right]^2} \qquad \text{(by eq 29)}$$

$K_P = 4.0196$

$$P_P = 4.0196 \cdot \frac{1}{2}(120\ \text{pcf})(20')^2 \qquad \text{(by eq 13)}$$

$P_P = 96{,}470$ lb per ft of wall

$$c_3 = \sqrt{[\tan(30+6)]\ [\tan(30+6) + \cot(30)][1 + \tan(3)\cot(30)]}$$

$c_3 = 1.3959$

$$c_4 = 1 + [[\tan(3)] \cdot [\tan(30+6) + \cot(30)]]$$

$c_4 = 1.1288$

$$\alpha_P = -30 + \tan^{-1}\left[\frac{\tan(30+6) + 1.3959}{1.1288}\right] \qquad \text{(by eq 30)}$$

$\alpha_P = 32.0°$ from the horizontal

Example No. 5 Reference Section: 3.4

For the Example No. 3 problem of a wall retaining a dry cohesionless backfill with $\phi' = 30$ degrees, $\delta = +3$ degrees, $\beta = +6$ degrees, and $\theta = 0$ degrees, compute K_A using the log spiral procedure of Figure 3.12. Compare this value with the K_A value computed in Example No. 3 using the Coulomb relationship.

$\delta/\phi = +0.1$ and $\beta/\phi = +0.2$

$K_A = 0.35$ from Figure 3.12 with $\beta/\phi = +0.2$ and using the curve for $\delta = \phi$.

This value for K_A agrees with the value computed using Coulomb's theory for active earth pressures in Example No. 3 ($K_A = 0.3465$).

Example No. 6 Reference Section: 3.4

For the Example No. 4 problem of a wall retaining a dry cohesionless backfill with ϕ = 30 degrees, δ = -3 degrees*, β = +6 degrees, and θ = 0 degrees, compute K_P. Compare this value with the K_P value computed in Example No. 4.

$$\delta/\phi = -0.1 \text{ and } \beta/\phi = +0.2$$

R (for δ/ϕ = -0.1) = 0.52 and K_P (for β/ϕ = +0.2) = 8 from Figure 3.12

$$\begin{aligned} K_P \text{ (for } \delta/\phi = -0.1) &= [R \text{ (for } \delta/\phi = -0.1)] \cdot [K_P \text{ (for } \beta/\phi = +0.2)] \\ &= 0.52 \cdot 8 \\ &= 4.16 \end{aligned}$$

The value for K_P is nearly the same as the value computed using Coulomb's theory for passive earth pressures in Example No. 4 (K_P = 4.0196) because $\delta < \phi/2$ (Section 3.3.4.1). The resultant force vector P_P acts in the same direction as shown in the Example No. 4 figure.

* Note the difference in sign for δ in the passive earth pressure solution using the Figure 3.12 log spiral solution procedure compared to that used in the Coulomb's solution, with sign convention as shown in Figure 3.4.

CHAPTER 4 DYNAMIC EARTH PRESSURES - YIELDING BACKFILLS

4.1 Introduction

Okabe (1926) and Mononobe and Matsuo (1929) extended Coulomb's theory of static active and passive earth pressures to include the effects of dynamic earth pressures on retaining walls. The Mononobe-Okabe theory incorporates the effect of earthquakes through the use of a constant horizontal acceleration in units of g, $a_h = k_h \cdot g$, and a constant vertical acceleration in units of g, $a_v = k_v \cdot g$, acting on the soil mass comprising Coulomb's active wedge (or passive wedge) within the backfill, as shown in Figure 4.1. The term k_h is the fraction of horizontal acceleration, k_v is the fraction of vertical acceleration, and g is the acceleration of gravity (1.0 g = 32.174 ft/sec/sec = 980.665 cm/sec/sec). In Figure 4.1, positive a_v values act downward, and positive a_h values act to the left. The acceleration of the mass in the directions of positive horizontal and positive vertical accelerations results in the inertial forces $k_h \cdot W$ and $k_v \cdot W$, as shown in Figure 4.1, where W is the weight of the soil wedge. These inertial forces act opposite to the direction in which the mass is accelerating. This type of analysis is described as a pseudostatic method of analysis, where the effect of the earthquake is modeled by an additional set of static forces, $k_h \cdot W$ and $k_v \cdot W$.

The Mononobe-Okabe theory assumes that the wall movements are sufficient to fully mobilize the shear resistance along the backfill wedge, as is the case for Coulomb's active and passive earth pressure theories. To develop the dynamic active earth pressure force, P_{AE}, the wall movements are away from the backfill, and for the passive dynamic earth pressure force, P_{PE}, the wall movements are towards the backfill. Dynamic tests on model retaining walls indicate that the required movements to develop the dynamic active earth pressure force are on the order of those movements required to develop the static active earth pressure force, as discussed in Section 2.2.2.

The Mononobe-Okabe theory gives the net static and dynamic force. For positive $k_h > 0$, P_{AE} is larger than the static P_A, and P_{PE} is less than the static P_P.

4.2 Dynamic Active Earth Pressure Force

The Mononobe-Okabe relationship for P_{AE} for dry backfills, given by Whitman and Christian (1990), is equal to

$$P_{AE} = K_{AE} \cdot \frac{1}{2} [\gamma_t (1 - k_v)] H^2 \tag{33}$$

and acts at an angle δ from the normal to the back of the wall of height H. The dynamic active earth pressure coefficient, K_{AE}, is equal to

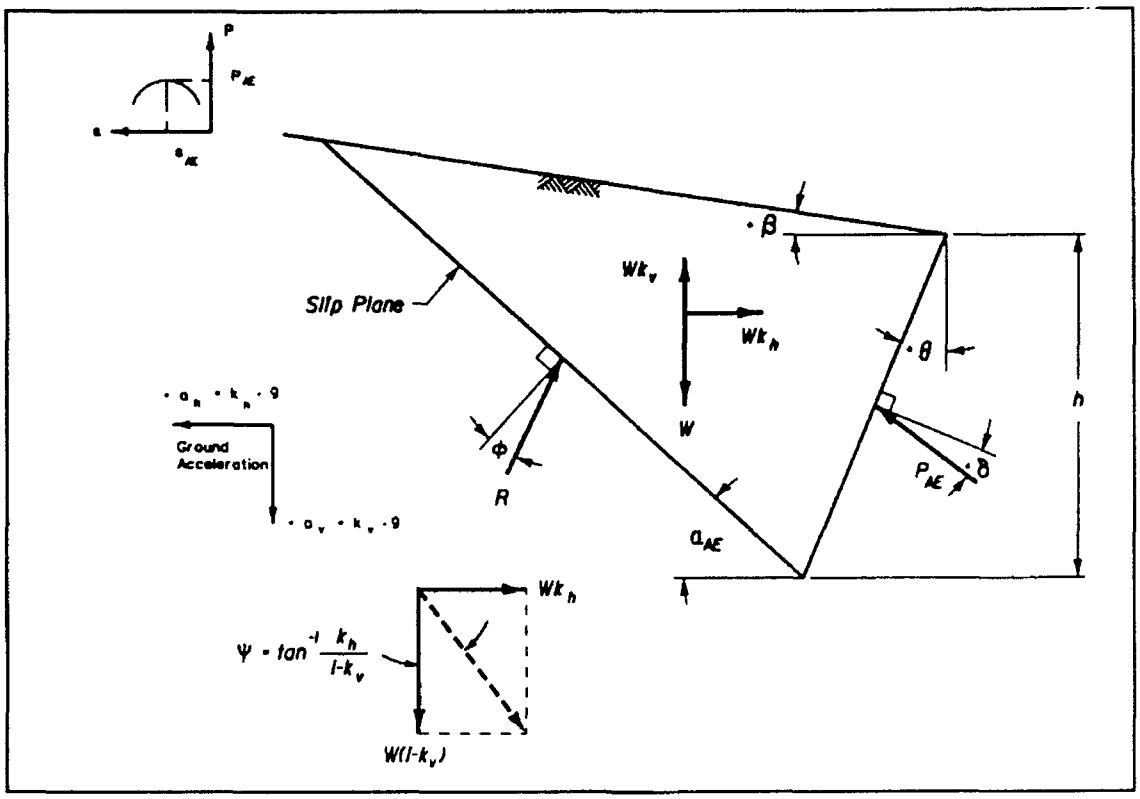

a. Mononobe-Okabe (active) wedge

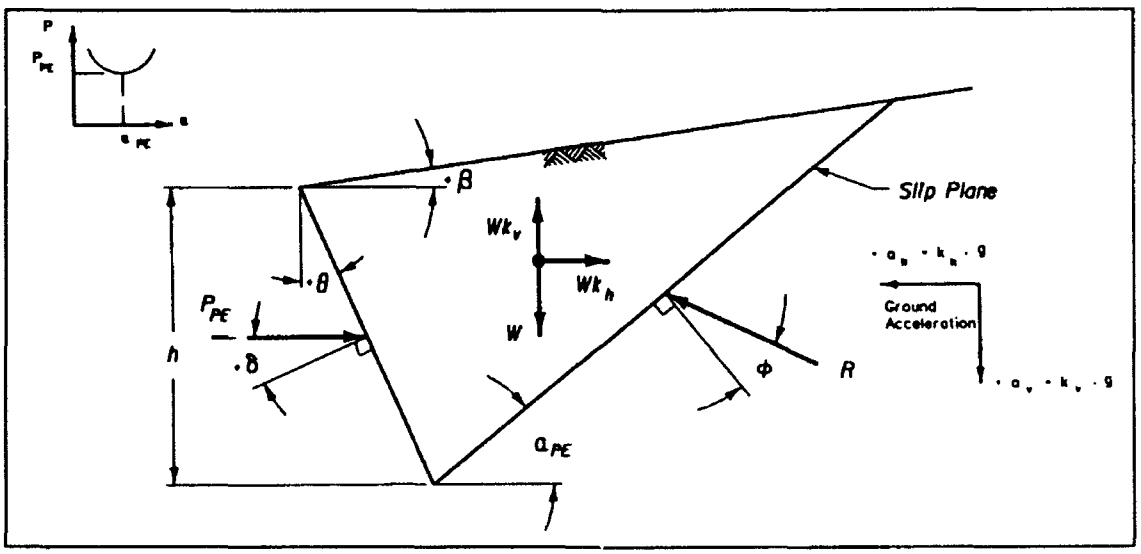

b. Passive wedge

From EM 1110-2-2502

Figure 4.1 Driving and resisting seismic wedges, no saturation

$$K_{AE} = \frac{\cos^2(\phi - \psi - \theta)}{\cos\psi\cos^2\theta\,\cos(\psi + \theta + \delta)\left[1 + \sqrt{\dfrac{\sin(\phi + \delta)\,\sin(\phi - \psi - \beta)}{\cos(\delta + \psi + \theta)\,\cos(\beta - \theta)}}\right]^2} \tag{34}$$

and the seismic inertia angle, ψ, is equal to

$$\psi = \tan^{-1}\left[\frac{k_h}{(1 - k_v)}\right]. \tag{35}$$

The seismic inertia angle represents the angle through which the resultant of the gravity force and the inertial forces is rotated from vertical. In the case of a vertical wall ($\theta = 0$) retaining a horizontal backfill ($\beta = 0$), Equation 34 simplifies to

$$K_{AE} = \frac{\cos^2(\phi - \psi)}{\cos\psi\,\cos(\psi + \delta)\left[1 + \sqrt{\dfrac{\sin(\phi + \delta)\,\sin(\phi - \psi)}{\cos(\delta + \psi)}}\right]^2}. \tag{36}$$

Figures 4.2 and 4.3 give charts from which values of K_{AE} may be read for certain combinations of parameters.

The planar slip surface extends upwards from the heel of the wall through the backfill and is inclined at an angle α_{AE} from horizontal. α_{AE} is given by Zarrabi (1978) to be equal to

$$\alpha_{AE} = \phi - \psi + \tan^{-1}\left[\frac{-\tan(\phi - \psi - \beta) + c_{1AE}}{c_{2AE}}\right] \tag{37}$$

where

$$c_{1AE} = \left[\sqrt{[\tan(\phi - \psi - \beta)][\tan(\phi - \psi - \beta) + \cot(\phi - \psi - \theta)]\cdot [1 + \tan(\delta + \psi + \theta)\cot(\phi - \psi - \theta)]}\right]$$

and

$$c_{2AE} = 1 + \left[[\tan(\delta + \psi + \theta)] \cdot [\tan(\phi - \psi - \beta) + \cot(\phi - \psi - \theta)]\right]$$

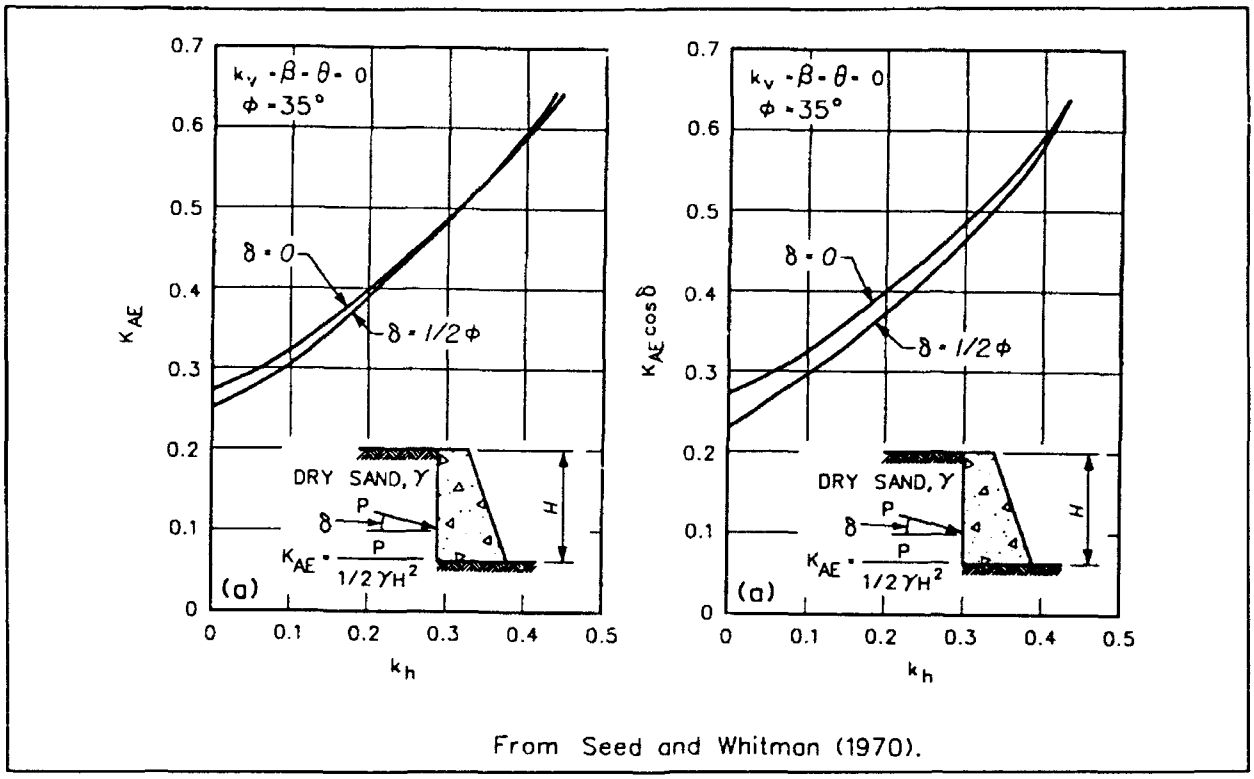

Figure 4.2 Variation in K_{AE} and $K_{AE} \cos \delta$ with k_h

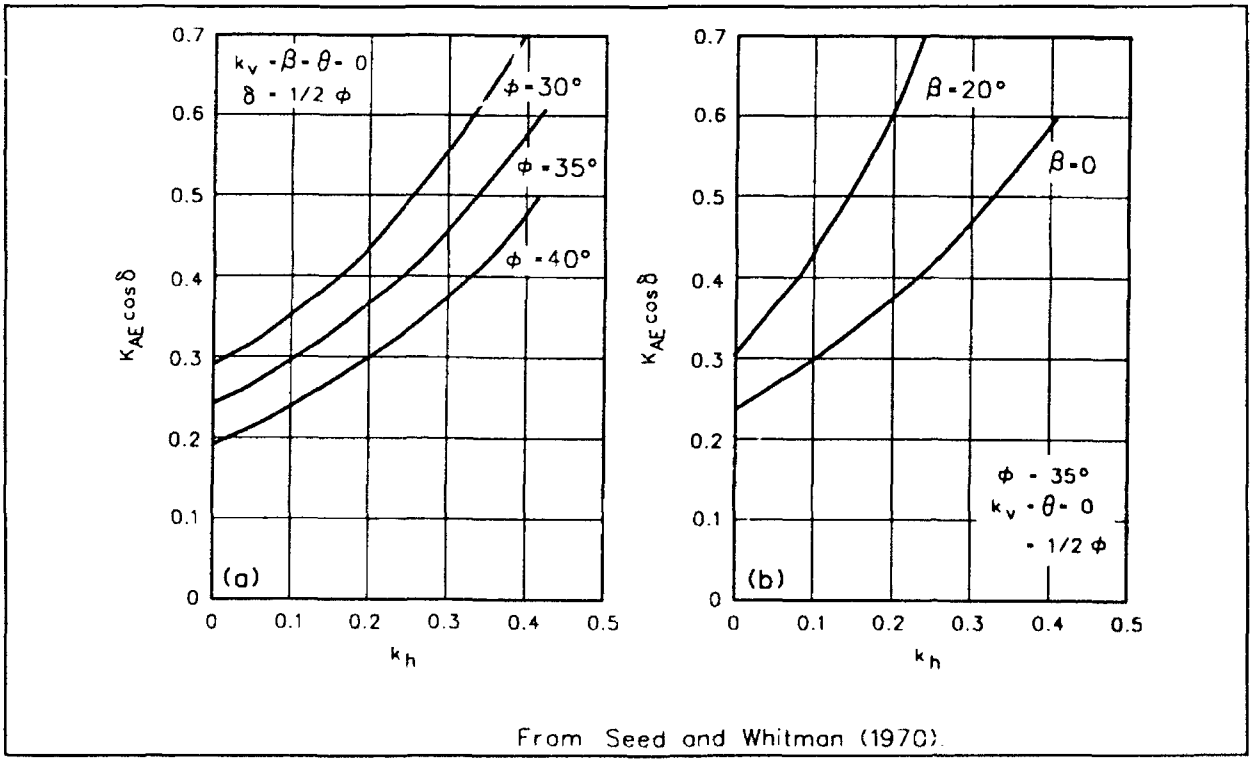

Figure 4.3 Variation in $K_{AE} \cos \delta$ with k_h, ϕ, and β

Figures 4.4 and 4.5 give α_{AE} as a function of ψ for several values of ϕ for vertical walls retaining level backfills.

A limited number of dynamic model retaining wall tests by Sherif and Fang (1983) and Ichihara and Matsuzawa (1973) on dry sands show δ to range from $\phi/2$ to $2\phi/3$, depending upon the magnitude of acceleration.

These procedures are illustrated in examples 7 and 8 at the end of this chapter.

The validity of the Mononobe-Okabe theory has been demonstrated by the shaking table tests described in Section 2.2.1. These tests were conducted at frequencies much less than the fundamental frequency of the backfill, so that accelerations were essentially constant throughout the backfill. Figure 4.6 gives a comparison between predicted and measured values of the seismic active pressure coefficient K_{AE}.

An alternative method for determining the value of K_{AE} using tabulated earth pressures was developed by Dr. I. Arango in a personal communication, as described by Seed and Whitman (1970). Dr. Arango recognized that by rotating a soil wedge with a planar slip surface through the seismic inertia angle, the resultant vector, representing vectorial sums of W, $k_h \cdot W$ and $k_v \cdot W$, becomes vertical, and the dynamic problem becomes equivalent to the static problem, as shown in Figure 4.7. The seismic active pressure force is given by

$$P_{AE} = [K_A(\beta^*, \theta^*) \cdot F_{AE}] \cdot \frac{1}{2}[\gamma_t(1 - k_v)]H^2 \tag{38}$$

where

H = actual height of the wall
$\beta^* = \beta + \psi$
$\theta^* = \theta + \psi$

and

$$F_{AE} = \frac{\cos^2(\theta + \psi)}{\cos\psi \cos^2\theta} \tag{39}$$

ψ is computed using Equation 35. Values of F_{AE} are also given as a function of ψ and θ in Figure 4.8. $K_A(\beta^*, \theta^*)$ is determined from the Coulomb static K_A values by Equation 16. An alternative procedure is to approximate $K_A(\beta^*, \theta^*)$ by using the static K_A values that were tabulated by Caquot and Kerisel (1948) or Kerisel and Absi (1990) as given in Table 3. The product of $K_A(\beta^*, \theta^*)$ times F_{AE} is equal to K_{AE}.

These procedures are illustrate in examples 9 and 10 at the end of this chapter.

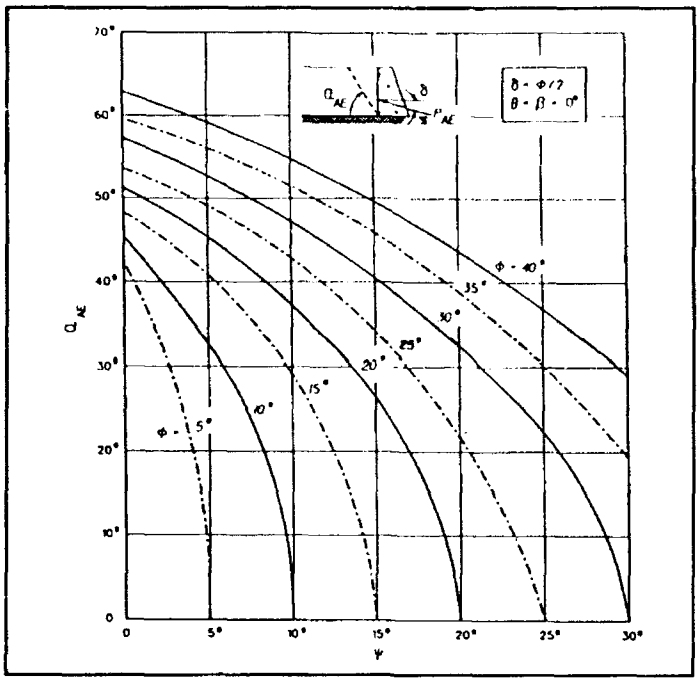

Figure 4.4 Variation in α_{PE} with ψ for δ equal to ϕ vertical wall and level backfill

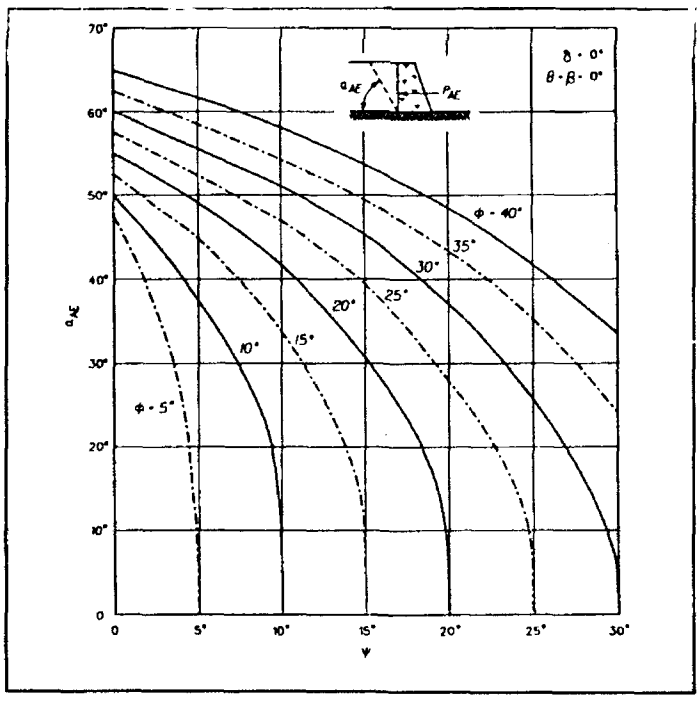

Figure 4.5 Variation in α_{AE} with Ψ for δ equal to zero degrees, vertical wall and level backfill

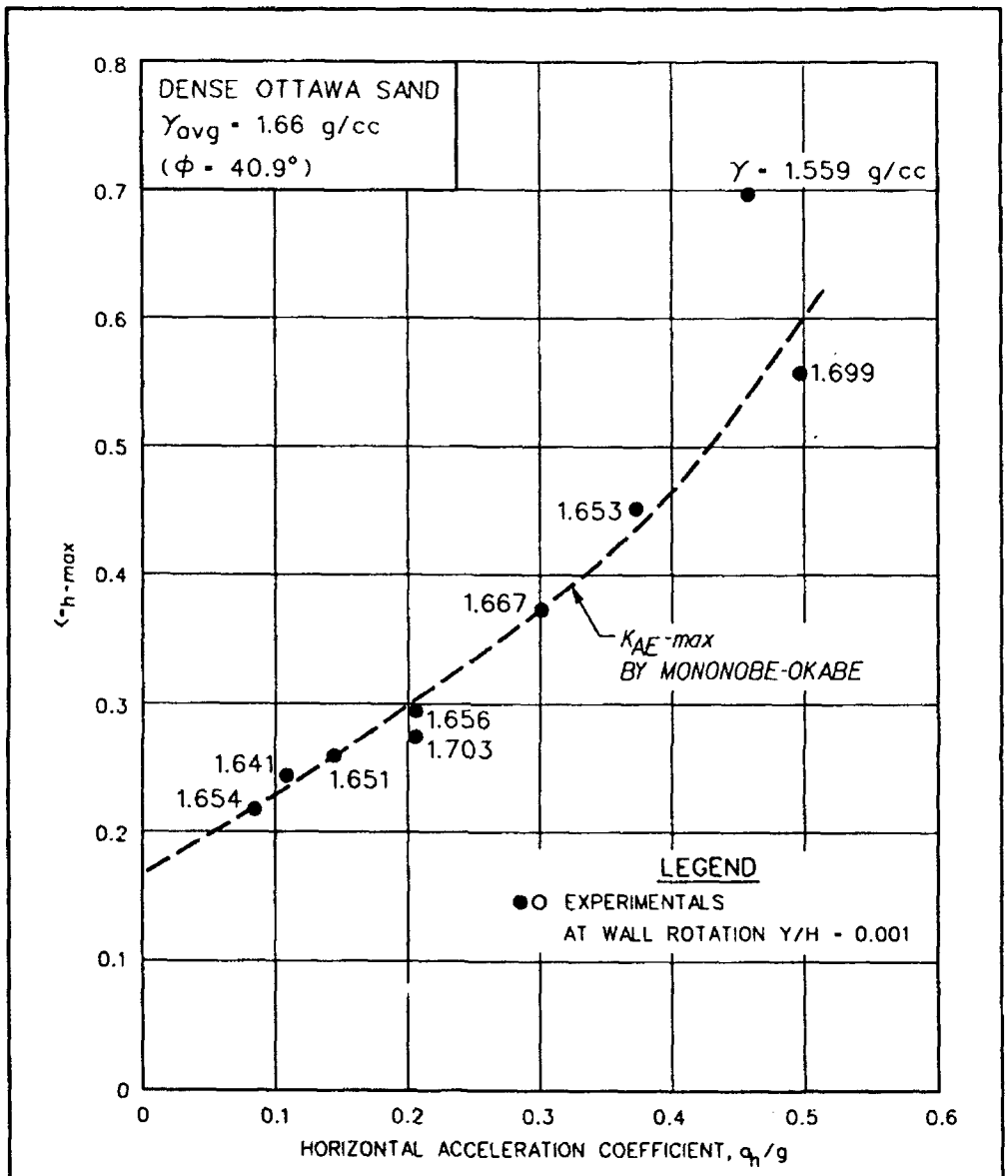

From Sherif and Fang (1983).

Figure 4.6 Variation in dynamic active horizontal earth pressure coefficient with peak horizontal acceleration

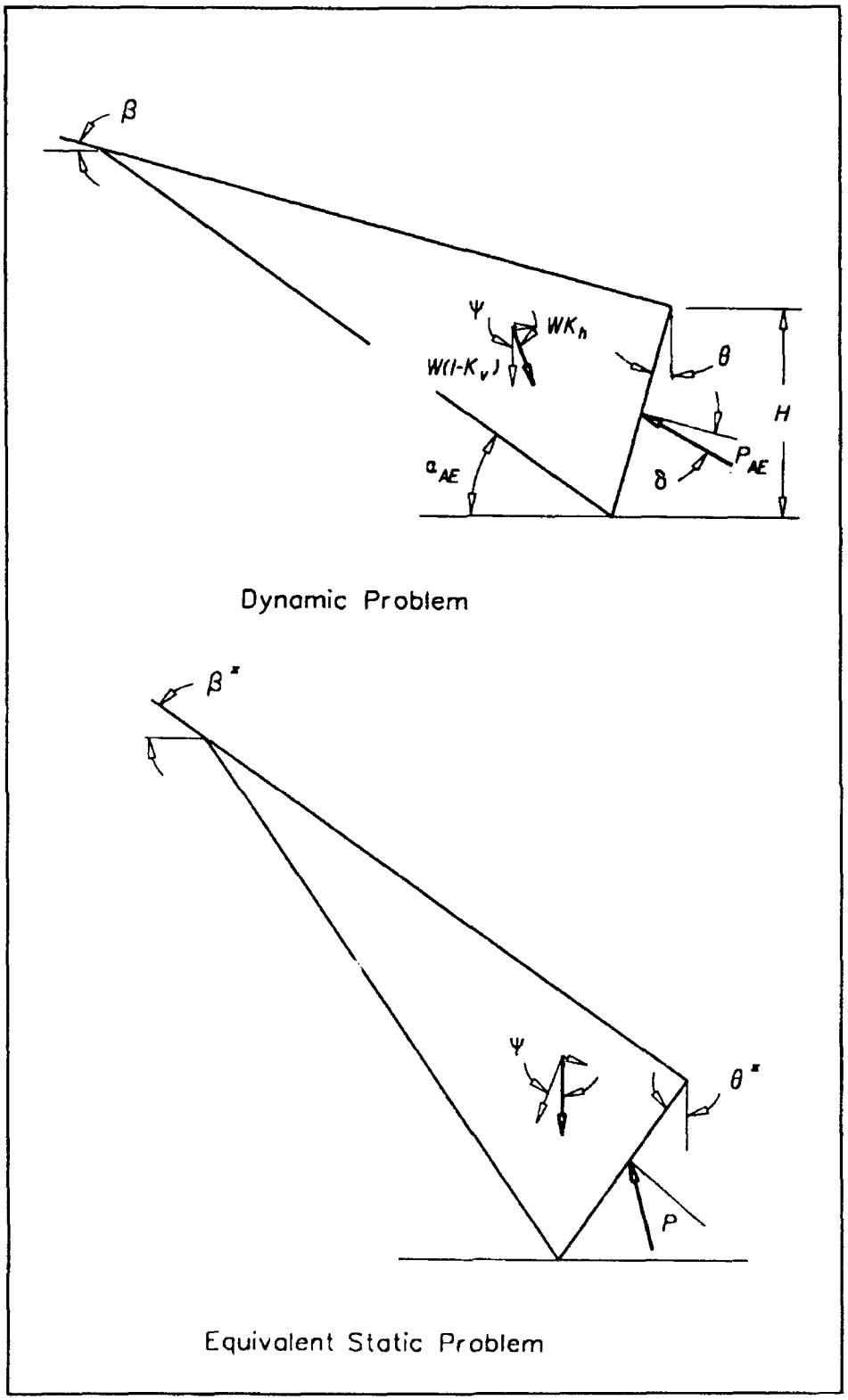

Figure 4.7 Equivalent static formulation of the Mononobe-Okabe active dynamic earth pressure problem

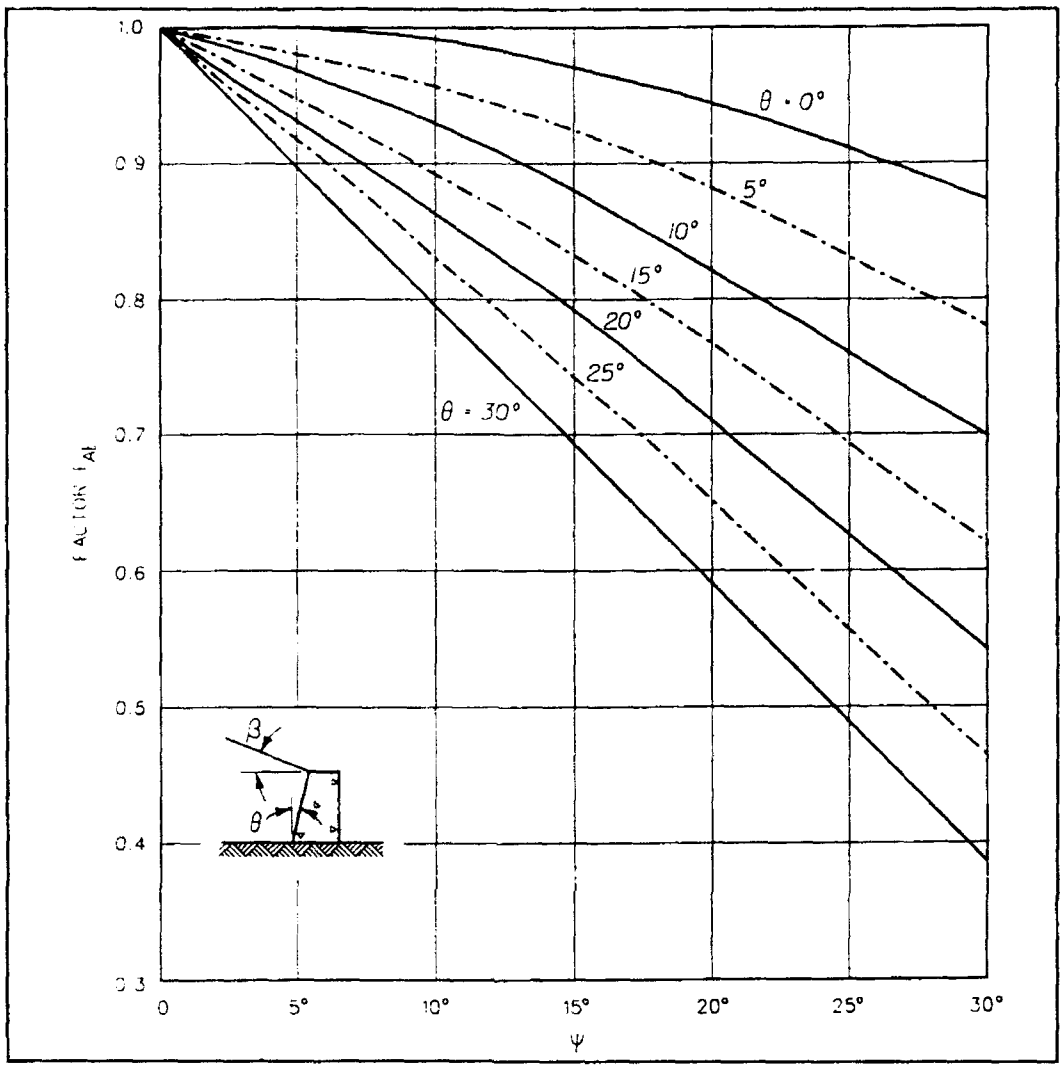

Figure 4.8 Values of factor F_{AE} for determination of K_{AE}

4.2.1 Vertical Position of P_{AE} along Back of Wall

The Mononobe-Okabe analysis procedure does not provide a means for calculating the point of action of the resulting force. Analytical studies by Prakash and Basavanna (1969) and tests on model walls retaining dry sands (Sherif, Ishibashi, and Lee 1982; Sherif and Fang 1984a; Sherif and Fang 1984b; and Ishibashi and Fang 1987) have shown that the position of P_{AE} along the back of the retaining wall depends upon the amount of wall movement and the mode in which these movements occur. These limited test results indicate that the vertical position of P_{AE} ranges from 0.4 to 0.55 times the height of the wall, as measured from the base of the wall. P_{AE} acts at a higher position along the back of the wall than the static active earth pressure force due to the concentration of soil mass comprising the sliding wedge above mid-wall height (Figure 4.1). With the static force component of P_{AE} acting below mid-wall height and the inertia force component of P_{AE} acting above mid-wall height, the vertical position of the resultant force, P_{AE}, will depend upon the magnitude of the accelerations applied to the mass comprising soil wedge.

This was shown to be the case in the Prakish and Basavanna (1969) evaluation of the moment equilibrium of a Mononobe-Okabe wedge. The results of their analyses are summarized in Figure 4.9.

4.2.2 Simplified Procedure for Dynamic Active Earth Pressures

Seed and Whitman (1970) presented a simplified procedure for computing the dynamic active earth pressure on a vertical wall retaining dry backfill. They considered the group of structures consisting of a vertical wall ($\theta = 0$) retaining a granular horizontal backfill ($\beta = 0$) with ϕ equal to 35 degrees, $\delta = \phi/2$ and k_v equal to zero. P_{AE} is defined as the sum of the initial static active earth pressure force (Equation 7) and the dynamic active earth pressure force increment,

$$P_{AE} = P_A + \Delta P_{AE} \tag{40}$$

where

$$\Delta P_{AE} = \Delta K_{AE} \cdot \frac{1}{2}\gamma_t H^2. \tag{41}$$

The dynamic active earth pressure coefficient is equal to

$$K_{AE} = K_A + \Delta K_{AE} \tag{42}$$

and

$$\Delta K_{AE} = \frac{3}{4} \cdot k_h. \tag{43}$$

Using this simplified procedure, K_A is computed using Equation 16, and ΔK_{AE} is computed using Equation 43. All forces act at an angle δ from the normal to the back of a wall, as shown in Figure 4.10. P_A acts at a height equal to H/3 above the heel of the wall, and ΔP_{AE} acts at a height equal to 0.6·H. P_{AE} acts at a height, Y, which ranges from H/3 to 0.6·H, depending upon the value of k_h.

$$Y = \frac{P_A \cdot (\frac{H}{3}) + \Delta P_{AE} \cdot (0.6H)}{P_{AE}} \tag{44}$$

The results of instrumented shake table tests conducted on model walls retaining dense sands show ΔP_{AE} acts at a height of between 0.43H and 0.58H, depending upon the mode of wall movement that occurs during shaking. The height of the model walls used in the shake table tests, as summarized in Matsuzawa, Ishibashi, and Kawamura (1985), were 2.5 and 4 feet.

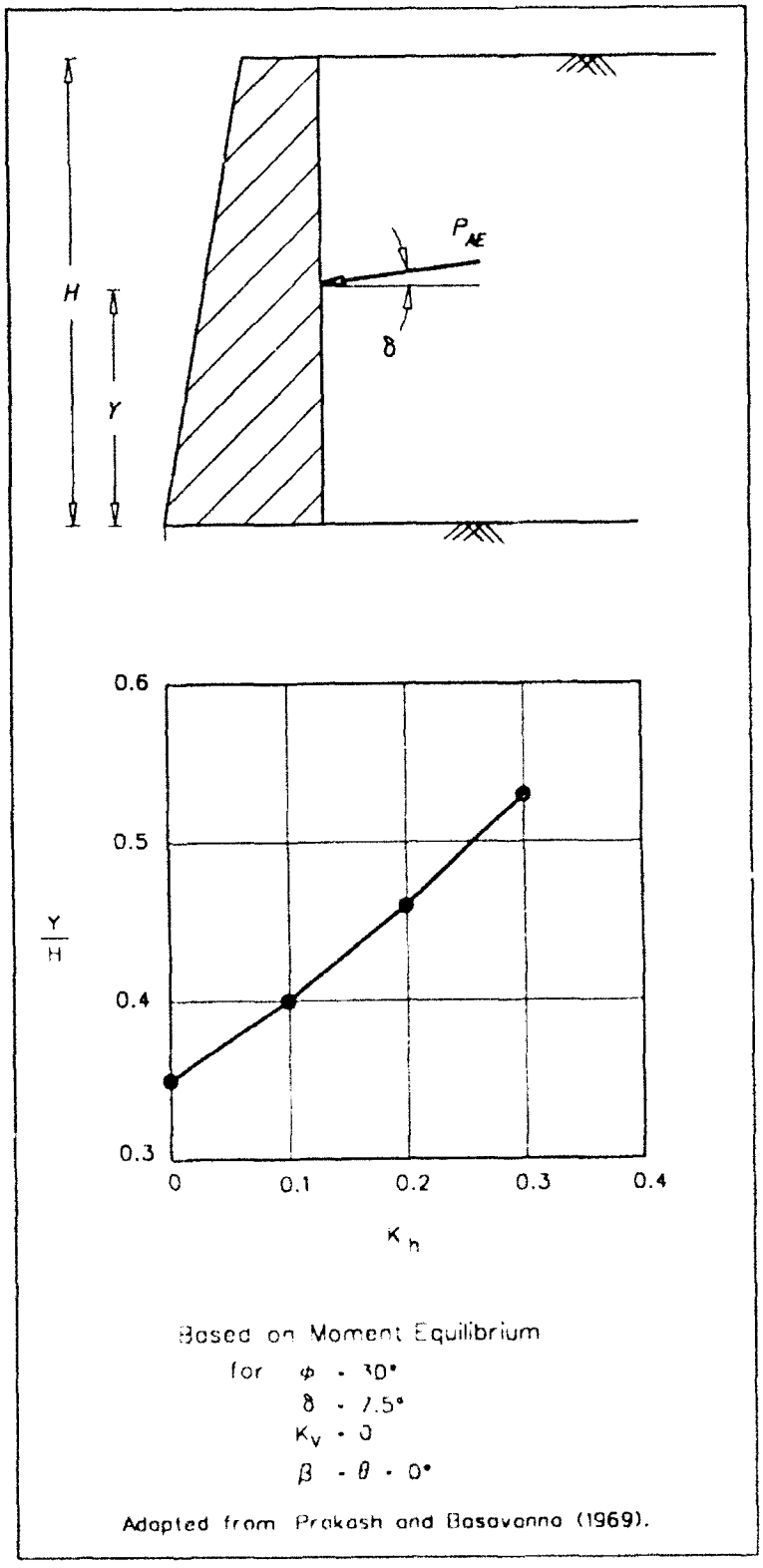

After Prakash and Basavanna (1969)

Figure 4.9 Point of action of P_{AE}

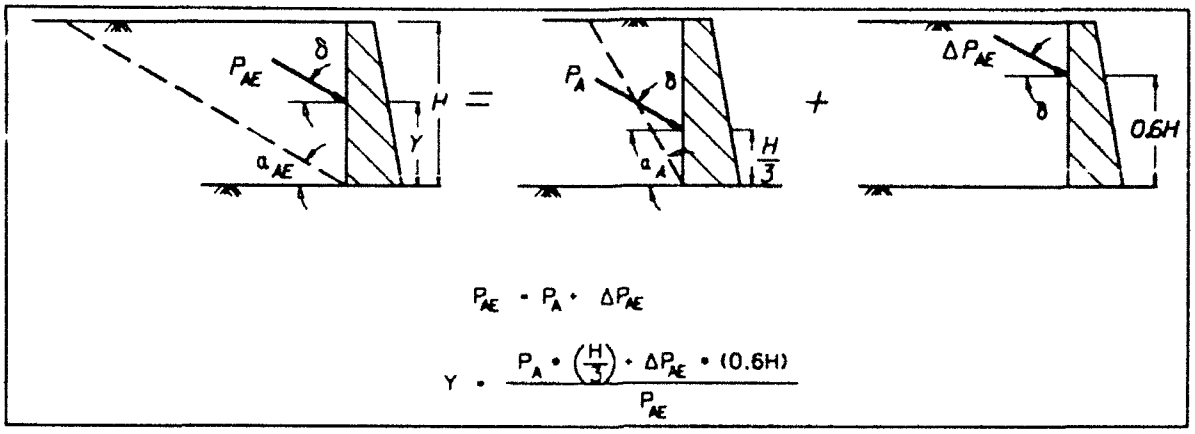

Figure 4.10 Static active earth pressure force and incremental dynamic active earth pressure force for dry backfill

Seed and Whitman (1970) approximate the value for α_{AE} as equal to ϕ, where ϕ equals 35 degrees. Thus, for a wall retaining a dry granular backfill of height H, the theoretical active failure wedge would intersect the top of the backfill at a distance equal to 1.5 times H, as measured from the top of the wall ($\tan 35° \approx 1/1.5$).

This procedure is illustrated in example 11 at the end of this chapter.

4.2.3 Limiting Value for Horizontal Acceleration

Richards and Elms (1979) show that Equations 34 and 36 are limited to cases where (ϕ - β) is greater than or equal to ψ. Substituting (ϕ - β) equal to ψ into Equation 37 results in α_{AE} equal to the slope of the backfill (β), which is the stability problem for an infinite slope. Zarrabi (1978) shows that this limiting value for ψ corresponds to a limiting value for k_h, which is equal to

$$k_h^* = (1 - k_v) \tan(\phi - \beta). \tag{45}$$

When k_h is equal to k_h^*, the shear strength along the failure surface is fully mobilized, and the backfill wedge verges on instability. Values of k_h^* are also shown in Figure 4.11.

This procedure is illustrated in examples 12 and 13 at the end of this chapter.

4.3 Effect of Submergence of the Backfill on the Mononobe-Okabe Method of Analysis

The Mononobe-Okabe relationships for P_{AE}, K_{AE}, and ψ will differ from those expressed in Equations 33, 34, and 35, respectively, when water is present in the backfill. Spatial variations in pore water pressure with constant elevation in the backfill will alter the location of the critical slip surface and thus the value of P_{AE}, similar to the case of P_A that was

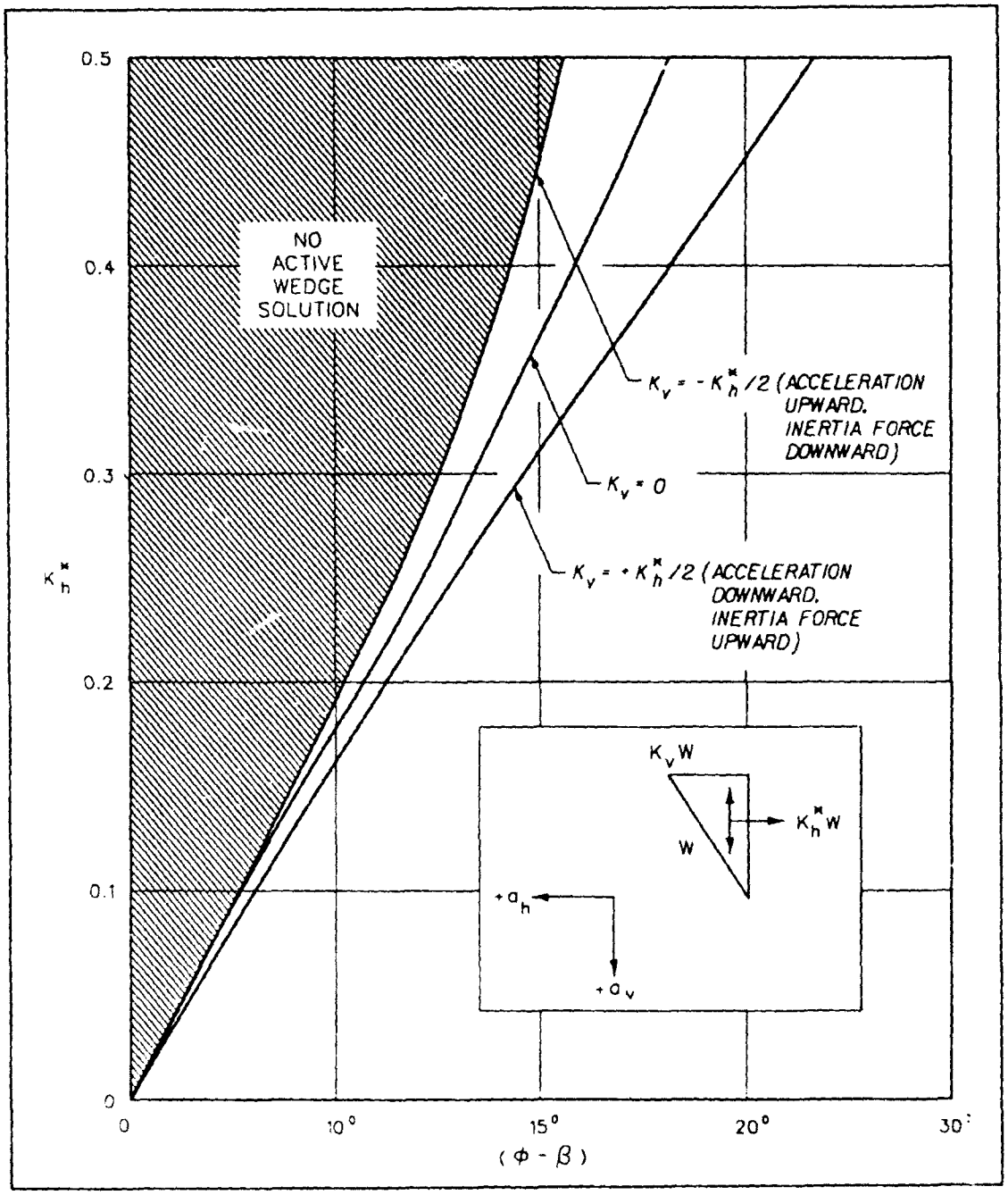

Figure 4.11 Limiting values for horizontal acceleration equals $k_h^* \cdot g$

discussed in Section 3.3.3. In addition, the pore water pressures may increase above their steady state values in response to the shear strains induced within the saturated portion of the backfill during earthquake shaking, as discussed in Tokimatsu and Yoshimi (1983), Tokimatsu and Seed (1987), Seed and Harder (1990), and Marcuson, Hynes, and Franklin (1990). The trial wedge procedure of analysis is used to locate the critical slip surface within the backfill and to compute P_{AE}, following the steps described in Section 3.4 and including the excess pore water pressures due to earthquake shaking in the analysis are described in Appendix A. In some situations, such as the case of a hydrostatic water table within the backfill or the case of excess pore water pressures equal to a constant fraction of the pre-earthquake effective overburden pressures throughout the backfill (r_u = constant), modified Mononobe-Okabe relationships may be used to compute P_{AE}.

4.3.1 Submerged Backfill with No Excess Pore Pressures

In this section it is assumed that shaking causes no associated buildup of excess pore pressure. The most complete study of this case appears in Matsuzawa, Ishibashi, and Kawamura (1985), Ishibashi, Matsuzawa, and Kawamura (1985), and Ishibashi and Madi (1990). They suggest two limiting conditions for design: (a) soils of low permeability - say $k < 1 \times 10^{-3}$ cm/sec where pore water moves with the mineral skeleton; and (b) soils of high permeability - say $k > 1$ cm/sec, where pore water can move independently of the mineral skeleton. Matsuzawa, Ishibashi, and Kawamura (1985) also suggest a parameter that can be used to interpolate between these limiting cases. However, understanding of case (b) and the interpolation parameter is still very incomplete.

<u>Restrained water case</u>: Here Matsuzawa Ishibaski, and Kawamura (1985) make the assumption that pore pressures do not change as a result of horizontal accelerations. Considering a Coulomb wedge and subtracting the static pore pressures, there is a horizontal inertia force proportional to $\gamma_t \cdot k_h$ and a vertical force proportional to γ_b. Thus, in the absence of vertical accelerations, the equivalent seismic angle is:

$$\psi_{el} = \tan^{-1} \frac{\gamma_t \cdot k_h}{\gamma_b}. \tag{46}$$

and the equivalent horizontal seismic coefficient is:

$$k_{hel} = \frac{\gamma_t}{\gamma_b} k_h. \tag{47}$$

Using k_{hel} in the Mononobe-Okabe theory together with a unit weight γ_b will give P_{AE}, to which the static water pressures must be added.

If vertical accelerations are present, Matsuzawa, Ishibashi, and Kawamura (1985) recommend using:

$$\psi_{e1} = \tan^{-1}\left[\frac{\gamma_t k_h}{\gamma_b(1 - k_v)}\right] \tag{48}$$

This is equivalent to assuming that vertical accelerations do affect pore pressures, and then it is not strictly correct to use the Mononobe-Okabe theory. However, the error in evaluating total thrust is small.

This procedure is illustrated in example 14 at the end of this chapter.

Free water case: It is difficult to come up with a completely logical set of assumptions for this case. Matsuzawa, Ishibaski, and Kawamura (1985) suggest that the total active thrust is made up of:

(1) A thrust from the mineral skeleton, computed using:

$$k_{he2} = \frac{\gamma_d}{\gamma_b} k_h = \frac{G_s}{G_s - 1} k_h \tag{49}$$

and

$$\psi_{e2} = \tan^{-1}\left[\frac{k_{he2}}{(1 - k_v)}\right] \tag{50}$$

where G_s is the specific gravity of the solids. A unit weight of γ_b is used in the equation for P_{AE}.

(2) The hydrodynamic water pressure force for the free water within the backfill, P_{wd}, is given by the Westergaard (1931) relationship (Appendix B)

$$P_{wd} = \frac{7}{12} \cdot k_h \cdot \gamma_w H^2 \tag{51}$$

and acts at 0.4 H above the base of the wall.

The total force behind the wall would also include the hydrostatic water pressure. This procedure is not totally consistent, since the effect of the increased pore pressures is ignored in the computation of the thrust from the mineral skeleton as is the effect of vertical acceleration upon pore pressure.

This procedure is illustrated in example 15 at the end of this chapter.

4.3.2 Submerged Backfill with Excess Pore Pressure

Excess pore pressures generated by cyclic shaking can be represented by $r_u = \Delta u/\sigma_v'$, where Δu is the excess pore pressure and σ_v' is the initial

vertical stress. While there is no rigorous approach for adapting the Mononobe-Okabe solution, the following approaches are suggested.

Restrained water case: Ignoring vertical accelerations, the effective unit weight of soil becomes:

$$\gamma_{e3} = \gamma_b(1 - r_u) \tag{52}$$

while the effective unit weight of water is

$$\gamma_{w3} = \gamma_w + \gamma_b \cdot r_u \tag{53}$$

The thrust from the soil skeleton, P_{AE}, is computed using

$$k_{he3} = \frac{\gamma_t}{\gamma_{e3}} k_h \tag{54}$$

and

$$\psi_{e3} = \tan^{-1}[k_{he3}] \tag{55}$$

together with a unit weight from Equation 52. The effective unit weight of water, Equation 53, is used to compute the "static" pore pressure. The effect of vertical acceleration may be accounted for by inserting $(1-k_v)$ in the denominator of Equation 55.

As r_u approaches unity, $\gamma_{e3} \rightarrow 0$ and $\gamma_{w3} = \gamma_t$, so that the fully-liquefied soil is a heavy fluid. It would now be logical to add a dynamic pore pressure computed using Equations 51 and 53.

This procedure is illustrated in example 16 at the end of this chapter.

Alternate Procedure:

An alternative approach is to use a reduced effective stress friction angle in which the effects of the excess pore water pressures are approximated within the analysis using a simplified shear strength relationship. In an effective stress analysis, the shear resistance on a potential failure surface is reduced by reducing the effective normal stress on this plane by the amount of excess residual pore water pressure, assuming the effective friction angle is unaffected by the cyclic loading. This is equivalent to using the initial, static effective normal stress and a modified effective friction angle, ϕ_{eq}, where

$$\tan\phi'_{eq} = (1 - r_u)\tan\phi' \tag{56}$$

as shown in Figure 4.12. In the case of r_u equal to a constant within the fully submerged backfill, the use of ϕ_{eq} in Equations 34 and 38 for K_{AE} and $K_A(\beta^*, \theta^*)$ approximating the effects of these excess pore water pressures

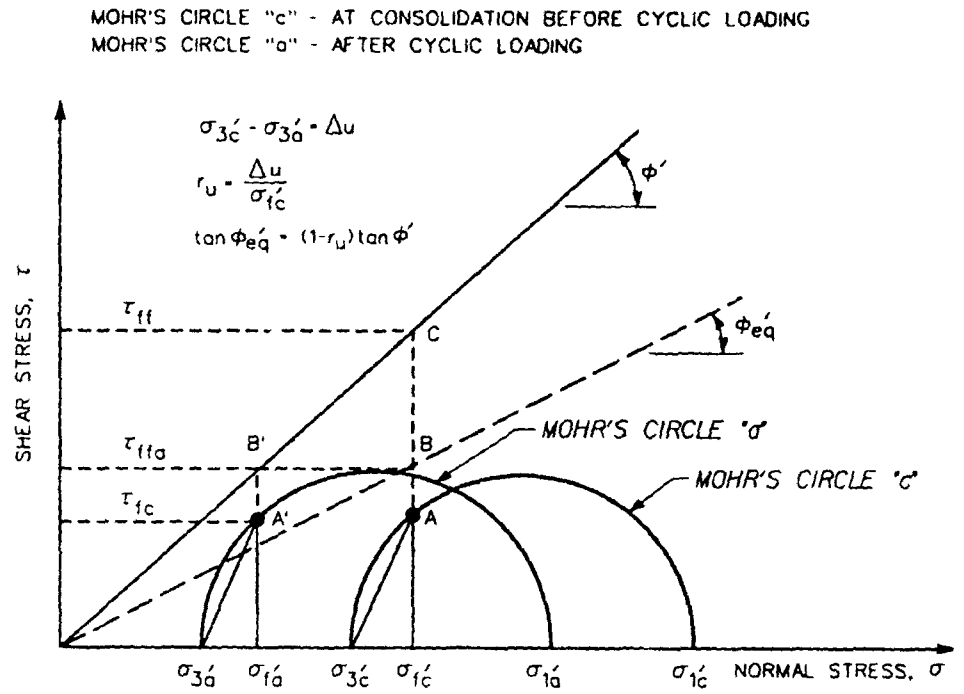

For the static stress path to failure from point A to point C

$$FS_{static} = \frac{\tau_{ff}}{\tau_{fc}} = \frac{\sigma_{fc}'\tan\phi'}{\tau_{fc}}$$

For the cyclic stress path to failure from point A′ to point B′

$$FS_{cyclic} = \frac{\tau_{ffa}}{\tau_{fc}} = \frac{\sigma_{fa}'\tan\phi'}{\tau_{fc}} = \frac{\sigma_{fc}'\tan\phi_{eq}'}{\tau_{fc}}$$

Figure 4.12 Modified effective friction angle

within the analysis. Using k_{hel}, ψ_{hel} (Equations 47 and 46 in Section 4.3.1) and ϕ_{eq} in the Mononobe-Okabe theory together with a unit weight γ_b will give P_{AE}.

Calculations by the authors of this report showed that reducing the effective stress friction angle of the soil so as to account for the excess pore water pressures when computing a value for P_{AE} is not exact. Comparisons between the exact value of P_{AE}, computed using γ_{e3}, k_{he3}, ψ_{he3} in the Mononobe-Okabe theory, and the value computed using the ϕ_{eq} procedure shows this approximation to overpredict the value of P_{AE}. The magnitude error in the computed value of P_{AE} increases with increasing values of r_u and increases with decreasing values of k_h. The error is largest for the k_h equal to 0 case.

This procedure is illustrated in example 17 at the end of this chapter.

Free water case: The thrust from the mineral skeleton may be estimated using:

$$k_{he4} = \frac{\gamma_d}{\gamma_{e3}} k_h . \tag{57}$$

where

$$\gamma_d = \frac{\gamma_t}{1 + w}$$

To this thrust are added the dynamic Westergaard water pressure (computed using γ_w) and a "static" water pressure computed using γ_{w3} from Equation 53.

This procedure is illustrated in example 18 at the end of this chapter.

4.3.3 Partial Submergence

Situations with partial submergence may be handled by weighing unit weights based on the volume of soil in the failure wedge above and below the phreatic surface, as shown in Figure 4.13.

This procedure is illustrated in example 19 at the end of this chapter.

4.4 Dynamic Passive Earth Pressures

The trial wedge procedure of analysis may be used to find the orientation of the critical slip surface that minimizes the value of the earth pressure force acting on the wall for the passive earth pressure problem shown in Figure 4.1b. This minimum earth pressure force corresponds to the dynamic passive earth pressure force, P_{PE}. The orientation of the inertial forces $k_h \cdot W$ and $k_v \cdot W$ that minimize the value of P_{PE} is directed away from the wall and upwards (Figure 4.1b). This corresponds to the case where the soil wedge is accelerating towards the wall (positive a_h values) and downwards (positive a_v values).

The Mononobe-Okabe relationship for P_{PE} for dry backfill, given by Whitman and Christian (1990), is equal to

$$P_{PE} = K_{PE} \cdot \frac{1}{2} [\gamma_t (1 - k_v)] H^2 \tag{58}$$

and acts at an angle δ from the normal to the back of the wall of height H. The dynamic passive earth pressure coefficient, K_{PE}, is equal to

$$K_{PE} = \frac{\cos^2 (\phi - \psi + \theta)}{\cos \psi \cos^2 \theta \cos (\psi - \theta + \delta) \left[1 - \sqrt{\frac{\sin (\phi + \delta) \sin (\phi - \psi + \beta)}{\cos (\delta + \psi - \theta) \cos (\beta - \theta)}} \right]^2} . \tag{59}$$

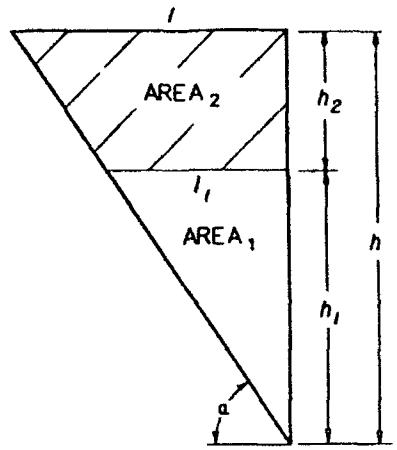

$$\tan(90^\circ - \alpha) = \frac{l_1}{h_1} = \frac{l}{h}$$

or

$$\frac{l_1}{l} = \frac{h_1}{h}$$

$$\text{Area} = \text{Area}_1 + \text{Area}_2$$

$$\frac{\text{Area}_1}{\text{Area}} = \frac{\frac{1}{2} l_1 h_1}{\frac{1}{2} l h} = \left(\frac{h_1}{h}\right)^2$$

$$\gamma_e = \frac{\gamma_1 \cdot \text{Area}_1 + \gamma_2 \cdot \text{Area}_2}{\text{Area}}$$

$$\gamma_e = \frac{\text{Area}_1}{\text{Area}} \gamma_1 + \left[1 - \frac{\text{Area}_1}{\text{Area}}\right] \gamma_2$$

$$\gamma_e = \left(\frac{h_1}{h}\right)^2 \gamma_1 + \left[1 - \left(\frac{h_1}{h}\right)^2\right] \gamma_2$$

NOTES:

(1) EXACT SOLUTION WHEN $r_u = 0$.

(2) APPROXIMATE SOLUTION WHEN $r_u > 0$.

Figure 4.13 Effective unit weight for partially submerged backfills

In the case of a vertical wall ($\theta = 0$) retaining a horizontal backfill ($\beta = 0$), Equation 59 simplifies to

$$K_{PE} = \frac{\cos^2(\phi - \psi)}{\cos\psi \cos(\psi + \delta) \left[1 - \sqrt{\dfrac{\sin(\phi + \delta) \sin(\phi - \psi)}{\cos(\delta + \psi)}}\right]^2} . \tag{60}$$

The planar slip surface extends upwards from the heel of the wall through the backfill and is inclined at an angle α_{PE} from the horizontal. α_{PE} is equal to

$$\alpha_{PE} = \psi - \phi + \tan^{-1} \left[\frac{\tan(\phi + \beta - \psi) + c_{3PE}}{c_{4PE}}\right] \tag{61}$$

where

$$c_{3PE} = \left[\sqrt{[\tan(\phi+\beta-\psi)][\tan(\phi+\beta-\psi)+\cot(\phi+\theta-\psi)]\cdot[1+\tan(\delta-\theta+\psi)\cot(\phi+\theta-\psi)]}\right]$$

and

$$c_{4PE} = 1 + \left[[\tan(\delta - \theta + \psi)] \bullet [\tan(\phi + \beta - \psi) + \cot(\phi + \theta - \psi)]\right].$$

Figures 4.14 and 4.15 give α_{PE} as a function of ψ for several values of ϕ.

This procedure is illustrated in example 20 and 21 at the end of this chapter.

The Mononobe-Okabe equation assumes a planar failure surface, which only approximates the actual curved slip surface. Mononobe-Okabe's relationship overpredicts the values for K_{PE} and the error increases with increasing values for δ and ψ.

Rotating the passive soil wedge with a planar slip surface through the seismic inertia angle, the resultant vector, representing vectorial sums of W, $k_h \cdot W$, and $k_v \cdot W$, becomes vertical, and the dynamic passive earth pressure force problem becomes equivalent to the static problem, as shown in Figure 4.16.

The seismic passive resistance is given by

$$P_{PE} = [K_P(\beta^*, \theta^*) \cdot F_{PE}] \cdot \frac{1}{2}[\gamma_t(1 - k_v)]H^2 \tag{62}$$

where

$$\beta^* = \beta - \psi$$
$$\theta^* = \theta - \psi$$

and

$$F_{PE} = \frac{\cos^2(\theta - \psi)}{\cos\psi \cos^2\theta} \tag{63}$$

ψ is computed using Equation 35. Values of F_{PE} are also given as a function of ψ and θ in Figure 4.17. $K_P(\beta^*, \theta^*)$ is determined from the Coulomb static K_P values by Equation 29. The Coulomb formulation assumes a planar failure surface which approximates the actual curved failure surface. The planar failure surface assumption introduces errors in determination of K_P and the error increases with increasing values of δ. The error in slip surface results in an overprediction of K_P. Thus the equivalent static formulation will be in error since the product of $K_P(\beta^*, \theta^*)$ times F_{PE} is equal to K_{PE}. An alternate procedure is to approximate $K_P(\beta^*, \theta^*)$ by using the static K_P values tabulated by Caquot and Kerisel (1948) or Kerisel and Absi (1990). Calculations show K_{PE} values by the alternate procedure are smaller than K_{PE} values by Mononobe-Okabe.

This procedure is illustrated in examples 22 and 23 at the end of this chapter.

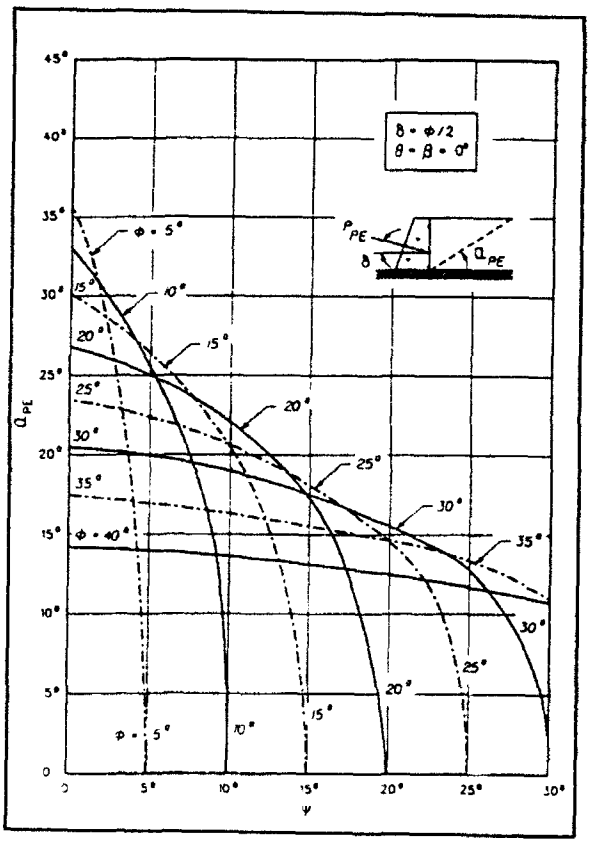

Figure 4.14 Variation α_{PE} with ψ for δ equal to $\phi/2$, vertical wall and level backfill

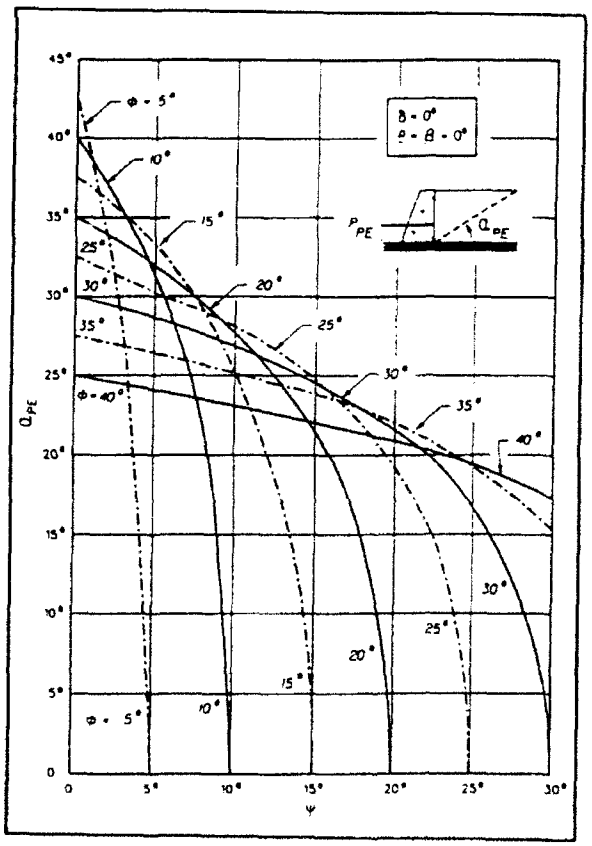

Figure 4.15 Variation in α_{PE} with ψ for δ equal to zero degrees, vertical wall and level backfill

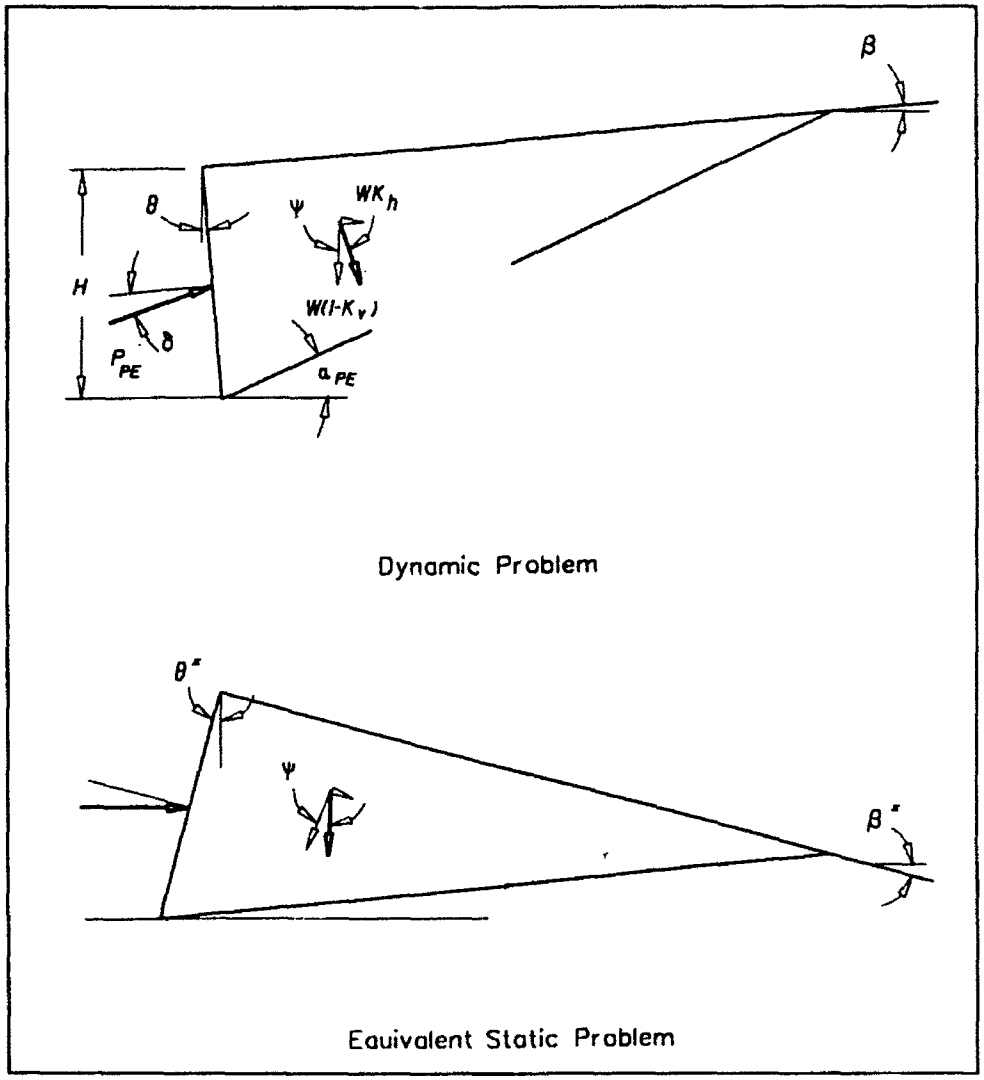

Figure 4.16 Equivalent static formulation of the Mononobe-Okabe passive dynamic earth pressure problem

This procedure is illustrated in the procedures outlined in Section 4.3. The procedures are used to account for the effect of submergence of the backfill in computing the value of P_{PE}. For example, in the restrained water case of a fully submerged backfill, an effective unit equal to γ_b is assigned to the backfill for the case of $r_u = 0$ or Equation 52 with $r_u > 0$. K_{PE} or $K_P(\beta^*, \theta^*)$ and F_{PE} are computed using an equivalent seismic inertia angle using Equation 48 for the case of $r_u = 0$ or Equation 55 with $r_u > 0$.

This procedure is illustrated in example 24 at the end of this chapter.

4.4.1 Simplified Procedure for Dynamic Passive Earth Pressures

Towhata and Islam (1987) recommended a simplified approach for computing the dynamic passive earth pressure force that is similar to the Seed and Whitman (1970) procedure for the dynamic active earth pressure force. They also considered the group of structures consisting of a vertical wall ($\theta = 0$)

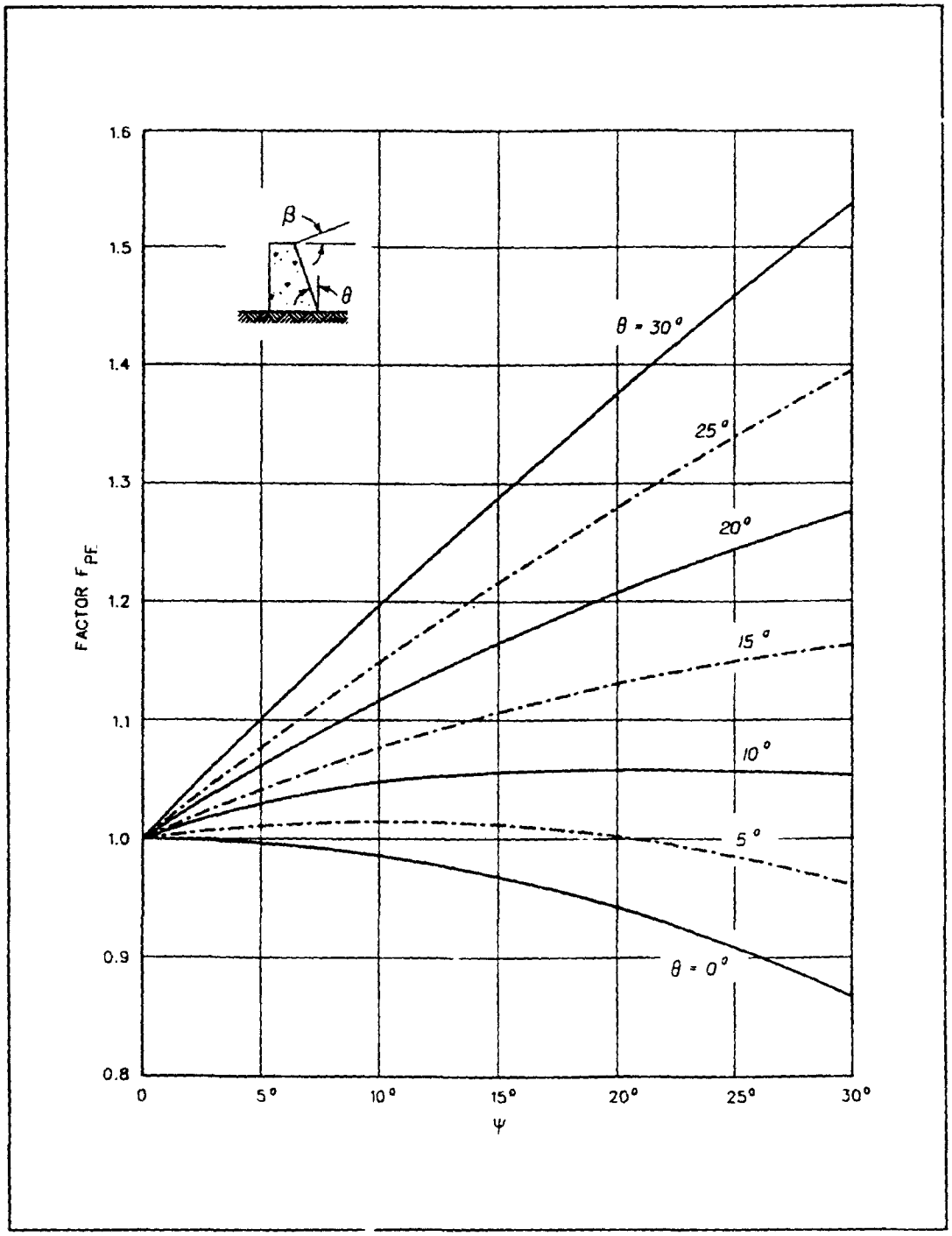

Figure 4.17 Values of factor F_{PE}

retaining a granular horizontal backfill ($\beta = 0$) with ϕ equal to 35 degrees, δ equal to 0, and k_v equal to zero. Equation 65 is presented as developed by Towhata and Islam, while Equations 64, 66, and 67 have been modified by the authors of this report. P_{PE} is defined as

$$P_{PE} = P_P - \Delta P_{PE} \tag{64}$$

where the reduction in the static passive earth pressure value P_p due to earthquake shaking is given by

$$\Delta P_{PE} = \frac{1}{2}\gamma_t H^2 \bullet \Delta K_{PE} \tag{65}$$

for a dry granular backfill. The dynamic passive earth pressure coefficient is equal to

$$K_{PE} = K_P - \Delta K_{PE} \tag{66}$$

and

$$\Delta K_{PE} = \frac{17}{8} \bullet k_h. \tag{67}$$

Using this simplified procedure, K_P is computed using Equation 11 (Rankine), and ΔK_{PE} is computed using Equation 67. The incremental dynamic force ΔP_{PE} acts counter to the direction of P_P, reducing the contribution of the static passive pressure force to P_{PE} . The resulting forces P_P (Equation 13) and ΔP_{PE} (Equation 65) act normal to the back of a wall.

This procedure is illustrated in example 25 at the end of this chapter.

The simplified procedure was developed for vertical walls retaining horizontal backfills with $\delta = 0$. This simplified procedure should not be applied to dynamic passive earth pressure problems involving values of $\delta > 0$, due to the magnitude of the error involved.

4.5 Effect of Vertical Accelerations on the Values for the Dynamic Active and Passive Earth Pressures

In a pseudo-static analysis the horizontal and vertical accelerations of the soil mass during an earthquake are accounted for by applying equivalent inertial forces $k_h \cdot W$ and $k_v \cdot W$ to the soil wedge, which act counter to the direction of the accelerating soil wedges, as shown in Figure 4.1. A positive horizontal acceleration value increases the value of P_{AE} and decreases the value of P_{PE}. The vertical component of acceleration impacts the computed values of both P_{AE} and P_{PE} and K_{AE} and K_{PE}.

Upward accelerations ($-k_v \cdot g$) result in smaller values of K_{AE} and larger values of P_{AE} as compared to the K_{AE} and P_{AE} values when k_v is set equal to zero. Upward accelerations ($-k_v \cdot g$) increase the value of P_{AE} due to the contribution of the term ($1 - k_v$) in Equation 33. This trend is reversed when

the vertical acceleration acts downward ($+k_v \cdot g$). Seed and Whitman (1970) and Chang and Chen (1982) showed that the change in the K_{AE} value varied with both the value of k_v and k_h. Calculations with k_v ranging from 1/2 to 2/3 of the k_h value show that the difference between the computed values of K_{AE} with a nonzero k_v value and k_v equal to zero is less than 10 percent. Seed and Whitman (1970) concluded that for typical gravity retaining wall design problems, vertical accelerations can be ignored when computing K_{AE}. The k_v value has a greater impact on the computed value of P_{PE} than on the value of P_{AE}.

Chang and Chen (1982) show that the change in the K_{PE} value varies with both the value of k_v and k_h. The difference between the values of K_{PE} with a nonzero k_v value and k_v set equal to zero increases with increasing magnitudes of both k_v and k_h. This difference can easily be greater than 10 percent. In general, vertical accelerations acting downward ($+k_v \cdot g$) will decrease the K_{PE} and P_{PE} values from the corresponding K_{PE} and P_{PE} values for which k_v is set equal to zero. The trend is reversed when the vertical acceleration acts upward ($-k_v \cdot g$). When P_{PE} acts as a stabilizing force for a structure, vertical accelerations should be considered in the computations of the value for P_{PE}. An example is the soil region below the dredge level and in front of an anchored sheet pile wall (refer to the design example in Section C.2 of Appendix C).

4.6 Cases with Surface Loadings

There are two approaches used to approximate the additional lateral earth pressures on walls due to surface loadings; (1) the wedge method of analysis and (2) finite element analyses.

In the case of a uniform surcharge q_s, the value of the dynamic active earth pressure force is computed using the modified Mononobe-Okabe relationships listed in Figure 4.18 and Equation 34 (or Equation 36 for a vertical wall retaining a horizontal backfill) for K_{AE}. The point of application of P_{AE} along the back of the wall is computed using the procedure outlined in Figures 4.19 and Figure 4.20. In this approximate procedure, the surcharge q_s is replaced by the addition of a layer of soil of height h_s equal to q_s/γ_t. The resulting problem is analyzed by adapting the Seed and Whitman's simplified procedure (of section 4.2.2) to the problem of a uniform surcharge loading as outlined in Figure 4.20.

This procedure is illustrated in example 26 at the end of this chapter.

Pseudo-static trial wedge analyses may be performed to account approximately for both uniformly and non-uniformly distributed surface loadings, as described in Section A.2 of Appendix A for dynamic active earth pressure problems. These analyses may be performed on walls whose movements satisfy the criteria listed in Table 1. Such analyses will give the total thrust against a wall. The effects of surface loading is included within the wedge analysis by including that portion of the surface loading between the back of the wall and the intersection of the slip surface and the backfill surface in the force equilibrium calculation for each wedge analyzed, as described in Section 3.6 for the static problem. The effect of the earthquake is modeled in the pseudo-static trial wedge analysis by an additional set of static forces, $k_h \cdot W$, $k_v \cdot W$, $k_h \cdot W_s$, and $k_v \cdot W_s$, where W is equal to the weight of the soil contained within the trial wedge and W_s is equal to the weight of surcharge contained within the region located above the trial wedge as shown in Figure A.3 for the active earth pressure problem. The difficult part of

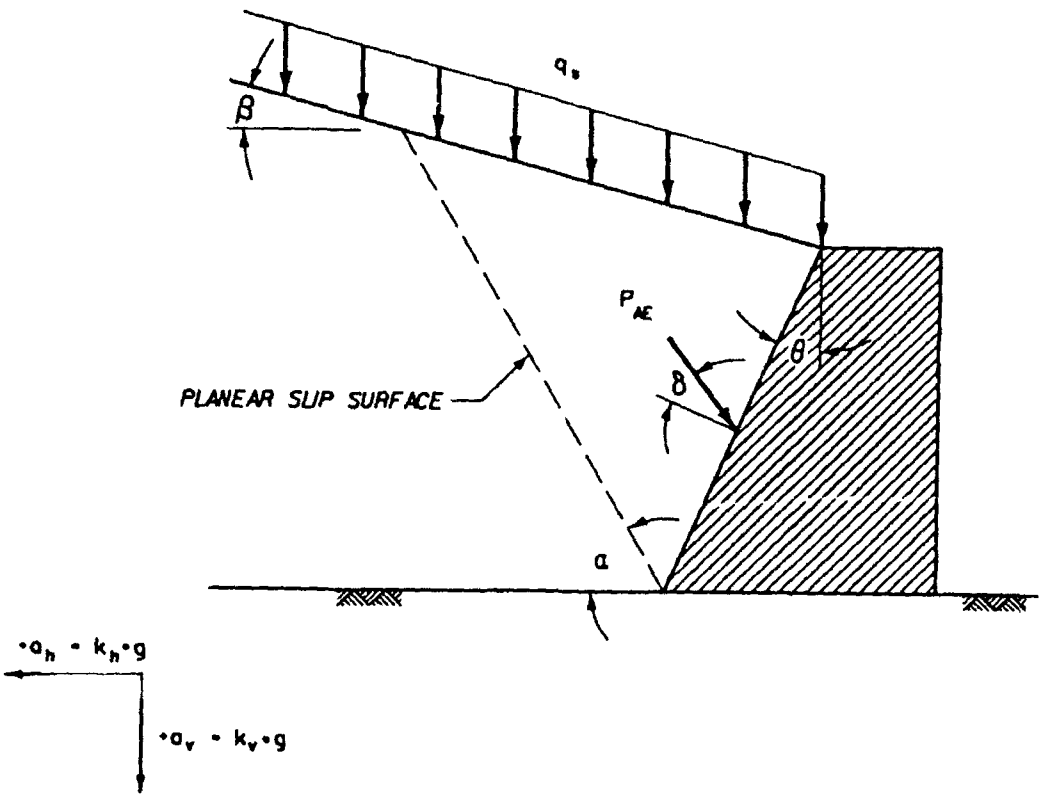

$$P_{AE} = K_{AE} \cdot \left\{ 1 + \frac{2\, q_s}{\gamma_t\, H} \cdot \left[\frac{\cos\theta}{\cos(\beta - \theta)} \right] \right\} \cdot \frac{1}{2} [\gamma_t (1 - k_v)] H^2$$

for a vertical wall ($\theta = 0$) retaining a horizontal backfill ($\beta = 0$) becomes

$$P_{AE} = K_{AE} \cdot \left\{ 1 + \frac{2\, q_s}{\gamma_t\, H} \right\} \cdot \frac{1}{2} [\gamma_t (1 - k_v)] H^2$$

These relationships are exact when the critical sliding surface is planar, as discussed in Chang and Chen (1982).

Figure 4.18 Mononobe-Okabe active wedge relationships including surcharge loading

the pseudo-static analysis is to determine the point of action of this force along the back of the wall (refer to Appendix A).

Two-dimensional finite element analyses may be used to estimate the dynamic forces against walls as a result of surface loadings. See Appendix D for a discussion of available methods.

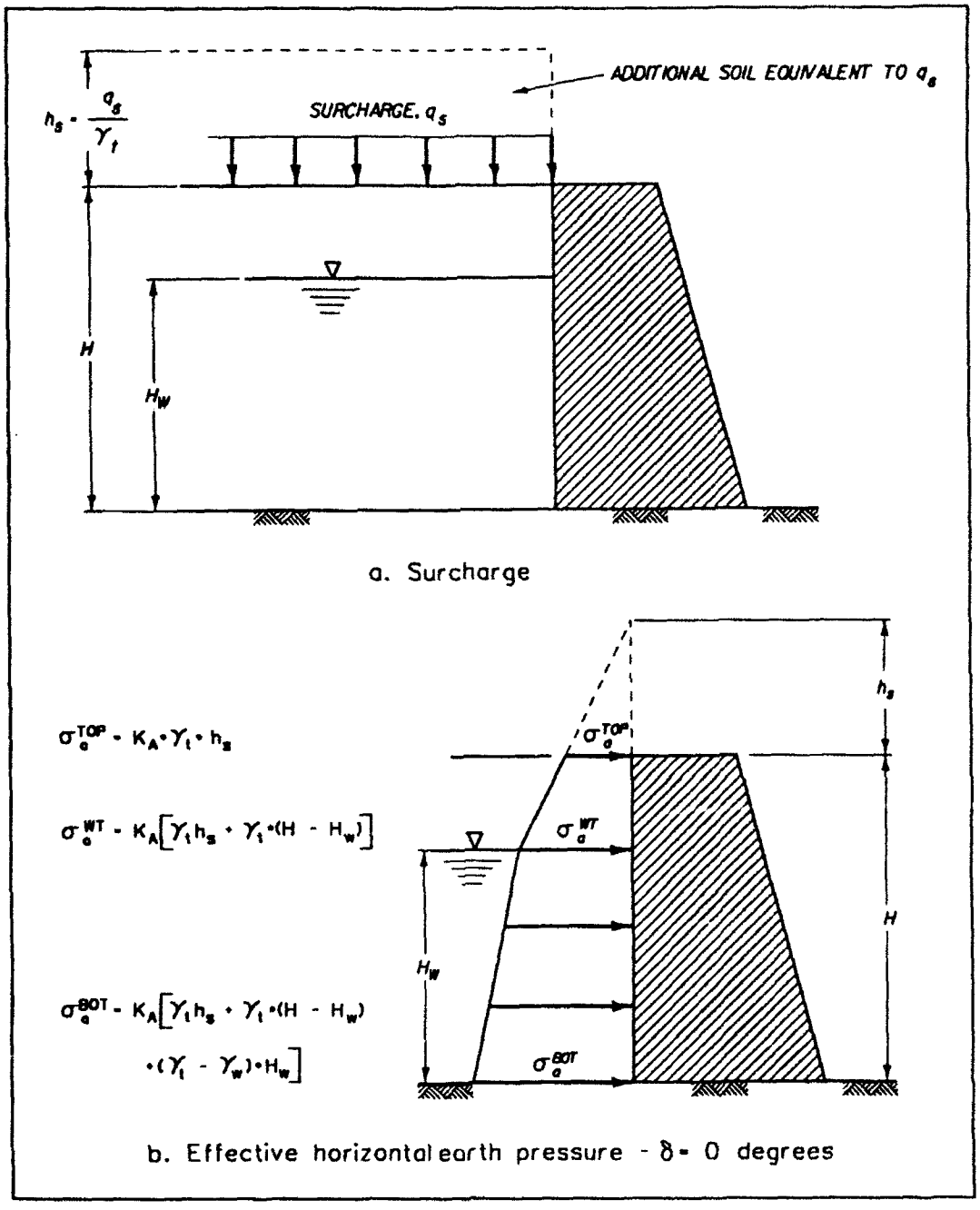

Figure 4.19 Static active earth pressure force including surcharge (Continued)

$$E_1 = \tfrac{1}{2}\left(\sigma_a^{WT} - \sigma_a^{TOP}\right)\cdot\left(H - H_w\right)$$

$$E_2 = \left(\sigma_a^{TOP}\right)\cdot\left(H - H_w\right)$$

$$E_3 = \tfrac{1}{2}\left(\sigma_a^{BOT} - \sigma_a^{WT}\right)\cdot\left(H_w\right)$$

$$E_4 = \left(\sigma_a^{WT}\right)\cdot\left(H_w\right)$$

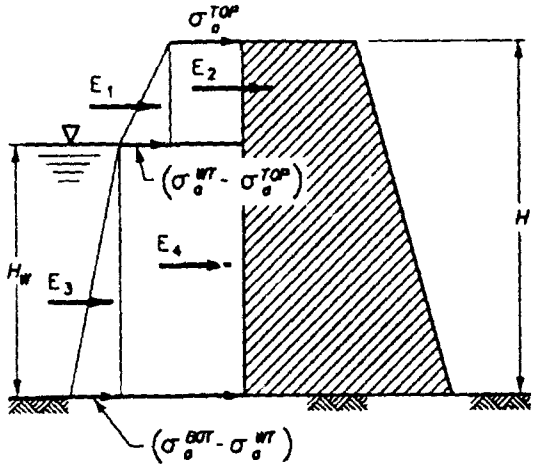

c. Equivalent forces

$$P_A = E_1 + E_2 + E_3 + E_4$$

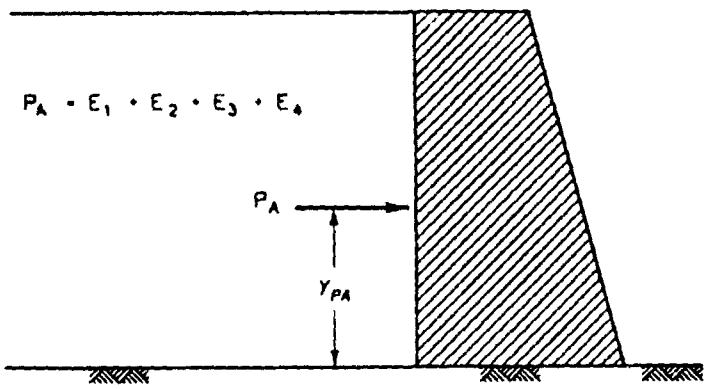

$$Y_{PA} = \frac{E_1\cdot\left[1/3(H - H_W) + H_W\right] + E_2\cdot\left[1/2(H - H_W) + H_W\right] + E_3\cdot\left[1/3H_W\right] + E_4\cdot\left[1/2H_W\right]}{P_A}$$

d. Resultant effective force and point of application

Figure 4.19 (Concluded)

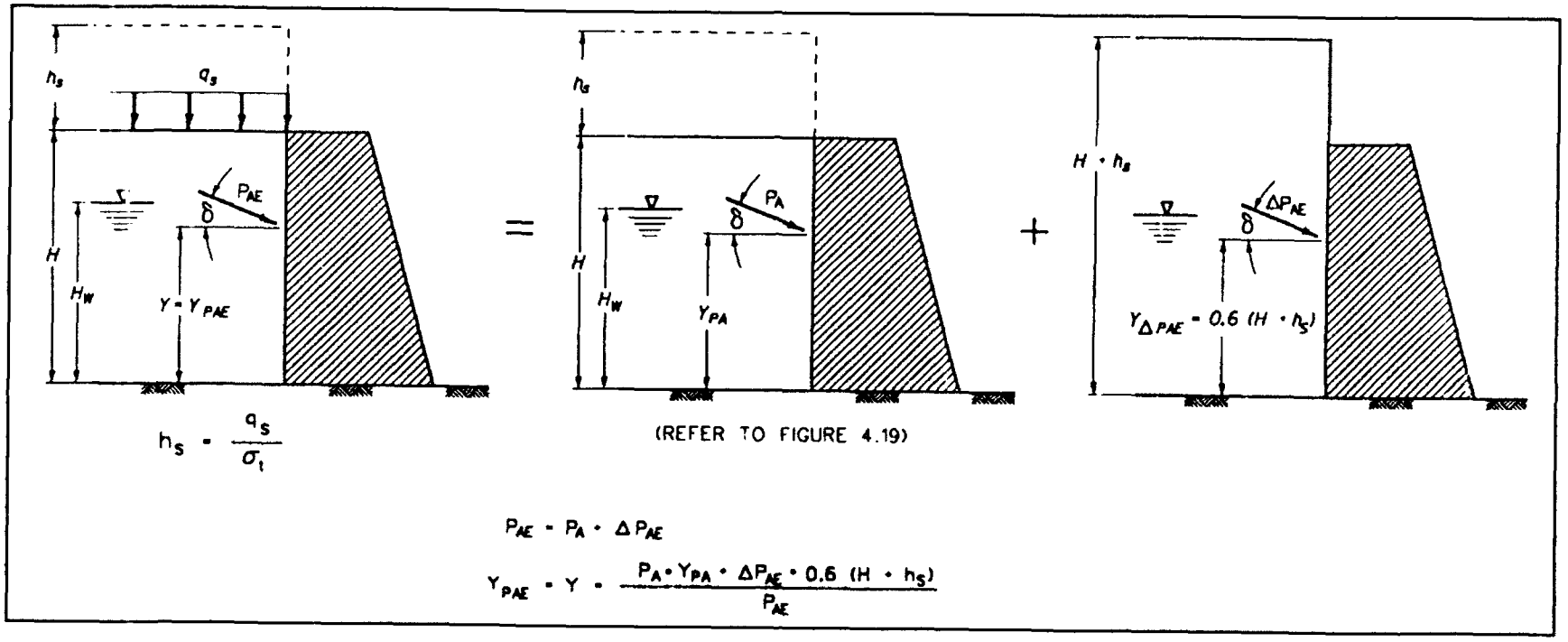

Figure 4.20 Static active earth pressure force and incremental dynamic active earth pressure force including surcharge

CHAPTER 4 - EXAMPLES

Contents

Example Problems 7 through 26.

Commentary

The following examples illustrate the procedures described in Chapter 4. The results of the computations shown are rounded for ease of checking calculations and not to the appropriate number of significant figures. Additionally, the values assigned to variables in these problems were selected for ease of computations.

Example No. 7 Reference Section: 4.2

For a wall of height H = 20 ft retaining a dry cohesionless backfill with $\phi' = 30$ degrees, $\delta = 3$ degrees, $\beta = 6$ degrees, $\theta = 0$ degrees, $k_h = 0.1$ (acceleration $k_h \cdot g$ away from the wall and inertia force $k_h \cdot W$ towards the wall) and $k_v = 0.067$ (acceleration $k_v \cdot g$ acting downward and inertia force $k_v W$ acting upward), compute K_{AE}, P_{AE}, and α_{AE}.

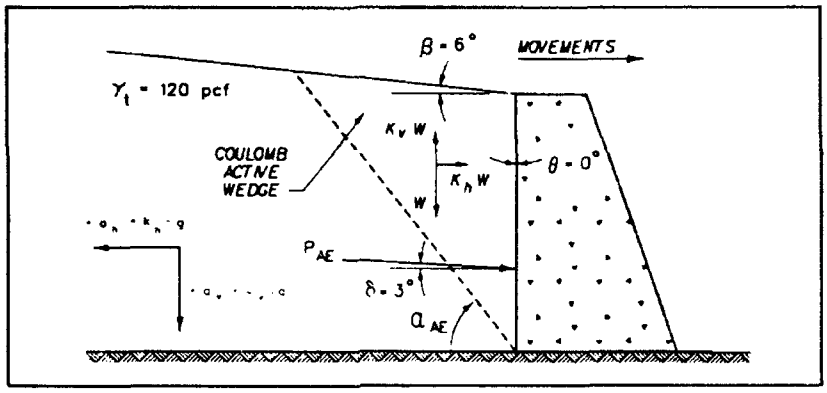

$$\psi = \tan^{-1}\left[\frac{0.1}{(1 - 0.067)}\right] \qquad \text{(by eq 35)}$$

$\psi = 6.12°$

$$K_{AE} = \frac{\cos^2(30-6.12)}{\cos(6.12)\cos^2(0)\cos(6.12+3)\left[1+\sqrt{\dfrac{\sin(30+3)\sin(30-6.12-6)}{\cos(3+6.12)\cos(6)}}\right]^2} \qquad \text{(by eq 34)}$$

$K_{AE} = 0.4268$

$$P_{AE} = 0.4268 \cdot \frac{1}{2}\left[120 \text{ pcf } (1 - 0.067)\right](20')^2 \qquad \text{(by eq 33)}$$

$P_{AE} = 9557$ lb per ft of wall

$$C_{1AE} = \left[\sqrt{[\tan(30-6.12-6)]\,[\tan(30-6.12-6) + \cot(30-6.12)]\cdot \frac{}{[1 + \tan(3+6.12)\cot(30-6.12)]}}\right]$$

$C_{1AE} = 1.0652$

$$C_{2AE} = 1 + \left[[\tan(3+6.12)] \cdot [\tan(30-6.12-6) + \cot(30-6.12)]\right]$$

$$C_{2AE} = 1.14144$$

$$\alpha_{AE} = 30 - 6.12 + \tan^{-1}\left[\frac{-\tan(30-6.12-6) + 1.0652}{1.14144}\right] \qquad \text{(by eq 37)}$$

$$\alpha_{AE} = 51.58°$$

Example No. 8 Reference Section: 4.2

Repeat Example 7 with $k_v = -0.067$ (acceleration $k_v \cdot g$ acting upward and inertia force $k_v \cdot W$ acting downward).

$$\psi = \tan^{-1}\left[\frac{0.1}{1 + 0.067}\right] \qquad \text{(by eq 35)}$$

$\psi = 5.35°$

$$K_{AE} = \frac{\cos^2(30-5.35)}{\cos(5.35)\cos^2(0)\cos(5.35+3)\left[1 + \sqrt{\frac{\sin(30+3)\sin(30-5.35-6)}{\cos(3+5.35)\cos(6)}}\right]^2} \qquad \text{(by eq 34)}$$

$K_{AE} = 0.4154$

$$P_{AE} = 0.4154 \cdot \frac{1}{2}\left[(120 \text{ pcf})(1 + 0.067)\right](20')^2 \qquad \text{(by eq 33)}$$

$P_{AE} = 10{,}639$ lb per ft of wall

$$C_{1AE} = \left[\sqrt{[\tan(30-5.35-6)]\,[\tan(30-5.35-6) + \cot(30-5.35)] \cdot [1 + \tan(3+5.35)\cot(30-5.35)]}\right]$$

$C_{1AE} = 1.0588$

$$C_{2AE} = 1 + \left[[\tan(3+5.35)] \cdot [\tan(30-5.35-6) + \cot(30-5.35)]\right]$$

$C_{2AE} = 1.3696$

$$\alpha_{AE} = 30-5.35 + \tan^{-1}\left[\frac{-\tan(30-5.35-6) + 1.0588}{1.3696}\right] \qquad \text{(by eq 37)}$$

$\alpha_{AE} = 52.45°$

Summary

Examples 7 and 8 show that when $k_v \cdot W$ acts downward (Example 8), in conjunction with the weight of the backfill wedge, the computed value for P_{AE} is about

11 percent larger than the value of P_{AE} computed for the case when $k_v W$ acts upward (Example 7).

Example No. 9 Reference Section: 4.2

For a wall of height H = 20 ft retaining a dry cohesionless backfill with ϕ' = 35 degrees, δ = 0 degrees, β = 5 degrees, θ = 0 degrees, k_h = 0.2 (acceleration $k_h \cdot g$ away from the wall and inertia force $k_h \cdot W$ towards the wall) and k_v = -0.1343 (acceleration $k_v \cdot g$ acting upward and inertia force $k_v \cdot W$ acting downward), compute K_{AE}, P_{AE}, α_{AE}, and $K_A(\beta^*, \theta^*)$.

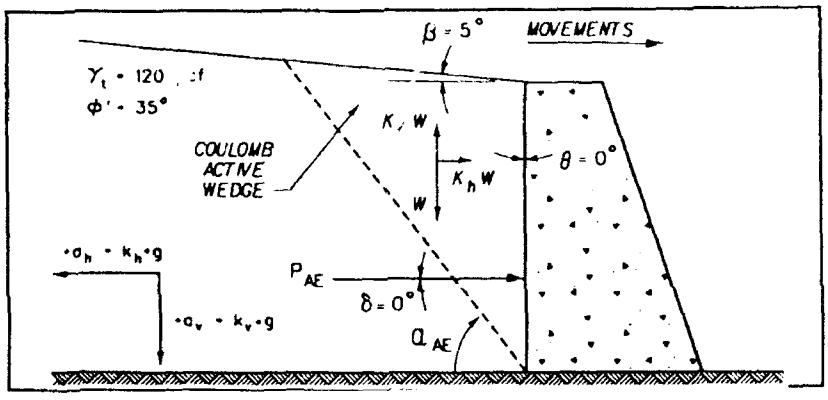

$$\psi = \tan^{-1}\left[\frac{0.2}{(1 + 0.1343)}\right] \qquad \text{(by eq 35)}$$

$\psi = 10°$

<u>Method 1</u> (K_{AE} by Mononobe-Okabe)

$$K_{AE} = \frac{\cos^2(35-10)}{\cos(10)\cos^2(0)\cos(10)\left[1 + \sqrt{\frac{\sin(35)\sin(35-10-5)}{\cos(10)\cos(5)}}\right]^2} \qquad \text{(by eq 34)}$$

$K_{AE} = 0.4044$

$$P_{AE} = 0.4044 \cdot \frac{1}{2}\left[(120 \text{ pcf})\ (1 + 0.1343)\right](20')^2 \qquad \text{(by eq 33)}$$

P_{AE} = 11,009 lb per ft of wall

$$C_{1AE} = \left[\sqrt{[\tan(35-10-5)][\tan(35-10-5) + \cot(35-10)] \cdot [1 + \tan(10)\cot(35-10)]} \right]$$

$C_{1AE} = 1.1217$

$$C_{2AE} = 1 + [[\tan(10)] \cdot [\tan(35-10-5) + \cot(35-10)]]$$

$C_{2AE} = 1.4423$

$$\alpha_{AE} = 35-10 + \tan^{-1}\left[\frac{-\tan(35-10-5) + 1.1217}{1.4423}\right] \qquad \text{(by eq 37)}$$

$\alpha_{AE} = 52.72°$

<u>Method 2</u> (Equivalent static formulation with K_A by Log Spiral Method)

$\beta^* = \beta + \psi = 15$ degrees
$\theta^* = \theta + \psi = 10$ degrees

$$F_{AE} = \frac{\cos^2(10)}{\cos(10)\cos^2(0)} \qquad \text{(by eq 39)}$$

$F_{AE} = 0.9848$

$K_A(\beta^*, \theta^*) = 0.41$ (from Table 3)

$K_{AE} = [K_A(\beta^*, \theta^*) \cdot F_{AE}] = 0.41 \cdot 0.9848 = \underline{0.404}$

$$P_{AE} = [0.404] \cdot \frac{1}{2}[(120 \text{ pcf})(1 + 0.1343)](20')^2 \qquad \text{(by eq 38)}$$

$P_{AE} = 10,998$ lb per ft of wall

<u>Method 3</u> (Equivalent static formulation with K_A from Coulomb Active wedge solution)

$$\left.\begin{array}{l} \beta^* = 15° \\ \theta^* = 10° \end{array}\right\} \text{from Method 2 calculations}$$

$$K_A(\beta^*,\theta^*) = \frac{\cos^2(35-10)}{\cos^2(10)\cos(10)\left[1+\sqrt{\frac{\sin(35)\sin(35-15)}{\cos(10)\cos(15-10)}}\right]^2} \qquad \text{(by eq 16)}$$

$K_A(\beta^*,\theta^*) = 0.4106$

$F_{AE} = 0.9848$ from Method 2 calculations

$K_{AE} = [K_A(\beta^*,\theta^*) \cdot F_{AE}] = 0.4106 \cdot 0.9848 = \underline{0.4044}$

$$P_{AE} = [0.4044] \cdot \frac{1}{2}\left[(120\text{ pcf})(1+0.1343)\right](20')^2 \qquad \text{(by eq 38)}$$

$P_{AE} = 11{,}008$ lb per ft of wall

Summary

The values for K_{AE} and P_{AE} by Equations 34 and 33, respectively, are equal to the values for the product $[K_A(\beta^*,\theta^*) \cdot F_{AE}]$ and P_{AE} (Equation 38).

Example No. 10 Reference Section: 4.2

For the example 9 problem, compute the increase in magnitude for the dynamic active earth pressure force above the static active earth pressure value, ΔP_{AE}.

$$K_A = \frac{\cos^2 (35)}{\cos^2 (0) \cos (0) \left[1 + \sqrt{\frac{\sin (35) \sin (35-5)}{\cos (0) \cos (5)}}\right]^2} \qquad \text{(by eq 16)}$$

$K_A = 0.2842$

$$P_A = 0.2842 \cdot \frac{1}{2} (120 \text{ pcf}) (20')^2 \qquad \text{(by eq 7)}$$

$P_A = 6{,}821$ lb per ft of wall

$P_{AE} = 11{,}008$ lb per ft of wall (from example 9)

$\Delta P_{AE} = P_{AE} - P_A$

$\Delta P_{AE} = 11{,}008 - 6{,}821$

$\Delta P_{AE} = 4{,}187$ lb per ft of wall

Summary

The dynamic active earth pressure force is 61 percent greater than the static active earth pressure force for the example 9 problem.

Example No. 11 Reference Section: 4.2.1

For a wall of height H = 20 ft retaining a dry cohesionless backfill with ϕ' = 35 degrees, δ = 17.5 degrees (= $\phi/2$), β = 0 degrees, θ = 0 degrees, k_h = 0.2 (acceleration $k_h g$ away from the wall and inertia force $k_h W$ towards the wall) and k_v = 0, compute K_{AE}, P_{AE}, and its point of action at elevation Y along the back of the wall using the simplified procedure for dynamic active earth pressures.

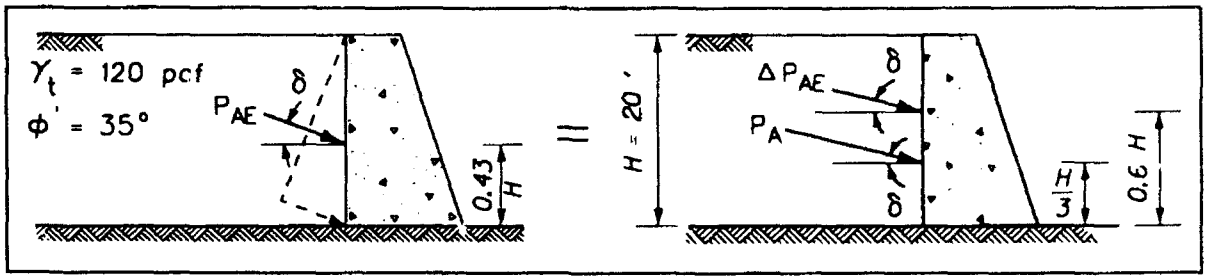

$$K_A = \frac{\cos^2(35)}{\cos^2(0)\cos(17.5)\left[1+\sqrt{\frac{\sin(35+17.5)\sin(35)}{\cos(17.5)\cos(0)}}\right]^2} \qquad \text{(by eq 16)}$$

K_A = 0.246

$$P_A = 0.246 \cdot \frac{1}{2}(120\text{ pcf})(20')^2 \qquad \text{(by eq 7)}$$

P_A = 5,904 lb per ft of wall, acting at 6.67 ft (H/3) above the base of the wall.

$$\Delta K_{AE} = \frac{3}{4} \cdot 0.2 \qquad \text{(by eq 43)}$$

ΔK_{AE} = 0.15

$$\Delta P_{AE} = 0.15 \cdot \frac{1}{2}(120\text{ pcf})(20')^2 \qquad \text{(by eq 41)}$$

ΔP_{AE} = 3,600 lb per ft of wall, acting at 12 ft (0.6 H) above the base of the wall.

$$K_{AE} = 0.246 + 0.15 \qquad \text{(by eq 42)}$$

K_{AE} = 0.396

$$P_{AE} = 5{,}904 + 3{,}600 \qquad \text{(by eq 40)}$$

P_{AE} = 9,504 lb per ft of wall

$$Y = \frac{5904 \left[\frac{20}{3}\right] + 3600\ (0.6 \cdot 20)}{9504} \qquad \text{(by eq 44)}$$

Y = 8.69 ft (0.43 H) above the base of the wall

Example No. 12 Reference Section: 4.2.3

For a wall retaining a dry cohesionless backfill with $\phi' = 35$ degrees, $\delta = 0$ degrees, $\beta = 15$ degrees, $\theta = 0$ degrees, and $k_v = - k_h/2$ (acceleration $k_v \cdot g$ acting upward and inertia force $k_v \cdot W$ acting downward), compute k_h^*, ψ, α_{AE}, K_{AE}, and P_{AE}.

Introducing $k_v = - k_h^*/2$ and rearranging, Equation 45 becomes

$$k_h^* = \frac{2 \tan(\phi - \beta)}{2 - \tan(\phi - \beta)}$$

For $(\phi - \beta) = 20$ degrees,

$k_h^* = 0.44494$

and $k_v = - 0.22247$

Note that the use of Figure 4.11 results in the same value for k_h^*.

By Equation 35, $\psi = 20$ degrees
By Equation 37, $\alpha_{AE} = 15$ degrees
By Equation 34, $K_{AE} = 1.05$

Example No. 13 Reference Section: 4.2.3

Repeat example 12 with $k_v = + k_h/2$ (acceleration $k_v \cdot g$ acting downward and inertia force $k_v \cdot W$ acting upward).

Introducing $k_v = + k_h^*/2$ and rearranging, Equation 45 becomes

$$k_h^* = \frac{2 \tan(\phi - \beta)}{2 + \tan(\phi - \beta)}$$

For $(\phi - \beta) = 20$ degrees,

$k_h^* = 0.307931$

and $k_v = 0.153966$

By Equation 35, $\psi = 20$ degrees
By Equation 37, $\alpha_{AE} = 15$ degrees
By Equation 34, $K_{AE} = 1.05$

Summary

Examples 12 and 13 show that for the limiting case of $(\phi - \beta)$ equal to ψ, the magnitude of k_h^* is dependent upon the orientation of the vertical inertia force. Both analyses result in the same values for ψ, K_{AE}, and α_{AE}. For these limiting cases the slip plane is orientated parallel to the slope of the backfill, $\alpha_{AE} = \beta$. Additionally, when the inertia force $k_v \cdot W$ acts downward (example 12) in conjunction with the weight of the backfill wedge, the value computed for P_{AE} is 44 percent greater than the value for P_{AE} when $k_v \cdot W$ acts upward (example 13) due to the term $(1 - k_v)$ in Equation 33.

Example No. 14 Reference Section: 4.3.1

For a wall of height H = 20 ft retaining a submerged cohesionless backfill with ϕ' = 35 degrees, δ = 17.5 degrees (= $\phi/2$), β = 0 degrees, θ = 0 degrees, k_h = 0.2 (acceleration $k_h \cdot g$ away from the wall and inertia force $k_h \cdot W$ towards the wall) and k_v = 0, compute the earth and water pressure forces acting on the wall for the case of <u>restrained water</u> within the backfill. Assume a hydrostatic water table within the backfill and r_u = 0.

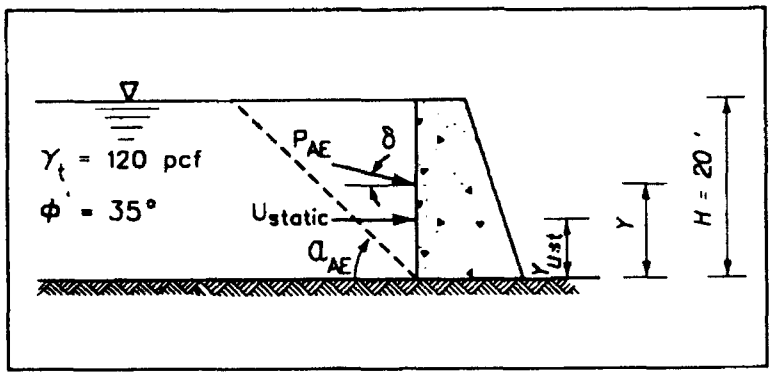

<u>Hydrostatic Water Pressure Force</u>

$$U_{static} = 1/2\ (62.4\ \text{pcf})\ (20')^2$$

U_{static} = 12,480 lb per ft of wall acting at Y_{ust} = 20'/3 = 6.67ft.

<u>Dynamic Earth Pressure Force</u>

$$\psi_{el} = \tan^{-1}\left[\frac{120 \cdot 0.2}{120 - 62.4}\right] \qquad \text{(by eq 46)}$$

ψ_{el} = 22.62 degrees

$$k_{hel} = \left[\frac{120}{120 - 62.4}\right] 0.2 = 2.08 \cdot 0.2 = 0.417 \qquad \text{(by eq 47)}$$

Method 1 (K_{AE} by Mononobe-Okabe, K_A by Coulomb)

$$K_{AE} = \frac{\cos^2(35 - 22.62)}{\cos(22.62)\cos(22.62+17.5)\left[1 + \sqrt{\dfrac{\sin(35 + 17.5)\sin(35 - 22.62)}{\cos(17.5 + 22.62)}}\right]^2} \qquad \text{(by eq 36)}$$

K_{AE} = 0.624

$$P_{AE} = 0.624 \cdot \frac{1}{2}\left[(120 - 62.4)\ (1 - 0)\right](20')^2$$ (adapted from eq 33)

P_{AE} = 7,188 lb per ft of wall

$(P_{AE})_x = P_{AE}\ (\cos\delta)$ = 6,855 lb per ft of wall

Determine Point of Application of P_{AE}

$$K_A = \frac{\cos^2(35)}{\cos^2(0) \cdot \cos(17.5)\left[1 + \sqrt{\dfrac{\sin(35 + 17.5)\sin(35)}{\cos(17.5)\cos(0)}}\right]^2}$$ (by eq 16)

$K_A = 0.246$

$$P_A = 0.246 \cdot \frac{1}{2}(120 - 62.4)\ (20)^2$$ (by eq 7)

P_A = 2,834 lb per ft of wall, acting at 6.67 ft (H/3) above the base of the wall.

$P_{AE} = P_A + \Delta P_{AE}$ (adapted from eq 40)

$\Delta P_{AE} = P_{AE} - P_A$

ΔP_{AE} = 7,188 - 2,834 = 4,354 lb per ft of wall acting at 12 ft (0.6H) above the base of the wall.

$$Y = \frac{2834\left(\frac{20}{3}\right) + 4354\ (0.6 \cdot 20)}{7188}$$ (by eq 44)

Y = 9.9 ft. (0.49 H)

Method 2 - Simplified Procedure (adapted from Seed and Whitman 1970)

Substitute k_{hel} for k_h in Equation 43:

$$\Delta K_{AE} = \frac{3}{4} \cdot 0.417 = 0.313$$

$$\Delta P_{AE} = 0.313 \cdot \frac{1}{2}\left[120 - 62.4\right](20')^2$$ (adapted from eq 41)

ΔP_{AE} = 3606 lb per ft of wall, acting at 12 ft (0.6 H) above the base of the wall.

From Method 1 calculations,

P_A = 2,834 lb per ft of wall acting at 6.67 ft above the base of the wall.

P_{AE} = 2,834 + 3,606 = 6,440 lb per ft of wall (by eq 40)

$$Y = \frac{2834\left(\frac{20}{3}\right) + 3606\,(0.6 \cdot 20)}{(6440)} \qquad \text{(by eq 44)}$$

Y = 9.65 ft (0.48 H)

Summary

The simplified procedure of analysis underestimates the P_{AE} value computed using the Mononobe-Okabe relationship by 10 percent due to the accuracy of the simplified relationship for large k_{hel} values (refer to the discussion on page 134 of Seed and Whitman 1970).

Static pore water pressures must be added for both methods.

Example No. 15 Reference Section: 4.3.1

For a wall of height H = 20 ft retaining a submerged cohesionless backfill with ϕ' = 35 degrees, δ = 17.5 degrees (= $\phi/2$), β = 0 degrees, θ = 0 degrees, k_h = 0.2 (acceleration $k_h \cdot g$ away from the wall and inertia force $k_h \cdot W$ towards the wall) and k_v = 0, compute the earth and water pressure forces acting on the wall for the case of free water within the backfill. Assume a hydrostatic water table within the backfill and r_u = 0.

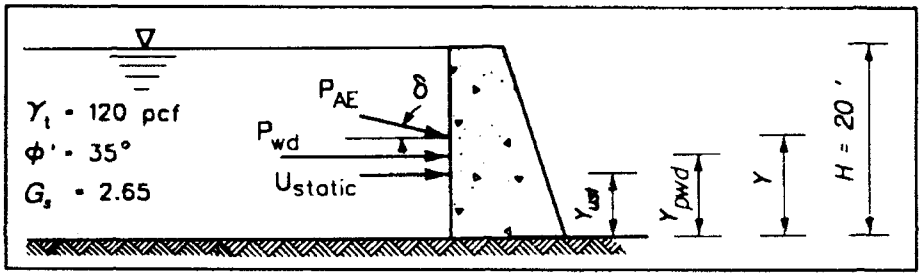

Hydrostatic Water Pressure Force

U_{static} = 1/2 (62.4 pcf) $(20')^2$

U_{static} = 12,480 lb per ft of wall,
acting at Y_{ust} = 20'/3 = 6.67 ft

Hydrodynamic Water Pressure Force

$$P_{wd} = \frac{7}{12} \cdot 0.2 \cdot (62.4 \text{ pcf})(20')^2 \qquad \text{(by eq 51)}$$

P_{wd} = 2,912 lb per ft of wall, acting at

Y_{pwd} = 0.4 · 20' = 8 ft

Dynamic Earth Pressure Force

$$k_{he2} = \frac{2.65}{2.65 - 1} 0.2 \qquad \text{(by eq 49)}$$

k_{he2} = 0.32

$$\psi_{e2} = \tan^{-1}\left[\frac{0.32}{1 - 0}\right] \qquad \text{(by eq 50)}$$

ψ_{e2} = 17.74 degrees

$$K_{AE} = \frac{\cos^2 (35 - 17.74)}{\cos (17.74) \cos (17.74 + 17.5) \left[1 + \sqrt{\frac{\sin (35 + 17.5) \sin (35 - 17.74)}{\cos (17.5 + 17.74)}}\right]^2} \quad \text{(by eq 36)}$$

$K_{AE} = 0.4965$

$$P_{AE} = 0.4965 \cdot \frac{1}{2} \left[(120 \text{ pcf} - 62.4 \text{ pcf}) (1 - 0)\right] (20')^2 \quad \text{(adapted from eq 33)}$$

$P_{AE} = 5{,}720$ lb per ft of wall

$(P_{AE})_x = P_{AE} (\cos \delta) = 5{,}455$ lb per ft of wall

Determine Point of Application of P_{AE}

From the Method 1 calculations in Example 14,

$K_A = 0.246$ and $P_A = 2{,}834$ lb per ft of wall.

$P_{AE} = P_A + \Delta P_{AE}$ (eq 40)

$\Delta P_{AE} = P_{AE} - P_A$

$\Delta P_{AE} = 5{,}720 - 2{,}834 = 2{,}886$ lb per ft of wall, acting at 12 ft (0.6 H) above the base of the wall.

$$Y = \frac{2{,}834 \left(\frac{20}{3}\right) + 2{,}886 (0.6 \cdot 20)}{5{,}720}$$

$Y = 9.4$ ft (0.47 H)

Summary

For the restrained water case (Example 14, Method 1), the total force acting normal to the wall $= P_{AE}(\cos\delta) + U_{static}$

$= 6{,}855 + 12{,}480$

$= 19{,}335$ lb per ft of wall.

For the free water case (Example 15), the total force acting on the wall $= P_{AE}(\cos\delta) + P_{wd} + U_{static} = 5{,}455 + 2{,}912 + 12{,}480 = 20{,}847$ lb per ft of wall

For this dynamic problem, the free water analysis results in an 8 percent larger total dynamic earth pressure force acting normal to the wall.

Example No. 16 Reference Section: 4.3.2

For a wall of height H = 20 ft retaining a submerged cohesionless backfill with ϕ' = 35 degrees, δ = 17.5 degrees (= $\phi/2$), β = 0 degrees, θ = 0 degrees, k_h = 0.2 (acceleration $k_h \cdot g$ away from the wall and inertia force $k_h \cdot W$ towards the wall) and k_v = 0, compute the earth and water pressure forces acting on the wall for the case of <u>restrained water</u> within the backfill. Assume a hydrostatic water table within the backfill and r_u = 0.3.

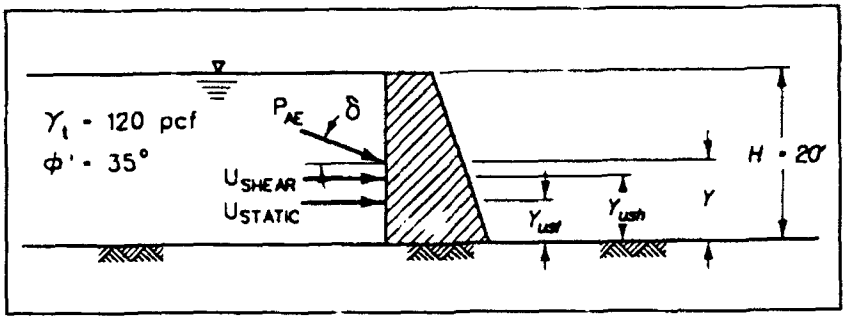

<u>Hydrostatic Water Pressure Force</u>

Linear pressure distribution with depth.

$$U_{static} = \frac{1}{2}\ 62.4\ \text{pcf}\ (20')^2$$

$$U_{static} = 12{,}480\ \text{lb per ft of wall}$$

$$\text{acting at}\quad Y_{ust} = \frac{20'}{3} = 6.67\ \text{ft above the base}$$

<u>Excess Pore Water Pressure Force</u>

Linear pressure distribution with depth for r_u = constant.

$$U_{shear} = \frac{1}{2}\left\{[\gamma_b \cdot r_u] \cdot H\right\} H \qquad \text{(adapted from eq A-9)}$$

$$U_{shear} = \frac{1}{2}\left[(120\ \text{pcf} - 62.4\ \text{pcf}) \cdot 0.3\right] \cdot (20')^2$$

U_{shear} = 3,456 lb per ft of wall, acting at

$Y_{ush} = 6.67\ \text{ft}\left(\frac{H_w}{3}\right)$ above the base of the wall with H_w = H and r_u = constant.

Dynamic Earth Pressure Force

$$\gamma_{e3} = (120 \text{ pcf} - 62.4 \text{ pcf})\ (1 - 0.3)$$
$$\gamma_{e3} = 40.32 \text{ pcf}$$ (by eq 52)

$$\gamma_{w3} = 62.4 \text{ pcf} + (120 \text{ pcf} - 62.4 \text{ pcf}) \cdot 0.3$$
$$\gamma_{w3} = 79.68 \text{ pcf}$$ (by eq 53)

$$k_{he3} = \frac{120 \text{ pcf}}{40.32 \text{ pcf}} \cdot 0.2$$
$$k_{he3} = 0.595$$ (by eq 54)

$$\psi_{e3} = \tan^{-1}[0.595]$$
$$\psi_{e3} = 30.75 \text{ degrees}$$ (by eq 55)

$$K_{AE} = \frac{\cos^2 (35 - 30.75)}{\cos (30.75) \cos (30.75 + 17.5) \left[1 + \sqrt{\dfrac{\sin (35 + 17.5) \sin (35 - 30.75)}{\cos (17.5 + 30.75)}}\right]^2}$$
$$K_{AE} = 1.033$$ (by eq 36)

$$P_{AE} = K_{AE} \cdot \frac{1}{2} \left[\gamma_{e3} (1 - k_v)\right] H^2$$
$$P_{AE} = 1.033 \cdot \frac{1}{2} \left[40.32 \text{ pcf } (1 - 0)\right] (20')^2$$ (adapted from eq 33)

$P_{AE} = 8,331$ lb per ft of wall
$(P_{AE})_x = P_{AE}(\cos\delta) = 7,921$ lb per ft of wall

Determine Point of Application of P_{AE}

$$K_A = \frac{\cos^2 (35)}{\cos^2 (0) \cos (17.5) \left[1 + \sqrt{\dfrac{\sin (35 + 17.5) \sin (35)}{\cos (17.5) \cos (0)}}\right]^2}$$ (by eq 16)

$$K_A = 0.246$$

$$P_A = 0.246 \cdot \frac{1}{2} (40.32 \text{ pcf}) (20')^2$$ (adapted from eq 7)

P_A = 1,984 lb per ft of wall, acting at 6.67 ft $\left(\frac{H}{3}\right)$ above the base of the wall.

$$\Delta P_{AE} = P_{AE} - P_A \qquad \text{(solve eq 40 for } \Delta P_{AE}\text{)}$$

ΔP_{AE} = 8,331 - 1,984 = 6,347 lb per ft of wall, acting at 12 ft (0.6 H) above the base of the wall.

$$Y = \frac{1{,}984\left(\frac{20}{3}\right) + 6{,}347\ (0.6 \cdot 20')}{8{,}331}$$

Y = 10.7 ft (0.54 • H)

Summary

Excess pore water pressures within the submerged portion of the backfill increased both the effective earth pressures and the total earth and water pressures acting along the back of the wall.

P_{AE} increased by 16 percent, from a value equal to 7,188 lb per ft of wall for the case of r_u = 0 (Method 1, example 14), to a value equal to 8,331 lb per ft of wall for the case of r_u = 0.3 (example 16).

The total force acting normal to the wall for the case of r_u equal to 0 (Method 1, example 14) = P_{AE} (cos δ) + U_{static} = 6,855 + 12,480 = 19,355 lb per ft of wall.

The total force acting normal to the wall for the case of r_u equal to 0.3 (example 16) = P_{AE} (cos δ) + U_{static} + U_{shear} = 7,921 + 12,480 + 3,456 = 23,857 lb per ft of wall.

The total force acting normal to the back of the wall increased by 23 percent from the case of r_u equal to 0, in the case of r_u equal to 0.3.

Example No. 17 Reference Section: 4.3.2

Repeat Example 16 using the reduced effective stress friction angle procedure to account for excess pore water pressures within the backfill and using $r_u = 0.3$.

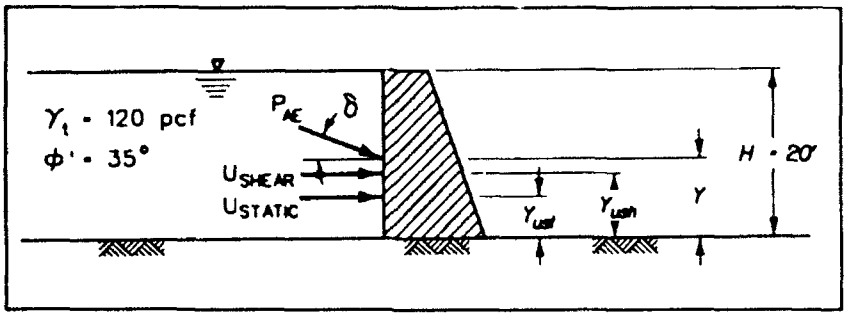

Hydrostatic Water Pressure Force

From Example 16,

U_{static} = 12,480 lb per ft of wall, acting at

$Y_{ust} = 6.67 \text{ ft} \left(\frac{H_w}{3}\right)$

Excess Pore Water Pressure Force

From Example 16,

U_{shear} = 3,456 lb per ft of wall acting at

$Y_{ush} = 6.67 \text{ ft} \left(\frac{H_w}{3}\right)$ due to r_u = constant.

Dynamic Earth Pressure Force

$$\tan\phi'_{eq} = (1 - 0.3) \tan 35° \qquad \text{(by eq 56)}$$

$$\phi'_{eq} = 26.11 \text{ degrees}$$

$$\psi_{el} = \tan^{-1}\left[\frac{120 \cdot 0.2}{(120 - 62.4)}\right] \qquad \text{(by eq 46)}$$

$$\psi_{el} = 22.62 \text{ degrees}$$

$$k_{hel} = \frac{120}{(120 - 62.4)} \cdot 0.2 \qquad \text{(by eq 47)}$$

$$k_{hel} = 0.417$$

$$K_{AE} = \frac{\cos^2 (26.1 - 22.62)}{\cos (22.62) \cos (22.62 + 17.5) \left[1 + \sqrt{\frac{\sin (26.1 + 17.5) \sin (26.1 - 22.62)}{\cos (17.5 + 22.62)}}\right]^2} \qquad \text{(by eq 36)}$$

$$K_{AE} = 0.928$$

$$P_{AE} = 0.928 \cdot \frac{1}{2} \left[(120 - 62.4)(1 - 0)\right] (20')^2 \qquad \text{(adapted from eq 33)}$$

$$P_{AE} = 10{,}690 \text{ lb per ft of wall}$$

$$(P_{AE})_x = P_{AE}(\cos\delta) = 10{,}196 \text{ lb per ft of wall}$$

Summary

The value of P_{AE} computed using the reduced effective friction angle is 28 percent larger than the value of P_{AE} computed in example 16.

Example No. 18 Reference Section: 4.3.2

For a wall of height H = 20 ft retaining a submerged cohesionless backfill with (water content = 15%) ϕ' = 35 degrees, δ = 17.5 degrees (= $\phi/2$), β = 0 degrees, θ = 0 degrees, k_h = 0.2 (acceleration $k_h \cdot g$ away from the wall and inertia force $k_h \cdot W$ towards the wall), and k_v = 0, compute the earth and water pressure forces acting on the wall for the case of free water within the backfill. Assume a hydrostatic water table within the backfill and r_u = 0.3.

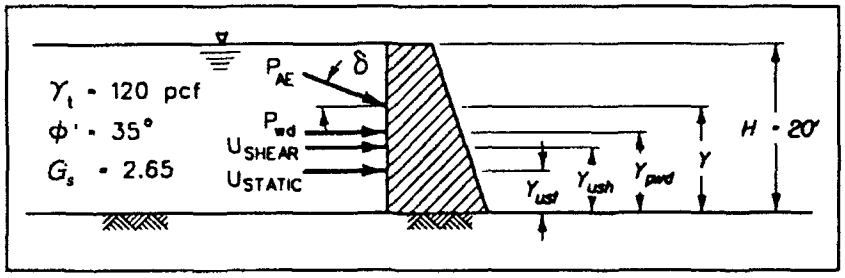

Hydrostatic Water Pressure Force

$$U_{static} = \frac{1}{2}\ (62.4\ \text{pcf})\ (20')^2$$

U_{static} = 12,480 lb per ft of wall, acting at

$$Y_{ust} = \frac{20'}{3} = 6.67\ \text{ft}$$

Excess Pore Water Pressure Force

$$U_{shear} = \frac{1}{2}\left[(120\ \text{pcf} - 62.4\ \text{pcf}) \cdot 0.3\right] \cdot (20')^2$$

U_{shear} = 3,456 lb per ft of wall, acting at

$Y_{ush} = 6.67\ \text{ft}\left(\frac{H_w}{3}\right)$ above the base of the wall with

H_w = H and r_u = constant.

Hydrodynamic Water Pressure Force

$$P_{wd} = \frac{7}{12} \cdot (0.2) \cdot (62.4\ \text{pcf})\ (20')^2 \qquad \text{(by eq 51)}$$

P_{wd} = 2,912 lb per ft of wall, acting at

$$Y_{pwd} = 0.4 \cdot 20' = 8\ \text{ft}$$

Dynamic Earth Pressure Force

$$\gamma_{e3} = (120 \text{ pcf} - 62.4 \text{ pcf})\ (1 - 0.3) \qquad \text{(by eq 52)}$$
$$\gamma_{e3} = 40.32 \text{ pcf}$$

$$\gamma_{w3} = 62.4 \text{ pcf} + (120 \text{ pcf} - 62.4 \text{ pcf}) \cdot 0.3 \qquad \text{(by eq 53)}$$
$$\gamma_{w3} = 79.68 \text{ pcf}$$

with a water content equal to 15 percent,

$$\gamma_d = \frac{\gamma_t}{1 + w}$$
$$\gamma_d = \frac{120 \text{ pcf}}{1 + 0.15} = 104.3 \text{ pcf}$$

$$k_{he4} = \frac{104.35 \text{ pcf}}{40.32 \text{ pcf}} \cdot 0.2 \qquad \text{(by eq 57)}$$
$$k_{he4} = 0.518$$

$$\psi_{e4} = \tan^{-1}\left[\frac{0.518}{1 - 0}\right]$$
$$\psi_{e4} = 27.38 \text{ degrees}$$

$$K_{AE} = \frac{\cos^2 (35 - 27.38)}{\cos (27.38) \cos (27.38 + 17.5) \left[1 + \sqrt{\dfrac{\sin (35 + 17.5) \sin (35 - 27.38)}{\cos (17.5 + 27.38)}}\right]^2} \qquad \text{(by eq 36)}$$
$$K_{AE} = 0.8136$$

$$P_{AE} = 0.8136 \cdot \frac{1}{2}\left[(40.32 \text{ pcf})\ (1 - 0)\right] (20')^2 \qquad \text{(adapted from eq 33)}$$

$$P_{AE} = 6{,}561 \text{ lb per ft of wall}$$
$$(P_{AE})_x = P_{AE}\ (\cos\delta) = 6{,}257 \text{ lb per ft of wall}$$

Determine Point of Application of P_{AE}

From example 16,

$K_A = 0.246$

$P_A = 1{,}984$ lb per ft of wall, acting at

6.67 ft $\left(\frac{H_w}{3}\right)$ above the base of the wall.

$\Delta P_{AE} = P_{AE} - P_A$ (solve eq 40 for ΔP_{AE})

$\Delta P_{AE} = 6{,}561 - 1{,}984 = 4{,}577$ lb per ft of wall, acting at 12 ft (0.6H) above the base of the wall.

$$Y = \frac{1{,}984\left(\frac{20}{3}\right) + 4{,}577\,(0.6 \cdot 20')}{6{,}561}$$

$Y = 10.4$ ft (0.52 H) above the base of the wall

Summary

For the restrained water case (example 16), the total force acting normal to the wall

$= P_{AE}\,(\cos\delta) + U_{static} + U_{shear}$

$= 7{,}921 + 12{,}480 + 3{,}456$

$= 23{,}857$ lb per ft of wall

For the free water case (example 18), the total force acting normal to the wall

$= P_{AE}\,(\cos\delta) + U_{static} + U_{shear} + P_{wd}$

$= 6{,}257 + 12{,}480 + 3{,}456 + 2{,}912$

$= 25{,}105$ lb per ft of wall

For this problem, the free water analysis results in a 5 percent larger total dynamic earth pressure force acting normal to the wall, as compared against the restrained water case.

Example No. 19 Reference Section: 4.3.3

For a wall of height H = 20 ft retaining a partially submerged cohesionless backfill with (H_w = 12 ft) with ϕ' = 35 degrees, δ = 17.5 degrees (= $\phi/2$), β = 0 degrees, θ = 0 degrees, k_h = 0.2 (acceleration $k_h \cdot g$ away from the wall and inertia force $k_h \cdot W$ towards the wall) and k_v = 0, compute the earth and water pressure forces acting on the wall for the case of <u>restrained water</u> within the backfill. Assume a hydrostatic water table within the backfill and r_u = 0.1.

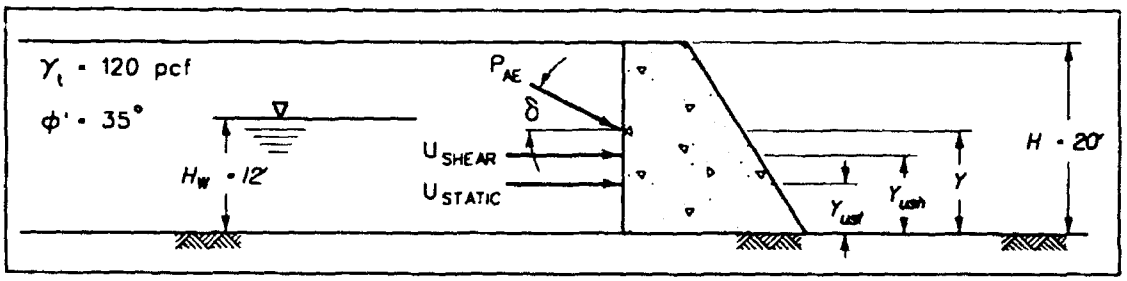

<u>Hydrostatic Water Pressure Force</u>

$$U_{static} = \frac{1}{2}\,(62.4\text{ pcf})\,(12')^2$$

$$U_{static} = 4{,}493 \text{ lb per ft of wall}$$

$$Y_{ust} = \frac{H_w}{3} = \frac{12'}{3} = 4 \text{ ft}$$

<u>Excess Pore Water Pressure Forces</u>

(refer to sections A.2.3 and A.2.4 of Appendix A)

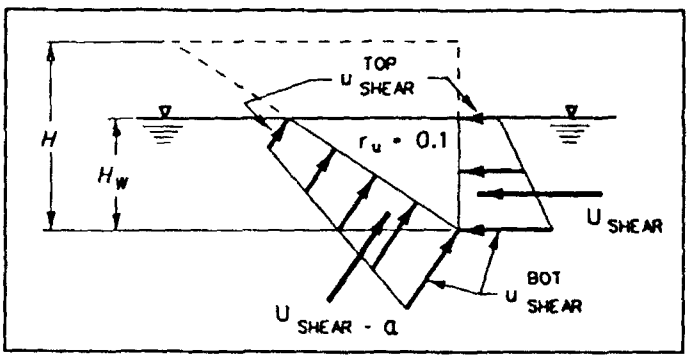

$$u^{top}_{shear} = (120\text{ pcf})\,(20' - 12')\,(0.1) \qquad \text{(by eq A-7)}$$

$$u^{top}_{shear} = 96 \text{ psf}$$

$$u_{shear}^{bot} = u_{shear}^{top} + (120\ pcf - 62.4\ pcf)(12')(0.1) \qquad \text{(by eqn. A-8)}$$
$$u_{shear}^{bot} = 165.1\ psf$$

$$U_{shear} = 1/2\ (96\ psf + 165.1\ psf)\ (12') \qquad \text{(by eq A-9)}$$
$$U_{shear} = 1{,}567\ lb\ per\ ft\ of\ wall$$

$$Y_{ush} = \frac{(96\ psf)\ (12')\ (12'/2) + 1/2\ (165.1\ psf - 96\ psf)\ (12')\ (12'/3)}{1567}$$

$$Y_{ush} = 5.47\ ft\ from\ the\ base\ of\ the\ wall$$

Dynamic Earth Pressure Force

Within the submerged backfill,

$$\gamma_{e3} = (120\ pcf - 62.4\ pcf)\ (1 - 0.1) \qquad \text{(by eq 52)}$$
$$\gamma_{e3} = 51.8\ pcf$$

For the partially submerged backfill,

$$\gamma_e = \left(\frac{12'}{20'}\right)^2 (51.8\ pcf) + \left[1 - \left(\frac{12}{20}\right)^2\right](120\ pcf) \qquad \text{(from Figure 4.13)}$$
$$\gamma_e = 95.45\ pcf$$

$$k_{he} = \left[\frac{120\ pcf}{95.45\ pcf}\right](0.2) \qquad \text{(adapted from eq 54)}$$
$$k_{he} = (1.257)\ (0.2) = 0.251$$

$$\psi_e = \tan^{-1}(0.251) \qquad \text{(adapted from eq 55)}$$
$$\psi_e = 14.11\ degrees$$

$$K_{AE} = \frac{\cos^2 (35 - 14.11)}{\cos (14.11) \cos (14.11 + 17.5) \left[1 + \sqrt{\frac{\sin (35 + 17.5) \sin (35 - 14.11)}{\cos (17.5 + 14.11)}}\right]^2}$$ (adapted from eq 36)

$K_{AE} = 0.4254$

$P_{AE} = (0.4254)\ (1/2)\ [95.45 \text{ pcf } (1 - 0)]\ (20')^2$ (adapted from eq 33)

$P_{AE} = 8{,}121$ lb per ft of wall

Determine Point of Application of P_{AE}

From example 16,

$K_A = 0.246$

Determine P_A and the point of application.

Find the vertical effective stresses slightly above the water table $(\sigma'_y)^{+WT}$ slightly below the water table $(\sigma'_y)^{-WT}$ and at the bottom of the wall $(\sigma'_y)^{BOT}$.

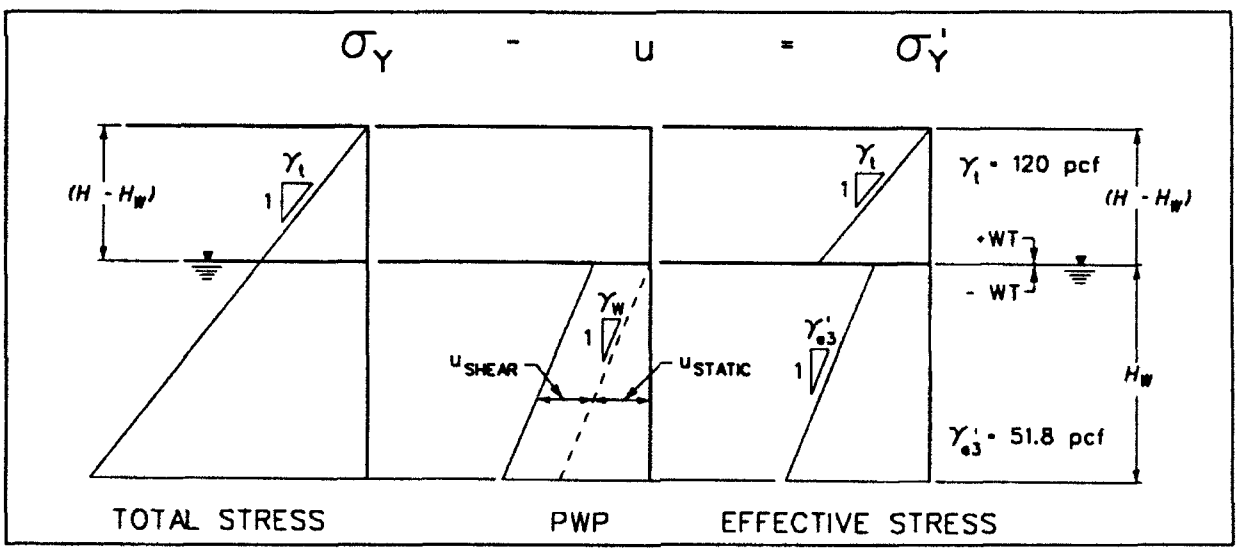

Vertical Total and Effective Stresses Slightly Above G.W.T.

$$\sigma_y = \gamma_t(H - H_w) = (120 \text{ pcf})\ (20' - 12') = 960 \text{ psf}$$

$$u = u_{static} + u_{shear} = 0$$

$$(\sigma_y')^{+WT} = \sigma_y - u = 960 \text{ psf}$$

Vertical Total and Effective Stresses Slightly Below G.W.T.

$$\sigma_y = \gamma_t(H - H_w) = (120 \text{ pcf})\ (20' - 12') = 960 \text{ psf}$$

$$u = u_{static} + u_{shear} = 0 + \gamma_t\ (H - H_w)\ r_u$$

$$u = 0 + (120 \text{ pcf})\ (20' - 12')\ (0.1) = 96 \text{ psf}$$

$$(\sigma_y')^{-WT} = \sigma_y - u = 960 \text{ psf} - 96 \text{ psf} = 864 \text{ psf}$$

Vertical Effective Stresses at the Base of the Wall

$$(\sigma_y')^{BOT} = (\sigma_y')^{-WT} + \gamma'_{e3}\ H_w = 864 \text{ psf} + (51.8 \text{ psf})\ (12')$$

$$(\sigma_y')^{BOT} = 1485.6 \text{ psf}$$

Determine the horizontal active effective stresses slightly above the water table (σ_a^{+WT}), slightly below the water table (σ_a^{-WT}), and at the bottom of the wall (σ_a^{BOT}).

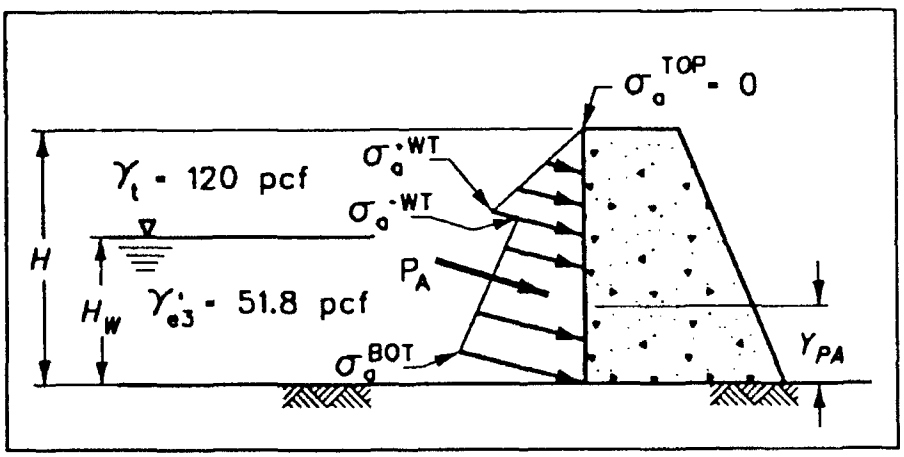

$\sigma_a^{+WT} = K_A\ (\sigma_y')^{+WT} = (0.246)\ (960\ psf)$

$\sigma_a^{+WT} = 236.2\ psf$

$\sigma_a^{-WT} = K_A(\sigma_y')^{-WT} = (0.246)\ (864\ psf)$

$\sigma_a^{-WT} = 212.5\ psf$

$\sigma_a^{BOT} = K_a(\sigma_y')^{BOT} = (0.246)\ (1{,}485.6\ psf)$

$\sigma_a^{BOT} = 365.5\ psf$

Break the effective stress distribution diagram into rectangles and triangles to find the magnitude of the resultant force and its point of application.

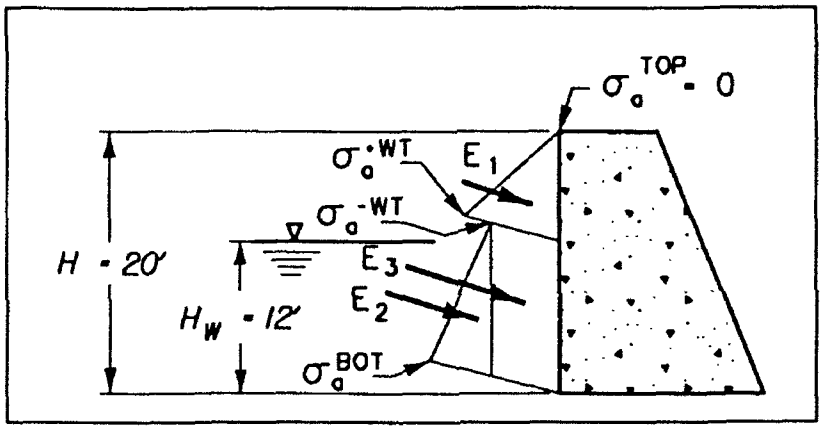

$E_1 = 1/2\ \sigma_a^{+WT}\ (H - H_W) = 1/2\ (236.2\ psf)\ (20' - 12')$

$E_1 = 944.8$ lb per ft of wall

$Y_{E1} = H_w + 1/3\ (H - H_w) = 12' + 1/3\ (20' - 12')$

$Y_{E1} = 14.67$ ft above the base of the wall

$E_2 = 1/2\left[\sigma_a^{BOT} - \sigma_a^{-WT}\right] H_W = 1/2\left[365.5\ psf - 212.5\ psf\right]\ (12')$

$E_2 = 918$ lb per ft of wall

$Y_{E2} = 1/3\ (H_w) = 1/3\ (12')$

$Y_{E2} = 4.00$ ft above the base of the wall

$E_3 = \sigma_a^{-WT}\ (H_w) = (212.5\ \text{psf})\ (12')$

$E_3 = 2{,}550$ psf

$Y_{E3} = 1/2\ (H_w) = 1/2\ (12')$

$Y_{E3} = 6.00$ ft above the base of the wall

$P_A = E_1 + E_2 + E_3 = 944.8 + 918 + 2{,}550$

$P_A = 4{,}413$ lb per ft of wall

Sum moments about the base of the wall and solve for:

$$Y_{PA} = \frac{E_1\ (Y_{E1}) + E_2\ (Y_{E2}) + E_3\ (Y_{E3})}{P_A}$$

$$Y_{PA} = \frac{(944.8)\ (14.67') + (918)\ (4.00') + (2{,}550)\ (6.00')}{4{,}413}$$

$Y_{PA} = 7.44$ ft above the base of the wall

$\Delta P_{AE} = P_{AE} - P_A$ (solve eq 40 for ΔP_{AE})

$\Delta P_{AE} = 8{,}121 - 4{,}413$

$\Delta P_{AE} = 3{,}708$ lb per ft of wall, acting at 12 ft (0.6H) above the base of the wall.

$$Y = \frac{P_A\ (Y_{PA}) + \Delta P_{AE}\ (0.6H)}{P_{AE}}$$

$$Y = \frac{(4{,}413)\ (7.44') + (3{,}708)\ (0.6)\ (20')}{8121}$$

$Y = 9.52$ ft (0.48H) above the base of the wall.

Example No. 20 Reference Section: 4.4

For a wall of height H = 20 ft retaining a dry cohesionless backfill with ϕ' = 30 degrees, δ = 3 degrees, β = 6 degrees, θ = 0 degrees, k_h = 0.1 (acceleration $k_h \cdot g$ towards the wall and inertia force $k_h W$ away from the wall), and k_v = 0.067 (acceleration $k_v \cdot g$ acting downward and inertia force $k_v W$ acting upward), compute K_{PE}, P_{PE}, and α_{PE}.

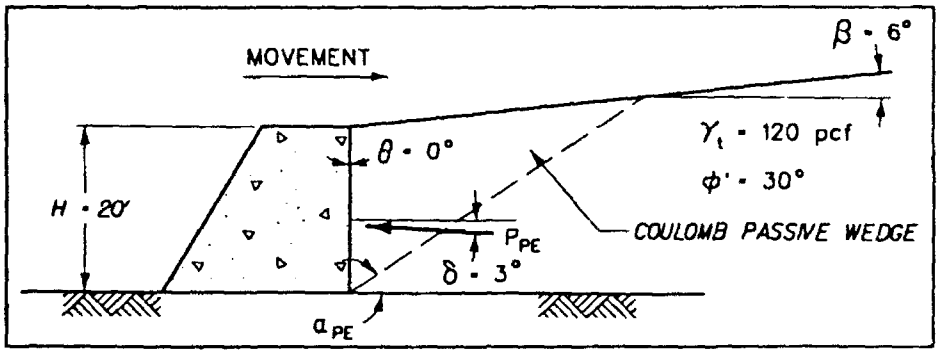

$$\psi = \tan^{-1}\left[\frac{0.1}{(1 - 0.067)}\right] \qquad \text{(by eq 35)}$$

$$\psi = 6.118°$$

$$K_{PE} = \frac{\cos^2(30 - 6.12 + 0)}{\cos(6.12)\cos^2(0)\cos(6.12 - 0 + 3)\left[1 - \sqrt{\dfrac{\sin(30 + 3)\sin(30 - 6.12 + 6)}{\cos(3 + 6.12 - 0)\cos(6 - 0)}}\right]^2} \qquad \text{(by eq 59)}$$

$$K_{PE} = 3.785$$

$$P_{PE} = 3.785\,(1/2)\,[(120\text{ pcf})\,(1 - 0.067)]\,(20')^2 \qquad \text{(by eq 58)}$$

$$P_{PE} = 84{,}754 \text{ lb per ft of wall}$$

$$c_{3PE} = \left[\sqrt{[\tan(30 + 6 - 6.12)]\,[\tan(30 + 6 - 6.12) + \cot(30 + 0 - 6.12)]\cdot [1 + \tan(3 - 0 + 6.12)\cot(30 + 0 - 6.12)]}\right]$$

$$c_{3PE} = 1.4893$$

$$c_{4PE} = 1 + \left[[\tan(3 - 0 + 6.12)] \cdot [\tan(30 + 6 - 6.12) + \cot(30 + 0 - 6.12)]\right]$$

$$c_{4PE} = 1.4547$$

$$\alpha_{PE} = 6.12 - 30 + \tan^{-1}\left[\frac{\tan(30 + 6 - 6.12) + 1.4893}{1.4547}\right] \quad \text{(by eq 61)}$$

$$\alpha_{PE} = 30.9°$$

Example No. 21 Reference Section: 4.4

Repeat Example 20 with $k_v = -0.067$ (acceleration $k_v \cdot g$ acting upward and inertia force $k_v \cdot W$ acting downward).

$$\psi = \tan^{-1}\left[\frac{0.1}{(1 - (-0.067))}\right] \qquad \text{(by eq 35)}$$

$$\psi = 5.354°$$

$$K_{PE} = \frac{\cos^2(30 - 5.35 + 0)}{\cos(5.35)\cos^2(0)\cos(5.35 - 0 + 3)\left[1 - \sqrt{\dfrac{\sin(30 + 3)\sin(30 - 5.35 + 6)}{\cos(3 + 5.35 - 0)\cos(6 - 0)}}\right]^2} \qquad \text{(by eq 59)}$$

$$K_{PE} = 3.815$$

$$P_{PE} = 3.815\,(1/2)\,[(120\text{ pcf})\,(1 - (-0.067))]\,(20')^2 \qquad \text{(by eq 58)}$$

$$P_{PE} = 97{,}695 \text{ lb per ft of wall}$$

$$c_{3PE} = \left[\sqrt{[\tan(30 + 6 - 5.35)]\,[\tan(30 + 6 - 5.35) + \cot(30 + 0 - 5.35)]\cdot [1 + \tan(3 - 0 + 5.35)\cot(30 + 0 - 5.35)]}\right]$$

$$c_{3PE} = 1.4724$$

$$c_{4PE} = 1 + \left[[\tan(3 - 0 + 5.35)] \cdot [\tan(30 + 6 - 5.35) + \cot(30 + 0 - 5.35)]\right]$$

$$c_{4PE} = 1.4071$$

$$\alpha_{PE} = 5.35 - 30 + \tan^{-1}\left[\frac{\tan(30 + 6 - 5.35) + 1.4724}{1.4071}\right] \qquad \text{(by eq 61)}$$

$$\alpha_{PE} = 31.1°$$

Summary

Examples 20 and 21 show that when the inertial force $k_v \cdot W$ acts downward (example 21) the computed value for P_{PE} is 15 percent larger than P_{PE} for the case when $k_v \cdot W$ acts upward (example 20).

Example No. 22 Reference Section: 4.4

For a wall of height H = 20 ft retaining a dry cohesionless backfill with ϕ' = 35 degrees, δ = 0 degrees, β = 0 degrees, θ = 5 degrees, k_h = 0.3 (acceleration $k_h \cdot g$ towards the wall and inertia force $k_h \cdot W$ away from the wall), and k_v = -0.12 (acceleration $k_v \cdot g$ acting upward and inertia force $k_v \cdot W$ acting downward) compute K_{PE}, P_{PE}, and α_{PE}.

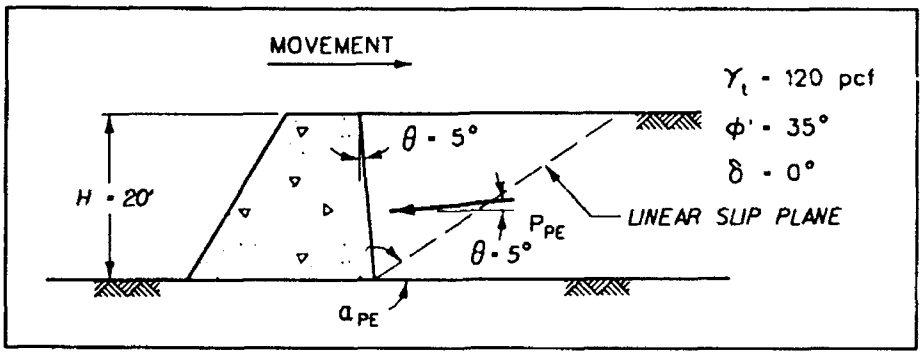

<u>Method 1</u> (K_{PE} by Mononobe - Okabe)

$$\psi = \tan^{-1}\left[\frac{0.3}{[1 - (-0.12)]}\right] \qquad \text{(by eq 35)}$$

$$\psi = 15.00°$$

$$K_{PE} = \frac{\cos^2(35 - 15 + 5)}{\cos(15)\cos^2(5)\cos(15 - 5 + 0)\left[1 - \sqrt{\dfrac{\sin(35 + 0)\sin(35 - 15 + 0)}{\cos(0 + 15 - 5)\cos(0 - 5)}}\right]^2}$$

$$K_{PE} = 2.847 \qquad \text{(by eq 59)}$$

$$P_{PE} = 2.847\,(1/2)\,(120 \text{ pcf } [1 - (-0.12)])\,(20')^2 \qquad \text{(by eq 58)}$$

$$P_{PE} = 76{,}527 \text{ lb per ft of wall}$$

$$c_{3PE} = \left[\sqrt{[\tan(35 + 0 - 15)]\,[\tan(35 + 0 - 15) + \cot(35 + 5 - 15)]\cdot [1 + \tan(0 - 5 + 15)\cot(35 + 5 - 15)]}\right]$$

$c_{3PE} = 1.1217$

$c_{4PE} = 1 + \left[[\tan(0 - 5 + 15)] \cdot [\tan(35 + 0 - 15) + \cot(35 + 5 - 15)]\right]$

$c_{4PE} = 1.4420$

$$\alpha_{PE} = (15 - 35) + \tan^{-1}\left[\frac{\tan(35 + 0 - 15) + 1.1217}{1.4420}\right] \quad \text{(by eq 61)}$$

$\alpha_{PE} = 25.8505°$

Method 2 (Equivalent Static Formulation with K_P by Log-Spiral Method)

$\beta^* = \beta - \psi = -15°$

$\theta^* = \theta - \psi = -10°$

$$K_p(\beta^*, \theta^*) = 2.52 \quad \text{(from Table 3)}$$

$$F_{PE} = \frac{\cos^2(5 - 15)}{\cos(15)\cos^2(5)}$$

$F_{PE} = 1.0117$

$P_{PE} = [2.52\ (1.0117)]\ (1/2)\ [(120\ [1 - (-0.12)])]\ (20)^2$ (by eq 62)

$P_{PE} = 68{,}530$ lb per ft of wall

Summary

The values for K_{PE} and P_{PE} computed using Mononobe - Okabe (by Equations 58 and 59) are 12 percent larger than the values for $[K_p\ (\beta^*,\ \theta^*) \cdot F_{PE}]$ and P_{PE} by Equation 62.

Example No. 23 Reference Section. 4.4

For a wall of height H = 20 ft (β = 0 degrees, θ = 5 degrees) retaining a dry cohesionless backfill with ϕ' = 35 degrees, $\delta = \phi$, compute the value of P_{PE} for the case of k_h = 0.3 (acceleration $k_h \cdot g$ towards the wall and inertia force $k_h \cdot W$ away from the wall), and k_v = -0.12 (acceleration $k_v \cdot g$ acting upward and inertia force $k_v \cdot W$ acting downward). Note that when using the log-spiral solutions, δ is set equal to -35 degrees (for Table 3 and $K_p(\beta^*, \theta^*)$. Calculate the magnitude error in the Mononobe-Okabe solution for the value of P_{PE} (K_{PE} by Equation 59 with δ = 35 degrees) versus the value of P_{PE} determined using the equivalent static formulation.

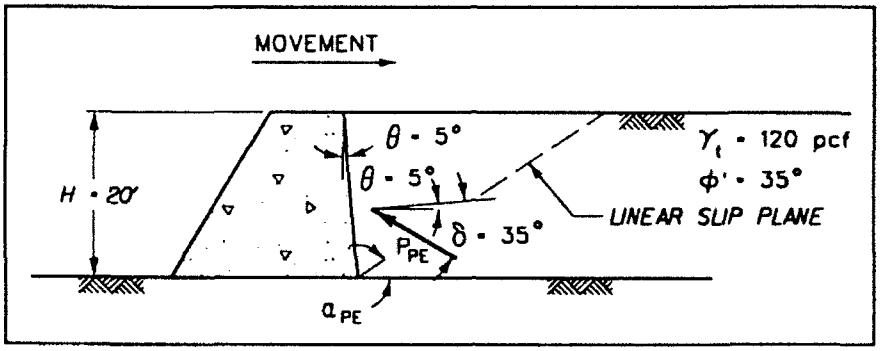

$$\psi = \tan^{-1}\left[\frac{0.3}{(1 - (-0.12))}\right] \qquad \text{(by eq 35)}$$

$$\psi = 15.00°$$

<u>Method 1</u> (Equivalent Static Formulation with K_p by Log-Spiral Method)

$$\beta^* = \beta - \psi = -15°$$

$$\theta^* = \theta - \psi = -10°$$

$$K_p(\beta^*, \theta^*) = 6.97 \qquad \text{(from Table 3)}$$

$$F_{PE} = \frac{\cos^2(5 - 15)}{\cos(15)\cos^2(5)}$$

$$F_{PE} = 1.0117$$

P_{PE} = [(6.97) (1.0117)] (1/2) [120 (1 - (-0.12))] $(20)^2$ (by eq 62)

P_{PE} = 189,546 lb per ft of wall

Method 2 (K_{PE} by Mononobe-Okabe Method)

$$K_{PE} = \frac{\cos^2 (35 - 15.0 + 5)}{\cos (15) \cos^2 (5) \cos (15 - 5 + 35) \left[1 - \sqrt{\frac{\sin (35 + 35) \sin (35 - 15 + 0)}{\cos (35 + 15 - 5) \cos (0 - 5)}}\right]^2}$$

K_{PE} = 11.507 (by eq 59)

P_{PE} = 11.507 (1/2) [(120 pcf) (1 - (-0.12))] $(20')^2$ (by eq 58)

P_{PE} = 309,308 lb per ft of wall

Summary

The Mononobe-Okabe procedure over predicts the value for P_{PE} by 63 percent. The accuracy of the Mononobe-Okabe solution decreases with increasing values of δ.

Example No. 24 Reference Section: 4.4

For a wall of height H = 20 ft retaining a submerged cohesionless backfill with ϕ = 35 degrees, δ = 17.5 degrees (= $\phi/2$), β = 0 degrees, θ = 0 degrees, k_h = 0.2 (acceleration $k_h \cdot g$ towards the wall and inertia force $k_h \cdot W$ away from the wall), and k_v = 0, compute the passive earth pressure force and water pressure forces acting on the wall for the case of restrained water within the backfill. Assume a hydrostatic water table within the backfill and r_u = 0.3.

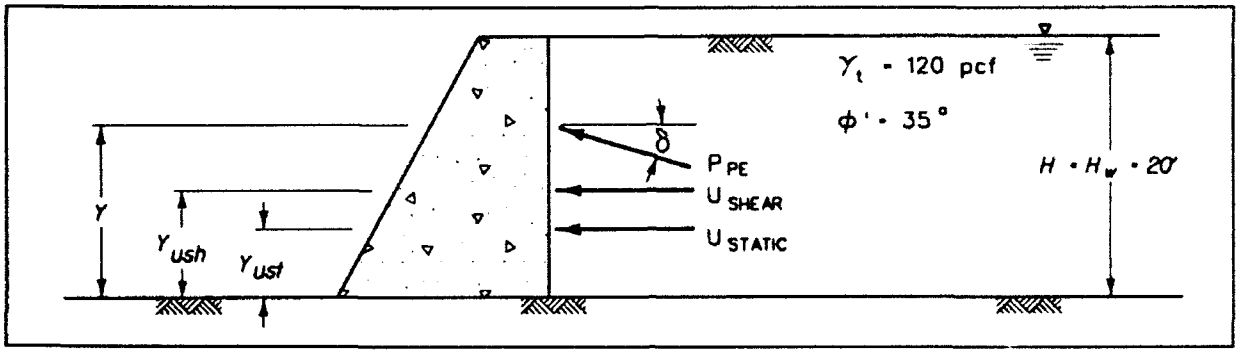

Hydrostatic Water Pressure Force

U_{static} = 1/2(62.4 pcf)(20)^2

U_{static} = 12,480 lb per ft of wall, acting at $Y_{ust} = \left(\frac{20'}{3}\right) = 6.67$ ft

Excess Pore Water Pressure Force

(refer to sections A.2.3 and A.2.4 of Appendix A)

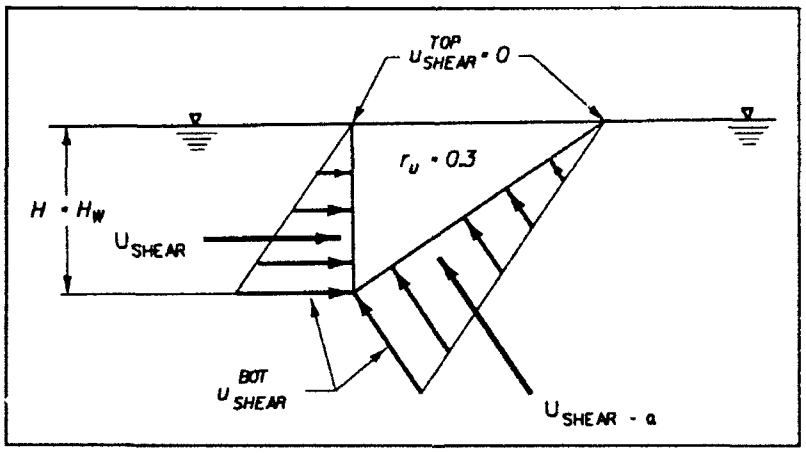

u^{top}_{shear} = 0

u^{bot}_{shear} = [(120 pcf - 62.4 pcf) · 20′](0.3) (by eq A-8)

u^{bot}_{shear} = 345.6 psf

$U_{shear} = 1/2(u^{bot}_{shear})(H_W)^2 = 1/2\ (345.6\ \text{psf})\ (20')^2$

U_{shear} = 3,456 lb per ft of wall

Y_{ush} = 1/3(H) = 6.67 ft from the base of the wall

Dynamic Earth Pressure Force

Within the submerged backfill,

$$\gamma_{e3} = (120 \text{ pcf} - 62.4 \text{ pcf})\ (1 - 0.3) \qquad \text{(by eq 52)}$$

$$\gamma_{e3} = 40.32 \text{ pcf}$$

$$k_{he3} = \left(\frac{120 \text{ pcf}}{40.32 \text{ pcf}}\right)(0.2) \qquad \text{(by eq 54)}$$

$$k_{he3} = 0.595$$

$$\psi_{e3} = \tan^{-1}[0.595] \qquad \text{(by eq 55)}$$

$$\psi_{e3} = 30.75°$$

$$K_{PE} = \frac{\cos^2(35 - 30.75 + 0)}{\cos(30.75)\cos^2(0)\cos(30.75 - 0 + 17.5)\left[1 - \sqrt{\dfrac{\sin(35 + 17.5)\sin(35 - 30.75 + 0)}{\cos(17.5 + 30.75 - 0)\cos(0 - 0)}}\right]^2}$$

$$K_{PE} = 3.518 \qquad \text{(by eq 59)}$$

$$P_{PE} = 3.518\ (1/2)\ (40.32 \text{ pcf } [1 - 0])\ (20')^2 \qquad \text{(adapted from eq 58)}$$

$$P_{PE} = 28{,}369 \text{ lb per ft of wall}$$

Example No. 25 Reference Section: 4.4.1

For a wall of height H = 20 ft retaining a dry cohesionless backfill with ϕ' = 35 degrees, δ = 0 degrees, β = 0 degrees, θ = 0 degrees, k_h = 0.2 (acceleration $k_h \cdot g$ towards the wall and inertia force $k_h \cdot W$ away from the wall), and k_v = 0, compute the value for P_{PE} using the simplified procedure for dynamic passive earth pressures.

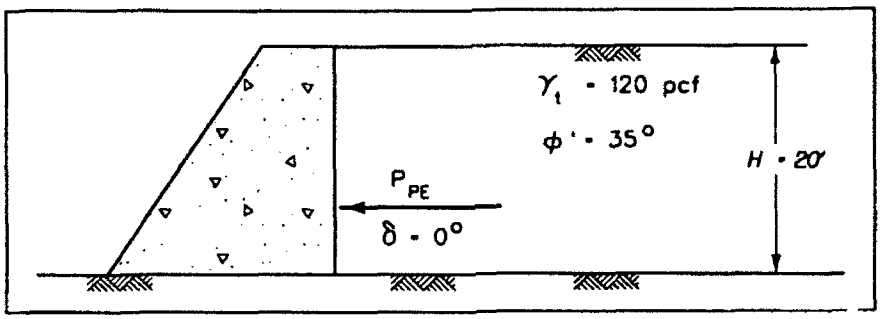

Since δ = 0, the Rankine equation gives the same result as the Coulomb equation.

$K_P = \tan^2 (45 + 35/2)$ (by eq 11)

$K_P = 3.69$

$P_P = 3.69\ (1/2)\ (120\ \text{pcf})\ (20')^2$ (by eq 13)

P_P = 88,560 lb per ft of wall, acting at 6.67 ft (1/3 H) above the base of the wall

$\Delta K_{PE} = 17/8\ (0.2)$ (by eq 67)

$\Delta K_{PE} = 0.425$

$\Delta P_{PE} = 1/2\ (120\ \text{pcf})\ (20')^2\ (0.425)$ (by eq 65)

ΔP_{PE} = 10,200 lb per ft of wall, acting at 13.33' (2/3 H) above the base of the wall.

$P_{PE} = 88{,}560 - 10{,}200$ (by eqn 64)

P_{PE} = 78,360 lb per ft of wall

Summary

The value of P_{PE} computed using the simplified procedure agrees with the value computed using the Mononobe-Okabe relationship (calculations not shown).

The simplified procedure is limited to values of δ = 0, vertical walls and level backfills.

Example No. 26 Reference Section: 4.6

For a wall of height H = 20 ft retaining a submerged cohesionless backfill with surcharge q_s = 500 psf, ϕ' = 35 degrees, δ = 17.5 degrees (= $\phi/2$), β = 0 degrees, θ = 0 degrees, k_h = 0.1 (acceleration $k_h \cdot g$ towards the wall and inertia force $k_h \cdot W$ away from the wall), and k_v = 0, compute the active earth pressure force and water pressure forces acting on the wall for the case of restrained water within the backfill. Assume a hydrostatic water table within the backfill and r_u = 0.1.

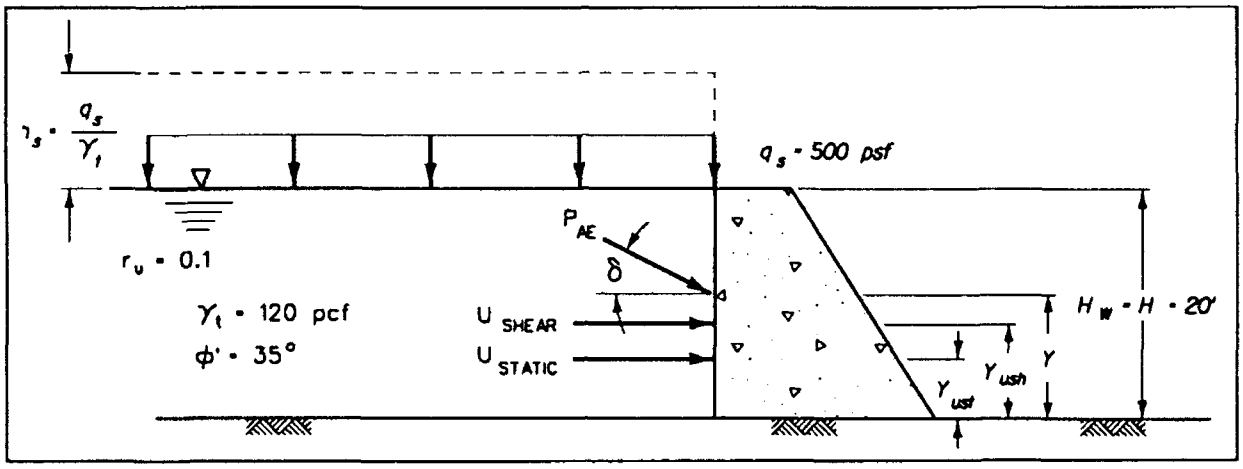

Hydrostatic Water Pressure Force

U_{static} = 1/2 (62.4 pcf) (20′) ^{2}

U_{static} = 12,480 lb per ft of wall

Y_{ust} = 20′/3 = 6.67′ (H_w/3) above the base of the wall.

Excess Pore Water Pressure Force

Linear pressure distribution with depth for r_u = constant.

$u^{top}_{shear} = q_s\ (r_u)$

u^{top}_{shear} = (500 psf) (0.1)

u^{top}_{shear} = 50 psf

$u^{bot}_{shear} = [q_s + (H - H_w)\ \gamma_t + H_w\ \gamma_b]\ r_u$

u^{bot}_{shear} = [500 psf + 0 + 20′ (120 pcf - 62.4 pcf)] (0.1)

u^{bot}_{shear} = 165.2 psf

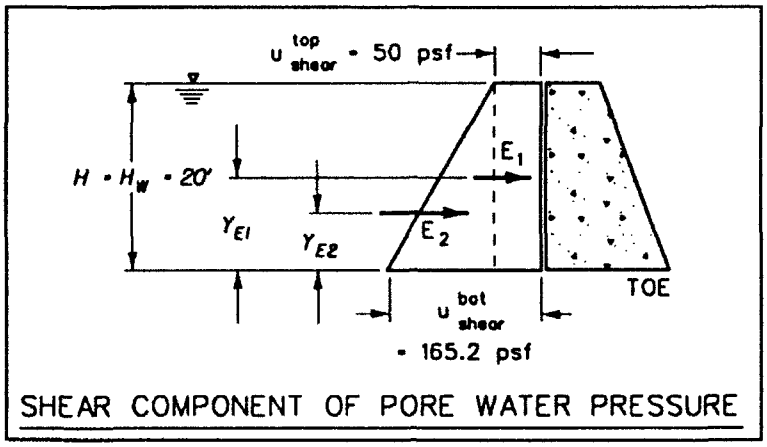

SHEAR COMPONENT OF PORE WATER PRESSURE

$E_1 = u^{top}_{shear}\ (H_w) = (50\ psf)\ (20')$

$E_1 = 1{,}000$ lb per ft of wall

$Y_{E1} = H_w/2 = 20'/2$

$Y_{E1} = 10'$ above the base of the wall

$E_2 = 1/2\left(u^{bot}_{shear} - u^{top}_{shear}\right) H_w = 1/2\ (165.2\ psf - 50\ psf)\ (20')$

$E_2 = 1{,}152$ lb per ft of wall

$Y_{E2} = 1/3\ (H_w) = 1/3\ (20')$

$Y_{E2} = 6.67'$ above the base of wall

$U_{shear} = E_1 + E_2 = 1{,}000 + 1{,}152$

$U_{shear} = 2{,}152$ lb per ft of wall

$$Y_{ush} = \frac{(E_1)\ (Y_{E1}) + (E_2)\ (Y_{E2})}{U_{shear}}$$

$$Y_{ush} = \frac{(1{,}000)\ (10') + (1{,}152)\ (6.67')}{2{,}152}$$

$Y_{ush} = 8.22$ ft above the base of the wall

Dynamic Earth Pressure Force

$\gamma_{e3} = (120\ pcf - 62.4\ pcf)\ (1 - 0.1)$ (by eq 52)

$\gamma_{e3} = 51.84$ pcf

$\gamma_{w3} = 62.4\ pcf + (120\ pcf - 62.4\ pcf)\ (0.1)$ (by eq 53)

$\gamma_{w3} = 68.16$ pcf

$$k_{he3} = \frac{120 \text{ pcf}}{51.84 \text{ pcf}} (0.1)$$ (by eq 54)

$$k_{he3} = 0.2315$$

$$\psi_{e3} = \tan^{-1} (0.2315)$$ (by eq 55)

$$\psi_{e3} = 13.03 \text{ degrees}$$

$$K_{AE} = \frac{\cos^2 (35 - 13.03)}{\cos (13.03) \cos (13.03 + 17.5) \left[1 + \sqrt{\frac{\sin (35 + 17.5) \sin (35 - 13.03)}{\cos (17.5 + 13.03)}}\right]^2}$$ (adapted from eq 36)

$$K_{AE} = 0.4069$$

$$P_{AE} = K_{AE} \left\{1 + \left[\frac{2q_s}{\gamma_{e3} H}\right]\right\} \cdot \frac{1}{2} \cdot (\gamma_{e3}) [1 - k_v] H^2$$ (adapted from Fig 4.18)

$$P_{AE} = (.4069) \left[1 + \frac{2 (500 \text{ psf})}{(51.84 \text{ pcf}) (20')}\right] \cdot \frac{1}{2} \cdot (51.84 \text{ pcf}) [1 - 0] (20')^2$$

$$P_{AE} = 8,288 \text{ lb per ft of wall}$$

<u>Determine Point of Application of P_{AE}</u>

$$K_A = \frac{\cos^2 (35 - 0)}{\cos^2(0) \cos (0 + 17.5) \left[1 + \sqrt{\frac{\sin (35 + 17.5) \sin (35 - 0)}{\cos (17.5 + 0) \cos (0 - 0)}}\right]^2}$$ (by eq 16)

$$K_A = 0.2461$$

Determine P_A and the point of application.

Find the vertical effective stress at the ground surface.

$$\sigma_y = q_s = 500 \text{ psf}$$

$$u_{static} = 0$$

$$u_{shear} = u_{shear}^{top} = 50 \text{ psf}$$

$$u = u_{static} + u_{shear} = 0 + 50 \text{ psf} = 50 \text{ psf}$$

$$(\sigma_Y')^{top} = \sigma_Y - u = 500 \text{ psf} - 50 \text{ psf} = 450 \text{ psf}$$

Find the vertical effective stress at the base of the wall.

$$(\sigma_Y')^{bot} = (\sigma_y')^{top} + \gamma_{e3}' H_w = 450 \text{ psf} + (51.84 \text{ pcf})\ (20')$$

$$(\sigma_Y')^{bot} = 1{,}487 \text{ psf}$$

Determine the horizontal active effective stress at the ground surface (σ_a^{top}), and at the bottom of the wall (σ_a^{bot}).

$$\sigma_a^{top} = K_A(\sigma_y')^{top} = (0.2461)\ (450 \text{ psf})$$

$$\sigma_a^{top} = 110.8 \text{ psf}$$

$$\sigma_a^{bot} = K_A\ (\sigma_y')^{bot} = (0.2461)\ (1{,}487 \text{ psf})$$

$$\sigma_a^{bot} = 366 \text{ psf}$$

Break the trapezoidal effective stress distribution diagram into a rectangle and a triangle to find the magnitude of the resultant force and its point of application.

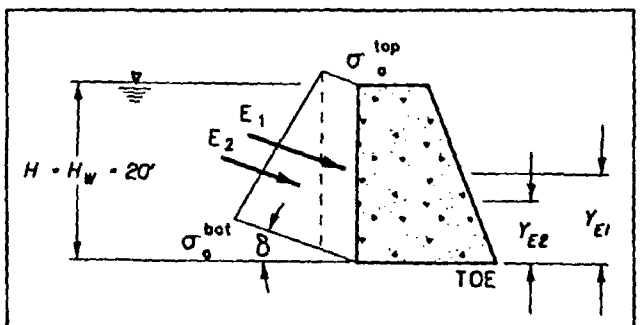

STATIC ACTIVE EARTH PRESSURE DIAGRAM

$E_1 = \sigma_a^{top}(H) = (110.8 \text{ psf})\ (20')$

$E_1 = 2{,}216$ lb per ft of wall

$Y_{E1} = 1/2(H) = 1/2\ (20')$

$Y_{E1} = 10$ ft above the base of the wall

$E_2 = 1/2\ (\sigma_a^{bot} - \sigma_a^{top})\ (H) = 1/2\ (366 \text{ psf} - 110.8 \text{ psf})\ (20')$

$E_2 = 2{,}552$ lb per ft of wall

$Y_{E2} = 1/3\ (H) = 1/3\ (20')$

$Y_{E2} = 6.67$ ft above the base of the wall

$P_A = E_1 + E_2 = 4{,}768$ lb per ft of wall

$$Y_{PA} = \frac{E_1\ (Y_{E1}) + E_2\ (Y_{E2})}{P_A} = \frac{(2216)\ (10') + (2552)\ (6.67')}{4768}$$

$Y_{PA} = 8.22$ ft above the base of the wall

$\Delta P_{AE} = P_{AE} - P_A = 8288 - 4768$ (solve eq 40 for ΔP_{AE})

$\Delta P_{AE} = 3{,}520$ lb per ft of wall

<u>Find the Point of Application of ΔP_{AE}</u>

$$h_s = \frac{q_s}{\gamma_t} = \frac{500 \text{ psf}}{120 \text{ pcf}}$$

$h_s = 4.17$ ft

$Y_{\Delta PAE} = 0.6\ (H + h_s) = 0.6\ (20' + 4.17')$ (from Figure 4.20)

$Y_{\Delta PAE} = 14.5$ ft above the base of the wall

$$Y = Y_{PAE} = \frac{P_A\ (Y_{iA}) + \Delta P_{AE}\ (Y_{\Delta PAE})}{P_{AE}} = \frac{(4768)\ (8.22') + (3520)\ (14.5')}{8{,}288}$$

$Y = 10.89$ ft $(0.54\ H)$ above the base of the wall

CHAPTER 5 EARTH PRESSURES ON WALLS RETAINING NONYIELDING BACKFILLS

5.1 Introduction

This part of the report describes two procedures that are used to compute the dynamic earth pressures acting along the back of walls retaining nonyielding backfills due to earthquake shaking. In practical terms, a wall retaining a nonyielding backfill is one that does not develop the limiting dynamic active or passive earth pressures because sufficient wall movements do not occur and the shear strength of the backfill is not fully mobilized - wall movements that are less than one-fourth to one-half of Table 1 wall movement values. Because of this, earth retaining structures such as massive concrete gravity retaining walls founded on firm rock or U-frame locks and dry docks are sometimes referred to as structures retaining "nonyielding" backfills in the literature. Two procedures for analyzing such cases are a simplified analytical procedure due to Wood (1973) and a complete soil-structure interaction analysis using the finite element method (see Appendix D).

5.2 Wood's Solution

Wood (1973) analyzed the response of a wall retaining nonyielding backfill to dynamic excitation assuming the soil backfill to be an elastic material. He provided normal mode solutions for the case of both a uniform modulus and a modulus varying linearly with depth. Since these solutions are slowly convergent for practical problems Wood (1973) presented approximate procedures based on findings from the normal mode solutions. Wood showed that a static elastic solution for a uniform 1·g horizontal body force gave very accurate results for the pressures, forces, and moments on the wall under harmonic excitation of frequency f (cyclic frequency) when dynamic amplification effects were negligible. This occurs when $\Omega = f/f_s$ is less than about 0.5 where f is the frequency of motion and $f_s = V_s/4H$ is the cyclic frequency of the first shear mode of the backfill considered as a semi-infinite layer of depth H. The limiting Ω depends on the value of V_s and the geometry of the elastic backfill but the value $\Omega < 0.5$ covers many practical cases.

In cases of wide backfills, the lateral seismic force against the wall when $\Omega < 0.5$ is given by

$$F_{sr} = \gamma H^2 \cdot k_h \tag{68}$$

acting at a height of 0.63·H above the back of the wall.

The normal stress distributions along the back of the wall were shown to be a function of (1) Poisson's ratio, υ, and (2) the lateral extent of the elastic medium behind the wall, expressed in terms of the ratio of the width of the elastic backfill divided by the height of the wall, L/H (see Figure 5.1). Two examples of the variation in the values for the normalized horizontal stresses with normalized elevations above the base of the wall are shown in Figure 5.2. A L/H value equal to 1 corresponds to a narrow backfill placed within rigid containment and a L/H value equal to 10 corresponds to a backfill of great width. The horizontal stresses at any elevation Y along the back of the wall, σ_x, are normalized by the product of γ·H in this figure.

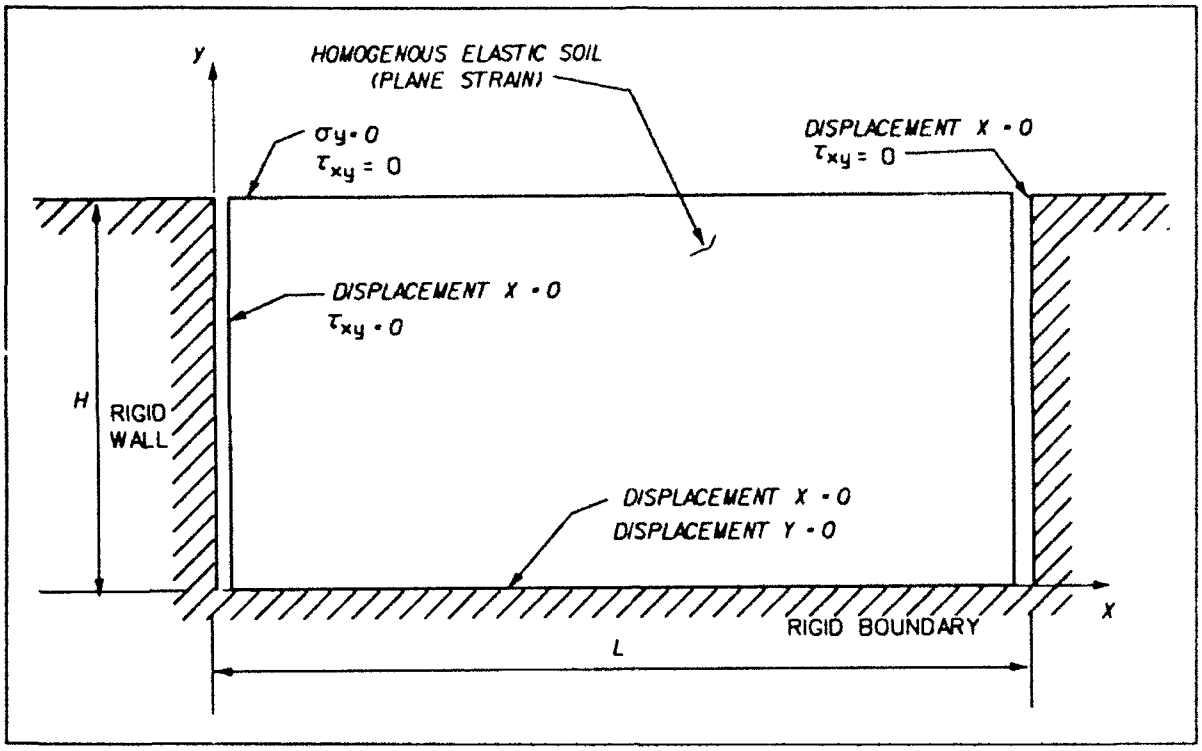

Figure 5.1 Model of elastic backfill behind a rigid wall

The resulting distributions for the horizontal stresses are parabolic, with larger values computed along the upper half of the wall, as compared to the values computed along the lower half. In addition, the results show σ_x to be larger for wide elastic backfills, as compared to those values computed for narrow elastic backfills. Figure 5.3 shows the corresponding resultant horizontal force, F_{sr}, along the back of the rigid wall and the corresponding seismic moment about the base of the rigid wall, M_{sr}, as a function of υ and L/H. Figure 5.3 presents the resultant force and moment in terms of their dimensionless values. F_{sr} acts at a height

$$Y_{sr} = \frac{M_{sr}}{F_{sr}} \tag{69}$$

The stresses shown in Figure 5.2 and the forces and moments shown in Figure 5.3 result from the application of a 1-g static horizontal body force. The values for σ_x and F_{sr} corresponding to other constant horizontal acceleration values are computed by multiplying the σ_x value from Figure 5.2 and the F_{sr} value from Figure 5.3 by the ratio of the new acceleration value coefficient, k_h.

Shaking table tests by Yong (1985) using dry sand backfill and one-half meter high walls have confirmed the applicability of Wood's simplified procedure when the predominant frequency of shaking is significantly less than the fundamental frequency of the backfill. The measured forces exceeded by a factor of 2 to 3 those predicted by the Mononobe-Okabe theory. The tests

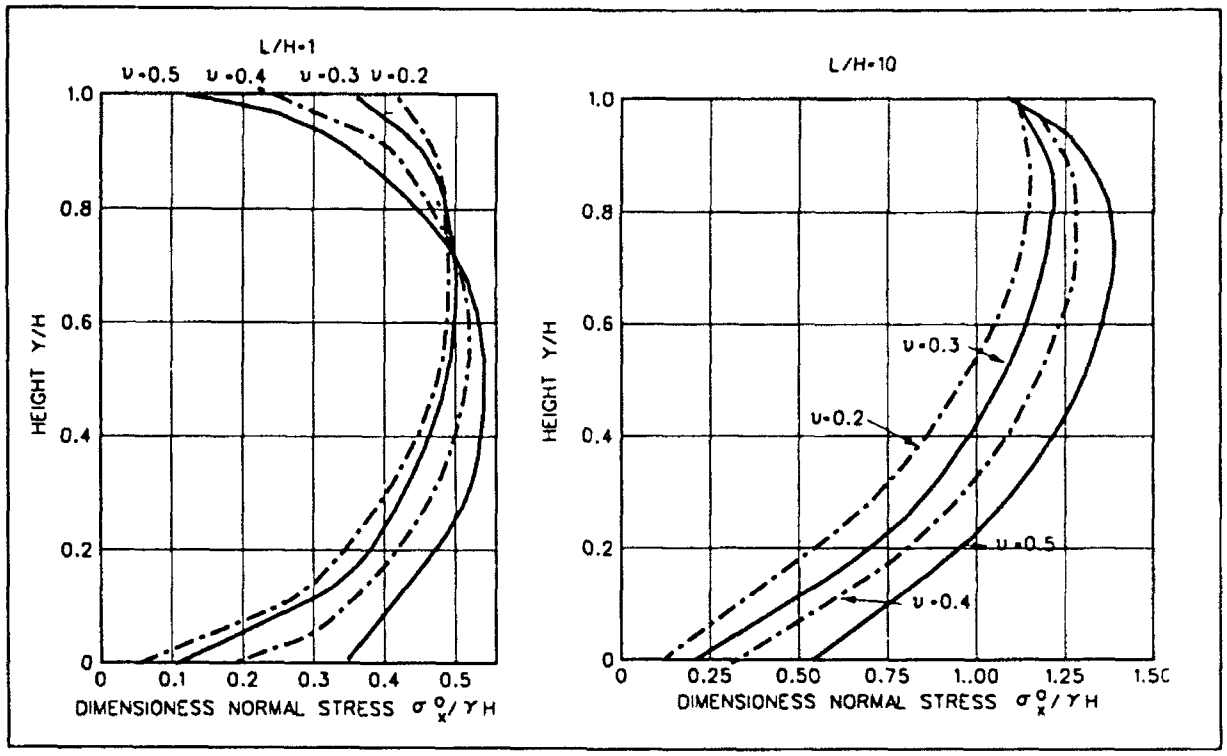

Figure 5.2 Pressure distributions on smooth rigid wall for 1-g static horizontal body force

clearly showed the limitations of Woods simplified procedure when this condition is not met. If the dynamic response of the backfill amplifies the accelerations at the level of the base of the backfill, the assumption of constant acceleration is not met and much greater earth pressures can result.

Woods (1973) has given two approximate procedures for estimating seismic soil pressures against walls retaining nonyielding backfills when dynamic effects are important; typically when $\Omega > 0.5$. In one procedure the dynamic response is represented by a number of low frequency modes together with a pseudomode called a rigid body mode to represent the combined effects of the higher modes.

The other procedure is based on the use of an equivalent two mode system with frequencies and damping ratios predefined to provide the best fit of the full dynamic modal solution.

Effective use of these procedures requires at least a broad understanding of Wood's general approach to the dynamic response of unyielding retaining structures. Therefore, the reader is referred to Wood (1973) for details on how to implement the approximate dynamic procedure.

Wood's simplified procedures do not account for: (1) vertical accelerations, (2) the typical increase of modulus with depth in the backfill, (3) the

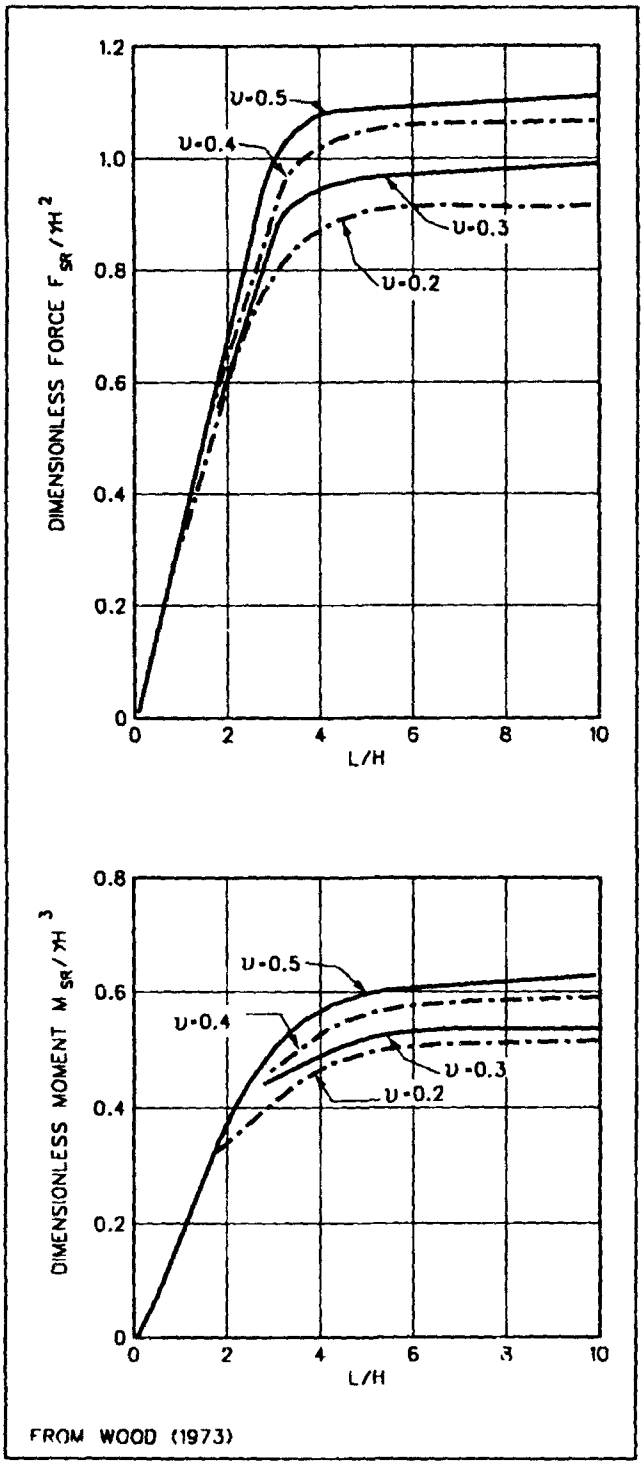

Figure 5.3 Resultant force and resultant moment on smooth rigid wall for 1-g static horizontal body force

influence of structures or other loads on the surface of the backfill, (4) the phased response at any given time for the accelerations and the dynamic earth pressures with elevation along the back of the wall, and (5) the effect of the reduced soil stiffness with the level of shaking induced in both the soil backfill and soil foundation. These and many other factors are addressed in the procedures used to simulate the dynamic response of earth retaining structures by a complete soil-structure interaction analysis.

CHAPTER 6 ANALYSIS AND DESIGN EXAMPLES FOR GRAVITY WALLS RETAINING YIELDING BACKFILLS

6.1 Introduction

Gravity walls generally are designed assuming that some permanent displacement will occur during the design seismic event. This assumption is implicit in procedures using a seismic coefficient significantly less than the acceleration coefficient corresponding to the design event. Newer methods, such as the displacement controlled approach developed by Richards and Elms (1979) explicitly consider such permanent displacements. If permanent displacements greater than about 1 inch per 20 foot height of wall ($Y/H = 0.004$, see Table 1) are not permissible, the analyses described in Chapter 8 should be used.

The procedures described in this chapter quantify the effect of earthquakes on the backfill by means of inertial forces acting on the soil mass comprising the sliding wedge within the backfill using the Mononobe-Okabe relationships for dynamic active and passive earth pressures. Where significant permanent displacements do occur, it is appropriate to use the Mononobe-Okabe theory to evaluate static and dynamic earth pressures. As discussed in Chapter 4, there is ample evidence that this theory is correct for dry sand backfills, although supporting evidence is very weak in the case of submerged backfills. With gravity walls, the dynamic increments of earth pressure generally are small compared to the inertia force on the wall itself and changes in water pressure on the poolside of the wall. Hence the exact values for dynamic earth pressures usually are not crucial. The procedures outlined in this chapter assume that all dynamic forces act simultaneously in the worst possible direction. This assumption is likely conservative (Whitman 1990; Anderson, Whitman, and Germaine 1987; Al Homound 1990), but is retained pending more complete studies of case histories from earthquakes.

Dynamic finite element analyses seldom are suitable for use during design of gravity walls, but will prove very useful for further research into issues such as the phasing of the various earth and water pressures acting upon a wall. When such studies are made, the wall should be modeled as movable in response to the forces acting upon it, and not as a rigid, nondisplacing wall.

The Mononobe-Okabe theory for computing P_{AE} and P_{PE} is described in Chapter 4. The presence of water within the backfill affects not only the static pressures acting on the wall, as discussed in Chapter 3, but also the dynamic pressures. During an earthquake, the saturated portion of the backfill that is below the water table may experience the development of additional pore water pressures due to the shear strains that occur within the backfill during earthquake shaking. These excess pore water pressures reduce the effective stresses within the backfill, resulting in both a reduction in the strength of the soil and adding to the destabilizing forces which act along the back of the wall. The magnitude of the excess pore water pressures generated within the soil during an earthquake can range from zero to the extreme case of pressures that are equal to the pre-earthquake vertical effective stresses, a state that corresponds to the liquefaction of the backfill. For those walls that have a pool of water in front of the wall, the earthquake shaking results in hydrodynamic pressures acting along the submerged portion at the front of the wall. The Westergaard procedure is used for computing the hydrodynamic

water pressures, which are superimposed on the static water pressure distribution along the front of the wall. The hydrodynamic pressure force acts to destabilize the wall and acts counter to the direction of the static water pressure force.

The seismic stability analysis of rigid walls that undergo movements during earthquakes is categorized as one of four types of analyses, as shown in Figure 6.1 and as listed in Table 4. These categories include rigid walls retaining dry backfills (Case 1), and three categories for rigid walls retaining submerged backfills, depending upon the magnitude of excess pore water pressures that are generated during the earthquake. They range from the case of no excess pore water pressures (Case 2) to the extreme case which corresponds to the complete liquefaction of the backfill (Case 4) and the intermediate case between the two (Case 3). In Figure 6.1, U_{static} corresponds to the steady state pore water pressure force acting along the back of the wall and the water pressure force when a pool exists in front of the wall. U_{shear} corresponds to the excess pore water pressure force acting along the back of the wall when excess pore water pressures are generated within the submerged portion of the backfill during the earthquake. $HF_{inertia}$ corresponds to the hydrodynamic water pressure force of a liquefied backfill. Procedures for determining the potential for liquefaction within the submerged backfill or the potential for the development of excess pore water pressures are discussed in Seed and Harder (1990) and Marcuson, Hynes, and Franklin (1990).

Experience gained with the evaluation of the stability and safety of existing Case 1 walls subjected to earthquake shaking over the last 20 years have established the validity of both the conventional equilibrium method of analysis and the displacement controlled approach for dry backfills. However, most of the case histories reported in the literature are for walls retaining submerged backfills that had liquified during earthquakes. The procedures outlined in this section for the analysis of the stability of the Case 2 through Case 4 retaining walls are proposed extensions of the procedures used for the analysis of walls retaining dry backfill.

The design of gravity walls generally begins with design for static loadings. Then the wall is checked for adequacy during the design seismic event, using the procedures described in the following sections. Adequacy for post-seismic conditions should also be checked, considering the effect of residual lateral earth pressures and any excess pore pressures as discussed in Chapter 2.

6.2 Procedure Based upon Preselected Seismic Coefficient

The force equilibrium method of analysis expresses the safety and stability of an earth retaining structure subjected to static and/or dynamic earth and water forces in terms of (1) the factor of safety against sliding along the base of the wall, (2) the ability of the wall to resist the earth and water forces acting to overturn the wall, and (3) the factor of safety against a bearing capacity failure or crushing of the concrete or rock at the toe in the case of a rock foundation. The ability of the retaining wall to resist the overturning forces is expressed in terms of the portion of the wall base remaining in contact with the foundation or, equivalently, the base area remaining in compression (Headquarters, Department of the Army EM 1110-2-2502, Ebeling et.al. 1990; Ebeling et al. 1992). Recommended minimum static and

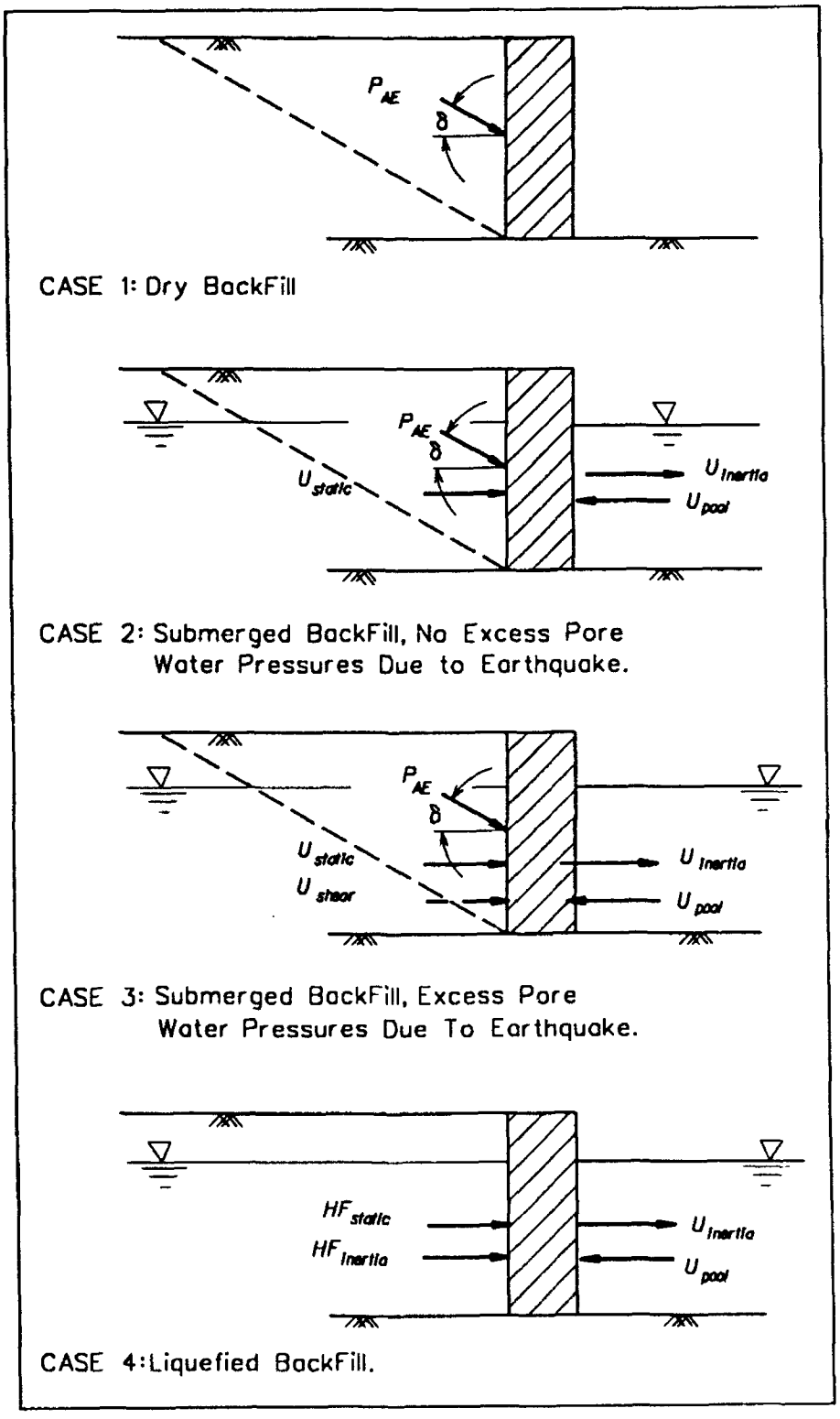

Figure 6.1 Rigid walls retaining backfills which undergo movements during earthquakes

Table 4 Section Numbers That Outline Each of the Two Design Procedures for Yielding Walls for the Four Categories of Retaining Walls Identified in Figure 6.1

	SECTION NUMBER			
Method of Analysis	Case 1 Dry Backfill	Case 2 Submerged Backfill with $r_u = 0$	Case 3 Submerged Backfill with $r_u > 0$	Case 4 Liquified Backfill ($r_u = 1$)
Preselected Seismic Coefficient	6.2.1	6.2.2	6.2.3	6.2.4
Displacement Controlled Approach for New Wall Design	6.3.1	6.3.3	6.3.5	
Displacement Controlled Approach for the Analysis of Existing Walls	6.3.2	6.3.4	6.3.6	

dynamic factors of safety and minimum base contact areas are listed in Table 5. Post-earthquake settlements should also be checked.

6.2.1 Stability of Rigid Walls Retaining Dry Backfills which Undergo Movements during Earthquakes

The force equilibrium procedure for evaluating the stability and safety of rigid walls retaining dry backfills, of the type shown in Figure 6.2, is described in Seed and Whitman (1970). This analysis, described as Case 1 in Figure 6.1, is an extension of traditional force equilibrium procedure that is used in the evaluation of the stability and safety of rigid walls under static loadings. The rigid wall is presumed to have undergone sufficient movements so that the active dynamic earth pressure force develops along the back of the wall. The eight steps in the stability analysis of the displaced rigid wall shown in Figure 6.2 are as follows:

(1) Select the k_h value to be used in the analysis; see Section 1.4 of Chapter 1.

(2) Select the k_v values to be used in the analysis; see Section 1.4.3 of Chapter 1.

Seed and Whitman (1970) found that for typical gravity earth retaining wall design problems with no toe fill in front of the wall, P_{AE} values varied

Table 5 Minimum Factors of Safety When Using the Preselected Seismic Coefficient Method of Analysis

From U.S. Army Corps of Engineers EM 1110-2-2502 (1989)

Failure Mode	Factor of Safety Static	Factor of Safety Earthquake
Sliding	1.5	1.1 - 1.2
B_E/B	100%	75% (50%-Rock)
Bearing*	3	>2

*Check for settlements, including differential settlements.

by less than 10 percent (as discussed in Section 4.5). In other cases vertical accelerations can contribute to the forces attempting to destabilize the wall (e.g. slender walls). In general, k_v values other than zero would be included in the analysis when vertical accelerations impact wall stability.

(3) Compute the dynamic active pressure force using the Mononobe-Okabe relationships as described in Chapter 4. P_{AE} is computed using equation number 33, with K_{AE} given by Equation 34 and acting at the height as given in Figure 4.7. For a vertical wall retaining a horizontal backfill, P_{AE} may be computed directly or defined in terms of the static force P_A and the incremental inertial force ΔP_{AE}. P_A is computed using Equation 7 with K_A given by Equation 16, using the Seed and Whitman's simplified procedure, and ΔP_{AE} is computed using Equation 41 with ΔK_{AE} given by Equation 43. P_{AE} is equal to the sum of these two forces (Equation 40) with a point of action, Y, given by Equation 44, as shown in Figure 4.8. For most engineered granular backfills, δ equal to $\phi/2$ is a reasonable value. Table 2 provides a list of ultimate friction angles for a variety of dissimilar materials that may interface with one another.

(4) Compute the weight of the wall W and point of application, and using the force P_{AE} and its point of application as determined in step 3, solve for the unknown forces N and T which act along the base of the wall using the horizontal and vertical force equilibrium equations.

The force W is computed per lineal foot of wall by multiplying the unit cross-sectional area of the wall by a representative value for the unit weight of the section. The resultant force acts at the center of mass for the cross section.

The total normal force between the wall and the foundation is equal to

$$N = W + (P_{AE})_Y \tag{70}$$

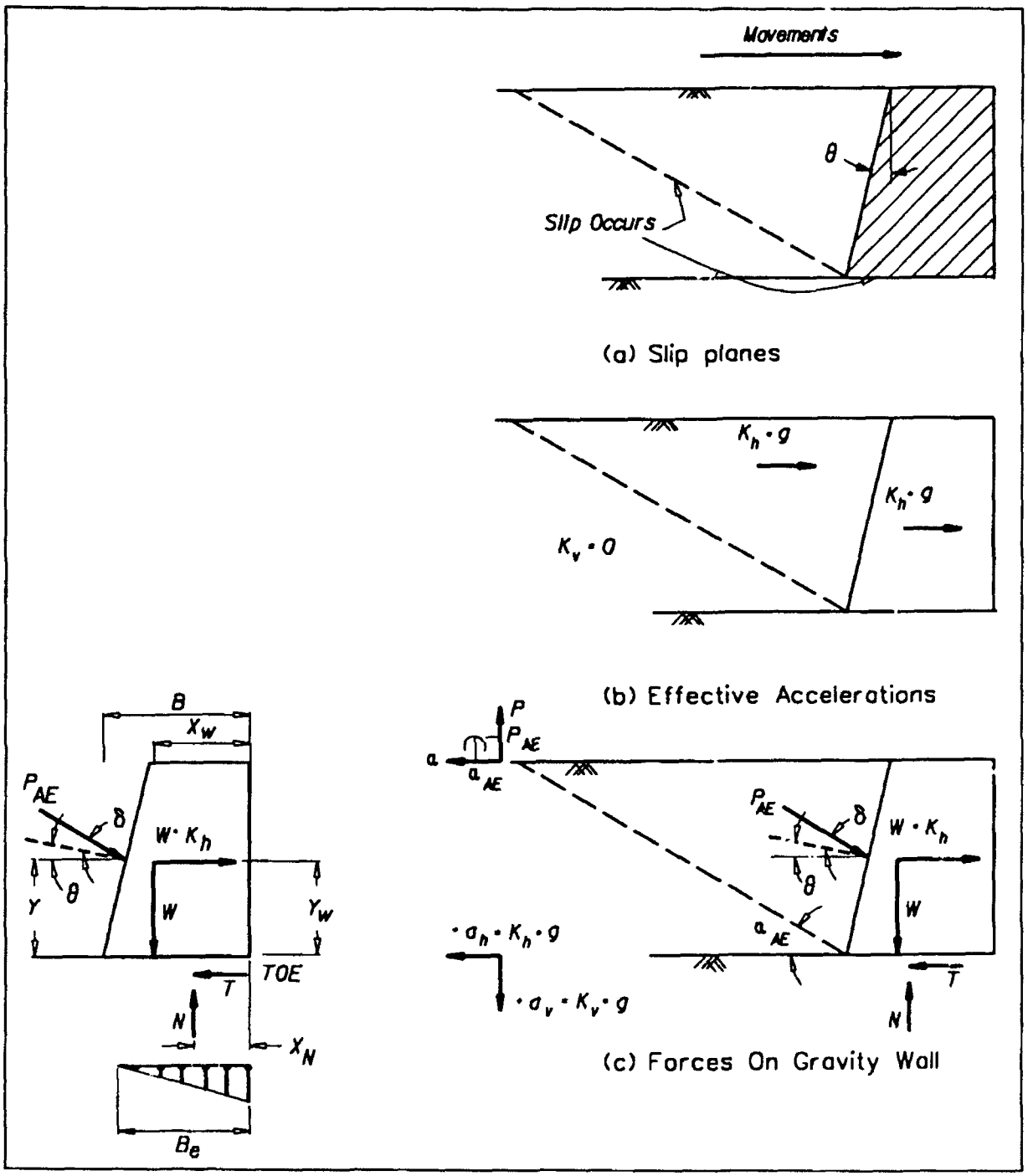

Figure 6.2 Rigid walls retaining dry backfill which undergo movements during earthquakes (case 1 in Figure 6.1)

where

W = weight of the wall
$(P_{AE})_Y$ = the vertical component of P_{AE}.

The point of action of the force N, X_N is computed by summing moments about the toe of the wall

$$X_N = \frac{W(X_W) + (P_{AE})_Y (X_{PAE}) - (P_{AE})_X (Y_{PAE}) - W(k_h)Y_W}{N} \tag{71}$$

where

$(P_{AE})_X = P_{AE} \cos(\delta + \theta)$
$(P_{AE})_Y = P_{AE} \sin(\delta + \theta)$
$X_{PAE} = B - (Y_{PAE}) \tan \theta$
$Y_{PAE} = Y$
X_W, Y_W = center of mass for the wall, as measured from the toe of the wall and the base of the wall, respectively.

The horizontal force T is the shear force required for sliding equilibrium of the wall and is equal to

$$T = (P_{AE})_X + W \cdot k_h \tag{72}$$

where

$W \cdot k_h$ = horizontal inertia force of the wall.

(5) Compute the factor of safety against sliding, F_s.

$$F_s = \frac{\text{ultimate shear force}}{\text{shear force required for equilibrium}} \tag{73}$$

The ultimate shear force along the base, T_{ult}, is given by

$$T_{ult} = N \cdot \tan\delta_b \tag{74}$$

where

δ_b = the base interface friction angle.

(6) Compare the computed factor of safety against sliding to the required factor of safety. Many retaining walls are designed using static active earth pressures with a factor of safety of 1.5 against sliding along the base. For temporary loading cases, such as earthquakes, the minimum required factor of safety is equal to 1.1 or 1.2 (Table 5). For a ductile wall to foundation interface, as the value of F_s approaches the minimum required value, the magnitude of the translation of the structure will increase as the value of F_s decreases (Newmark 1965). For a bonded interface, the displacements will be small until the bond is ruptured (at $F_s = 1.0$) and a brittle failure results.

(7) The overturning criterion is expressed in terms of the percentage of base contact area B_e/B, where B_e is the width of the area of effective base contact. Assuming that the bearing pressure varies linearly between the base of the wall and the foundation, the normal stress is a maximum at the toe ($q = q_{max}$) and a minimum at the inner edge ($q = 0$) as shown in Figure 6.3.

$$B_e = 3 \cdot x_N \tag{75}$$

An alternative assumption regarding base pressure distribution and contact area was suggested by Meyerhof (1953). Meyerhof assumed a uniform distribution of pressure along the base, resulting in an effective base contact equal to

$$B_e' = 2 \cdot x_N . \tag{76}$$

Meyerhof's pressure distribution has been used widely for foundations on soil and is most appropriate for foundation materials that exhibit ductile mechanisms of failure. The assumption is less appropriate for brittle materials.

Many retaining walls are designed using static active earth pressures with full contact along the base, B_e/B (or B'_e/B), equal to 100 percent. For temporary loading cases, such as earthquakes, this criteria is relaxed to a minimum value of 75 percent, 50 percent for rock foundations (Table 5).

(8) For those structures founded on rock, the factor of safety against bearing capacity failure, or crushing of the concrete or the rock at the toe, can be expressed as

$$F_b = \frac{q_{ult}}{q_{max}} \tag{77}$$

where q_{ult} is the ultimate bearing capacity or compressive strength of the concrete or the rock at the toe and q_{max} is the maximum bearing pressure at the toe. For brittle materials like unconfined concrete, the ultimate bearing capacity is equal to the compressive strength of the material. Building codes are commonly used to obtain values for the allowable bearing stress on rock, q_{all}. Alternately, a large factor of safety is applied to the unconfined compressive strength of intact samples. The maximum bearing pressure q_{max} is restricted to an allowable bearing capacity q_{all}. For ductile foundation materials that undergo plastic failure, the ultimate bearing capacity is greater than the compressive strength of the material, excluding those foundation materials exhibiting a loss in shear resistance due to earthquake-induced deformations or due to the development of residual excess pore water pressures. In these cases, a conventional bearing capacity evaluation is conducted to establish the post-earthquake stability of the structure.

In stability analyses in which the vertical accelerations are considered, the force acting downward through the center of mass of the wall that represents the weight of the wall, W, in Figure 6.2, is replaced by the force

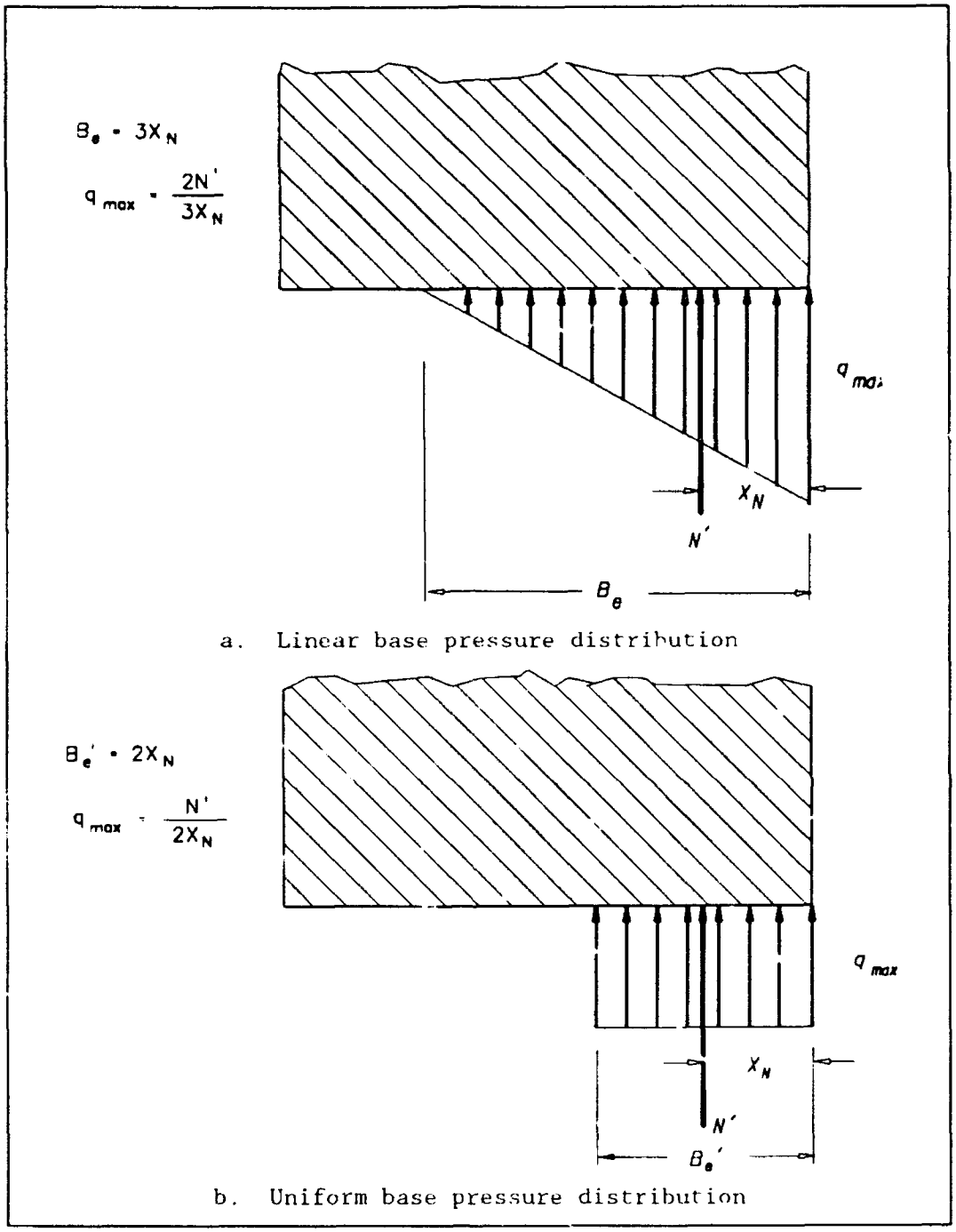

Figure 6.3 Linear and uniform base pressure distributions

$W \cdot (1 - k_v)$ acting downward. The first term in Equations 70 and 71, W and $W \cdot X_w$ are replaced by $W \cdot (1-k_v)$ and $W \cdot (1-k_v) \cdot X_w$, respectively The direction in which the vertical inertia force, $k_v \cdot W$, acts is counter to the direction assigned to the effective vertical acceleration, $k_v \cdot g$. Vertical accelerations will also affect the values for P_{AE} (Equation 33) and K_{AE} (Equation 34), as described in

Section 4.2. The stability should be checked for the possibility of k_v acting in either direction.

This procedure is illustrated in example 27 at the end of this chapter.

6.2.2 Stability of Rigid Walls Retaining Submerged Backfills which Undergo Movements During Earthquakes - No Excess Pore Water Pressures

The presence of water within the backfill and in front of the wall results in additional static and dynamic forces acting on the wall and alters the distribution of forces within the active soil wedge developing behind the wall. This section describes the first of three proposed force equilibrium procedures used in the evaluation of the stability and safety of rigid walls retaining submerged or partially submerged backfills and including a pool of water in front of the wall, as shown in Figure 6.4. This analysis, described as Case 2 in Figure 6.1, assumes that no excess pore water pressures are generated within the submerged portion of the backfill or within the foundation during earthquake shaking. The evaluation of the potential for the generation of excess pore water pressures during the shaking of the submerged soil regions is determined using the procedure described in Seed and Harder (1990) or Marcuson, Hynes, and Franklin (1990). The rigid wall is presumed to have undergone sufficient movements so that the active dynamic earth pressure force develops along the back of the wall. Many of the details regarding the procedures used in the eight steps of the stability analysis of walls retaining dry backfills (Section 6.2.1) are similar to those procedures used for submerged backfills, and the explanations for these common steps are not repeated in this section. The eight steps in the stability analysis of the displaced rigid wall retaining submerged backfill as shown in Figure 6.4 are as follows:

(1) Select the k_h value to be used in the analysis; see Section 1.4 of Chapter 1.

(2) Consider k_v, as discussed in Section 1.4.3.

(3) Compute P_{AE} using the procedure described in Section 4.3. U_{static} is determined from the steady state flow net for the problem. By definition, only steady state pore water pressures exist within the submerged backfill and foundation of a Case 2 retaining structure ($r_u = 0$). In the restrained water case of a fully submerged soil wedge with a hydrostatic water table, P_{AE} is computed (Equations 33 and 38) using an effective unit weight equal to γ_b. K_{AE} (Equation 34) or $K_A(\beta^*,\theta^*)$ (Equation 38) are computed using an equivalent horizontal acceleration, k_{hel}, and an equivalent seismic inertia angle, ψ_{el}, given by Equation 47 and 48. In the case of a partially submerged backfill, this simplified procedure will provide approximate results by increasing the value assigned to the effective unit weight based upon the proportion of the soil wedge that is above and below the water table. A more refined analysis may be conducted using the trial wedge procedure (Section 3.4) for the forces shown in Figure 6.4. For most engineered granular backfills, δ equal to $\phi/2$ is a reasonable value (Table 2).

(4) Compute the weight of the wall W and point of application, and using the force P_{AE} and the point of application as determined in step 3, solve for the unknown forces N' and T which act along the base of the wall using the horizontal and vertical force equilibrium equations.

The force W is computed per lineal foot of wall by multiplying the unit cross-sectional area of the wall by a representative value for the unit weight of the section. The resultant force acts at the center of mass for the cross section.

The effective normal force between the wall and the foundation is equal to

$$N' = W + (P_{AE})_Y - U_b \tag{78}$$

where

W = weight of the wall

$(P_{AE})_Y$ = the vertical component of P_{AE}

U_b = resultant pore water pressure force along the base of the wall

The point of action of the force N', $X_{N'}$ is computed by summing moments about the toe of the wall

$$X_{N'} = \frac{M_W + M_{PAE} - U_{static}(Y_{ust}) - U_b(X_{ub}) + M_{pool}}{N'} \tag{79}$$

where

$$M_W = W(X_W) - W(k_h)Y_W$$

$$M_{PAE} = (P_{AE})_Y\ (X_{PAE}) - (P_{AE})_X\ (Y_{PAE})$$

$$M_{pool} = U_{pool}(Y_{up}) - U_{inertia}(Y_{ui})$$

$(P_{AE})_X = P_{AE} \cos(\delta + \theta)$

$(P_{AE})_Y = P_{AE} \sin(\delta + \theta)$

$X_{PAE} = B - (Y_{PAE}) \tan \theta$

$Y_{PAE} = Y$

Y_{ust} = point of action of U_{static} (from flow net)

Y_{up} = point of action of U_{pool} ($= H_p/3$)

Y_{ui} = point of action of $U_{inertia}$ (see Appendix B)

Y_{ub} = point of action of U_b (from flow net)

X_W, Y_W = center of mass for the wall, as measured from the toe of the wall and the base of the wall, respectively.

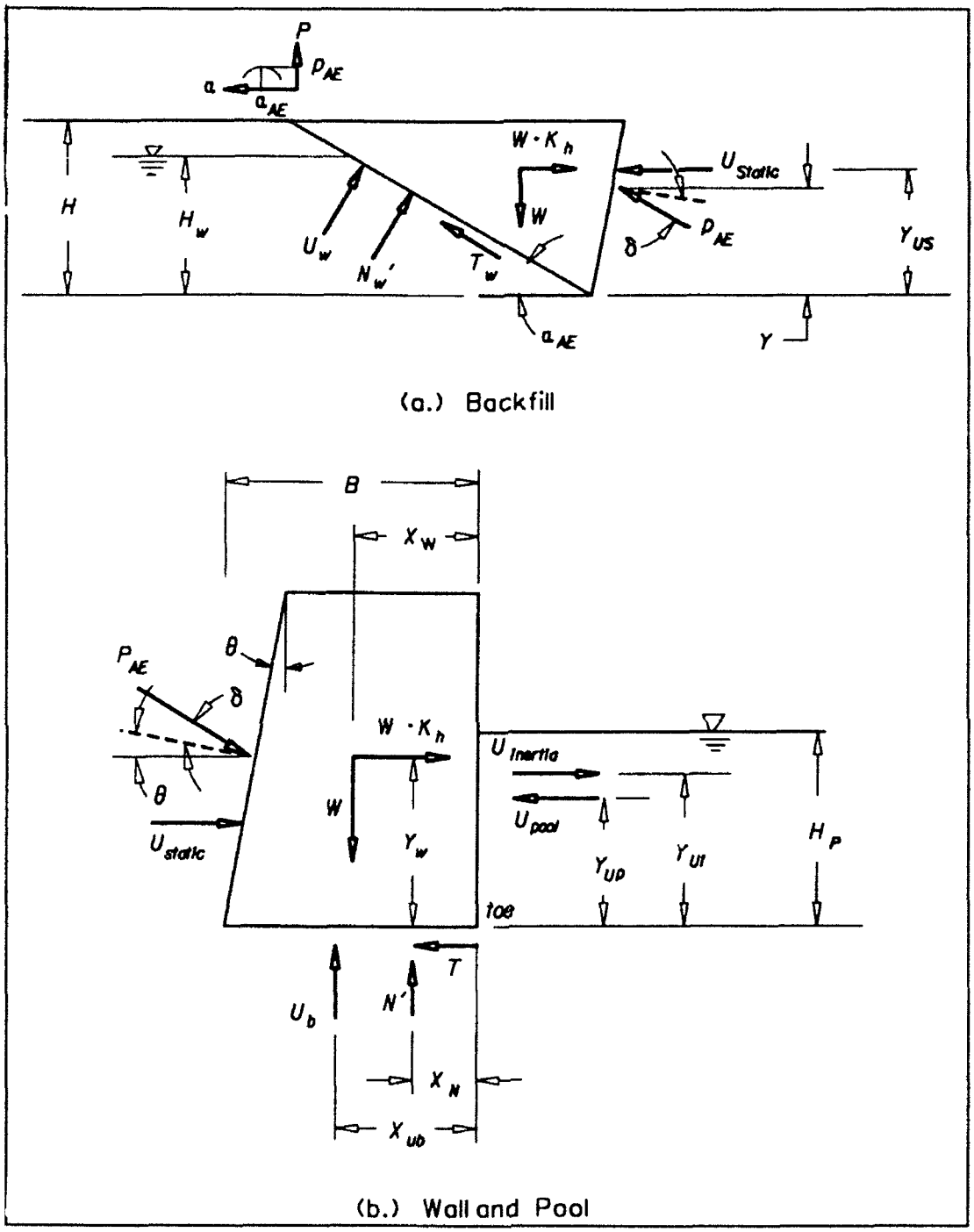

Figure 6.4 Rigid wall retaining submerged backfill which undergo movements during no excess pore water pressures (Case 2 in Figure 6.1)

The horizontal force T is the shear force required for equilibrium of the wall and is equal to

$$T = (P_{AE})_X + W(k_h) + U_{static} - U_{pool} + U_{inertia} \tag{80}$$

where

$W \cdot k_h$ = horizontal inertia force of the wall.

U_{static} = resultant steady state pore water pressure force along the back of the wall.

U_{pool} = resultant hydrostatic water pressure force for the pool

$U_{inertia}$ = hydrodynamic water pressure force for the pool directed away from the wall (see Appendix B).

(5) Compute the factor of safety against sliding, F_s, using Equation 73. The ultimate shear force along the base, T_{ult}, is given by

$$T_{ult} = N' \cdot \tan\delta_b \tag{81}$$

where

δ_b = the effective base interface friction angle.

(6) Compare the computed factor of safety against sliding to the required factor of safety of 1.1 or 1.2 for temporary loading cases (Table 5).

(7) The stability against overturning is expressed in terms of the base area in compression, B_e. B_e is computed by either Equation 75 or 76, as described in Section 6.2.1. Many retaining walls are designed using static active earth pressures with full contact along the base, B_e/B (or B'_e/B), equal to 100 percent. For temporary loading cases, such as earthquakes, this criteria is relaxed to a minimum value of 75 percent, 50 percent for rock foundations (Table 5).

(8) Check the stability of the wall against a bearing capacity failure, as discussed in step 8 of Section 6.2.1.

6.2.3 Stability of Rigid Walls Retaining Submerged Backfills which Undergo Movements During Earthquakes - Excess Pore Water Pressures

This section describes the second of three proposed force equilibrium procedures for evaluating the stability and safety of rigid walls retaining submerged or partially submerged backfills and including a pool of water in front of the wall, as shown in Figure 6.5. This analysis, described as Case 3 in Figure 6.1, assumes that excess pore water pressures, in addition to the steady state pore water pressures, are generated within the submerged portion of the backfill or within the foundation during earthquake shaking. The magnitude and distribution of these excess pore water pressures depend upon several factors including the magnitude of the earthquake, the distance from the

site to the fault generating the earthquake and the properties of the submerged soils. The evaluation of the magnitude of the residual excess pore water pressures within the submerged soil regions due to earthquake shaking is determined using the procedure described in Seed and Harder (1990) or Marcuson, Hynes, and Franklin (1990). The rigid wall is presumed to have undergone sufficient movements so that the active dynamic earth pressure force develops along the back of the wall. Many of the details regarding the procedures used in the nine steps of the stability analysis are common to the Case 1 and Case 2 analyses. The nine steps in the stability analysis of Figure 6.5 displaced rigid wall retaining a submerged backfill with excess pore water pressures within the soil regions are as follows:

(1) Select the k_h value to be used in the analysis; see Section 1.4 of Chapter 1.

(2) Consider k_v, as discussed in Section 1.4.3.

(3) Compute P_{AE} using the procedure described in Section 4.3. The total pore water pressures existing near the end of earthquake shaking are equal to the sum of the steady state pore water pressures and the residual excess pore water pressures. U_{static} is determined from the steady state flow net for the problem. The post-earthquake residual excess pore water pressures are identified as U_{shear} and ΔU, respectively, in Figure 6.5 and are determined using the procedures described in Seed and Harder (1990) or Marcuson, Hynes, and Franklin (1990). In the restrained water case of a fully submerged soil wedge with a hydrostatic water table and r_u equal to the average value within the backfill, P_{AE} is computed (Equations 33 and 38) using an effective unit weight (Equation 52). K_{AE} (Equation 34) or $K_A(\beta^*,\theta^*)$ (Equation 38) is computed using an equivalent horizontal acceleration, k_{he3}, and an equivalent seismic inertia angle, ψ_{e3}, given by Equations 54 and 55.

An alternative approach is to compute P_{AE} using an effective unit weight equal to γ_b and a modified effective friction angle, ϕ_{eq} (Equation 56). K_{AE} (Equation 34) or $K_A(\beta^*,\theta^*)$ (Equation 38) are computed using an equivalent horizontal acceleration, k_{he1}, and an equivalent seismic inertia angle, ψ_{e1}, given by Equations 47 and 48.

In the case of a partially submerged backfill, either of the simplified procedures provides for approximate results by increasing the value assigned to the effective unit weight based upon the proportion of the soil wedge that is above and below the water table. A more refined analysis may be conducted using the trial wedge procedure (Section 3.4) for the forces shown in Figure 6.5. For most engineered granular backfills, δ equal to $\phi/2$ is a reasonable value (Table 2).

(4) Compute the weight of the wall W and corresponding point of application, with the forces determined in step 3 and their points of application, solve for the unknown forces N' and T which act along the base of the wall using the horizontal and vertical force equilibrium equations.

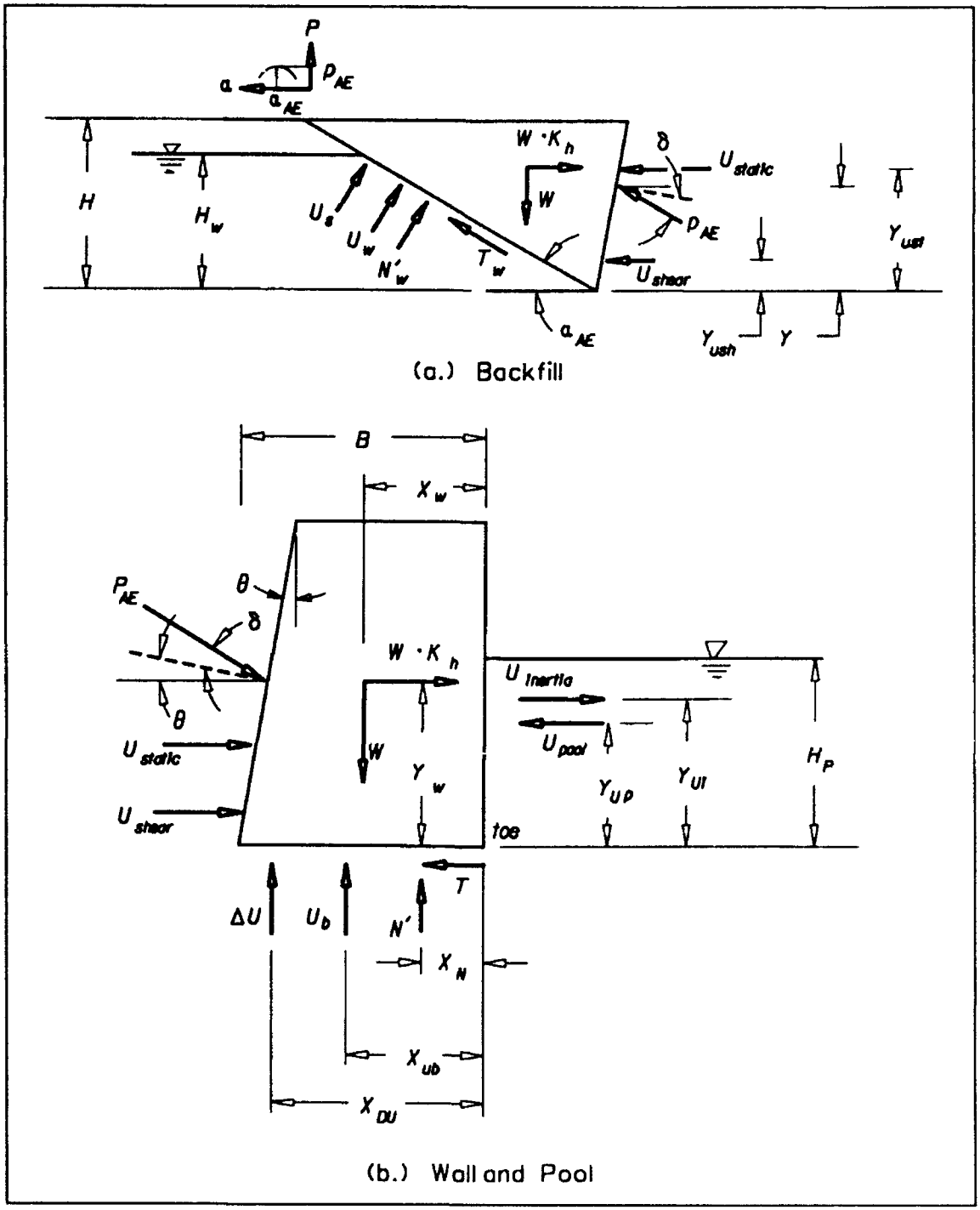

Figure 6.5 Rigid wall retaining submerged backfill which undergo movements during earthquakes, including excess pore water pressures (Case 3 in Figure 6.1)

The force W is computed per lineal foot of wall by multiplying the unit cross-sectional area of the wall by a representative value for the unit weight of the section. The resultant force acts at the center of mass for the cross section.

The effective normal force between the wall and the foundation is equal to

$$N' = W + (P_{AE})_Y - U_b - \Delta U \tag{82}$$

where

ΔU = resultant excess pore water pressure force along the base of the wall

The point of action of the force N', $X_{N'}$ is computed by summing moments about the toe of the wall

$$X_{N'} = \frac{M_W + M_{PAE} + M_{pwp} - \Delta U(X_{DU}) - U_b(X_{ub}) + M_{pool}}{N'} \tag{83}$$

where

$$M_W = W(X_W) - W(k_h)Y_W$$

$$M_{PAE} = (P_{AE})_Y\ (X_{PAE}) - (P_{AE})_X\ (Y_{PAE})$$

$$M_{pool} = U_{pool}(Y_{up}) - U_{inertia}(Y_{ui})$$

$$M_{pwp} = -U_{static}(Y_{ust}) - U_{shear}(Y_{ush})$$

and

$$(P_{AE})_X = P_{AE} \cos(\delta + \theta)$$

$$(P_{AE})_Y = P_{AE} \sin(\delta + \theta)$$

$$X_{PAE} = B - (Y_{PAE}) \tan \theta$$

$$Y_{PAE} = Y$$

Y_{ush} = point of action of U_{shear}

X_{DU} = point of action of ΔU

The horizontal force T is the shear force required for equilibrium of the wall and is equal to

$$T = (P_{AE})_X + W(k_h) + U_{static} + U_{shear} - U_{pool} + U_{inertia} \tag{84}$$

where

U_{shear} = resultant excess pore water pressure force along the back of the wall.

Procedures for the computation of values for U_{shear}, Y_{ush}, ΔU, and X_{DU} are discussed in Seed and Harder (1990) or Marcuson, Hynes, and Franklin (1990).

(5) Compute the factor of safety against sliding, F_s, using Equation 73. The ultimate shear force along the base, T_{ult}, is given by Equation 81.

(6) Compare the computed factor of safety against sliding to the required factor of safety of 1.1 or 1.2 for temporary loading cases (Table 5).

(7) The stability against overturning is expressed in terms of the base area in compression, B_e. B_e is computed by either Equation 75 or 76, as described in Section 6.2.1. Many retaining walls are designed using static active earth pressures with full contact along the base, B_e/B (or B'_e/B), equal to 100 percent. For temporary loading cases, such as earthquakes, this criteria is relaxed to a minimum value of 75 percent, 50 percent for rock foundations (Table 5).

(8) Check the stability of the wall against a bearing capacity failure, as discussed in step 8 of Section 6.2.1.

(9) Additional stability considerations for the retaining wall are discussed in Chapter 2. Some of the factors to be considered are the potential for strength loss within looser foundation materials and the post-earthquake redistribution of excess pore water pressures. Post-earthquake stability of the wall and post-earthquake settlements should also be considered.

This procedure is illustrated in example 28 at the end of this chapter.

6.2.4 Stability of Rigid Walls Retaining Submerged Backfills which Undergo Movements During Earthquakes - Liquified Backfill

This section describes the force equilibrium procedure used in the evaluation of the stability and safety of displaced rigid walls retaining submerged or partially submerged backfills and including a pool of water in front of the wall, as shown in Figure 6.6. This analysis, described as Case 4 in Figure 6.1, assumes that the submerged portion of the backfill has liquified (r_u = 100%) during the earthquake and that excess pore water pressures (r_u < 100%) are generated within the foundation during earthquake shaking. The evaluation of the liquefaction potential for the backfill and the magnitude of the residual excess pore water pressures within the foundation are determined using the procedure described in Seed and Harder (1990) or Marcuson, Hynes, and Franklin (1990). Many of the details regarding the procedures used in the nine steps of the stability analysis are common to the previously described analyses. The steps in the stability analysis of Figure 6.6 displaced rigid wall retaining a liquified backfill with excess pore water pressures within the soil foundation are as follows:

(1) Select the k_h value to be used in the analysis; see Section 1.4 of Chapter 1.

(2) Consider k_v, as discussed in Section 1.4.3.

(3) Compute the forces acting along the back of the wall,

$$HF_{static} = \frac{1}{2}\gamma_t H^2 \tag{85}$$

identified as HF_{static} and $HF_{inertia}$ in Figure 6.6. Upon liquefaction of the backfill during the earthquake, the earth pressure forces acting along the back of the wall are equivalent to a heavy fluid with a density equal to the total unit weight of the backfill, γ_t. The inertial force of the heavy fluid during shaking is approximated using the Westergaard procedure (Appendix B) for the inertia force of a fluid as acting at 0.4·H above the base of the wall.

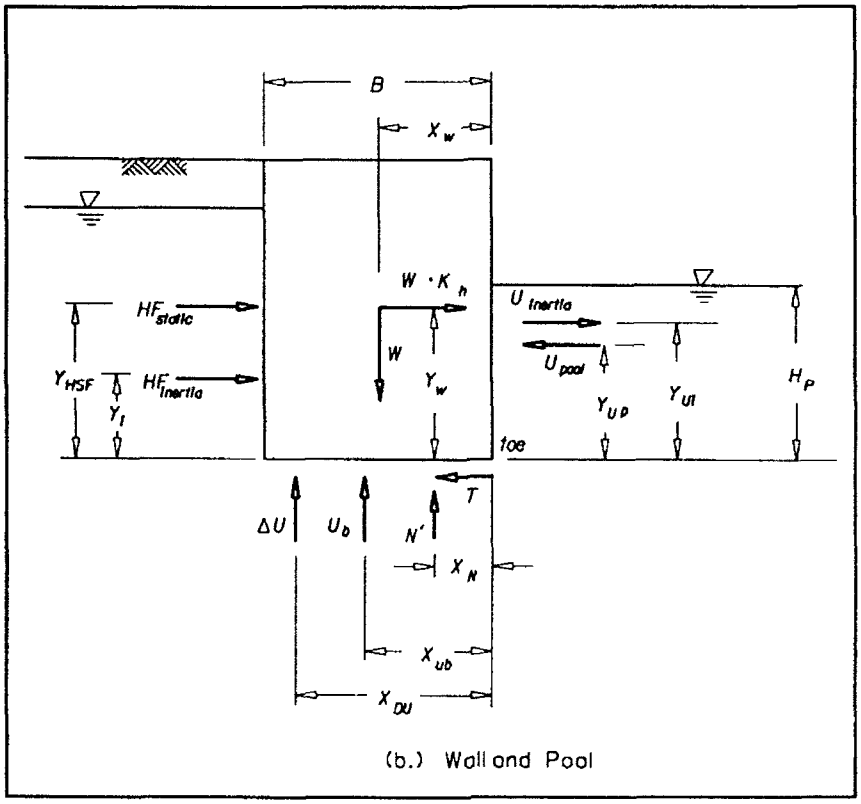

Figure 6.6 Rigid wall retaining submerged backfill which undergo movements during earthquakes - liquified backfill (Case 4 in Figure 6.1)

$$HF_{inertia} = \frac{7}{12} k_h \gamma_t H^2 \tag{86}$$

(4) Compute the weight of the wall W and corresponding point of application with the forces determined in step 3 and their points of application; solve for the unknown forces N′ and T which act along the base of the wall using the horizontal and vertical force equilibrium equations.

The force W is computed per lineal foot of wall by multiplying the unit cross-sectional area of the wall by a representative value for the unit weight of the section. The resultant force acts at the center of mass for the cross section.

The effective normal force between the wall and the foundation is equal to

$$N' = W - U_b - \Delta U \tag{87}$$

The point of action of the force N', $X_{N'}$ is computed by summing moments about the toe of the wall

$$X_{N'} = \frac{M_W + M_{HF} - \Delta U(X_{DU}) - U_b(X_{ub}) + M_{pool}}{N'} \tag{88}$$

where

$$M_W = W(X_W) - W(k_h)Y_W$$

$$M_{HF} = -HF_{static}(Y_{HFS}) - HF_{inertia}(Y_i)$$

$$M_{pool} = U_{pool}(Y_{up}) - U_{inertia}(Y_{ui})$$

and

Y_{HFS} = point of action of HF_{static} (= H/3)

Y_i = point of action of $HF_{inertia}$ (= 0.4H)

In the case where excess pore water pressures are generated within the foundation, the steady state flow net is used to compute the steady state pore water pressure force U_b along the base of the wall, and the excess pore water pressure force ΔU is computed using the procedure described in Seed and Harder (1990) or Marcuson, Hynes, and Franklin (1990). The horizontal force T is the shear force required for equilibrium of the wall and is equal to

$$T = HF_{static} + HF_{inertia} + W \bullet k_h - U_{pool} + U_{inertia} \tag{89}$$

(5) Compute the factor of safety against sliding, F_s, using Equation 73. The ultimate shear force along the base, T_{ult}, is given by Equation 81.

(6) Compare the computed factor of safety against sliding to the required factor of safety of 1.1 or 1.2 for temporary loading cases (Table 5).

(7) The stability against overturning is expressed in terms of the base area in compression, B_e. B_e is computed by either Equation 75 or 76, as described in Section 6.2.1. Many retaining walls are designed using static active earth pressures with full contact along the base, B_e/B (or B'_e/B), equal to 100 percent. For temporary loading cases, such as earthquakes, this criteria is relaxed to a minimum value of 75 percent, 50 percent for rock foundations (Table 5).

(8) Check the stability of the wall against a bearing capacity failure, as discussed in step 8 of Section 6.2.1.

(9) Additional stability considerations for the retaining wall are discussed in Chapter 2. Some of the factors to be considered are the potential for strength loss within looser foundation materials and the post-earthquake redistribution of excess pore water pressures. Post-earthquake stability of the wall and post-earthquake settlements should also be considered.

6.3 Displacement Controlled Approach

The displacement controlled approach incorporates wall movements explicitly in the stability analysis of earth retaining structures. It is, in effect, a procedure for choosing a seismic coefficient based upon explicit choice of an allowable permanent displacement. Having selected the seismic coefficient, the usual stability analysis against sliding is performed, including use of the Mononobe-Okabe equations. No safety factor is applied to the required weight of wall evaluated by this approach; the appropriate level of safety is incorporated into the step used to calculate the horizontal seismic coefficient. This procedure of analysis represents an alternative to the conventional equilibrium method of analysis which expresses the stability of a rigid wall in terms of a preselected factor of safety against sliding along its base, as described in Section 6.2.

The analytical procedure that was developed by Richards and Elms (1979) recognizes that for some limiting value of horizontal acceleration, identified as $N^* \cdot g$ in Figure 6.7, the horizontal inertia force acting on a retaining wall with no toe fill will exceed the shear resistance provided by the foundation along the interface between the base of the wall and the foundation. This implies that although the soil base may be accelerating horizontally at values greater than $N^* \cdot g$, the wall will be sliding along the base under the action of the horizontal inertial force that corresponds to the horizontal acceleration $N^* \cdot g$. This results in the movement of the soil base relative to the movement of the wall and vice-versa. The relative movement commences at the point in time designated as point a in Figure 6.8 and continues until the velocity of the base is equal to the velocity of the wall, designated as time point b in this same figure. The velocity of the soil base is equal to the integral over time of the soil acceleration, and the velocity of the wall between time points a and b is equal to the integral of the wall acceleration, which is a constant $N^* \cdot g$. The relative velocity of the wall, v_r, is equal to the integral of the difference between the base acceleration and the constant wall acceleration $N^* \cdot g$ between time points a and b, as shown in Figure 6.8. The relative displacement of the wall is equal to the integral of the relative velocity of the wall, which occurs between the two points in time labeled a and b in Figure 6.8. Additional relative displacements occur for the wall between the two latter points in time labeled c and d in Figure 6.8, with the residual relative wall displacements, d_r, equal to the cumulative relative displacements computed during the entire time of earthquake shaking.

This problem was first studied in detail by Newmark (1965) using the sliding block on a sloping plane analogy, with procedural refinements contributed by Franklin and Chang (1977), Wong (1982), Whitman and Liao (1985), Ambraseys and Menu (1988) and others. Makdisi and Seed (1978) and Idriss (1985, Figure 47), proposed relationships based on a modification to the Newmark permanent displacement procedure to allow for the dynamic response of embankments. The approach has been reasonably well validated for the case of wall retaining dry backfills. The major problem is the selection of a suitable friction angle. This is particularly troublesome when the peak friction angle is significantly greater than the residual friction angle. It is conservative to use the residual friction angle, and this should be the usual practice.

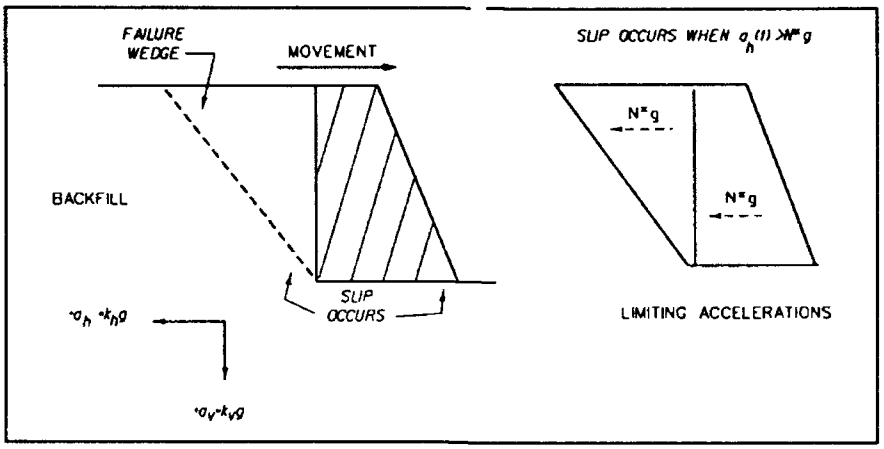

From Whitman (1990)

Figure 6.7 Gravity retaining wall and failure wedge treated as a sliding block

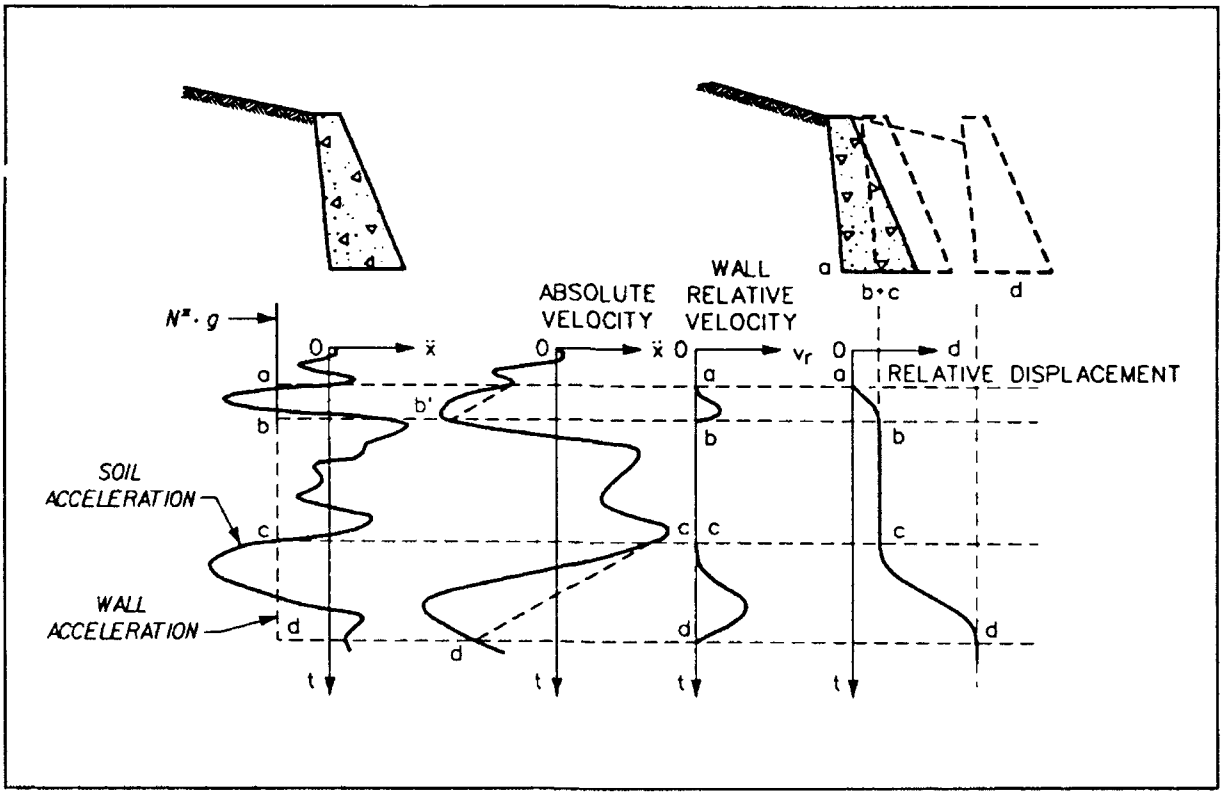

From Elms and Richards (1990)

Figure 6.8 Incremental displacement

The Richards and Elms procedure was developed using a sliding block analogy to calculate the magnitude of wall displacements in sliding during earthquake shaking. Whitman and Liao improved this procedure by using statistical methods to address the several sources of uncertainty in the

displacement controlled procedure. However, the reader is cautioned against relying solely upon this simplified procedure for waterfront structures located within severe seismic environments or epicentral regions, structures with significant deformations, or critical structures. It does not include wall displacements due to post-earthquake settlements or due to creep displacements. The method has not yet been extended to take into account tilting of walls; this matter is discussed by Whitman (1990).

Among the uncertainties are the effects of vertical and transverse accelerations, including their influence upon the passive stabilizing force for walls with toe fill. Results of studies by Sharama (1989), as described by Elms and Richards (1990), indicate that the effect of the vertical acceleration component is negligible. Other research as described by Whitman (1979) indicated that the effect of vertical acceleration can be to increase the total displacement by 50 to 100 percent for $N^*/A > 0.6$. Whitman and Liao (1985) determined that the detrimental effects of vertical accelerations on wall stability were offset by consideration of other variables. Sharama (1989), as reported by Elms and Richards (1990), determined that transverse accelerations oriented along the length of the wall contribute to wall displacement. Sliding block displacements must always increase due to transverse accelerations. Displacement increases of 70 percent or higher for N^*/A values between 0.5 and 0.9 were found. These additional displacements are based on analysis of a wall with no transverse support other than base friction. A more sophisticated analysis is required to investigate, or to consider the effects of k_v (or vertical acceleration) in the deformations of waterfront structures.

The stabilizing force for sliding resistance may be less than the full passive earth pressure force because of insufficient wall displacements. A conservative evaluation of this resistance should be used.

The displacement controlled procedure for the analysis of earth retaining structures is categorized as one of four types of analyses, as was done for the conventional equilibrium method of analysis. These categories, that are shown in Figure 6.1, include rigid walls retaining dry backfills (Case 1) and three categories for rigid walls retaining submerged backfills, depending upon the magnitude of excess pore water pressures that are generated during the earthquake. They range from the case of no excess pore water pressures (Case 2) to the extreme case which corresponds to the complete liquefaction of the backfill (Case 4) and the intermediate case between the two (Case 3). This proposed procedure for submerged backfills is not applied to the case of liquified backfills due to the complexity of the post-earthquake behavior within the soil regions. In addition, the steps in the application of the displacement controlled approach to the design of a new wall are distinguished from the steps in the application of the displacement controlled approach to the analysis of an existing wall. Table 4 identifies the appropriate Chapter 6 section that describes either the design of a new wall or the analysis of an existing wall for the first three Figure 6.1 categories of displacement controlled analyses.

6.3.1 Displacement Controlled Design Procedure for a Wall Retaining Dry Backfill

This section describes the application of the displacement controlled approach to the design of a wall retaining dry backfill identified as Case 1

in Figure 6.1. Richards and Elms (1979) first applied this analysis procedure to walls that retain dry backfill. The eight steps in the design of the earth retaining structure shown in Figure 6.9 are as follows:

(1) Decide upon the value for the permanent relative displacement d_r that is acceptable for the wall. For most walls, displacements on the order of several inches would be acceptable. The value for d_r must be consistent with the dynamic active earth pressure used in step 5 during the design of the wall (see the discussions in Sections 6.1 and 2.2.2).

(2) Select the site specific average peak horizontal acceleration, $A \cdot g$, and the site specific average peak horizontal velocity, V, within the soil backfill comprising the dynamic active wedge and the retaining structure. Refer to the discussion in Section 1.4 of Chapter 1.

(3) In typical earth retaining wall design problems, by Whitman and Liao displacement controlled procedure, $k_v = 0$.

(4) Calculate the maximum transmissible acceleration, $N^* \cdot g$, coefficient N^* using the Whitman and Liao (1985) relationship

$$N^* = A \cdot \left\{ 0.66 - \frac{1}{9.4} \ln \left[\frac{d_r \cdot (A \cdot g)}{V^2} \right] \right\} \tag{90}$$

where

$A \cdot g$ = base acceleration in units of in/sec^2
V is expressed in units of inches per second
d_r is expressed in units of inches
g = 386 in/sec^2

According to Whitman and Liao, this relationship for the maximum transmissible acceleration coefficient, N^*, ensures that there will be 95 percent confidence that the prescribed allowable permanent displacement will not be exceeded during an earthquake for the assigned A and V values. Equation 90 was derived using 14 earthquake records. All but two of the records were for earthquakes with magnitudes between 6.3 and 6.7. For severe seismic environments, structures located in epicentral regions, significant deformations, or critical structures, additional calculations should be made using other relationships (see Section 6.2).

(5) Compute the value for the dynamic active earth pressure force P_{AE} using the Mononobe-Okabe relationship described in Section 4.2, or for vertical walls and level backfills, in terms of P_A and ΔP_{AE} using the simplified Mononobe-Okabe procedure described in Section 4.2.2. When using the relationships for ψ, K_{AE}, ΔK_{AE}, and α_{AE}, N^* is substituted for k_h, and k_v is set equal to zero. Additional comments regarding these calculations are given in step 7 in Section 6.2.1.

(6) Compute the required weight of wall. Horizontal force equilibrium requires that the shear stress required for equilibrium, T, (Equation 72) be equal to the ultimate shear force along the base of the wall, T_{ult} (Equation 74). Setting Equation 72 equal to Equation 74, and introducing the normal force N (Equation 70) and solving for W results in the relationship

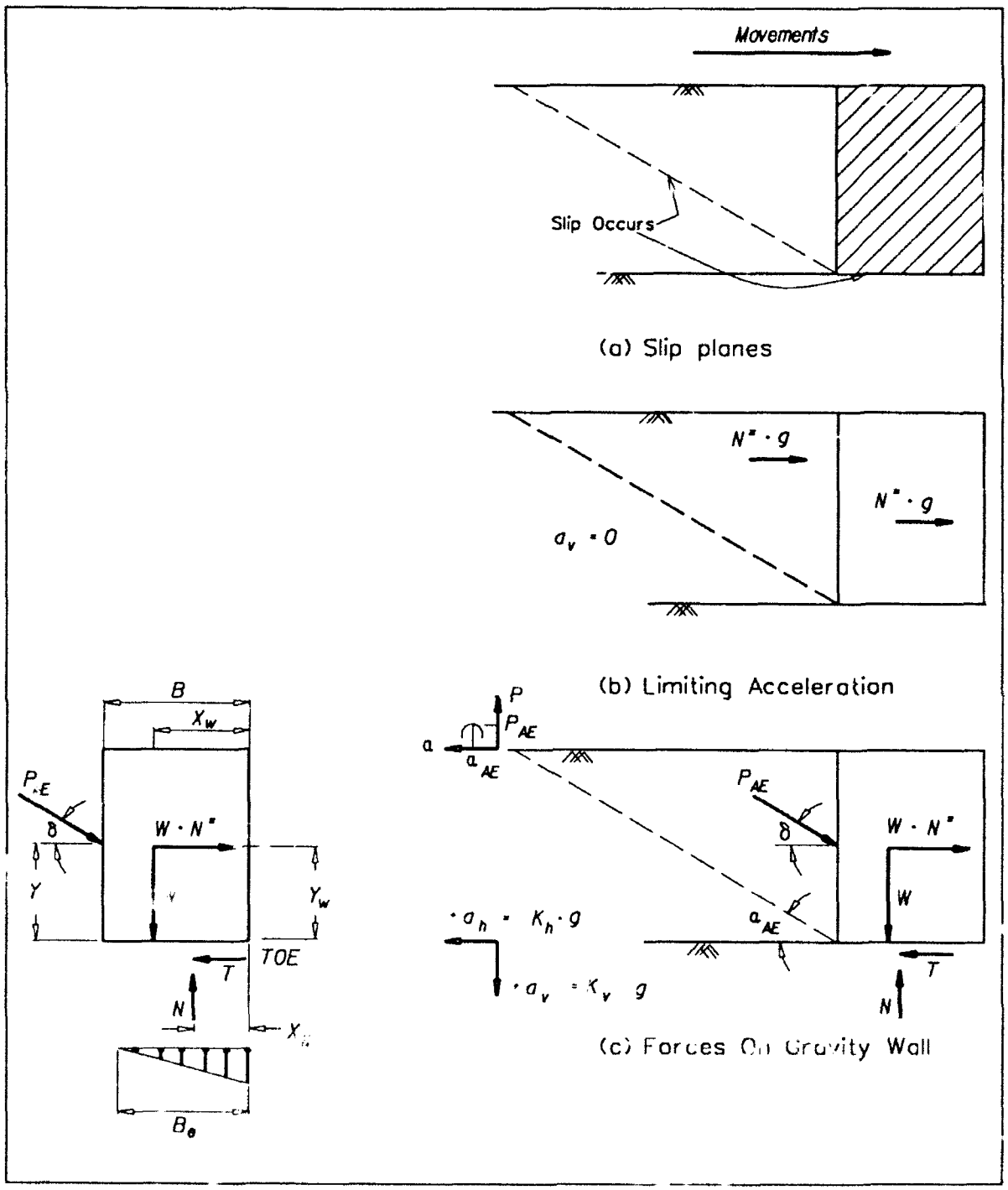

Figure 6.9 Forces acting on a gravity wall for a limiting acceleration equal to N*·g

$$W = \frac{(P_{AE})_X - (P_{AE})_Y(\tan\delta_b)}{\tan\delta_b - N^*} \tag{91}$$

where

$$(P_{AE})_X = P_{AE}\cos(\delta + \theta)$$

$$(P_{AE})_Y = P_{AE}\sin(\delta + \theta)$$

(7) No factor of safety needs to be applied to the wall weight W computed in step 6 when using Equation 90 ($FS_W = 1.0$).

(8) Proportion the geometry of the wall so that the overturning criterion is satisfied. This is expressed in terms of the percentage of base contact area B_e/B, where B_e is the width of the area of effective base contact, as described in step 7 in Section 6.2.1. For a given trial geometry, the point of action of the normal force along the base, x_N, is computed using Equation number 71, followed by the computation of the value of B_e using either Equation 75 or 76, depending upon the foundation material. This B_e value is then compared to the minimum B_e value, which is equal to 75 percent of the base width B for earthquake loading conditions (50 percent for rock foundations).

This procedure is illustrated in example 29 at the end of this chapter.

6.3.2 Analysis of Earthquake Induced Displacements for a Wall Retaining Dry Backfill

This section describes the analysis of the earthquake induced displacements of an existing wall retaining dry backfill, identified as Case 1 in Figure 6.1. The four steps in the analysis of the earth retaining structure shown in Figure 6.9 are as follows:

(1) Determine the value for the average site specific peak horizontal acceleration, A·g, and the value for the average peak horizontal velocity, V, at the site. Refer to the discussion in step 2 of Section 6.3.1.

(2) In typical earth retaining wall design problems by Whitman and Liao displacement controlled procedure, $k_v = 0$.

(3) Compute the value for the maximum transmissible acceleration, N^* g, coefficient N^*. An iterative method consisting of the following five steps is used to determine the value for N^*.

(3-A) Using the assumed value for N^*, compute the value for the dynamic active earth pressure force P_{AE} using either the Mononobe-Okabe relationship described in Section 4.2 or in terms of P_A and ΔP_{AE} assuming the simplified Mononobe-Okabe procedure described in Section 4.2.2 applies. When using the relationships for ψ, K_{AE}, ΔK_{AE}, and α_{AE}, N^* is substituted for k_h, and k_v is set equal to zero. Additional comments regarding these calculations are given in step 3 in Section 6.2.1.

(3-B) Calculate the value of the shear force required for equilibrium along the base of the wall, T, using Equation 72.

(3-C) Calculate the value for the normal force, N, using Equation 70.

(3-D) Calculate the value for the ultimate shear force along the base of the wall, T_{ult}, using Equation 74.

(3-E) If the value for T is not equal to the value for T_{ult}, adjust the value used for N^* and repeat steps 3-A through step 3-D until $T = T_{ult}$. The resulting value for N^* is equal to the limit acceleration.

(4) Calculate the permanent relative displacement d_r using the Whitman and Liao (1985) relationship

$$d_r = \left[\frac{495 \cdot V^2}{(A \cdot g)}\right] \cdot \exp^{\left(-9.4 \cdot \frac{N^*}{A}\right)} \tag{92}$$

where

$N^* \cdot g$ = maximum transmissible acceleration in units of in/sec^2
$A \cdot g$ = base acceleration in units of in/sec^2
V is expressed in units of inches per second
d_r is expressed in units of inches
g = 386 in/sec^2.

The value of d_r must be consistent with those movements that are required to develop the dynamic active earth pressure (used in step 3-A). Refer to the discussion in Section 2.2.2. The actual earthquake induced displacement will be of the same relative magnitude as the computed d_r value.

This procedure is illustrated in example 30 at the end of this chapter.

6.3.3 Displacement Controlled Design Procedure for a Wall Retaining Submerged Backfill - No Excess Pore Water Pressures

The displacement controlled approach was originally formulated by Richards and Elms (1979) for gravity walls retaining dry backfills. This section outlines a proposed procedure for extending this method of analysis to problems involving walls retaining submerged backfills that do not develop excess pore water pressures during earthquake shaking, the Case 2 structure of Figure 6.1. A pool of water is also present in front of the retaining wall. The same procedures that were described in the conventional force equilibrium method of analysis to compute the effective earth pressures (P_{AE}) and both steady state pore water pressure forces, U_{static} and U_b, and residual excess water pressure forces, U_{shear} and ΔU, acting on the wall, are used in the displacement controlled design approach. The procedure used to evaluate the liquefaction potential within the backfill and foundation and the magnitude of the residual excess pore water pressures after shaking are described in Seed and Harder (1990) or Marcuson, Hynes, and Franklin (1990).

This section describes the application of the displacement controlled approach to the design of a wall retaining submerged backfill, identified as Case 2 in Figure 6.1. No excess pore water pressures result from earthquake shaking. There are eight steps in the design of the earth retaining structure shown in Figure 6.4. The first four steps are the same as those listed in Section 6.3.1, with the first being the selection of the value for the permanent relative displacement d_r that is acceptable for the wall.

For steps (1) through (4), see Section 6.3.1.

(5) Compute the value for the effective dynamic active earth pressure force P_{AE} using the procedure described in step 3 of Section 6.2.2. When using the relationships for ψ, K_{AE}, and α_{AE}, N^* is substituted for k_h, and k_v is set equal to zero (a more sophisticated analysis is required to consider k_v).

(6) Compute the required weight of wall. Horizontal force equilibrium requires that the shear stress required for equilibrium, T, (Equation 80) be equal to the ultimate shear force along the base of the wall, T_{ult} (Equation 81). Setting Equation 80 equal to Equation 81, and introducing the effective normal force N' (Equation 78) and solving for W results in the relationship

$$W = \frac{(P_{AE})_X - (P_{AE})_Y(\tan\delta_b) + U_{static} - U_{pool} + U_{inertia} + U_b}{\tan\delta_b - N^*} \qquad (93)$$

where

$$(P_{AE})_X = P_{AE}\cos(\delta + \theta)$$

$$(P_{AE})_Y = P_{AE}\sin(\delta + \theta)$$

(7) No factor of safety needs to be applied to the wall weight W computed in step 6 when using Equation 90 ($FS_W = 1.0$).

(8) Proportion the geometry of the wall so that the overturning criterion is satisfied. This is expressed in terms of the percentage of base contact area B_e/B, where B_e is the width of the area of effective base contact, as described in step 7 in Section 6.2.2. For a given trial geometry, the point of action of the effective normal force along the base, $x_{N'}$, is computed using Equation 79, followed by the computation of the value for B_e using either Equation 75 or 76, depending upon the foundation material. This B_e value is then compared to the minimum B_e value, equal to 75 percent of the base width B for earthquake loading conditions.

With no residual excess pore water pressures generated within the backfill nor the soil foundation during earthquake shaking, there is no redistribution of excess pore water pressures after the earthquake. This implies that the wall displacements are due entirely to inertial effects during the earthquake (and not due to any post earthquake consolidation). Additional wall movements would occur should the foundation soils exhibit creep behavior as discussed in Seed (1987) and Whitman (1985). Creep displacements are not included in this procedure.

6.3.4 Analysis of Earthquake Induced Displacements for a Wall Retaining Submerged Backfill - No Excess Pore Water Pressures

This section describes the proposed procedure for the analysis of the earthquake induced displacements of an existing wall retaining submerged backfill, identified as Case 2 in Figure 6.1. No excess pore water pressures are generated within the backfill and the foundation during earthquake shaking. The four steps in the analysis of Figure 6.4 retaining wall are as follows:

For steps (1) and (2), see Section 6.3.2.

(3) Compute the value for the maximum transmissible acceleration, $N^* g$, coefficient N^*. An iterative method consisting of the following five steps are used to determine the value for N^*.

(3-A) Using the assumed value for N^*, compute the value for the dynamic active earth pressure force P_{AE} using the procedure described in step 3-A of Section 6.2.2. When using the relationships for ψ_e, K_{AE}, ΔK_{AE}, and α_{AE}, N^* is substituted for k_h, and k_v is set equal to zero.

(3-B) Calculate the value the shear force requires for equilibrium along the base of the wall, T, using Equation 80.

(3-C) Calculate the value for the effective normal force, N', using Equation 78.

(3-D) Calculate the value for the ultimate shear force along the base of the wall, T_{ult}, using Equation 81.

(3-E) If the value for T is not equal to the value for T_{ult}, adjust the value used for N^* and repeat steps 3-A through 3-D until $T = T_{ult}$. The resulting value for N^* is equal to the limit acceleration.

(4) Calculate the permanent relative displacement d_r using Equation 92. The value of d_r must be consistent with those movements that are required to develop the dynamic active earth pressure (used in step 3-A), as described in Section 2.2.2. The commentary following step 8 in Section 6.3.3 also applies in this case.

6.3.5 Displacement Controlled Design Procedure for a Wall Retaining Submerged Backfill - Excess Pore Water Pressures

This section describes the application of the proposed displacement controlled approach to the design of a wall retaining a submerged backfill that develops excess pore water pressures within the backfill or within the foundation during earthquake shaking, the Case 3 structure of Figure 6.1. A pool of water is also present in front of the retaining wall. There are nine steps in the design of the earth retaining structure shown in Figure 6.5. The first four steps are the same as those listed in Section 6.3.1, with the first being the selection of the value for the permanent relative displacement d_r that is acceptable for the wall.

For steps (1) through (4) see Section 6.3.1.

(5) Compute the value for the effective dynamic active earth pressure force P_{AE} using the procedure described in step 3 of Section 6.2.3. When using the

relationships for ψ_{e2}, K_{AE}, and α_{AE}, N^* is substituted for k_h, and k_v is set equal to zero (a more sophisticated analysis is required to consider k_v).

(6) Compute the required weight of wall. Horizontal force equilibrium requires that the shear stress required for equilibrium, T, (Equation 84) be equal to the ultimate shear force along the base of the wall, T_{ult} (Equation 81). Setting Equation 84 equal to Equation 81, and introducing the effective normal force N′ (Equation 82) and solving for W results in the relationship

$$W = \frac{(P_{AE})_X - (P_{AE})_Y(\tan\delta_b) + U_{static} + U_{shear} - U_{pool} + U_{inertia} + U_b + \Delta U}{\tan\delta_b - N^*} \qquad (94)$$

where

$$(P_{AE})_X = P_{AE}\cos(\delta + \theta)$$

$$(P_{AE})_Y = P_{AE}\sin(\delta + \theta)$$

(7) No factor of safety needs to be applied to the wall weight W computed in step 6 when using Equation 90 ($FS_W = 1.0$).

(8) Proportion the geometry of the wall so that the overturning criterion is satisfied. This is expressed in terms of the percentage of base contact area B_e/B, where B_e is the width of the area of effective base contact, as described in step 7 in Section 6.2.2. For a given trial geometry, the point of action of the effective normal force along the base, $x_{N'}$, is computed using Equation 83, followed by the computation of the value for B_e using either Equation 75 or 76, depending upon the foundation material. This B_e value is then compared to the minimum B_e value, which is equal to 75 percent of the base width B for earthquake loading conditions.

(9) Compute the additional wall movements that occur as a result of the dissipation of the residual excess pore water pressures. In this problem, residual excess pore water pressures are generated during earthquake shaking within the backfill and/or the soil foundation, resulting in a redistribution of excess pore water pressures after the earthquake. The design wall displacement selected in step 1 results from the inertial forces acting during the earthquake and do not include the post earthquake settlements.

The cautions expressed regarding wall stability during the dissipation of these excess pore water pressures as expressed in step 9 of Section 6.2.3 remain applicable.

This procedure is illustrated in Example 31 at the end of this chapter.

6.3.6 Analysis of Earthquake Induced Displacements for a Wall Retaining Submerged Backfill - Excess Pore Water Pressures

This section describes the proposed procedure for the analysis of the earthquake induced displacements of an existing wall retaining a submerged backfill that develops excess pore water pressures within the backfill or within the foundation during earthquake shaking, the Case 3 structure of

Figure 6.1. A pool of water is also present in front of the retaining wall. The five steps in the analysis of Figure 6.4 retaining wall are as follows:

For steps (1) and (2) see Section 6.3.2.

(3) Compute the value for the maximum transmissible acceleration, $N^* \cdot g$, coefficient N^*. An iterative method consisting of the following five steps are used to determine the value for N^*.

(3-A) Using the assumed value for N^*, compute the value for the dynamic active earth pressure force P_{AE} using the procedure described in step 3 of Section 6.2.3. When using the relationships for ψ_{e2}, K_{AE}, ΔK_{AE}, and α_{AE}, N^* is substituted for k_h, and k_v is set equal to zero.

(3-B) Calculate the value the shear force requires for equilibrium along the base of the wall, T, using Equation 84.

(3-C) Calculate the value for the effective normal force, N', using Equation 81.

(3-D) Calculate the value for the ultimate shear force along the base of the wall, T_{ult}, using Equation 81.

(3-E) If the value for T is not equal to the value for T_{ult}, adjust the value used for N^* and repeat steps 3-A through step 3-D until $T = T_{ult}$. The resulting value for N^* is equal to the limit acceleration.

(4) Calculate the permanent relative displacement d_r using Equation 92.

(5) Compute the additional settlements that occur during the dissipation of the excess pore water pressures and add these computed values to the lateral displacement value calculated in step 4. Note that this value of displacement does not include any creep displacements that may occur within the foundation soils. The resulting displacements must be consistent with those movements that are required to develop the dynamic active earth pressure (used in step 3-A), as described in Section 2.2.2.

The commentary included in step 9 of Section 6.2.3 also applies in this case.

CHAPTER 6 - EXAMPLES

Contents

Example Problems 27 through 31.

Commentary

The following examples illustrate the procedures described in Chapter 6. The results of the computations shown are rounded for ease of checking calculations and not to the appropriate number of significant figures. Additionally, the wall geometry and values for the material properties were selected for ease of computations.

Example No. 27 Reference Section: 6.2.1

For a wall of height H = 40 ft and base width B = 32 ft founded on rock and retaining a dry dense sand backfill, determine if the wall satisfies the stability criterion listed in Table 5 for a peak horizontal site acceleration equal to 0.3 g. Assume the contact surface between the wall and the foundation rock to be entirely frictional (no bond).

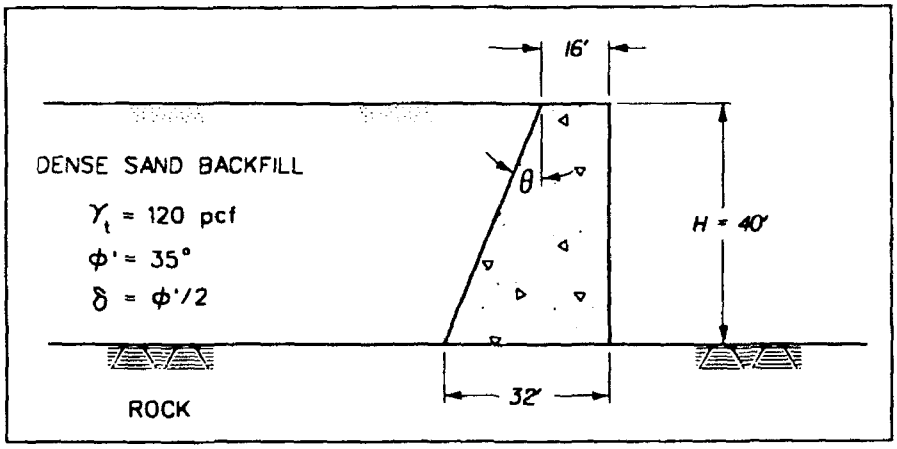

Step 1

Determine Seismic Coefficient k_h

$a_h = 0.3$ g

$k_h = 0.2$

Step 2

Determine Seismic Coefficient k_v

$k_v = 0.$

Step 3

Determine P_{AE} from Mononobe-Okabe relationships

$$\psi = \tan^{-1}\left[\frac{0.2}{(1 - 0)}\right] \qquad \text{(by eq 35)}$$

$\psi = 11.31°$

$$\theta = \tan^{-1}\left(\frac{16}{40}\right)$$

$\theta = 21.8°$

$$K_{AE} = \frac{\cos^2(35-11.31-21.8)}{\cos(11.31)\cos^2(21.8)\cos(11.31+21.8+17.5)\left[1+\sqrt{\frac{\sin(35+17.5)\sin(35-11.31-0)}{\cos(17.5+11.31+21.8)\cos(0-21.8)}}\right]^2}$$

$K_{AE} = 0.618$ (by eq 34)

$P_{AE} = 0.618\ (1/2)\ (120\ \text{pcf}\ [1 - 0])\ (40')^2$ (by eq 33)

$P_{AE} = 59{,}328$ lb per ft of wall

Determine Point of Application of P_{AE}

$$K_A = \frac{\cos^2(35 - 21.8)}{\cos^2(21.8)\cos(21.8 + 17.5)\left[1 + \sqrt{\frac{\sin(35 + 17.5)\sin(35 - 0)}{\cos(17.5 + 21.8)\cos(0 - 21.8)}}\right]^2}$$

(by eq 16)

$K_A = 0.441$

$P_A = (0.441)\ (1/2)\ (120\ \text{pcf})\ (40')^2$ (by eq 7)

$P_A = 42{,}336$ lb per ft of wall, acting at 13.33 ft (1/3 H) above the base of the wall

$P_{AE} = P_A + \Delta P_{AE}$ (eq 40)

$\Delta P_{AE} = 59{,}328 - 42{,}336$

$\Delta P_{AE} = 16{,}992$ lb per ft of wall, acting at 24 ft (0.6 H) above the base of the wall

$$Y = \frac{(42{,}336)\ (13.33')\ +\ (16{,}992)\ (24')}{59{,}328}$$

(by eq 44)

Y = 16.4 ft above the base of the wall

Step 4

Determine the weight of the wall.

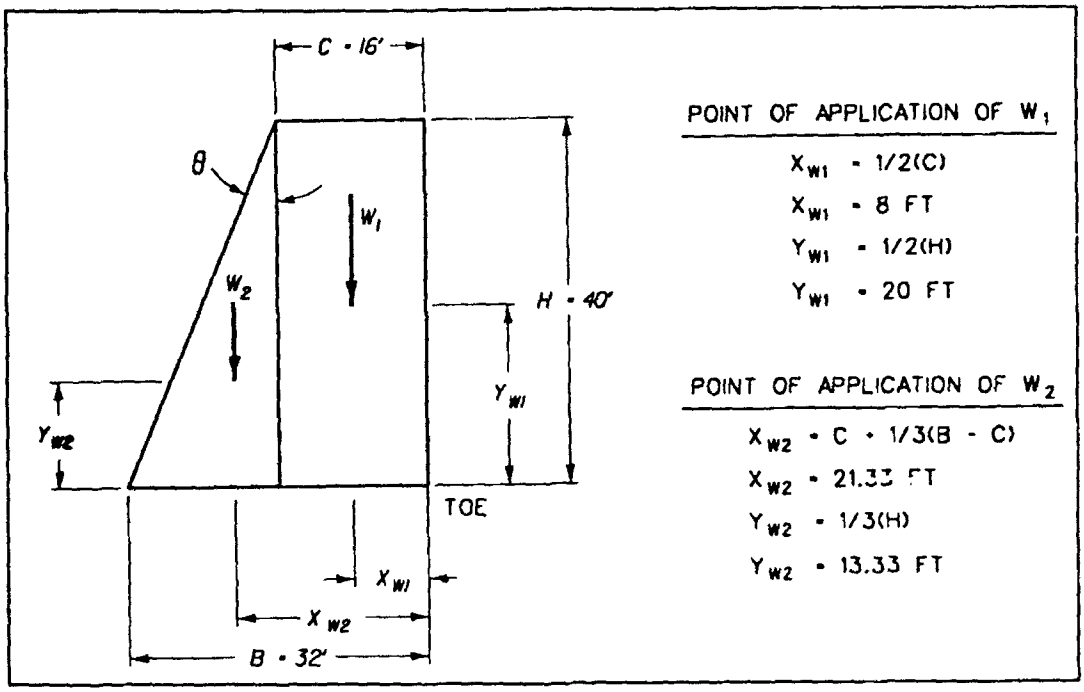

W_1 = (40′) (16′) (150 pcf)

W_1 = 96,000 lb per ft of wall

W_2 = (1/2) (16′) (40′) (150 pcf)

W_2 = 48,000 lb per ft of wall

$W = W_1 + W_2$

W = 96,000 + 48,000

W = 144,000 lb per ft of wall

Determine the Horizontal Point of Application of W

$$X_w = \frac{W_1 (X_{W1}) + W_2 (X_{W2})}{W}$$

$$X_w = \frac{(96,000)\ (8')\ +\ (48,000)\ (21.33')}{144,000}$$

X_w = 12.44′ from the toe of the wall

Determine the Vertical Point of Application of W

$$Y_w = \frac{W_1 (Y_{W1}) + W_2 (Y_{W2})}{W} = \frac{96,000\ (20')\ +\ (48,000)\ (13.33')}{144,000}$$

Y_W = 17.78 ft from the base of the wall

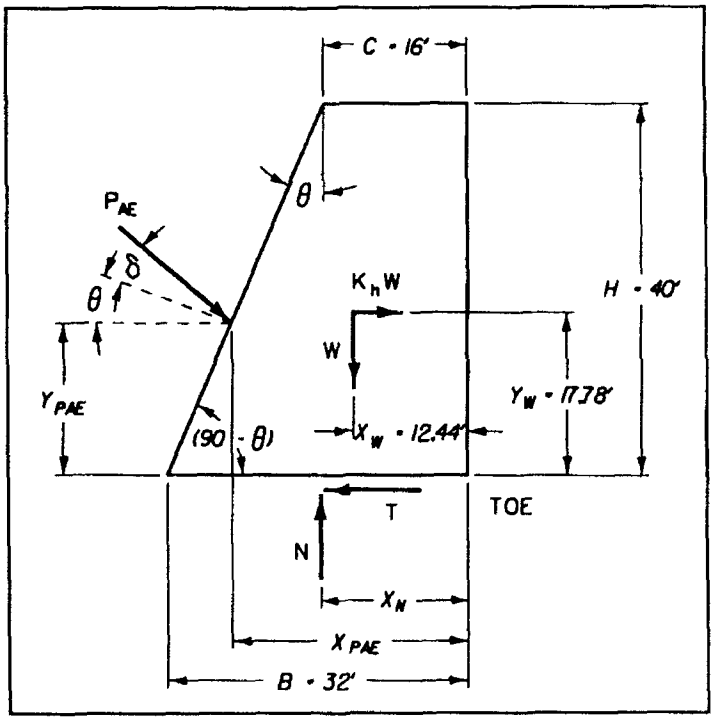

Determine the total normal force between the wall and the foundation:

N = 144,000 + (59,328) [sin (17.5 + 21.8)] (by eq 70)

N = 181,577 lb per ft of wall

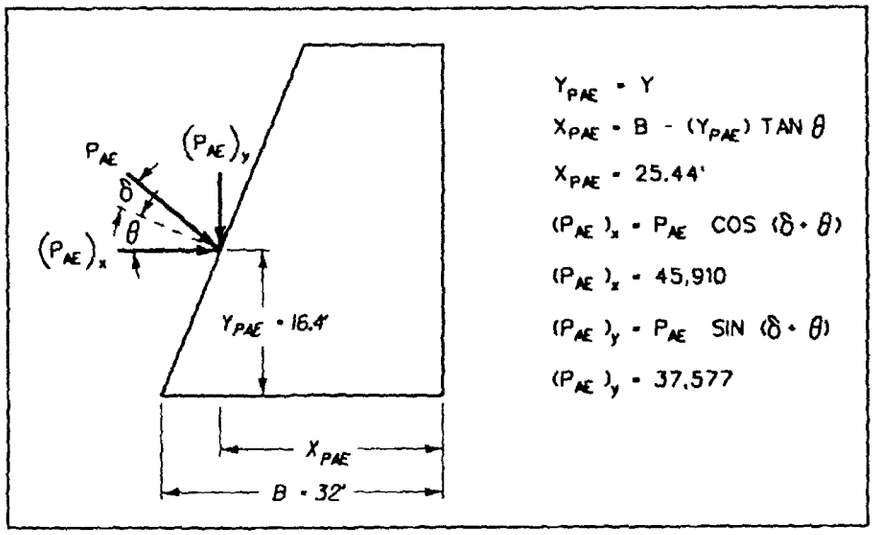

Determine the Point of Application of the Normal Force (N)

$(P_{AE})_Y$ = (59,328) sin (17.5° + 21.8°) (see Figure)

$(P_{AE})_Y$ = 37,577 lb per ft of wall

X_{PAE} = 32' - (16.4) tan (21.8)

X_{PAE} = 25.44'

$(P_{AE})_X$ = (59,328) cos (17.5 + 21.8) (see Figure)

$(P_{AE})_X$ = 45,910 lb per ft of wall

Y_{PAE} = Y

Y_{PAE} = 16.4' above the base of the wall

$$X_N = \frac{(144,000)\ (12.44')\ +\ (37,577)\ (25.44')\ -\ (45,910)\ (16.4)\ -\ (144,000)\ (0.2)\ (17.78)}{181,577}$$

X_N = 8.16' from the toe of the wall (by eq 71)

Find the horizontal shear force (T) required for equilibrium of the wall.

T = 45,910 + (144,000) (0.2) (by eq 72)

T = 74,710 lb per ft of wall

Step 5

Find the ultimate shear force along the base (T_{ult})

$\delta_b = 35°$, for clean sound rock. (from Table 2)

$T_{ult} = (181,577) \tan (35)$ (by eq 74)

$T_{ult} = 127,142$ lb per ft of wall

Compute the factor of safety against sliding (F_s)

$$F_s = \frac{127,142}{74,710}$$ (by eq 73)

$(F_s)_{actual} = 1.70$

Step 6

Compare the computed factor of safety against sliding to the required factor of safety

$(F_s)_{required} = 1.2$ (from Table 5)

$(F_s)_{actual} > (F_s)_{required}$, therefore o.k.

Step 7

Determine the width of the area of effective base contact (B_e)

$B_e = 3\ (8.16')$ (by eq 75)

$B_e = 24.48$

For temporary loading cases, such as earthquakes, B_e/B should be greater than or equal to 0.5 (rock foundation, Table 5) to avoid overturning of the structure.

$$\left(\frac{B_e}{B}\right)_{actual} = \frac{24.48}{32}$$

$$\left(\frac{B_e}{B}\right)_{actual} = 0.765$$

$(B_e/B)_{actual} > (B_e/B)_{required}$, therefore o.k.

Step 8

Determine the factors of safety against bearing capacity failure, or crushing of both the concrete and rock at the toe.

Compute q_{max}

$$q_{max} = (2/3)\ (N'/X_N) = (2/3)\ [(181,577)/(8.16)]$$ (see Figure 6.3)

$$q_{max} = 14,835 \text{ lb per ft of wall}$$

Check F_b for concrete

Assume for concrete:

$$q_{ult} = (4,000 \text{ psi})\ (144 \text{ in.}^2/\text{ft}^2)$$

$$q_{ult} = 576,000 \text{ lb per ft of wall}$$

$$(F_b)_{concrete} = \frac{q_{ult}}{q_{max}} = \frac{576,000}{14,835}$$ (by eq 77)

$$(F_b)_{concrete} = 38.8$$

Values of F_b for concrete is adequate.

Check F_b for rock

Calculations omitted.

Summary

The effect of vertical accelerations on the wall are summarized in the following table.

Example 27 with varying k_v

$k_h = 0.2$
$k_v = 0,\ +0.1,\ -0.1$

Example No. 27 (Continued) Reference Section: 6.2.1

Case	k_v	P_{AE}		Y_{PAE}		F_s		B_e/B		F_b	
Vertical Accelera-tion	Value	Value	%	Value	%	Value	%	Value	%	Value	%
None	0	59,328	0	16.4	0	1.7	0	0.765	0	38.8	0
Downward	+0.1	55,728	-6	15.89	-3	1.61	-5	0.751	-1	42.0	+8
Upward	-0.1	63,128	+6	16.84	+3	1.79	+5	0.778	+2	36.2	-7

For structures with borderline values of F_s, B_e/B or F_b, vertical accelerations must be considered to correctly evaluate wall stability.

Example No. 28 Reference Section: 6.2.3

For a wall of height H = 20 ft and base width B = 20 ft founded on "weathered" rock and retaining a partially submerged cohensionless backfill (H_w = 12 ft), determine if the wall satisfies the stability criterion listed in Table 5 for a peak horizontal site acceleration equal to 0.3 g. Assume the contact surface between the wall and the foundation rock to act as a granular material (i.e. with no bond), r_u is equal to 0.1.

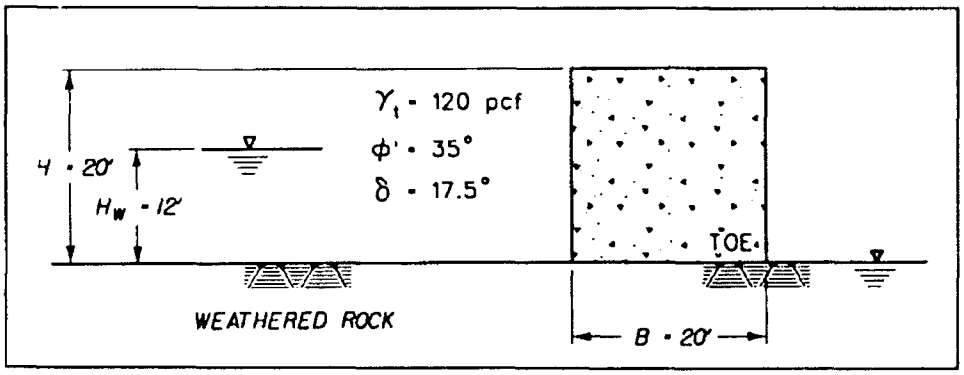

Step 1

Determine the seismic coefficient k_h

a_h = 0.3 g

$$k_h = 0.2$$

Step 2

Determine seismic coefficient k_v

k_v = 0.

Step 3

Determine P_{AE} from the Mononobe-Okabe relationships.

P_{AE} = 8,121 lb per ft of wall (see Example 19)

Y_{PAE} = Y = 9.52 ft (0.49 H) above the base of the wall (see Example 19)

$(P_{AE})_x$ = 8,121 cos (17.5)

$(P_{AE})_x$ = 7,745 lb per ft of wall

$(P_{AE})_y$ = 8,121 sin (17.5)

$(P_{AE})_y$ = 2,442 lb per ft of wall

X_{PAE} = B = 20 ft

Determine hydrostatic water pressure force

U_{static} = 4,493 lb per ft of wall (see Example 19)

Y_{ust} = 4 ft (see Example 19)

Assume 80 percent of the base in compression (B_e = 16 ft) with full uplift pressures acting along 4 ft ($B - B_e$) of the wall to rock interface.

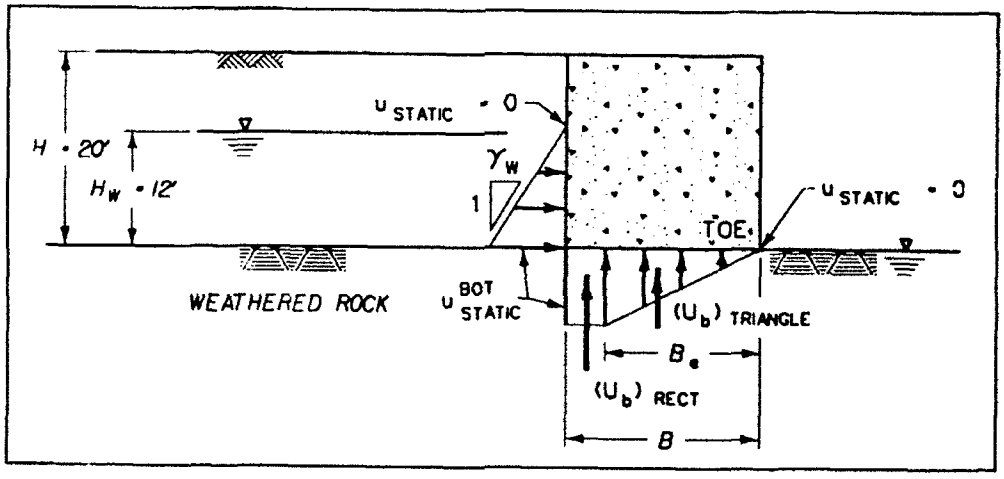

$(U_b)_{rect} = \gamma_w (H_w) (B - B_e) = (62.4 \text{ pcf}) (12') (20' - 16')$

$(U_b)_{rect}$ = 2,995 lb per ft of wall

$(X_{ub})_{rect} = B - [(B - B_e)/2] = 20 - [(20 - 16)/2]$

$(X_{ub})_{rect}$ = 18 ft from the toe of the wall

$(U_b)_{triangle} = 1/2\ \gamma_w H_w B_e = 1/2 (62.4 \text{ pcf}) (12') (16')$

$(U_b)_{triangle}$ = 5,990 lb per ft of wall

$(X_{ub})_{triangle} = 2/3\ B_e = 2/3(16')$

$(X_{ub})_{triangle}$ = 10.67 ft

$U_b = (U_b)_{rect} + (U_b)_{triangle} = 2{,}995 + 5{,}990$

U_b = 8,985 lb per ft of wall

$$X_{ub} = \frac{(2{,}995)\ (18')\ +\ (5{,}990)\ (10.67')}{8{,}985}$$

X_{ub} = 13.11 ft from the toe of the wall

Determine the excess pore water pressure force along the back of the wall

U_{shear} = 1,567 lb per ft of wall (see ex 19)

Y_{ush} = 5.47 ft above the base of the wall (see ex 19)

Determine the pore water pressure force along the base of the wall

Assuming redistribution of excess pore water pressure within the backfill along the interface between the base of the wall and the foundation, the pressure distribution will be distributed as discussed for U_b.

u_{shear}^{bot} = 165.1 psf (see Example 19)

$(\Delta U)_{rect} = u_{shear}^{bot} (B - B_e) = (165.1 \text{ psf}) (4') = 660 \text{ lb/ft}$

$(\Delta U)_{tria} = 1/2(u_{shear}^{bot})(B_e) = 1/2(165.1 \text{ psf}) (16') = 1,321 \text{ lb/ft}$

$\Delta U = \Delta U_{rect} + \Delta U_{tria} = 660 + 1,321 = 1,981 \text{ lb/ft}$

X_{DU} = 13.11 ft from the toe of the wall

Step 4

Compute the weight of the wall and point of application

$W = H(B)\gamma_{conc} = (20') (20') (150 \text{ pcf})$

$W = 60,000 \text{ lb/ft}$

$X_w = B/2 = 20'/2 = 10'$ from the toe of the wall

$Y_w = H/2 = 20'/2 = 10'$ from the base of the wall

Determine the effective normal force (N') between the wall and the foundation

$N' = 60,000 + 2,442 - 8,985 - 1,981$ (by eq 82)

$N' = 51,476$

Determine the point of application of the effective normal force (N')

$M_w = 60,000 (10') - 60,000 (0.2) (10')$

$M_w = 480,000 \text{ lb - ft}$

$M_{PAE} = 2,242\ (20') - 7,745\ (9.52')$

$M_{PAE} = -24,892$

$M_{pool} = 0$

$M_{pwp} = -(4,493)(4') - (1,567)\ (5.47')$

$M_{pwp} = -26,544$ lb - ft

$$X_{N'} = \frac{480,000 + (-24,892) + (-26,544) - (1,981)\ (13.11) - (8,985)\ (13.11) + 0}{51,476}$$

$$X_{N'} = \frac{284,800}{51,476} \qquad \text{(by eq 83)}$$

$X_{N'} = 5.53$ ft from the toe of the wall

Find the horizontal shear force (T) required for equilibrium of the wall.

$$T = 7,745 + 60,000\ (0.2) + 4,493 + 1,567 - 0 + 0 \qquad \text{(by eq 84)}$$

$T = 25,805$ lb per ft of wall

Step 5

Find the ultimate shear force along the base (T_{ult})

$\delta_b = 31°$ (from Table 2)

$T_{ult} = 51,476 \tan (31)$ (by eq 81)

$T_{ult} = 30,930$ lb per ft of wall

Compute the factor of safety against sliding (F_s).

$$F_s = \frac{30,930}{25,805} = 1.2 \qquad \text{(by eq 73)}$$

Step 6

$$(F_s)_{actual} = 1.2 = (F_s)_{req'd} = 1.2 \therefore \text{o.k.} \qquad \text{(from Table 5)}$$

Step 7

Determine the width of the area of effective base contact (B_e)

$$B_e = 3\ (5.53')$$
$$B_e = 16.59' \qquad \text{(by eq 75)}$$

$$\frac{B_e}{B} = \frac{16.59'}{20'} = 0.83 > 0.5 \text{ req'd} \therefore \text{o.k.}$$

Calculations show B_e/B = 83 percent as compared to the initially assumed value of 80 percent. If the calculated B_e value differed sufficiently from the assumed value, it would be necessary to recompute the uplift pressure distribution and repeat the analysis.

Step 8

Determine the factors of safety against bearing capacity failure or crushing of the concrete and the rock at the toe of the wall.

Compute q_{max}

$$q_{max} = (2/3)\ (N'/X_{N'}) = 2/3 \left(\frac{51,476}{5.53}\right) = 6,206$$

Check F_b for concrete

Assume for concrete:

$$q_{ult} = 576,000 \text{ lb per ft of wall} \qquad \text{(see ex 27)}$$

$$(F_b)_{concrete} = \frac{q_{ult}}{q_{max}} = \frac{576,000}{6,206} = 92.8 \qquad \text{(by eq 77)}$$

Value for F_b for concrete is adequate.

Check F_b for rock

Calculations omitted.

Example No. 29 Reference Section: 6.3.1

Design a rectangular wall of height H = 20 ft to be founded on "weathered" rock and retaining a dense sand backfill for a peak average horizontal site acceleration equal to 0.3 g and a peak average velocity equal to 12 in/sec. Assume the contact surface between the wall and the foundation rock to act as a granular material (i.e. with no bond). Use the displacement controlled design procedure for a wall retaining a dry backfill.

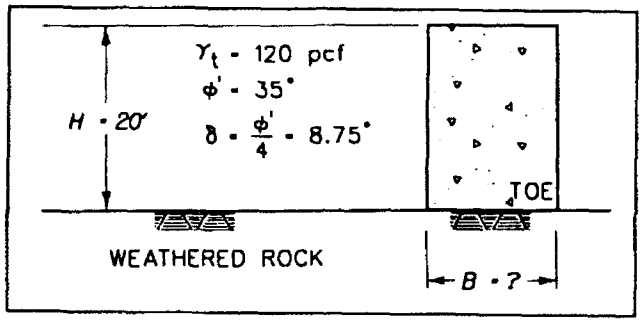

Step 1 Decide upon a value for d_r

Minimum value for d_r. To achieve active earth pressures behind a 20 ft high wall retaining a dense sand backfill, the minimum wall displacement equals 0.24 inch (Y/H = 0.001 from Table 1).

Specify a maximum allowable wall displacement d_r equal to 0.5 inch (use the Whitman and Liao method).

Step 2

$A \cdot g = 0.3\ g$

$A \cdot g = 0.3 \cdot (386\ \text{in/sec/sec}) = 116\ \text{in/sec/sec}$

$A = 0.3$

$V = 12\ \text{in/sec}$

Step 3

$k_v = 0$

Example No. 29 (Continued) Reference Section: 6.3.1

Step 4

$$N^* = (0.3)\cdot\left\{0.66 - \frac{1}{9.4}\ \ln\left[\frac{(0.5\text{ in})\ (116\text{ in/sec}^2)}{(12\text{ in/sec})^2}\right]\right\} \qquad \text{(by eq 90)}$$

$$N^* = 0.227,\ \left[\frac{N^*}{A} = 0.76\right]$$

Step 5

$k_h = N^* = 0.227$

$k_v = 0$

Use the simplified Mononobe-Okabe procedure, described in Section 4.2.2.

$$\Delta K_{AE} = 3/4\ (0.227) = 0.170 \qquad \text{(by eq 43)}$$

$\Delta P_{AE} = (0.170)\ (1/2)\ (120\text{ pcf})\ (20')^2 = 4{,}080$ lb per ft of wall

$Y_{\Delta PAE} = 0.6H = 0.6\ (20') = 12$ ft above from the base of the wall

$$K_A = \frac{\cos^2(35 - 0)}{\cos^2(0)\cos(0 + 8.75)\left[1 + \sqrt{\dfrac{\sin(35 + 8.75)\sin(35 - 0)}{\cos(8.75 + 0)\cos(0 - 0)}}\right]^2} \qquad \text{(by eq 16)}$$

$K_A = 0.2544$

$$P_A = (0.2544)\ (1/2)\ (120\text{ pcf})(20')^2 \qquad \text{(by eq 7)}$$

$P_A = 6{,}106$ lb per ft of wall

$$P_{AE} = 6{,}106 + 4{,}080 \qquad \text{(by eq 40)}$$

$P_{AE} = 10{,}186$ lb per ft of wall

$$Y = Y_{PAE} = \frac{6,106\ (20'/3) + 4,080\ (0.6)\ (20')}{10,186} \qquad \text{(by eq 44)}$$

$$Y = Y_{PAE} = 8.80 \text{ ft above the base of the wall}$$

Step 6

Compute the required weight of the wall.

$(P_{AE})_X = 10,186 \cos (8.75 + 0) = 10,068$ lb per ft of wall

$(P_{AE})_Y = 10,186 \sin (8.75 + 0) = 1,550$ lb per ft of wall

$$\delta_b = 29° \qquad \text{(from Table 2)}$$

$$W = \frac{10,068 - 1,550\ [\tan(29)]}{\tan (29) - 0.227} \qquad \text{(by eq 91)}$$

$$W = 28,135 \text{ lb per ft of wall}$$

Assuming a rectangular block with H = 20 ft, compute B.

$$W = H(B)\,\gamma_{conc}$$

$$B = \frac{28,135}{(20')\ (150 \text{ pcf})} = 9.38' \approx 9.5'$$

$$W = (20')\ (9.5')\ (150 \text{ pcf}) = 28,500 \text{ lb per ft of wall}$$

$$X_W = B/2 = 9.5'/2 = 4.75 \text{ ft from the toe of the wall}$$

$$Y_W = H/2 = 20'/2 = 10.00 \text{ ft above the base of the wall}$$

$$X_{PAE} = B = 9.5 \text{ ft from the toe}$$

Step 7

$FS_W = 1.0$

Step 8

$$N = 28,500 + 1,550 = 30,050 \text{ lb ft of wall} \qquad \text{(by eq 70)}$$

$$X_N = \frac{28{,}500\ (4.75') + 1{,}550\ (9.5') - 10{,}186\ (8.8') - 28{,}500\ (.227)\ (10')}{30{,}050}$$

$X_N = -0.1'$ ft (by eq 71)

The negative X_N value indicates overturning controls the design width of the wall, not shear.

Try B = 12.5 ft. (B/H = 0.60)

$W = H(B)\gamma_{conc}$

W = (20') (12.5') (150 pcf) = 37,500 lb per ft of wall

X_W = B/2 = 12.5'/2 = 6.25 ft from the toe of the wall

Y_W = H/2 = 20'/2 = 10.00 ft above the base of the wall

X_{PAE} = B = 12.5 ft from the toe of the wall

$$X_N = \frac{(37{,}500)\ (6.25') + 1{,}550\ (12.5') - (10{,}068)\ (8.80') - 37{,}500\ (0.227)\ (10.00')}{39{,}050}$$

X_N = 2.05 ft from the toe of the wall (by eq 71)

B_e = 3 (2.05') = 6.15 ft (by eq 75)

$$\left(\frac{B_e}{B}\right)_{actual} = \frac{6.15\ ft.}{12.5'} = 0.5 = \left(\frac{B_e}{B}\right)_{req'd} = 0.5$$ (from Table 5)

Check F_b

Compute q_{max}

q_{max} = 2/3 (39,050/2.05) = 12,700 lb/ft (see Figure 6.3)

Check F_b for concrete

Assume for concrete:

$$q_{ult} = 576{,}000 \text{ lb/ft} \qquad \text{(see ex 27)}$$

$$(F_b)_{concrete} = \frac{q_{ult}}{q_{max}} = \frac{576{,}000}{12{,}700} = 45 \qquad \text{(by eq 77)}$$

Value for F_b for concrete is adequate.

Check F_b for rock

Calculations omitted.

Summary

Overturning stability governs the design of the gravity wall (refer to step 7). It would be more efficient to make a gravity wall thinner at top than at the base. Doing so lowers the center of gravity and hence the seismic overturning moment. A T-wall may be more economical for structures of this height. In contrast with gravity walls, the addition of reinforced concrete to the toe of the T-wall increases the overturning resistance with a relatively minor increase in mass (and cost) of the structure.

Example No. 30 Reference Section: 6.3.2

Compute the value of d_r (Equation 92) for a rectangular wall of height H = 20 ft and width equal to 12.5 ft to be founded on "weathered" rock and retaining a dense sand backfill for a peak average horizontal site acceleration equal to 0.3 g and a peak average velocity equal to 12 in/sec. Assume active earth pressure forces acting along the back of the wall and the contact surface between the wall and the foundation rock to act as a granular material (i.e. with no bond).

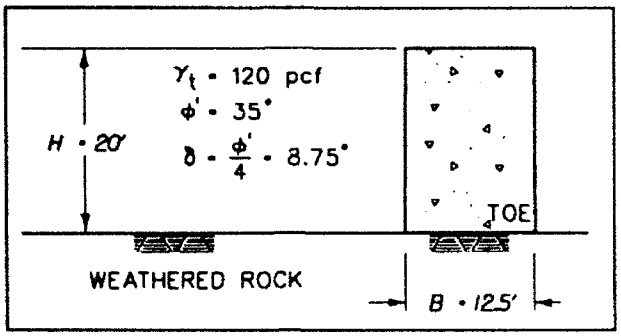

Step 1

$A \cdot g = 0.3g$

$A \cdot g = 0.3\ (386\ in/sec^2) = 116\ in/sec^2$

$A = 0.3$

$V = 12\ in/sec$

Step 2

$k_v = 0$

Step 3

$N^* = 0.227$ (from example 29)

Step 3-A

P_{AE} = 10,186 lb per ft of wall (see ex 29)

Y_{PAE} = 8.80 ft above the base of the wall (see Ex 29)

Step 3-B

$T = 10{,}068 + (37{,}500)\ (0.227)$ (by eq 72)

$T = 18{,}581$ lb per ft of wall

Step 3-C

$N = 37{,}500 + 1.550$ (by eq 70)

$N = 39{,}050$ lb per ft of wall

Step 3-D

$\delta_b = 29°$ (from Table 2)

$T_{ult} = 39{,}050 \tan (29)$ (by eq 74)

$T_{ult} = 21{,}646$ lb per ft of wall

Step 3-E

Adjust the value used for N^*

$$F_s = \frac{T_{ult}}{T} = \frac{21{,}646}{18{,}581} = 1.165$$

$k_h = N^* = (N^*)_{old}\ (F_s) = (0.227)\ (1.165)$

$k_h = N^* = 0.264$

Step 3-A 2nd Iteration

$\Delta K_{AE} = 3/4\ (0.264) = 0.198$ (by eq 43)

$$\Delta P_{AE} = (0.198)\ (1/2)\ (120\ \text{pcf})\ (20')^2$$
$$\Delta P_{AE} = 4{,}752\ \text{lb per ft of wall}$$ (by eq 41)

$$P_A = 6{,}106\ \text{lb per ft of wall}$$ (see ex 29)

$$P_{AE} = 6{,}106 + 4{,}752$$
$$P_{AE} = 10{,}858\ \text{lb per ft of wall}$$ (by eq 40)

$$(P_{AE})_X = 10{,}858 \cos (8.75 + 0) = 10{,}732\ \text{lb per ft of wall}$$
$$(P_{AE})_Y = 10{,}858 \sin (8.75 + 0) = 1{,}652\ \text{lb per ft of wall}$$

Step 3-B 2nd Iteration

$$T = 10{,}732 + 37{,}500\ (0.264)$$
$$T = 20{,}632\ \text{lb per ft of wall}$$ (by eq 72)

Step 3-C 2nd Iteration

$$N = 37{,}500 + 1{,}652$$
$$N = 39{,}152\ \text{lb per ft of wall}$$ (by eq 70)

Step 3-D 2nd Iteration

$$\delta_b = 29°$$ (see ex 29)

$$T_{ULT} = 39{,}152 \tan (29) = 21{,}702\ \text{lb per ft of wall}$$ (by eq 74)

Step 3-E 2nd Iteration

Adjust the value used for N^*

$$F_s = \frac{T_{ULT}}{T} = \frac{21,702}{20,632} = 1.05 \approx 1.1$$

$$k_h = N^* = (N^*)_{old}\ (F_s) = (0.264)\ (1.1) = 0.290$$

Step 3-A 3rd Iteration

$$\Delta K_{AE} = 3/4\ (0.290) = 0.218 \qquad \text{(by eq 43)}$$

$$\Delta P_{AE} = (0.218)\ (1/2)\ (120\ pcf)\ (20')^2 = 5,232\ lb\ per\ ft\ of\ wall \qquad \text{(by eq 41)}$$

$$P_A = 6,106 \text{ lb per ft of wall} \qquad \text{(see ex 29)}$$

$$P_{AE} = 6,106 + 5,232 = 11,338 \text{ lb per ft of wall} \qquad \text{(by eq 40)}$$

$$(P_{AE})_X = 11,338 \cos (8.75 + 0) \approx 11,206 \text{ lb per ft of wall}$$

$$(P_{AE})_Y = 11,338 \sin (8.75 + 0) \approx 1,725 \text{ lb per ft of wall}$$

Step 3-B 3rd Iteration

$$T = 11,206 + 37,500\ (0.290) \qquad \text{(by eq 72)}$$
$$T = 22,081 \text{ lb per ft of wall}$$

Step 3-C 3rd Iteration

$$N = 37,500 + 1,725 = 39,225 \text{ lb per ft of wall} \qquad \text{(by eq 70)}$$

Step 3-D 3rd Iteration

$$\delta_b = 29° \qquad \text{(see ex 29)}$$

$$T_{ULT} = 39,225 \tan(29) = 21,743 \text{ lb per ft of wall} \qquad \text{(by eq 74)}$$

Step 3-E 3rd Iteration

Adjust the value used for N^*

$$F_s = \frac{T_{ULT}}{T} = \frac{21,743}{22,081} = 0.985$$

Assume $T_{ULT} \approx T$ since F_s is less than 2 percent from a value of 1.0 and use $N^* = 0.290$.

$$\frac{N^*}{A} = \frac{0.290}{0.30} = 0.967$$

Step 4

$$d_r = \left[\frac{495\ (12 \text{ in/sec})^2}{(116 \text{ in/sec}^2)}\right] \exp^{(-9.4 \cdot 0.967)} \qquad \text{(by eq 92)}$$

$d_r = 0.07$ inches

$$d_r \approx \frac{1}{4} \text{ of } \frac{1}{4} \text{ inch}, \left(\frac{1}{4} \text{ inch} = 0.001 \cdot H\right)$$

Check F_b

Calculation omitted.

Summary

The calculated earthquake induced displacement (approximately 1/10 inch) is less than 1/4 inch displacement, the minimum value that is required to develop active earth pressures in a dense sand backfill of 20 ft height (refer to Example 29). The computed d_r value is less than this required minimum value due to the fact that to satisfy the stability criterion against overturning, the required width of the gravity wall was increased. The additional concrete mass increased the shear resistance along the base of the wall and thus reduced the magnitude of wall displacement for the design earthquake load.

Since the computed displacement of the rectangular gravity wall is less than that minimum value required to develop active earth pressures for the design earthquake by a factor of four, the procedures discussed in Chapter 5

(walls retaining nonyielding backfills) would be used to compute the dynamic earth pressure acting on the gravity wall. In general, the dynamic earth pressures for "nonyielding backfills" are two to three times larger than the dynamic active earth pressure force. Analysis and design of walls retaining nonyielding backfills are discussed in Chapter 8.

If the wall had been made thinner at the top than at the base, as discussed in the summary to Example 29, then the necessity to design the wall to retain a nonyielding backfill might be avoided.

Example No. 31 Reference Section: 6.3.5

Design a rectangular wall of height H = 20 ft to be founded on "sound" rock and retaining a dense sand backfill for a peak average horizontal site acceleration equal to 0.275 g and a peak average velocity equal to 10 in./sec. Assume active earth pressure forces acting along the back of the wall and the contact surface between the wall and the foundation rock acts as a granular material (i.e. with no bond). Use the displacement controlled design procedure for a wall retaining a submerged backfill, with d_r = 0.5 inches and r_u = 0.1.

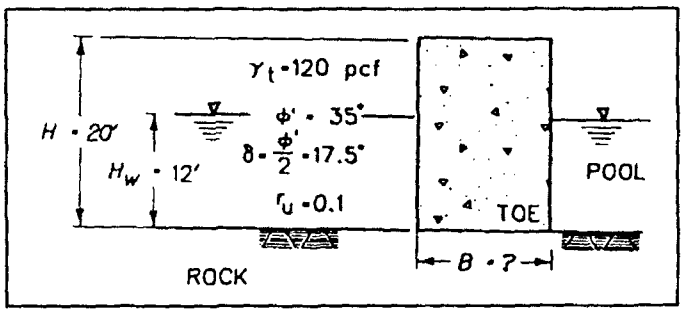

Step 1

Specify a maximum allowable wall displacement d_r equal to 0.5 inch.

Step 2

$A \cdot g = 0.275\ g$

$A \cdot g = 0.275\ (386.4\ \text{in./sec}^2) = 106.3\ \text{in./sec}^2$

$A = 0.275$

$V = 10\ \text{in./sec}$

Step 3

$k_v = 0$

Step 4

$$N* = 0.275 \cdot \left[0.66 - \frac{1}{9.4} \ln \left\{\frac{(0.5\ \text{in.})\ (106.3\ \text{in./sec}^2)}{(10\ \text{in./sec})^2}\right\}\right]$$

$$k_h = N* = 0.2 \text{ with } \left[\frac{N*}{A} = 0.73\right]$$

Step 5

$k_{he} = 0.251$ (see ex 19)

$(P_{AE})_x = 8{,}121 \cos 17.5°$ (see ex 19)

$(P_{AE})_x = 7{,}745$ lb per ft of wall (see ex 19)

$X_{PAE} = B$

$(P_{AE})_Y = 8{,}121 \sin 17.5°$ (see ex 19)

$(P_{AE})_Y = 2{,}442$ lb per ft of wall (see ex 19)

$Y_{PAE} = Y = 9.52$ ft (0.49 H) above the base of the wall (see ex 19)

Determine hydrostatic water pressure force

$U_{static} = 4{,}493$ lb per ft of wall (see ex 19)

$Y_{ust} = 4$ ft from the base of the wall (see ex 19)

Assume full hydrostatic pressure beneath the base of the wall.

$U_b = (H_w)\ (\gamma_w)\ (B) = (12')\ (62.4 \text{ pcf})\ B$

$U_b = 748.8\ B$

$X_{ub} = B/2 = 0.5\ B$

Determine the excess pore water pressure force along the back of the wall.

$U_{shear} = 1{,}567$ lb per ft of wall (see ex 19)

$Y_{ush} = 5.47$ ft (see ex 19)

Determine the excess pore water pressure force along the base of the wall

Assume $B_e/B = 0.5$

Assume the excess pore water pressure generated in the backfill during earthquake shaking will propagate under the wall at a constant value in the base separation zone ($B - B_e$). The pore water pressure in the base under compression (B_e) will linearly decrease from the maximum value to zero at the toe of the wall.

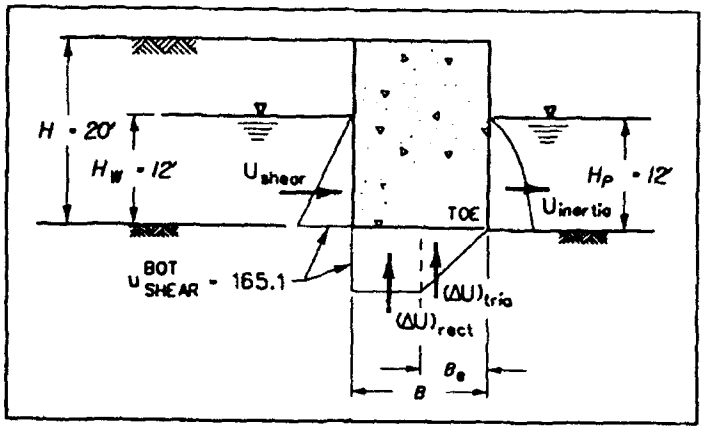
H = 20'
H_W = 12'
U_{shear}
TOE
H_P = 12'
$U_{inertia}$
u^{BOT}_{SHEAR} = 165.1
$(\Delta U)_{tria}$
$(\Delta U)_{rect}$
B_e
B

$u_{shear}^{bot} = 165.1$ psf (see ex 19)

$(\Delta U)_{rect} = u_{shear}^{bot} (B - B_e) = (165.1 \text{ psf}) (1/2) (B)$

$(\Delta U)_{rect} = 82.55 B$

$(\Delta U)_{tria} = 1/2(u_{shear}^{bot}) B_e = 1/2 (165.1 \text{ psf}) (1/2) (B)$

$(\Delta U)_{tria} = 41.28 B$

$$\Delta U = \Delta U_{rect} + \Delta U_{tria} = 82.55 B + 41.28 B = 123.83 B$$

$$X_{DU} = \frac{(82.55 B) [B_e + ((B - B_e)/2)] + 41.28 B [2/3 B_e]}{123.83 B}$$

with $B_e = 0.5 B$,

$$X_{DU} = \frac{(82.55 B) (0.75 B) + (41.28 B) (2/3) (B/2)}{123.83 B} = 0.6111 B$$

<u>Determine the hydrostatic water pressure force in front of the wall (due to the pool)</u>

$U_{pool} = 1/2 \gamma_w H_p^2 = 1/2 (62.4 \text{ pcf}) (12')^2$

$U_{pool} = 4,493$ lb per ft of wall

$Y_{up} = H_p/3 = 12'/3 = 4.00'$ above the base of the wall

<u>Determine the inertia force in front of the wall</u>

(see Appendix B)

$P_{wd} = (7/12) (0.2) (62.4 \text{ pcf}) (12')^2$

$U_{inertia} = P_{wd} = 1,048$ lb per ft of wall $\left(\frac{U_{inertia}}{U_{pool}} = 0.23\right)$

$Y_{ui} = 0.4 H_p = (0.4) (12') = 4.8$ ft above the base of the wall

Step 6

Compute the required weight of wall.

$\delta_b = 35°$ (Table 2)

$$W = \frac{7,745 - 2,442[\tan(35)] + 4,493 + 1,567 - 4,493 + 1,048 + 748.8\ B + 123.8\ B}{\tan(35) - 0.20} \quad \text{(by eq 94)}$$

$$W = \frac{8,650.1 + 872.6\ B}{0.5002}$$

$$W = B\ (H)\ \gamma_{conc}$$

$$\text{with } W = W, \quad B = \frac{17,293}{[(20)\ (150) - 1,744.5]}$$

$B = 13.77'$

Let $B = 14.0$ ft

$W = B(H)\gamma_{conc} = (14')\ (20')\ (150\ \text{pcf}) = 42,000$ lb per ft of wall

$X_w = B/2 = 14'/2 = 7.0$ ft from the toe of the wall

$Y_w = H/2 = 20'/2 = 10.0$ ft from the base of the wall

Step 7

$FS_w = 1.0$

Step 8

$\Delta U = 123.83\ B = 123.83\ (14') = 1,734$ lb per ft of wall

$X_{DU} = 0.6111\ B = 0.6111\ (14') = 8.56$ ft from the toe of the wall

$U_b = 748.8\ B = 748.8\ (14') = 10,483$ lb per ft of wall

$X_{ub} = 0.5\ B = 0.5\ (14') = 7.00$ ft from the toe of the wall

$N' = 42,000 + 2,442 - 748.8\ (14') - 123.8\ (14')$ (by eq 82)

$N' = 32,226$ lb per ft of wall

$M_w = 42,000\ (7.0') - 42,000\ (0.2)\ (10.0') = 210,000$

$M_{PAE} = 2{,}442\ (14') - 7{,}745\ (9.52') = -39{,}544$

$M_{pool} = 4{,}493\ (4') - 1{,}048\ (4.8') = 12{,}942$

$M_{pwp} = -4{,}493\ (4) - 1{,}567\ (5.47) = -26{,}544$

$$X_{N'} = \frac{210{,}000 + (-39{,}544) + (-26{,}544) - (1{,}734)(8.56') - (10{,}483)(7') + 12{,}942}{32{,}226} \quad \text{(by eq 83)}$$

$X_{N'} = 2.13'$ from the toe of the wall

$B_e = 3(\ 2.13') = 6.39$ ft (by eq 75)

$$\left(\frac{B_e}{B}\right)_{actual} = \frac{6.39\ ft}{14\ ft} = 0.46 < \left(\frac{B_e}{B}\right)_{req'd} = 0.5 \quad \text{(from Table 5)}$$

∴ overturning controls the design

The wall must be designed to resist overturning forces. Start from the minimum overturning stability requirement,

$$\left(\frac{B_e}{B}\right)_{req'd} = 0.5 \quad \text{(from Table 5)}$$

$B_e = 3X_{N'}$ (adapted from eq 75)

$$\frac{3X_{N'}}{B} = 0.5$$

$$X_{N'} = \frac{0.5\ B}{3} = \frac{1}{6}\ B$$

$$M_w = (H)\ (B)\ (\gamma_{conc})\ (B/2) - (H)\ (B)\ (\gamma_{conc})\ (0.2)\ (H/2)$$

$$M_w = \left[\frac{(H)\ (B)\ (\gamma_{conc})}{2}\right] [B - 0.2H] = (20')\ (150\ pcf)\ B[B - (0.2)\ 20]$$

$$M_w = 1{,}500\ B\ (B - 4)$$

$$M_{PAE} = 2{,}442\ B - 7{,}745\ (9.52') = (2{,}442\ B - 73{,}732)$$

$$M_{pool} = 4{,}493\ (4') - 1{,}048\ (4.8') = 12{,}942$$

$$U_b\ (X_{Ub}) = (748.8\ B)\ (0.5\ B) = 374.4\ B^2$$

$$\Delta U(X_{DU}) = (123.83\ B)\ (0.6111\ B) = 75.7\ B^2$$

$$N' = (H)\ (B)\ (\gamma_{conc}) + 2{,}442 - 748.8\ B - 123.83\ B$$

$$N' = (20')\ (150\ pcf)\ B + 2{,}442 - 872.6B = (2{,}127.4\ B + 2{,}442)$$

Solution continues on following page.

Summary

The width of the retaining wall cannot be directly determined because the resultant pore water pressure forces (both hydrostatic and excess) along the base of the wall vary as a function of the base width. Pressure distribution diagrams, for a specified value of the ratio B_e/B, are expressed as a function of the width of wall B for both hydrostatic and excess pore pressures.

The design procedure is based on determining the weight of wall (using Equation 94) which will satisfy base shear requirements. Values of N′ and $X_{N'}$ are next calculated. The value of $X_{N'}$ defines the value of B_e. B_e/B is used to express the stability of the wall against overturning. If the value of B_e/B is sufficient and consistent with the assumed uplift pressures used in the calculations, then base shear would have controlled the design width. If B_e/B is not acceptable (as in this example) then overturning controls the design width which must be increased such that the minimum value for B_e/B is satisfied.

B	M_w	M_{PAE}	M_{pwp}	$\Delta U(X_{DU})$	$-U_b(X_{Ub})$	$+M_{pool}$	N'	$X_{N'}$ Calc	1/6B	$\frac{B_e}{B}$
B	1,500 B (B - 4)	2,442 B - 73,732	-26,544	75.7 B^2	374.4 B^2	12,942	2,127.4 B + 2,442			
15	247,500	-37,102	-26,544	17,033	83,240	12,942	34,352	2.781	2.5	.556
14.5	228,375	-38,323	-26,544	15,916	78,718	12,942	33,289	2.458	2.417	.509

Since $\left(\frac{B_e}{B}\right)_{actual} = 0.509 \approx \left(\frac{B_e}{B}\right)_{assumed} = 0.5$

B = 14.5 ft

Check F_b

Calculations omitted.

CHAPTER 7 ANALYSIS AND DESIGN OF ANCHORED SHEET PILE WALLS

7.1 Introduction

This section describes the procedures for evaluating the stability and safety of anchored sheet pile walls during earthquakes. Anchored sheet pile walls are comprised of interconnected flexible sheet piles that form a continuous and permanent waterfront structure. The free earth support method is used to determine the required depth of sheet pile penetration below the dredge level and the force the anchor must resist so that excessive sheet pile wall movements do not occur during earthquake shaking. The forces acting on both the sheet pile wall and anchor during the earthquake include the static and dynamic earth pressure forces, the static and hydrodynamic pool water pressure forces and the steady state and residual excess pore water pressure forces within the submerged backfill and foundation soils. Because anchored walls are flexible and because it is difficult to prevent some permanent displacement during a major seismic event, it is appropriate to use active and passive earth pressure theories to evaluate dynamic as well as static earth pressures. The Mononobe-Okabe theory is used to evaluate the dynamic earth pressures.

There have been very few documented cases of waterfront anchored walls that have survived earthquakes or of walls that have failed for reasons other than liquefaction. Hence uncertainty remains concerning the procedures outlined in this chapter and the difficulty of ensuring adequacy of anchored sheet pile walls during strong earthquake shaking (e.g. one rough index is seismic coefficients above 0.2).

One of the few seismic design procedures for anchored sheet pile walls is the Japanese Code, which is summarized in Section 7.2.1. Using the observations regarding the performance of anchored sheet pile walls during earthquake shaking (summarized in Section 7.2), the following improvements over past practice are recommended:

(1) Anchors must be placed further away from the wall.

(2) Larger seismic coefficients are required. They are to be assigned with consideration of the seismotectonic structures as well as the characteristics of soil and structural features comprising the wall, the anchorage and its foundation.

(3) There is a limitation upon the build-up of excess pore pressures in backfill.

The procedures outlined in this chapter are to be viewed as interim guidance, an improvement over past practice. An anchored sheet pile wall is a complex structure and its performance (e.g. displacements) during earthquake shaking depends upon the interactions between the many components of the structural system (e.g. sheet pile wall, backfill, soil below dredge level, foundation, and anchorage), which impact overall wall performance. The seismic design of anchored sheet pile walls using the procedures described in this chapter requires considerable judgement during the course of design by an earthquake engineer experienced in the problems associated with the seismic design of anchored sheet pile walls.

As a general design principle, anchored sheet pile walls sited in seismic environments should be founded in dense and dilative cohesionless soils with no silt or clay size particles. The proposed design procedure presume this to be the case. Strength parameters are to be assigned in accordance with the criteria in Section 2.3. Additionally, the design procedure is limited to the case where excess pore water pressures are less than 30 percent of the initial vertical effective stress (see Section 1.3, Chapter 1).

7.2 Background

Agbabian Associates (1980) summarize the performance of anchored sheet pile walls at 26 harbors during earthquakes in Japan, the United States, and South America. Their survey indicates that the catastrophic failures of sheet pile walls are due to the large-scale liquefaction of the backfill and/or the foundation, including the foundation soil located in front of the sheet pile wall and below the dredge level. For those structures that underwent excessive movements but did not suffer a catastrophic failure, there was little or no evidence of damage due to the vibrations of structures themselves. For those walls whose backfill and foundation soils did not liquify but did exhibit excessive wall moments during the earthquake, the survey identified the source of these excessive sheet pile wall movements as (1) the soil in front of the sheet pile wall and below the dredge level moved outward (toe failure), (2) the anchor block moved towards the pool (anchor failure), or (3) the entire soil mass comprising the sheet pile structure and the anchor block moved as one towards the pool (block movement). These three potential failure modes within the backfill and the foundation soils are idealized in Figure 2.1, along with the two potential structural failure modes during earthquake shaking of anchored sheet pile walls. The report identified a number of factors which may contribute to the excessive wall movements, including (1) a reduction in soil strength due to the generation of excess pore water pressures within the submerged soils during the earthquake shaking, (2) the action of the inertial forces due to the acceleration of the soil masses in front and behind the sheet pile wall and the anchor block, and (3) the hydrodynamic water pressures along the front of the wall during the earthquake.

The Japanese Ports and Harbors commissioned a study by Kitajima and Uwabe (1979) to summarize the performance of 110 quay walls during various earthquakes that occurred in Japan during the past several decades. This survey included a tally of both damaged and undamaged waterfront structures and the dates on which the earthquakes occurred. Most of these waterfront structures were anchored bulkheads, according to Gazetas, Dakoulas, and Dennehy (1990). In their survey, Kitajima and Uwabe were able to identify the design procedure that was used for 45 of the bulkheads. This is identified as the Japanese code. Their survey showed that (1) the percentage of damaged bulkheads was greater than 50 percent, including those designed using the Japanese design procedure and (2) the percentage of bulkhead failures did not diminish with time. These two observations indicate that even the more recently enacted Japanese code is not adequate. To understand the poor performance of anchored sheet pile walls during earthquakes, it is useful to review the Japanese code that was used in the design of the most recent sheet pile walls that were included in the Kitajima and Uwabe survey.

7.2.1 Summary of the Japanese Code for Design of Anchored Sheet Pile Walls

Most of the case histories regarding the performance of anchored sheet pile walls during earthquakes that were included in the Agbabian Associates (1980) and the Kitajima and Uwabe (1979) surveys are for Japanese waterfront structures. To understand the performance of these Japanese waterfront structures, it is useful to review the Japanese design procedures that were used for the most recently constructed waterfront structures included in the surveys. The Japanese code for the design of anchored sheet pile walls as described by Gazetas, Dakoulas, and Dennehy (1990) consists of the following five steps:

(1) Estimate the required sheet pile embedment depth using the free earth support method, with the factor of safety that is applied to the shear strength of the soil reduced from 1.5 for static loadings to 1.2 for dynamic loadings. The effect of the earthquake is incorporated in the analysis through the inertial forces acting on the active and passive soil wedges by using the Mononobe-Okabe method to compute P_{AE} and P_{PE}.

(2) The horizontal seismic coefficient, k_h, used in the Mononobe-Okabe relationships for P_{AE} and P_{PE} is a product of three factors: a regional seismicity factor (0.10 ± 0.05), a factor reflecting the subsoil conditions (1 ± 0.2), and a factor reflecting the importance of the structure (1 ± 0.5).

(3) Design the tie rod using a tension force value computed on the assumption that the sheet pile is a simple beam supported at the dredge line and by the tie rod connection. Allowable stress in the tie rod steel is increased from 40 percent of the yield stress in a design for static loadings to 60 percent of the yield stress in the design for dynamic loadings.

(4) Design the sheet pile section. Compute the maximum bending moment, referred to as the free earth support moment, in the sheet pile using the simple beam of step 3. In granular soils Rowe's procedure is used to account for flexure of the sheet pile below the dredge level. A reduction of 40 to 50 percent in the free earth support moment value is not unusual. Allowable stress in the sheet pile steel is increased from 60 percent of the yield stress in a design for static loadings to 90 percent of the yield stress in the design for dynamic loadings.

(5) Design the anchor using the tie rod force of step 2 increased by a factor equal to 2.5 in the design for both static and dynamic loadings and assume the slip plane for the active wedge starts at the dredge line.

From the modes of failure observed in the Kitajima and Uwabe study of anchored sheet pile walls that were designed using the Japanese code, Gazetas, Dakoulas and Dennehy (1990) identified the following as the primary deficiencies in the Japanese code procedure:

(1) The values for the seismic coefficients, k_v and k_h, used in the Mononobe-Okabe relationships for P_{AE} and P_{PE} are not determined from a site response analysis but are specified within the Japanese code (k_v =

0, and k_h is within a narrow range of values for most of the waterfront structures involved in the study).

(2) The resistance provided by the anchor is over estimated because the code allows the anchor to be placed too close to the sheet pile wall such that the passive wedge that develops in front of the anchor interferes with the active wedge developing within the backfill behind the sheet pile wall.

(3) The code does not account for the earthquake induced excess pore water pressures within the submerged soils and the corresponding reduction in the shear strength for the submerged soil regions, nor the excess water pressure forces and hydrodynamic forces acting on the sheet pile structure.

Gazetas, Dakoulas, and Dennehy (1990) listed only one of the failures of the sheet pile walls designed using the Japanese Code as a general flexural failure. In this case, the structural failure was attributed to corrosion of the steel at the dredge level.

Each of these deficiencies is addressed in the steps used in the design of anchored sheet pile walls using the free earth support method of analysis as described in Section 7.4.

7.2.2 Displacements of Anchored Sheet Piles during Earthquakes

In the Kitajima and Uwabe (1979) survey of damage to anchored sheet pile walls during earthquakes, the level of damage to the waterfront structure was shown to be a function of the movement of the top of the sheet pile during the earthquake. Kitajima and Uwabe (1979) categorized the damage as one of five levels as given in Table 6 and reported in Gazetas, Dakoulas, and Dennehy (1990). Their survey shows that for sheet pile wall displacements of 10 cm (4 inches) or less, there was little or no damage to the Japanese waterfront structures as a result of the earthquake shaking. Conversely, the level of damage to the waterfront structure increased in proportion to the magnitude of the displacements above 10 cm (4 inches). Using the information on the anchored sheet pile walls survey reported in Kitajima and Uwabe (1979) and using simplified theories and the free earth support method of analysis, Gazetas, Dakoulas, and Dennehy (1990) showed that the post-earthquake displacements at the top of the sheet pile wall correlated to (1) the depth of sheet pile embedment below the dredge level and (2) the distance between the anchor and the sheet pile.

Two anchored bulkheads were in place in the harbor of San Antonio, Chile, during the very large earthquake of 1985. A peak horizontal acceleration of about 0.6g was recorded within 2 km of the site. One experienced a permanent displacement of nearly a meter, and use of the quay was severely restricted. There was evidence of liquefaction or at least poor compaction of the backfill, and tie rods may not have been preloaded. The second bulkhead developed a permanent displacement of 15 cm, but the quay remained functional after the earthquake. This bulkhead had been designed using the Japanese procedure with a seismic coefficient of 0.15, but details concerning compaction of the backfill are unknown.

Table 6 Qualitative and Quantitative Description of the Reported Degrees of Damage

DEGREE OF DAMAGE		DESCRIPTION OF DAMAGE	PERMANENT DISPLACEMENT AT TOP OF SHEETPILE	
+ A +	+ B +		CM	INCHES
I	0	No damage	<2	<1
	1	Neglible damage to the wall itself; noticeble damage to related structures (i.e. concrete apron)	10	4
II	2	Noticable damage to wall	30	12
III	3	General shape of anchored sheetpile preserved, but significantly damaged	60	24
	4	Complete destruction, no recognizable shape of wall	120	48

+ A + Damaged Criteria Grouping by Gazetas, Dakoulas, and Denneby (1990).
+ B + Damage criteria Grouping by Kitajima and Uwake (1978).

7.3 Design of Anchored Sheet Pile Walls - Static Loadings

In the design of anchored sheet pile walls for static earth pressure and water pressure loads, the free earth support method or any other suitable method may be used to determine the required depth of sheet pile embedment below the dredge level and the magnitude of the design anchor force required to restrict the wall movements to acceptable levels. The interrelationship between the changes in earth pressures, the corresponding changes in the sheet pile displacements, and the changes in the distribution of bending moments along the sheet pile make the free earth support method of analysis an attractive design tool, as discussed in Section 7.4. Rowe's (1952) free earth support method of analysis assumes that the sheet pile wall moves away from the backfill and displaces the foundation soils that are below the dredge level and in front of the wall, as shown in Figure 7.1. These assumed displacements are sufficient to fully mobili the shear resistance within the backfill and foundation, resulting in active earth pressures along the back of the sheet pile wall and passive earth pressures within the foundation in front of the sheet pile wall, as shown in Figure 7.1.

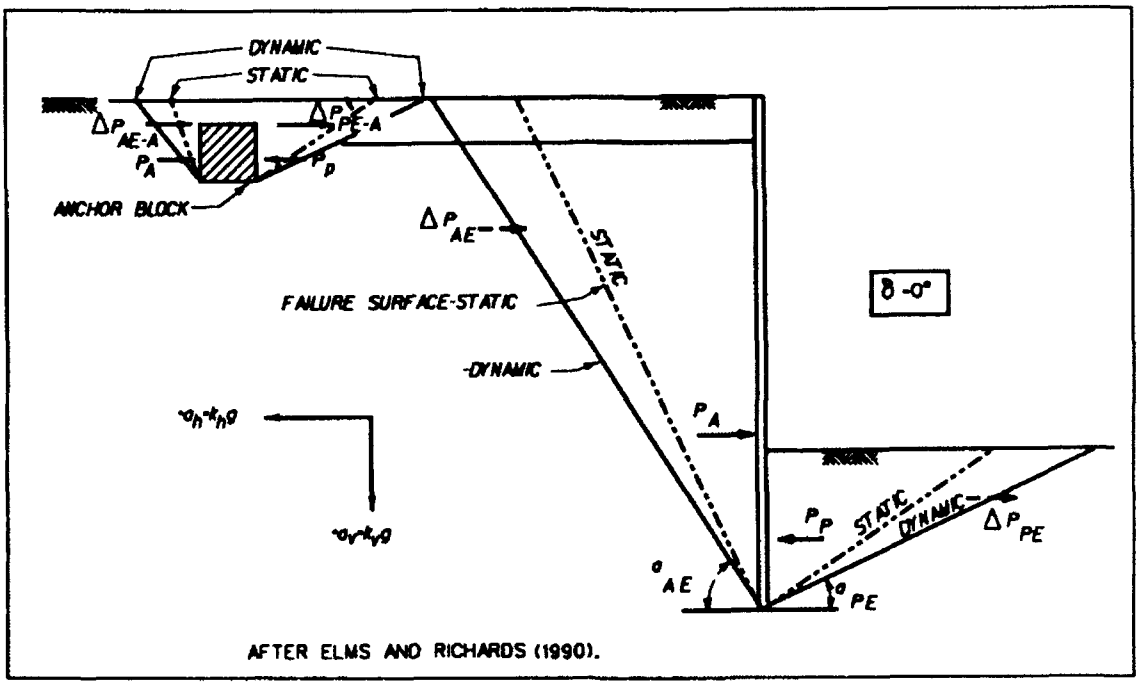

Figure 7.1 Decrease in failure surface slope of the active and passive sliding wedges with increasing lateral accelerations

To begin the analysis, a factor of safety equal to 1.5 is applied to the shear strength of the soil comprising the passive block in front of the sheet pile wall, while active earth pressures are presumed behind the sheet pile wall (factor of safety on shear strength of the backfill = 1.0). Equilibrium of the moments for the active earth pressure distribution and the factored passive earth pressure distribution about the anchor results in the minimum required depth of sheet pile penetration. Horizontal equilibrium of the active earth pressure distribution and the factored passive pressure earth distribution results in the computation of the equilibrium anchor force. The distribution of moments along the sheet pile is then computed using the earth pressure distributions and the equilibrium anchor force.

Rowe's (1952) model studies showed that because of flexure in the sheet pile below the dredge level, the free earth support analysis predicts larger moments than those developing under working loads. According to Rowe's work, the maximum moment to be used in the design of the sheet pile wall is equal to the maximum moment corresponding to the free earth support analysis times a correction factor; r_d, where

r_d = the moment reduction factor due to flexure below the dredge level, as developed by Rowe. r_d is typically less than 1.0. Values for r_d are given in Figure 7.2. The value of r_d is a function of the flexibility of the sheet pile and the type and characteristics of the foundation soil below the dredge level.

The value of the correction factor is a value less than or equal to one, dependent upon (1) the flexibility of the sheet pile and (2) the type and

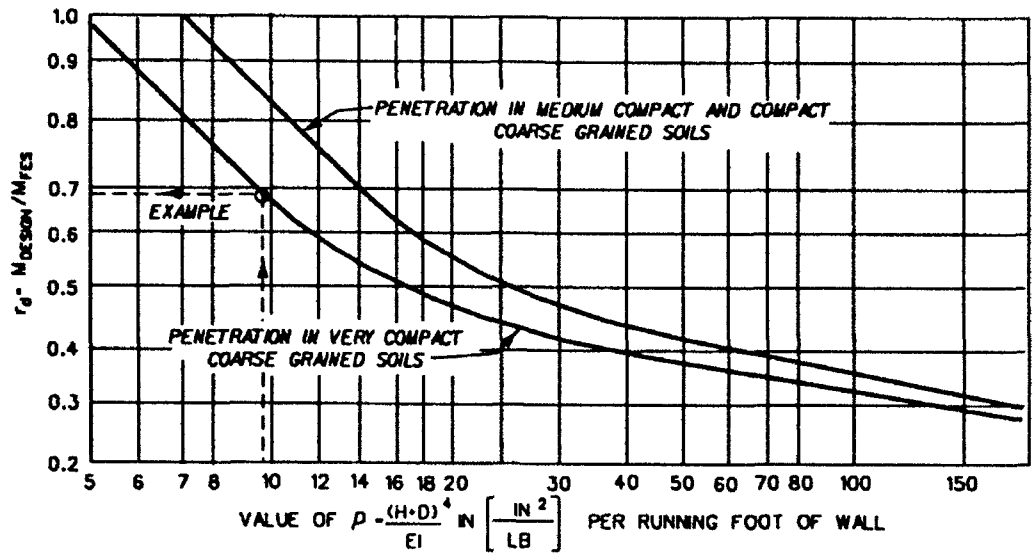

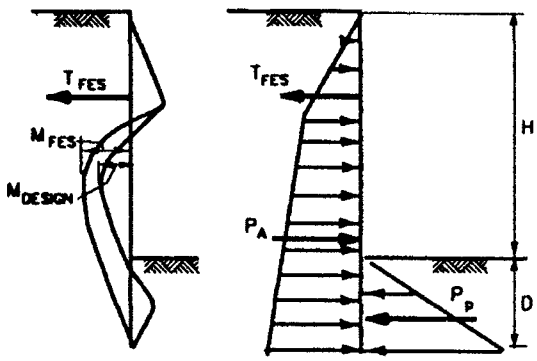

MOMENT DIAGRAM LOAD DIAGRAM

EXAMPLE: PENTRATION IN VERY COMPACT SAND

M_{FES} = 950,000 IN. LB/FT

H = 33 FT, D = 15FT.

fs = 25,000 PSI, E = 30,000.000 PSI

TRY ZP32, I = 385.7 $IN.^4$, S = 38.3 $IN.^3$

$$\rho = \frac{(33+15)^4 \times 12^4}{30{,}000{,}000 \times 385.7} = 9.5 \frac{IN.^2}{LB.}$$

$$\frac{M_{DESIGN}}{M_{FES}} = 0.68, \; M_{DESIGN} = 645.000 \text{ IN.LB/FT}$$

$$fs = \frac{M}{S} = \frac{645{,}000}{38.3} = 16{,}800 \text{ PSI}$$

16,800 < 25,000 PSI

TRY A SMALLER SECTION

LEGEND

M_{FES} - MAXIMUN POSITIVE MOMENT IN SHEETING COMPUTED BY FREE EARTH SUPPORT METHOD

M_{DESIGN} - MAXIMUM POSITIVE MOMENT FOR DESIGN OF SHEETING

ρ - FLEXIBILITY NUMBER = $\frac{(H+D)^4}{EI}$

E - SHEETING MODULUS OF ELASTICITY, PSI

I - SHEETING MOMENT OF INERTIA, $IN.^4$ PER RUNNING FOOT OF WALL

NOTES

1. M_{DESIGN} IS OBTAINED BY SUCCESSIVE TRIALS OF SHEETING SIZE UNTIL MAX. BENDING STRESS IN SHEETING EQUALS ALLOWABLE BENDING STREAA.
2. NO REDUCTION IN M_{FES} IS PERMITTED FOR PENETRATION IN FINE GRAINED SOILS OR LOOSE OR VERY LOOSE COARSE GRAINED SOILS
3. FLEXIBLTY NUMBER IS COMPUTED ON THE BASIS OF LUBRICATED INTERLOCKS.

FROM NAVFAC DM7.2

Figure 7.2 Reduction in bending moments in anchored bulkhead from wall flexibility

characteristics of the foundation soil. The entire moment diagram is altered due to incorrect earth pressure assumptions, idealized in Figure 7.3.

The corresponding design load, sheet pile displacements shown in Figure 7.3 reflect the flexure that occurs below the dredge level. In sand foundations the flexure below the dredge level increases with increasing density for the foundation sand. These **reduced** outward displacements along the bottom of the sheet pile explain why the free earth support method overpredicts the required design moment values for flexible sheet pile structures. Note that the point of contraflexure is now above the tip of the sheet pile in the case of the design loads.

For those anchored walls in which the water table within the backfill differs from the elevation of the pool, the differences in the water pressures are incorporated in the analysis. Terzaghi (1954) describes a simplified procedure used to analyze the case of unbalanced water pressures and steady state seepage. The distributions for the unbalanced water pressures along the sheet pile for the case of no seepage and for the case of steady state seepage are shown in Figure 7.4. In an effective stress analysis of frictional soils are computed within these two regions, and the effective unit weights (Equation 27) are used to compute the active and passive earth pressures along the sheet pile wall using the simplified relationship of the type described in Section 3.3.3. The seepage force acts downward behind the sheet pile, increasing the effective unit weight and the active earth pressures, and acts upward in front of the sheet pile, decreasing the effective unit weight with steady state seepage, and the passive earth pressures. For the case of no flow, the buoyant unit weights are assigned to the frictional soils below the water table to compute the active and passive earth pressures using the simplified relationships of the type described in Section 3.3.2.

Various important load and material factors in common practice are as follows: The allowable stress in the sheet pile is usually restricted to between 50 percent and 65 percent of the yield stress of the steel (60 percent in the Japanese Code). The allowable stress (gross area) in the tie rod steel is usually between 40 and 60 percent of the yield stress, and the tie rod force is designed using the equilibrium anchor force increased by a factor equal to 1.3. The anchor is designed using the equilibrium anchor force increased by a factor equal to between 2.0 and 2.5.

This design procedure for static loadings is extended to dynamic problems in the following sections.

7.4 Design of Anchored Sheet Pile Walls for Earthquake Loadings

The first step is to check for the possibility of excess pore pressures or liquefaction (see Seed and Harder (1990) or Marcuson, Hynes, and Franklin 1990). The presence or absence of these phenomenon will have a major influence on design. The potential for excessive deformations is to be considered (see National Research Council, 1985).

The proposed design procedure quantifies the effect of earthquake shaking in the free earth support analysis of anchored sheet pile walls through the use of inertial forces within the backfill, the soil below the dredge level in front of the sheet pile wall and the hydrodynamic water pressure force in the pool in front of the wall. These inertial forces are

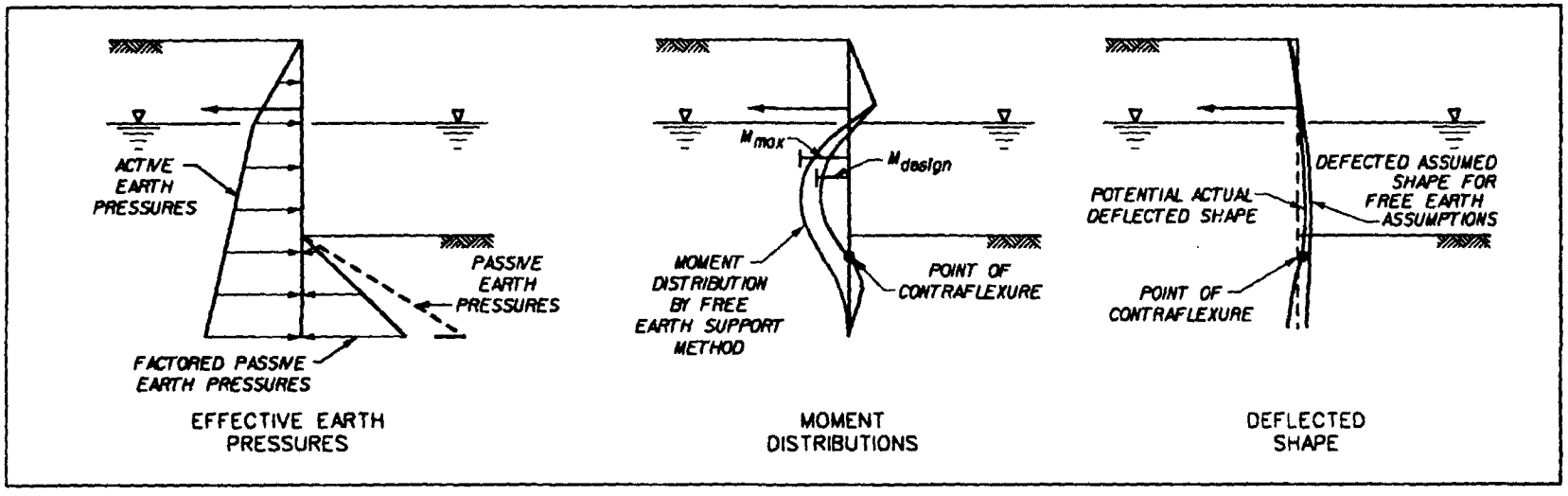

Figure 7.3 Free earth support analysis distribution of earth pressures, moments and displacements, and design moment distributions

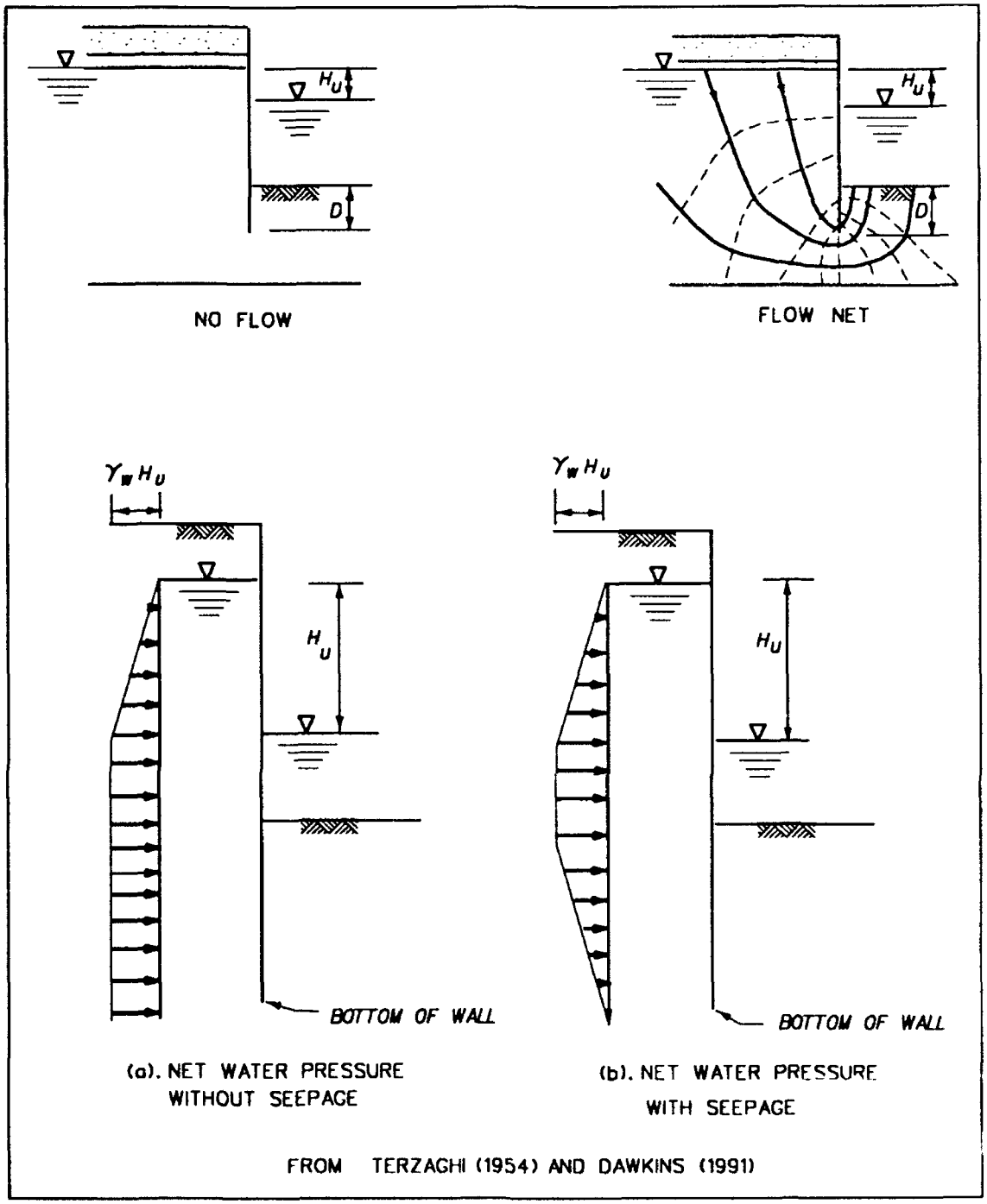

Figure 7.4 Two distributions for unbalanced water pressures

superimposed on the static forces along the sheet pile wall. Certain adjustments are made to the load and material factors, as is detailed in the following sections, when earthquake loads are included in the analysis.

An important design consideration is the placement of the anchor. It should be located far enough from the wall such that the active wedge from the wall (starting at the bottom of the wall) and the passive wedge from the

anchor do not intersect. The inertial forces due to the acceleration of the soil mass have the effect of decreasing the slope of the active and passive soil wedge failure surfaces, as shown in Figure 7.1 and described in Chapter 4. The slope angles α_{AE} and α_{PE} for the slip planes decrease (the slip planes become flatter) as the acceleration levels increase in value.

When the horizontal accelerations are directed towards the backfill ($+k_h \cdot g$), the incremental increases in the earth pressure forces above the static earth pressure forces, denoted as ΔP_{AE} and ΔP_{PE} in Figure 7.1, are directed away from the backfill. This has the effect of increasing the driving force behind the sheet pile wall and decreasing the stabilizing force in front of the sheet pile wall. The effect of increased accelerations on the distribution of moments are twofold, (1) increased values for the maximum moment within the sheet pile and (2) a lowering of the elevation of the point of conflexure along the sheet pile (refer to Figure 7.3 for definition). The anchored sheet pile wall model tests in dry sands by Kurata, Arai, and Yokoi (1965), Steedman and Zeng (1988) and Kitajima and Uwabe (1979) have confirmed this interrelationship, as shown in Figure 7.5. This type of sheet pile response shows that as the value for acceleration increases, the point of conflexure moves down the pile, and the response of the sheet pile (described in terms of sheet pile displacements, earth pressures along the sheet pile and distribution of moments within the sheet pile) will approach those of the free earth support. This increase in the value of the maximum moment and the movement of the point of contraflexure towards the bottom of the sheet pile with increasing acceleration reflects the development of a fully active stress state within the soil that is located below the dredge level and behind the sheet pile wall. Thus, the value for Rowe's moment reduction factor that is applied to the moment distribution corresponding to the free earth support method will increase in value, approaching the value of one, with increasing values for accelerations. This effect is not taken into account directly in the design. However, it is indirectly considered if the moment equilibrium requirement of the free earth method requires a greater depth of embedment when earthquake loadings are included.

Another factor affecting the orientation of the failure planes and thus the corresponding values for the dynamic earth pressure forces is the distribution of total pore water pressures within the backfill and foundation. The total pore water pressure is a combination of the steady state seepage and any excess pore water pressures resulting from earthquake induced shear strains within the submerged soils.

The proposed procedures for the seismic stability analysis of anchored sheet pile walls that undergo movements during earthquakes are categorized as one of three types of analyses, depending upon the magnitude of excess pore water pressures generated during the earthquake (Figure 7.6). They range from the case of no excess pore water pressures (Case 1) to the extreme case corresponding to the complete liquefaction of the backfill (Case 3) and the intermediate case of residual excess pore water pressures within the backfill and/or the soil in front of the sheet pile (Case 2).

In Figure 7.6, $U_{static-b}$ corresponds to the steady state pore water pressure force along the back of the sheet pile wall, $U_{static-t}$ the steady state pore water pressure force along the front toe of the wall and U_{pool} the hydrostatic water pressure force exerted by the pool along the front of the wall. In the case of balanced water pressures, the sum of $U_{static-b}$ is equal to U_{pool}

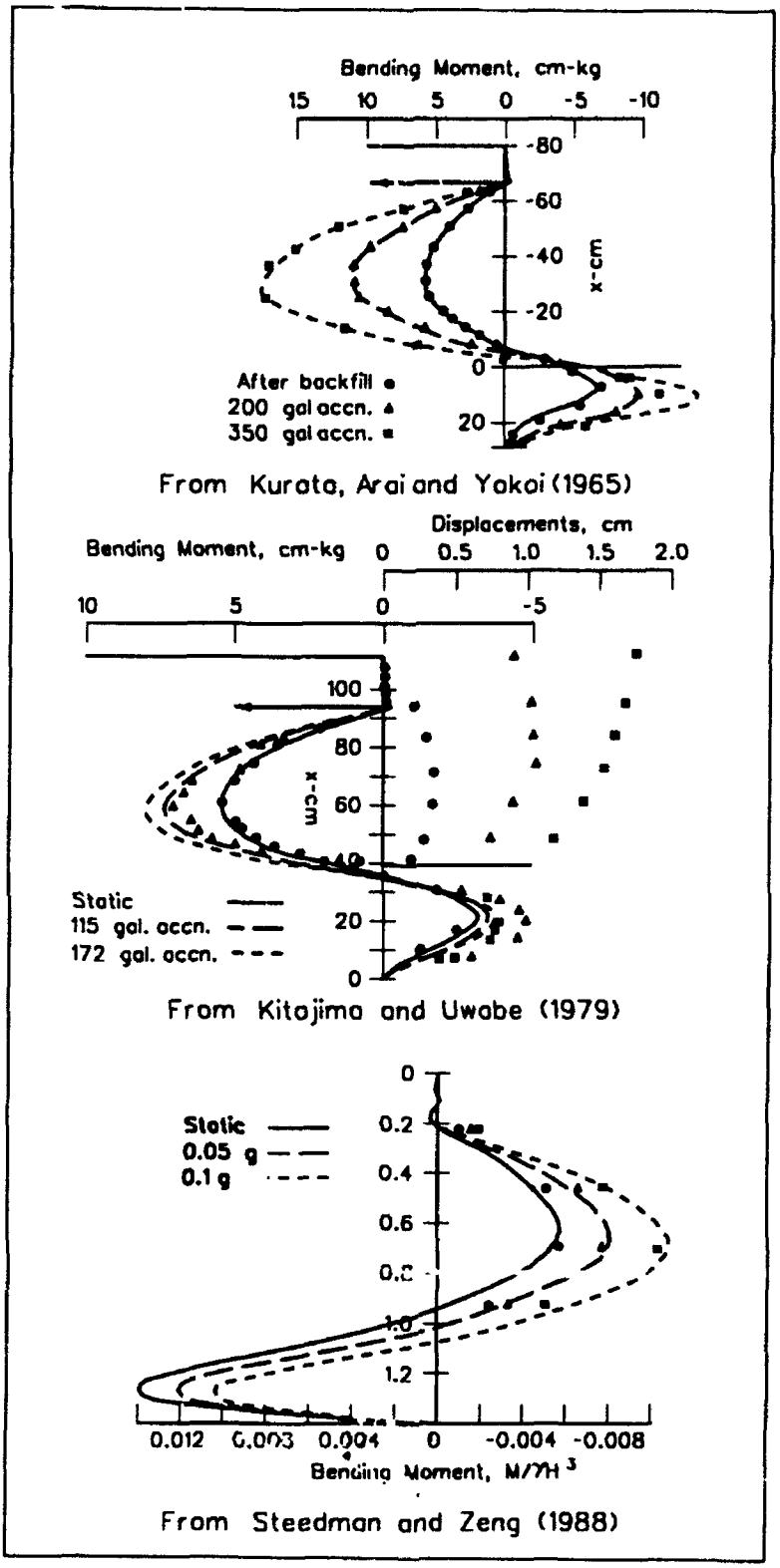

Figure 7.5 Measured distributions of bending moment in three model tests on anchored bulkhead

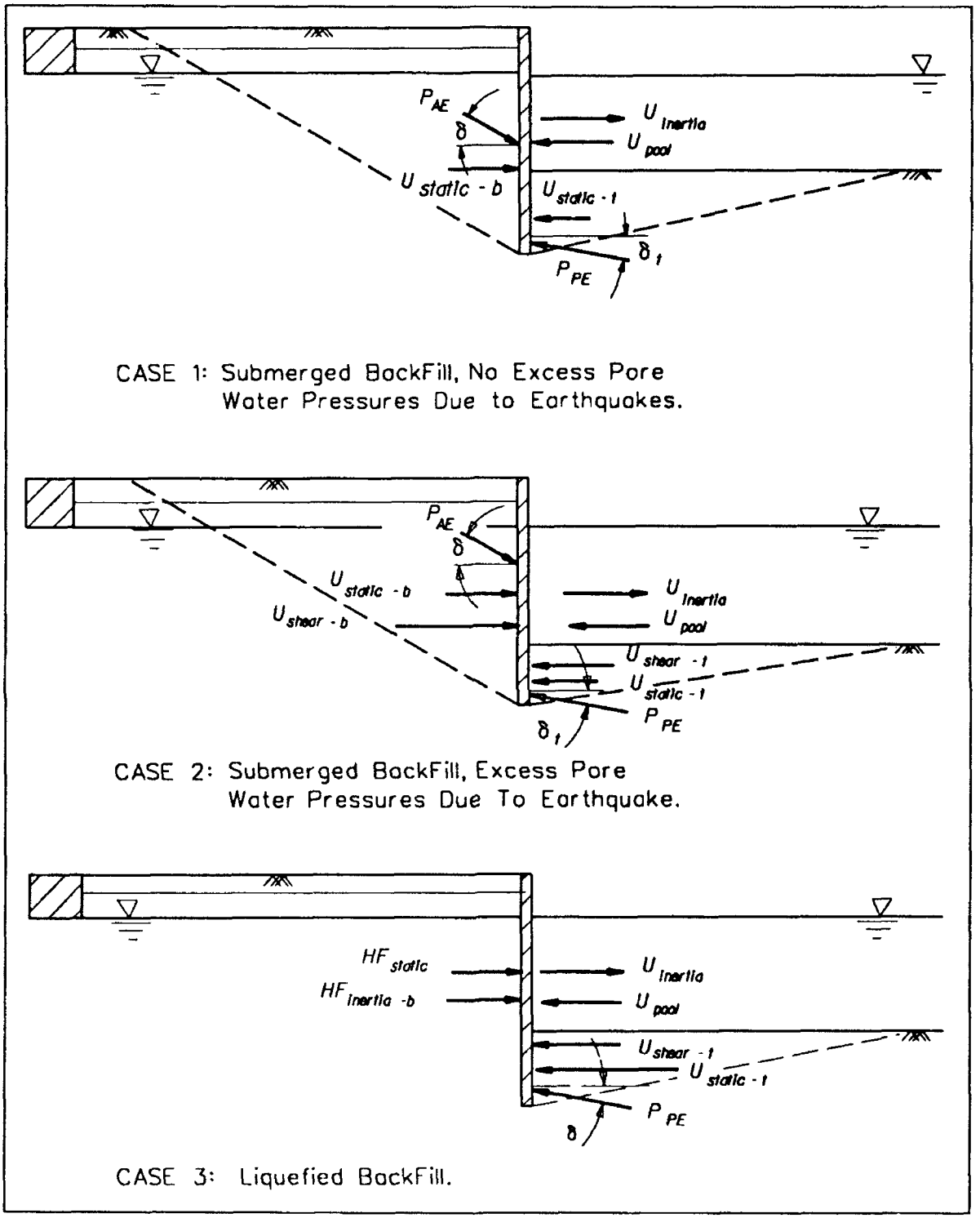

Figure 7.6 Anchored sheet pile walls retaining backfills which undergo movements during earthquakes

and $U_{static-t}$. $U_{inertia}$ corresponds to the hydrodynamic water pressure force along the front of the wall due to earthquake shaking of the pool. $U_{shear-b}$ and $U_{shear-t}$ correspond to the excess pore water pressure force acting along the back of the wall and along the front of the wall (Case 2). In the case of a liquified backfill, HF_{static} and $HF_{inertia-b}$ are equal to the equivalent heavy fluid hydrostatic pressure of the liquified backfill and the inertia force due to the acceleration of a liquified backfill.

An anchored sheet pile wall cannot be designed to retain a liquified backfill and foundation, and hence Case 3 is only of academic interest. Site improvement techniques (the National Research Council 1985) or the use of alternative structures should be investigated in this situation. A procedure for determining the potential for liquefaction within the submerged backfill or the potential for the development of excess pore water pressures is discussed in numerous articles, including the National Research Council (1985), Seed, Tokimatsu, Harder, and Chung (1985), Seed and Harder (1990) or Marcuson, Hynes, and Franklin (1990). The design procedure (Section 7.4.2) is limited to the case where excess pore water pressures are less than 30 percent of the initial vertical effective stress.

Flexure of the Sheet Pile Wall Below the Dredge Level:

Justification of the use of Rowe's moment reduction factor values, obtained from static tests (Rowe 1952) on dynamic problems, is empirical. The damage surveys of anchored sheet pile walls that failed due to earthquake shaking listed one sheet pile wall that exhibited a general flexural failure (Section 7.2.1). The structural failure of this wall, designed using the Japanese Code, was attributed to corrosion at the dredge level. The Japanese Code uses the Rowe's reduction factor values to reduce the maximum free earth support moment in the design of the sheet pile section, thus relying on flexure of the sheet pile wall below the dredge level during earthquake shaking. Flexure of the sheet pile below the dredge level is caused by several factors, including the depth of penetration and flexural stiffness of the sheet pile wall and the strength and compressibility of the soil (Rowe 1952, 1956, and 1957, Tschebotarioff 1973). In Rowe's procedure, the dependence of the value of r_d on the soil type incorporates the dependence of the level of moment reduction on the compressibility and strength of the soil as well as the magnitude and distribution of sheet pile displacements below the dredge level.

The ability of the system to develop flexure below the dredge level during earthquake shaking must be carefully evaluated prior to application of Rowe's moment reduction factor or any portion of the reduction factor. This is especially true when analyzing the seismic stability of an existing sheet pile wall founded in a contractive soil. A sheet pile wall founded in dense granular soils is far more likely to develop flexure below the dredge level during earthquake shaking than one founded in loose soils. Dense soils that dilate during shearing are far less susceptible to large displacements during earthquake shaking than are loose soils (Seed, 1987 and Seed, Tokimatsu, Harder, and Chung, 1985). Loose soils contract during shearing and are susceptible to large displacements and even flow failures caused by earthquake shaking (National Research Council, 1985, and Whitman, 1985). As a general design principle, anchored sheet pile walls sited in seismic environments should be founded in dense and dilative cohesionless soils with no silt or clay site particles.

7.4.1 Design of Anchored Sheet Pile Walls - No Excess Pore Water Pressures

The presence of water within the backfill and in front of the sheet pile wall results in additional static and dynamic forces acting on the wall and alters the distribution of forces within the active and passive soil wedges developing behind and in front of the sheet pile wall. This section describes the first of two proposed design procedures using the free earth support method to design anchored sheet pile walls retaining submerged or partially submerged backfills and including a pool of water in front of the sheet pile wall, as shown in Figure 7.7. This analysis, described as Case 1 in Figure 7.6, assumes that no excess pore water pressures are generated within the submerged portion of the backfill or within the foundation during earthquake shaking. The evaluation of the potential for the generation of excess pore water pressures during the shaking of the submerged soil regions is determined using the procedure described in the National Research Council (1985), Seed, Tokimatsu, Harder, and Chung (1985), Seed and Harder (1990) or Marcuson, Hynes, and Franklin (1990). Stability of the structure against block movements, as depicted in Figure 2.1, should also be checked during the course of the analysis. The ten stages of the analyses in the design of anchored walls for seismic loadings using the free earth support method of analysis are labeled A through J in Table 7. Appendix C contains a worked example. The 13 steps in the design of the anchored sheet pile wall retaining submerged backfill as shown in Figure 7.7 are as follows:

(1) Perform a static loading design of the anchored sheet pile wall using the free earth support method of analysis, as described in Section 7.3, or any other suitable method of analysis.

(2) Select the k_h value to be used in the analysis; see Section 1.4 of Chapter 1.*

(3) Consider k_v as discussed in Section 1.4.3.

(4) Compute P_{AE} using the procedure described in Section 4.3 and with the shear strength of the backfill fully mobilized. P_{AE} acts at an angle δ to the normal to the back of the wall. The pore pressure force $U_{static-b}$ is determined from the steady state flow net for the problem. By definition, only steady state pore water pressures exist within the submerged backfill and foundation of a Case 1 anchored sheet pile wall ($r_u = 0$). In the restrained water case of a <u>fully submerged</u> soil wedge with a hydrostatic water table, P_{AE} is computed (Equations 33 and 38) using an effective unit weight equal to the buoyant unit weight. K_{AE} (Equation 34) or $K_A(\beta^*, \theta^*)$ (Equation 38) is computed using an equivalent horizontal acceleration, k_{hel}, and an equivalent seismic inertia angle, ψ_{el}, given by Equations 47 and 46 (Section 4.3.1).

---

* The values for seismic coefficients are to be established by the seismic design team for the project considering the seismotectonic structures within the region, or as specified by the design agency. The earthquake-induced displacements for the anchored sheet pile wall are dependent upon numerous factors, including how conservatively the strengths, seismic coefficients (or accelerations), and factors of safety have been assigned, as well as the compressibility and density of the soils, and the displacement at the anchorage.

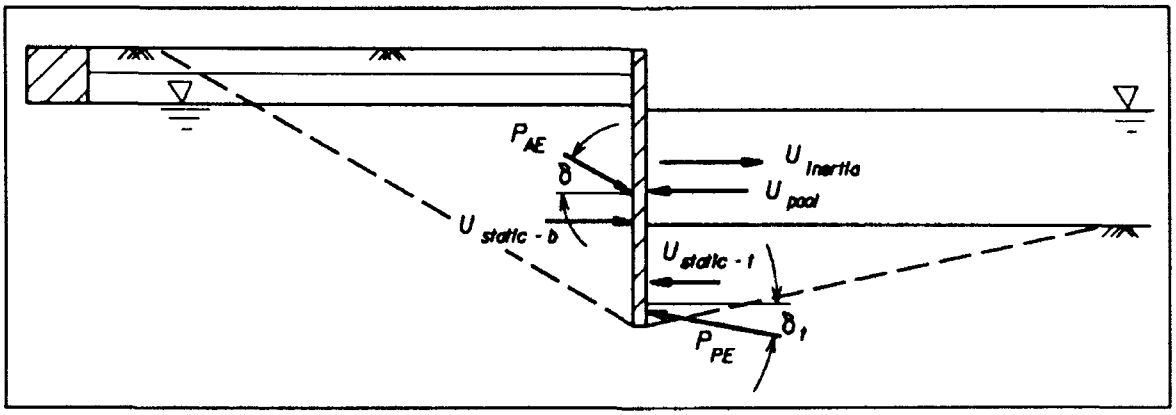

Figure 7.7 Anchored sheet pile wall with no excess pore water pressure due to earthquake shaking (Case 1).

Table 7 Ten Stages of the Analyses in the Design of Anchored Walls for Seismic Loadings

Stage of Analysis	Section 7.4.1 Design Steps	Description
A		Evaluate potential for liquefaction or excessive deformations.
B	1	Static design: Provides initial depth of penetration for seismic analysis.
C	2, 3	Determine the average site specific acceleration for wall design.
D	4, 5	Compute dynamic earth pressure forces and water pressure forces.
E	6	Sum the moments due to the driving forces and the resisting forces about the tie rod elevation.
F	4-6	Alter the depth of penetration and repeat steps 4 and 6 until moment equilibrium is achieved. The minimum depth of embedment has been computed when moment equilibrium is satisfied.
G	7	Sum horizontal forces to compute the tie rod force (per foot of wall).
H	8, 9	Compute the maximum bending moment, apply Rowe's moment reduction factor and size the flexible wall (if applicable).
I	10	Size the tie rods and select their spacing.
J	11-13	Design and site the anchorage.

In the case of a partially submerged backfill, this simplified procedure will provide approximate results by increasing the value assigned to the effective unit weight, γ_e, based upon the proportion of the soil wedge that is above and below the water table (see Figure 4.13 in Section 4.3.3). P_{AE} is computed (Equations 33 and 38) with γ_t replaced by γ_e. K_{AE} (Equation 34) or $K_A(\beta^*,\theta^*)$ (Equation 38) is computed using an equivalent horizontal acceleration, k_{hel}, and an equivalent seismic inertia angle, ψ_{el}, given by Equations and 46 in Section 4.3.1 with γ_b replaced by γ_e. A more refined analysis may be conducted using the trial wedge procedure (Appendix A) for the forces shown in Figure 7.7.

To compute the point of action of P_{AE} in the case of a partially submerged backfill, redefine P_{AE} in terms of the static force, P_A, and the dynamic active earth pressure increment, ΔP_{AE}, using Equation 40. This procedure is demonstrated in Figure 7.8. First compute K_A and the static effective earth pressure distribution along the back of sheet pile wall using one of the procedures described in Chapter 3. P_A is equal to the resultant force for this static effective stress distribution along the back of the wall, which also provides for the point of action for P_A. Solve for the force ΔP_{AE} as equal to the difference between P_{AE} and P_A. Assume that ΔP_{AE} acts at a height equal to 0.6·H above the base of the sheet pile. Compute the point of action of force P_{AE} using Equation 44 and correcting this relationship for the new locations along the back of the sheet pile for the forces P_A and ΔP_{AE} (refer to Example 19).

(5) Compute P_{PE} acting in front of the sheet pile using the procedure described in Section 4.4 (Chapter 4) and using a factor of safety, FS_P, applied to both the shear strength of the soil and the effective angle of friction along the interface. δ equal to $\phi'/2$ (Section 3.3.1) is a reasonable value for dense frictional soils. In a static free earth support method of analysis, FS_P is set equal to 1.5, and in a dynamic earth pressure analysis, the minimum value assigned to FS_P is 1.2. $U_{static-t}$ is determined from the steady state flow net for the problem. By definition, only steady state pore water pressures exist within the submerged backfill and foundation of a Case 1 anchored sheet pile

$$\tan\phi_t = \frac{\tan\phi'}{FS_P} \tag{95}$$

and

$$\tan\delta_t = \frac{\tan\delta}{FS_P} \tag{96}$$

wall ($r_u = 0$). In the restrained water case of a fully submerged soil wedge with a hydrostatic water table, P_{PE} is computed (Equations 58 and 62) using an effective unit weight equal to the buoyant unit weight. For low to moderate levels of earthquake shaking, assume that P_{PE} acts at a height equal to approximately 1/3 of the height of the soil in front of the sheet pile wall and at an angle δ_t to the normal to the face of the

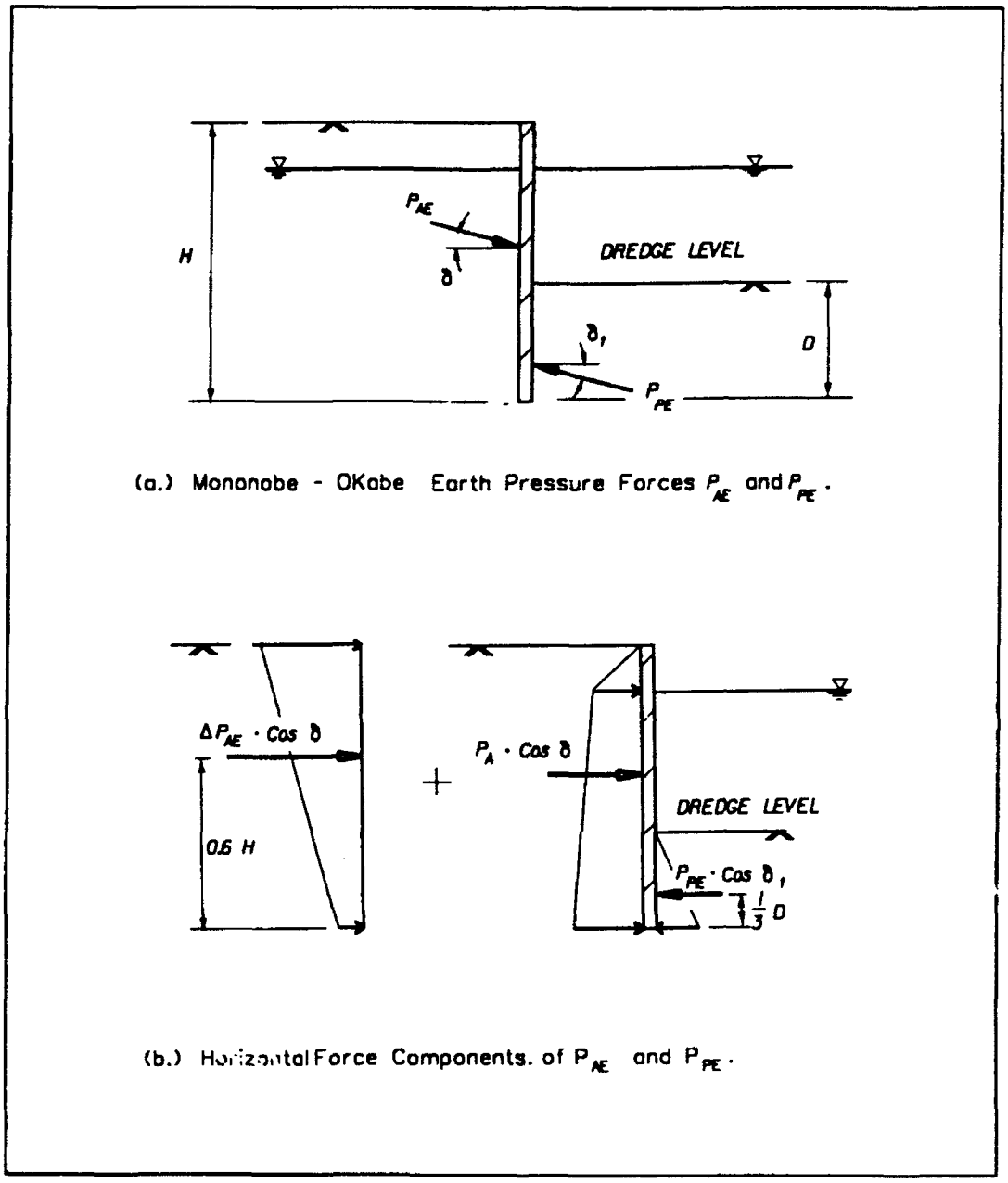

Figure 7.8 Static and inertial horizontal force components of the Mononobe-Okabe earth pressure forces

wall.* K_{PE} (Equation 59) or $K_P(\beta^*,\theta^*)$ (Equation 62) is computed using an equivalent horizontal acceleration, k_{hel}, and an equivalent seismic inertia angle, ψ_{el}, given by Equations 47 and 46. In the case of a steady state seepage, this simplified procedure will provide approximate results by decreasing the value assigned to the effective unit weight (Equation 27) according to the magnitude of the upward seepage gradient (Equation 26).

Equation 59 for K_{PE} is restricted to cases where the value of ϕ (Equation 95) is greater than ψ_{el} (Equation 46). This limiting case may occur in cases of high accelerations and/or low shear strengths. One contributing factor is the submergence of the soil in front of the anchored wall, which approximately doubles the value of the equivalent seismic inertia angle over the corresponding dry soil case.

(6) To determine the minimum required depth of sheet pile penetration, the clockwise and counterclockwise moments of the resultant earth pressure forces and resultant water pressure forces about Figure 7.7 anchor are computed as follows:

$$\text{Counterclockwise Moment} = P_{AE}\cos\delta_b \cdot (Y_a - Y_{AE}) + U_{static\text{-}b} \cdot (Y_a - Y_{ub}) + U_{inertia} \cdot (Y_a - Y_i) \tag{97}$$

and

$$\text{Clockwise Moment} = -U_{pool} \cdot (Y_a - Y_{up}) - P_{PE} \cdot \cos\delta_t \cdot (Y_a - Y_{PE}) - U_{static\text{-}t} \cdot (Y_a - Y_{ut}) \tag{98}$$

---

* In a static design by the free earth support method of analysis, a triangular earth pressure is assumed along the front of the wall, with the resulting force P_P assigned to the lower third point. Experience has shown that reasonable static designs resulted when the appropriate strength parameters and adequate factors of safety were used in conjunction with this simplified assumption. A similar approach is used in the dynamic design. The point of application of P_{PE} may move downward from its static point of application for anchored sheet pile walls as the value for k_h increases. However, no satisfactory procedure was found for computing the point of application of P_{PE} for this structure. In the interim, the assumption of P_{PE} acting at approximately 1/3 of the height of the soil in front of the wall is restricted to low to moderate levels of earthquake shaking (e.g. one rough index is $k_h < 0.1$) and with conservative assumptions regarding all parameters used in the analysis. For higher levels of shaking and less conservative assumptions for parameters, a larger value for FS_P than 1.2 and/or a lower point of application would be assigned.

where

δ_b = effective angle of friction along the backfill to sheet pile wall interface

δ_t = effective angle of friction along the toe foundation to sheet pile wall interface

$U_{static-b}$ = resultant steady state pore water pressure force along the back of the wall

$U_{static-t}$ = resultant steady state pore water pressure force below the dredge level along the front of the wall

U_{pool} = resultant hydrostatic water pressure force for the pool

$U_{inertia}$ = hydrodynamic water pressure force for the pool, directed away from the wall (see Appendix B)

Y_a = distance from the base of sheet pile to the anchor

Y_{AE} = distance from the base of sheet pile to P_{AE}

Y_{ub} = distance from the base of sheet pile to $U_{static-b}$ (from a flow net)

Y_i = distance from the base of sheet pile to $U_{inertia}$ (see Appendix B)

Y_{up} = distance from the base of sheet pile to U_{pool}

Y_{PE} = distance from the base of sheet pile to P_{PE}

Y_{ut} = distance from the base of sheet pile to $U_{static-t}$ (from a flow net).

The value for the Clockwise Moment about Figure 7.7 anchor is compared to the value for the Counterclockwise Moment, resulting in the following three possibilities:

(6a) If the value of the Clockwise Moment is equal to the value of the Counterclockwise Moment, the sheet pile wall is in moment equilibrium, and the depth of penetration below the dredge level is correct for the applied forces.

(6b) If the value of the Clockwise Moment is greater than the value of the Counterclockwise Moment, the trial sheet pile embedment depth below the dredge level is too deep and should be reduced.

(6c) If the value of the Clockwise Moment is less than the value of the Counterclockwise Moment, the trial sheet pile embedment depth below the dredge level is shallow and should be increased.

Note that the sheet pile wall is in moment equilibrium for only one depth of sheet pile penetration within the foundation. For those trial sheet pile penetration depths in which moment equilibrium is not achieved, a new trial depth of sheet pile penetration is assumed, and step 4 through step 6 are repeated.

(7) Once the required depth of sheet pile penetration is determined in step 6, the equilibrium anchor force per foot width of wall, T_{FES}, is computed using the equations for horizontal force equilibrium.

$$T_{FES} = P_{PE}\cos\delta_t + U_{static-t} + U_{pool} - U_{inertia} - P_{AE}\cos\delta_b - U_{static-b} \qquad (99)$$

In some situations the value for T_{FES} computed in a seismic analysis can be several times the value computed in the static analysis due to the effect of the inertial forces acting on both the active and passive soil wedges and the pool of water. Large anchor forces per foot width of wall will impact

both the selection of the type of anchorage, anchor geometry and the number of rows and spacing of tie rods along the wall (see steps 10 through 12).

(8) The distribution of the moments within the sheet pile is computed from the external earth pressures along the front and back of the sheet pile and from the anchor force. To accomplish this, the earth pressure forces shown in Figure 7.7 must be converted to equivalent earth pressures distributions. One approach for doing this is to separate P_{AE} into its static and incremental dynamic components and corresponding points of action, as discussed in step 4 and shown in Figures 7.8 and 7.9. Figure 7.10 is used to define the variation in horizontal stress with depth for the dynamic earth pressure force increment ΔP_{AE}. At a given elevation, an imaginary section is made through the sheet pile, as shown in Figure 7.10, and the internal shear force V and internal bending moment M are represented. The internal shear force V is equal to the sum of earth pressures and water pressures and T_{FES} acting on the free body diagram of the sheet pile above Section A-A'. The internal bending moment M is equal to moment of the earth pressures, water pressures about Section A-A'. The maximum bending moment within the sheet pile is denoted as M_{FES}. The value for M_{FES} is determined by calculating the internal bending moment at the elevation at which the shear is equal to zero.

(9) The design moment for the sheet pile, M_{design}, is equal to

$$M_{design} = M_{FES} \cdot r_d \tag{100}$$

where M_{FES} is the value of the maximum moment calculated using the Free Earth Support Method, and r_d is the Rowe's moment reduction factor discussed in Section 7.3. Using the currently available moment reduction curve shown in Figure 7.2, the value of correction factor will change from the static case only if the depth of penetration or the flexural stiffness, EI, of the wall changes in order to meet moment equilibrium requirements for seismic loadings. The ability of the system to develop flexure below the dredge level during earthquake shaking must be carefully evaluated prior to application of Rowe's moment reduction factor or any portion thereof. This aspect of the design is discussed in Section 7.4.

In a static design, the allowable stress in the sheet pile is usually restricted to between 50 and 65 percent of the yield strength. Higher allowable stresses may be considered for use in the design for dynamic earth pressures, given the short duration of loading during earthquakes. The allowable stresses for earthquake loading may be increased 33 percent above the value specified for static loading. This corresponds to an allowable stress in the sheet pile restricted to between 67 and 87 percent of the yield strength. The effects of corrosion should be considered during the course of wall design for static and seismic loadings.

(10) In a static design, the design tie rod force per foot width of wall, T_{design}, is equal to

$$T_{design} = 1.3 \cdot T_{FES} \tag{101}$$

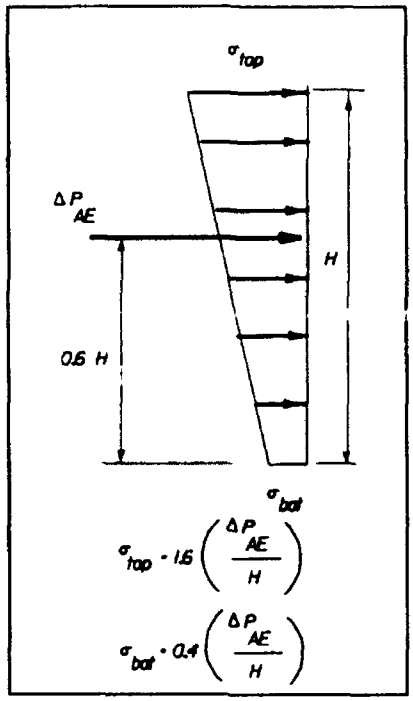

Figure 7.9 Distributions of horizontal stresses corresponding to ΔP_{AE}

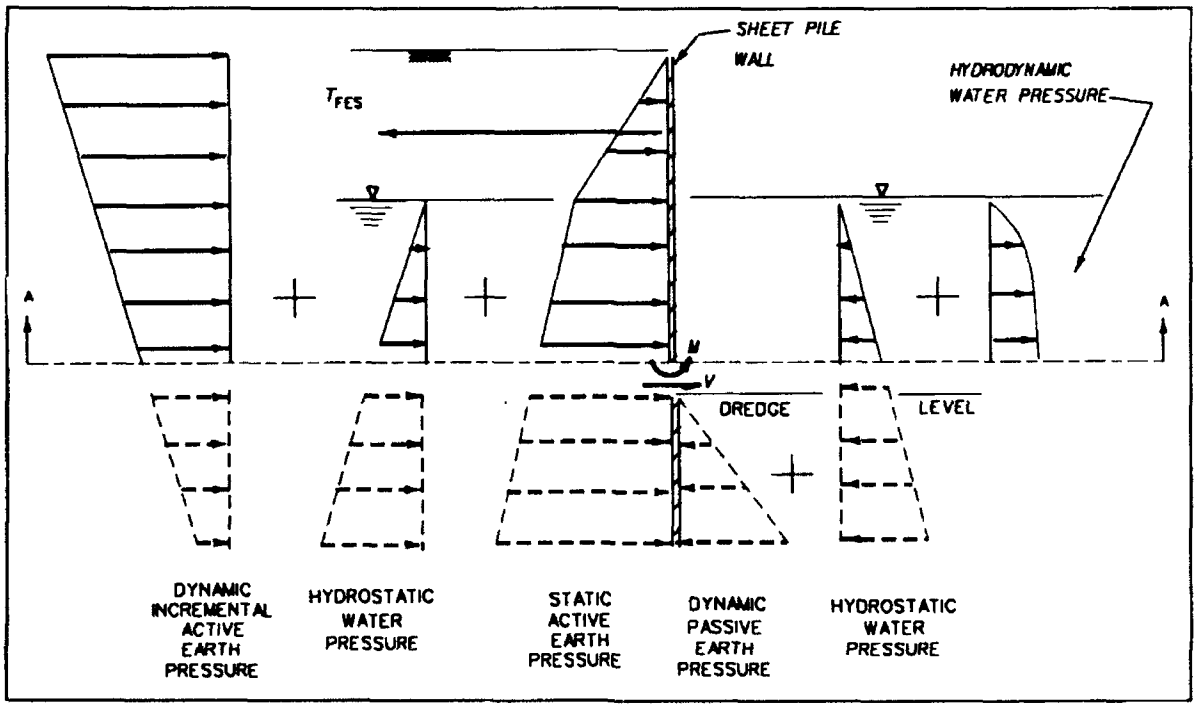

Figure 7.10 Horizontal pressure components and anchor force acting on sheet pile wall

and the allowable stress in the tie rods is usually restricted to between 40 and 60 percent of the yield strength. The factor 1.3 is also recommended for earthquake loading conditions. The Japanese code restricts the allowable stresses to 60 percent of the yield strength for earthquake loading (see the discussion at the end of step 9). The value of 60 percent is recommended. The effects of corrosion should be considered during the course of wall design for both static and seismic loadings.

(11) The design of the anchorage for seismic loadings follows the approach that is proposed for the design of the flexible wall and differs from the approach used when designing for static loadings. In the case of static loads, the ultimate force (per foot width of wall) which the anchor is to be designed, T_{ult-a}, is equal to

$$T_{ult-a} = 2.5 \cdot T_{FES} \tag{102}$$

and the static earth pressure forces P_A and P_P on the front and back of the anchor block are computed using the ultimate shear strength with $\delta = 0°$ for slender anchorage (refer to discussion in Section C.1.9 of Appendix C or to Dismuke (1991). The proposed design procedure for seismic loadings is described in steps 12 and 13. Seismic loads usually control the anchorage design.

(12) For those waterfront structures in which the anchor consists of a plate or a concrete block, a major contribution to the forces resisting the pulling force T_{ult-a} is provided by the formation of a passive soil wedge in front of the block, as shown in Figure 7.11a. In a seismic analysis, T_{ult-a} is set equal to T_{FES}. The Mononobe-Okabe equations 33 and 58 are used to compute the dynamic active earth pressure force, P_{AE}, and the dynamic passive earth pressure force, P_{PE}, acting on the anchor block during earthquake shaking (Figure 7.11b). P_{AE} is computed with the shear strength of the backfill fully mobilized and $\delta = 0°$ for slender anchorage and $\delta \leq \phi/2$ for mass concrete anchorage (Section C.1.9 of Appendix C). P_{PE} is computed using a factor of safety FS_P applied to the shear strength of the soil (Equation 95) and the effective angle of friction along the interface (Equation 96). At a minimum, FS_P is set equal to a value between 1.2 and 1.5, depending on the allowable displacement and on how conservatively the strengths and seismic coefficients have been assigned. In general and with all parameters constant, the larger the factor of safety, the smaller the anchorage displacement due to earthquake shaking.

Water pressure forces are not included along the sides of the block because most anchor blocks are constructed on or just above the water table, as idealized in this figure. If the water table extends above the base of the block, these forces are to be included in the analysis.

The size of the block is proportioned such that

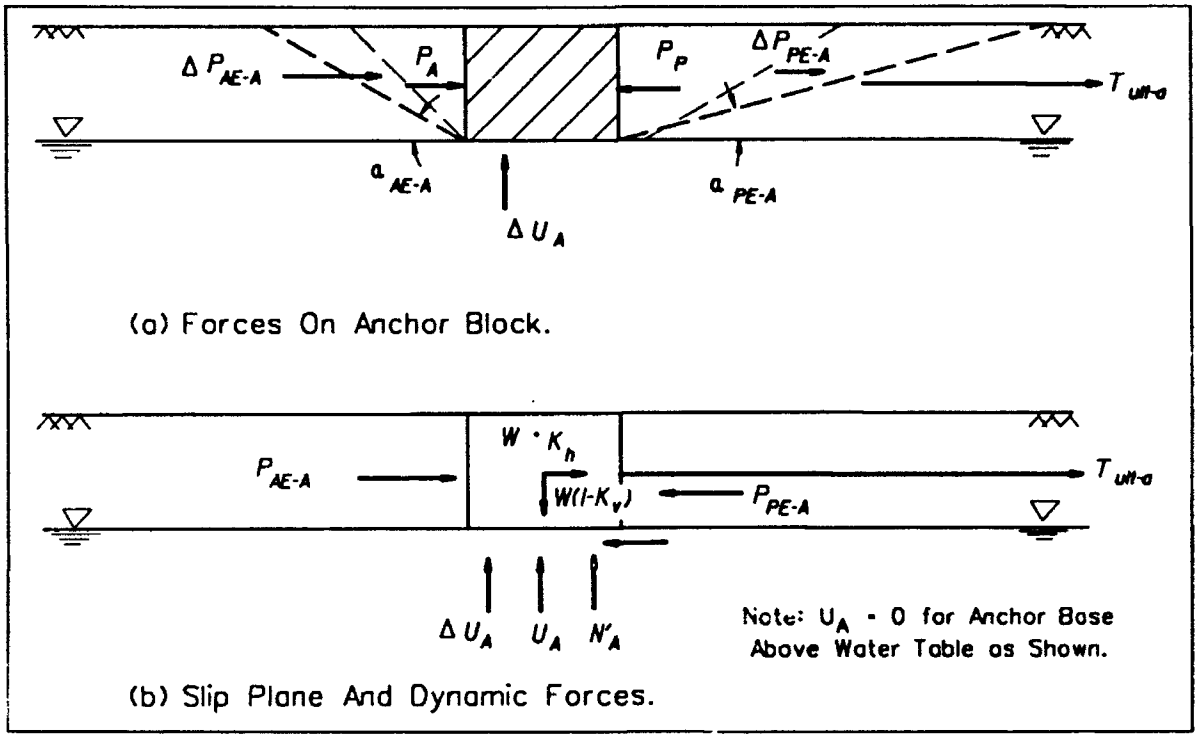

Figure 7.11 Dynamic forces acting on an anchor block (for δ = 0°)

$$T_{ult-a} = P_{PE} \cdot \cos\delta_t - P_{AE} \cdot \cos\delta_b - W \cdot k_h + N' \cdot \tan\delta_A \tag{103}$$

where

$$N' = W(1 - k_v) - U_A. - P_{PE} \cdot \sin\delta_t + P_{AE} \cdot \sin\delta_b \tag{104}$$

When the magnitude of computed anchor block forces prohibit the use of shallow anchor blocks, alternative anchorage systems are to be investigated. These include the use of multiple tie rods and anchorage, A-frame anchors, sheet pile anchorage, soil or rock anchors and tension H-piles. Discussions of anchorage are readily available in numerous textbooks and sheet pile design manuals, including the USS Steel Sheet Piling Design Manual (1969), Dismuke (1991), McMahon (1986) and U. S. Army Corps of Engineers Manual EM 1110-2-2906 (Headquarters, Department of the Army 1991).

By definition, no excess pore water pressures are generated within the backfill (ΔU_A = 0) for the Case 1 anchored sheet pile walls. U_A is equal to the resultant steady state pore water pressure force along the base of the anchor. The orientation of a linear failure plane in front of the anchor block, α_{PE}, in Figure 7.11a is approximated using Equation 61.

(13) The anchor block is to be located a sufficient distance behind the sheet pile wall so that the active failure surface behind the sheet pile wall does

not intersect the passive failure surface developing in front of the anchor during earthquake shaking. The required minimum distance between the back of the sheet pile and the anchor block increases with increasing values of acceleration, as shown in Figure 7.1. The orientation of the active slip surface behind the sheet pile wall, α_{AE}, is calculated in step 4, and the orientation of the passive slip surface in front of the anchor block, α_{PE}, is calculated in step 12.

7.4.2 Design of Anchored Sheet Pile Walls - Excess Pore Water Pressures

This section describes the proposed procedure, using the free earth support method to design anchored sheet pile walls retaining submerged or partially submerged backfills and including a pool of water in front of the sheet pile wall, as shown in Figure 7.12. This analysis, described as Case 2 in Figure 7.6, assumes that excess pore water pressures are generated within the submerged portion of the backfill or within the foundation during earthquake shaking. The magnitude and distribution of these excess pore water pressures depend upon several factors, including the magnitude of the earthquake, the distance from the site to the fault generating the earthquake and the properties of the submerged soils. The evaluation of the magnitude of these excess pore water pressures is estimated using the procedure described in Seed and Harder (1990) or Marcuson, Hynes, and Franklin (1990). This design procedure is limited to the case where excess pore water pressures are less than 30 percent of the initial vertical effective stress. Stability of the structure against block movements, as depicted in Figure 2.1, should also be checked during the course of the analysis. Many of the details regarding the procedures used are common to the Case 1 analysis. The 14 steps in the design of the anchored sheet pile wall retaining submerged backfill as shown in Figure 7.12 are as follows:

(1) Perform a static loading design of the anchored sheet pile wall using the free earth support method of analysis, as described in Section 7.3, or any other suitable method of analysis.

(2) Select the k_h value to be used in the analysis; see Section 1.4 of Chapter 1.*

(3) Consider k_v, as discussed in Section 1.4.3.

(4) Compute P_{AE} using the procedure described in Section 4.3 and with the shear strength of the backfill fully mobilized. P_{AE} acts at an angle δ to the normal to the back of the wall. The pore pressure force $U_{static-b}$ is determined from the steady state flow net for the problem. The post-earthquake residual excess pore water pressures are identified as U_{shear} in Figure 7.12 and are determined using the procedures described in Seed and Harder (1990) or

---

* The values for seismic coefficients are to be established by the seismic design team for the project considering the seismotectonic structures within the region, or as specified by the design agency. The earthquake-induced displacements for the anchored sheet pile wall are dependent upon numerous factors, including how conservatively the strengths, seismic coefficients (or accelerations), and factors of safety have been assigned, as well as the compressibility and density of the soils, and the displacement at the anchorage.

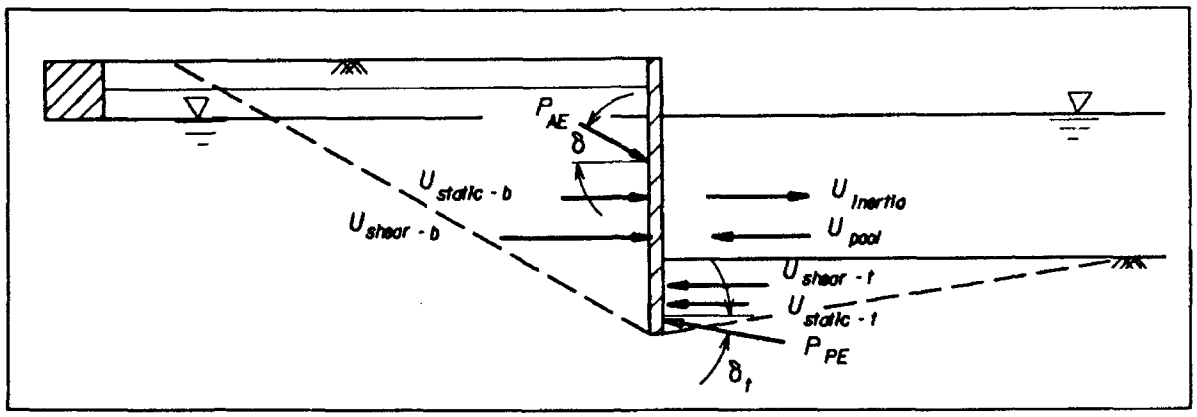

Figure 7.12 Anchored sheet pile wall with excess pore water pressures generated during earthquake shaking (Case 2)

Marcuson, Hynes, and Franklin (1990). In the restrained water case of a <u>fully submerged</u> soil wedge with a hydrostatic water table, P_{AE} is computed (Equations 33 and 38) using an effective unit weight equal to the buoyant unit weight. K_{AE} (Equation 34) or $K_A(\beta^*,\theta^*)$ (Equation 38) is computed using an equivalent horizontal acceleration, k_{he3}, and an equivalent seismic inertia angle, ψ_{e3}, given by equations 55 and 54 (Section 4.3.2). An alternative approach is to use a modified effective friction angle, ϕ_{eq} (Equation 56), with r_u equal to the average value within the backfill.

In the case of a <u>partially submerged backfill</u>, this simplified procedure will provide approximate results by increasing the value assigned to the effective unit weight, γ_e, based upon the proportion of the soil wedge that is above and below the water table (see Figure 4.13 in Section 4.3.3). P_{AE} is computed (Equations 33 and 38) with γ_t replaced by γ_e. The unit weight assigned to the soil below the water table is given by Equation 52 when using the procedure described in Figure 4.13 to compute the value of γ_e. K_{AE} (Equation 34) or $K_A(\beta^*,\theta^*)$ (Equation 38) is computed using an equivalent horizontal acceleration, k_{he3}, and an equivalent seismic inertia angle, ψ_{e3}, given by Equations 54 and 55 in Section 4.3.2 with γ_{e3} replaced by γ_e. For this case, the excess residual pore water pressures are superimposed upon the hydrostatic pore water pressures.

To compute the point of action of P_{AE} in the case of a partially submerged backfill, redefine P_{AE} in terms of the static force, P_A, and the dynamic active earth pressure increment, ΔP_{AE}, as described in step 4 of Section 7.4.1.

(5) Compute P_{PE} acting in front of the sheet pile using the procedure described in Section 4.4 of Chapter 4 and apply a factor of safety FS_P equal to 1.2 to both the shear strength of the soil and the effective angle of friction along the interface. Refer to step 5 of Section 7.4.1. The pore pressure force $U_{static-t}$ is determined from the steady state flow net for the problem. In the restrained water case of a <u>fully submerged</u> soil wedge with a hydrostatic water table, P_{PE} is computed (Equations 58 and 62) with γ_t replaced by the effective unit weight of soil below the water table, γ_{e3} (Equation 52 in Section 4.3.2). An average r_u value is used within the soil in front of the wall. K_{PE} (Equation 59) or $K_P(\beta^*,\theta^*)$ (Equation 62) is computed

using an equivalent horizontal acceleration, k_{he3}, and an equivalent seismic inertia angle, ψ_{e3}, given by Equations 54 and 55 in Section 4.3.2. In the case of a steady state seepage, this simplified procedure will provide approximate results by decreasing the value assigned to the effective unit weight (Equation 27) according to the magnitude of the upward seepage gradient (Equation 26). For low to moderate levels of earthquake shaking, assume that P_{PE} acts at a height equal to approximately 1/3 of the height of the soil in front of the sheet pile wall and at an angle δ_t to the normal to the face of the wall.*

(6) To determine the required depth of sheet pile penetration, the clockwise and counterclockwise moments of the resultant earth pressure forces and resultant water pressure forces about Figure 7.12 anchor are computed as follows:

$$\text{Counterclockwise Moment} = P_{AE}\cos\delta_b \cdot (Y_a - Y_{AE}) + U_{static\text{-}b} \cdot (Y_a - Y_{ub}) + U_{shear\text{-}b} \cdot (Y_a - Y_{utaub}) + U_{inertia} \cdot (Y_a - Y_i) \tag{105}$$

and

$$\text{Clockwise Moment} = -U_{pool} \cdot (Y_a - Y_{up}) - P_{PE} \cdot \cos\delta_t \cdot (Y_a - Y_{PE}) - U_{static\text{-}t} \cdot (Y_a - Y_{ut}) - U_{shear\text{-}t} \cdot (Y_a - Y_{utaut}) \tag{106}$$

where

$U_{shear\text{-}b}$ = resultant excess pore water pressure force along the back of the wall

$U_{shear\text{-}t}$ = resultant excess pore water pressure force below the dredge level along the front of the wall

Y_{utaub} = distance from the base of sheet pile to $U_{shear\text{-}b}$

Y_{utaut} = distance from the base of sheet pile to $U_{shear\text{-}t}$

Values for Y_{utaub}, $U_{shear\text{-}b}$, Y_{utaut} and $U_{shear\text{-}t}$ are computed using the procedure described in Seed and Harder (1990) or Marcuson, Hynes, and Franklin (1990).

---

* In a static design by the free earth support method of analysis, a triangular earth pressure is assumed along the front of the wall, with the resulting force P_P assigned to the lower third point. Experience has shown that reasonable static designs resulted when the appropriate strength parameters and adequate factors of safety were used in conjunction with this simplified assumption. A similar approach is used in the dynamic design. The point of application of P_{PE} may move downward from its static point of application for anchored sheet pile walls as the value for k_h increases. However, no satisfactory procedure was found for computing the point of application of P_{PE} for this structure. In the interim, the assumption of P_{PE} acting at approximately 1/3 of the height of the soil in front of the wall is restricted to low to moderate levels of earthquake shaking (e.g. one rough index is $k_h < 0.1$) and with conservative assumptions regarding all parameters used in the analysis. For higher levels of shaking and less conservative assumptions for parameters, a larger value for FS_P than 1.2 and/or a lower point of application would be assigned.

The value for the Clockwise Moment is compared to the value for the Counter-clockwise Moment, resulting in one of three possibilities listed in steps 6a through step 6c in Section 7.4.1. The sheet pile wall is in moment equilibrium for only one depth of sheet pile penetration within the foundation. For those trial sheet pile penetration depths in which moment equilibrium is not achieved, a new trial depth of sheet pile penetration is assumed, and step 4 through step 6 is repeated.

(7) Once the required depth of sheet pile penetration is determined in step 6, the equilibrium anchor force per foot width of wall, T_{FES}, is computed using the equations for horizontal force equilibrium.

$$T_{FES} = P_{PE}\cos\delta_t + U_{static-t} + U_{shear-t} + U_{pool} - U_{inertia} - P_{AE}\cos\delta_b - U_{static-b} - U_{shear-b} \quad (107)$$

Additional commentary is provided in step 7 of Section 7.4.1.

(8) The distribution of the moments within the sheet pile, M_{FES}, is computed using the procedure described in step 8 of Section 7.4.1.

(9) The computation of the design moment for the sheet pile, M_{design}, is described in step 9 of Section 7.4.1.

(10) The design tie rod force, T_{design}, is computed using the procedure described in step 10 of Section 7.4.1.

(11) The design of the anchor block for seismic loadings differs from the approach used when designing for static loadings. The reader is referred to the discussion in step 11 of Section 7.4.1.

(12) For those waterfront structures in which the anchor consists of slender anchorage or mass concrete anchorage, a major contribution to the forces resisting the pulling force T_{ult-a} is provided by the formation of a passive soil wedge in front of the block, as shown in Figure 7.11a. The procedure described in step 12 of Section 7.4.1 is used to compute P_{AE}, P_{PE}, and α_{PE} (Figure 7.11b). The size of the block is proportioned using Equation 103 relationship, where N′ is equal to

$$N' = W(1 - k_v) - U_A - \Delta U_A. - P_{PE}\cdot\sin\delta_t + P_{AE}\cdot\sin\delta_b \quad (108)$$

The excess pore water pressure force along the base of the block is equal to ΔU_A (see Seed and Harder (1990) or Marcuson, Hynes, and Franklin (1990)).

An alternative procedure for incorporating residual excess pore water pressures in the analysis is by using r_u and an equivalent angle of interface friction along the base of block, δ_A.

$$\tan\delta_{A\,eq} = (1 - r_u)\tan\delta_A \quad (109)$$

In this case, the value for N′ in Equation 103 is given by

$$N' = W(1 - k_v) - U_{A'} - P_{PE} \cdot \sin\delta_t + P_{AE} \cdot \sin\delta_b \tag{110}$$

Reducing the effective stress friction angle along the soil to concrete interface so as to account for the excess pore water pressures is not an exact procedure (see discussion in Section 4.3.2).

(13) The required minimum distance between the back of the sheet pile and the anchor block is computed following the procedure described in step 1 of Section 7.4.1.

(14) The residual excess pore water pressures within the submerged backfill and foundation will be redistributed after earthquake shaking has ended. The post earthquake static stability (k_h and k_v equal to zero) of any earth retaining structure should be evaluated during the redistribution of the excess pore water pressures within the soil regions (see discussions in the National Research Council 1985 or Seed 1987).

7.5 Use of Finite Element Analyses

Finite element analyses should be considered only if: (a) the cost implications of the simplified design procedures indicate that more detailed study is warranted, (b) it is necessary to evaluate permanent displacements that might result from the design seismic event, or (c) there is concern about the influence of surface loadings. It is particularly difficult to model well the various features of an anchored wall, especially when there is concern about excess pore pressures. One example of a detailed analysis of an actual failure is given by Iai and Kameoka (1991).

CHAPTER 8 ANALYSIS AND DESIGN OF WALLS RETAINING NONYIELDING BACKFILLS

8.1 Introduction

This chapter applies to design problems in which the allowable movement of a wall is small - less than one-fourth to one-half of Table 1 wall movement values. Typical situations include the walls of U-shaped structures such as dry docks, walls of basements, and the lateral walls of underground structures. Under these conditions it may be inappropriate to base design upon earth pressures computed using the Mononobe-Okabe theory, which assumes that active stress conditions are achieved. Hence, earth pressures generally should be computed using the theory set forth in Chapter 5.

Design criteria for such situations will involve permissible combined static plus dynamic bending stresses within the wall. In many cases it may be necessary to ensure that such moments do not cause yielding of the material composing the wall. If the wall is free-standing, then avoidance of sliding or overturning will be design criteria.

In many cases it may be appropriate to use Wood's simplified theory to compute the dynamic increment of stresses. In this case, a key decision will be the choice of the horizontal acceleration coefficient k_h. Important considerations are:

* If displacement of the wall is not permissible, the assigned peak acceleration coefficient should be used. Use of a seismic coefficient less than the peak acceleration coefficient implies that some displacement of the backfill is acceptable during the design earthquake event.

* The acceleration at ground surface should be used to define k_h. This is a conservative assumption. If the peak acceleration varies significantly over the height of the backfill, which may often be the situation when the high side walls of dry docks are involved, consideration should be given to the use of dynamic finite element studies (see Appendix D).

Use of finite element studies should also be considered when there are important surface loadings. In many cases an elastic analysis using soil moduli and damping adjusted for expected levels of strain will suffice.

There may be cases in which it is overly conservative to design structures using lateral pressures from the theory for walls retaining nonyielding backfills. If the structure is founded upon soil with the same stiffness as the backfill (see Figure 8.1), the structure itself will experience movements that may be sufficient to develop active stress conditions. Finite element studies, and measurements as large scale field models in Taiwan (Chang et al. 1990), have shown this to be the case. However, in such situations, it would seem that larger, passive-type stresses should develop on the opposite wall. If there are large cost implications for design using stresses computed assuming nonyielding backfills, finite element studies should again be considered.

If liquefaction is of concern, methods for evaluating residual pore pressures may be found in Seed and Harder (1990) or Marcuson, Hynes, and Franklin (1990). In principle it is possible to design walls to resist the pressures from fully liquefied soil, including Westergaard's dynamic pressure

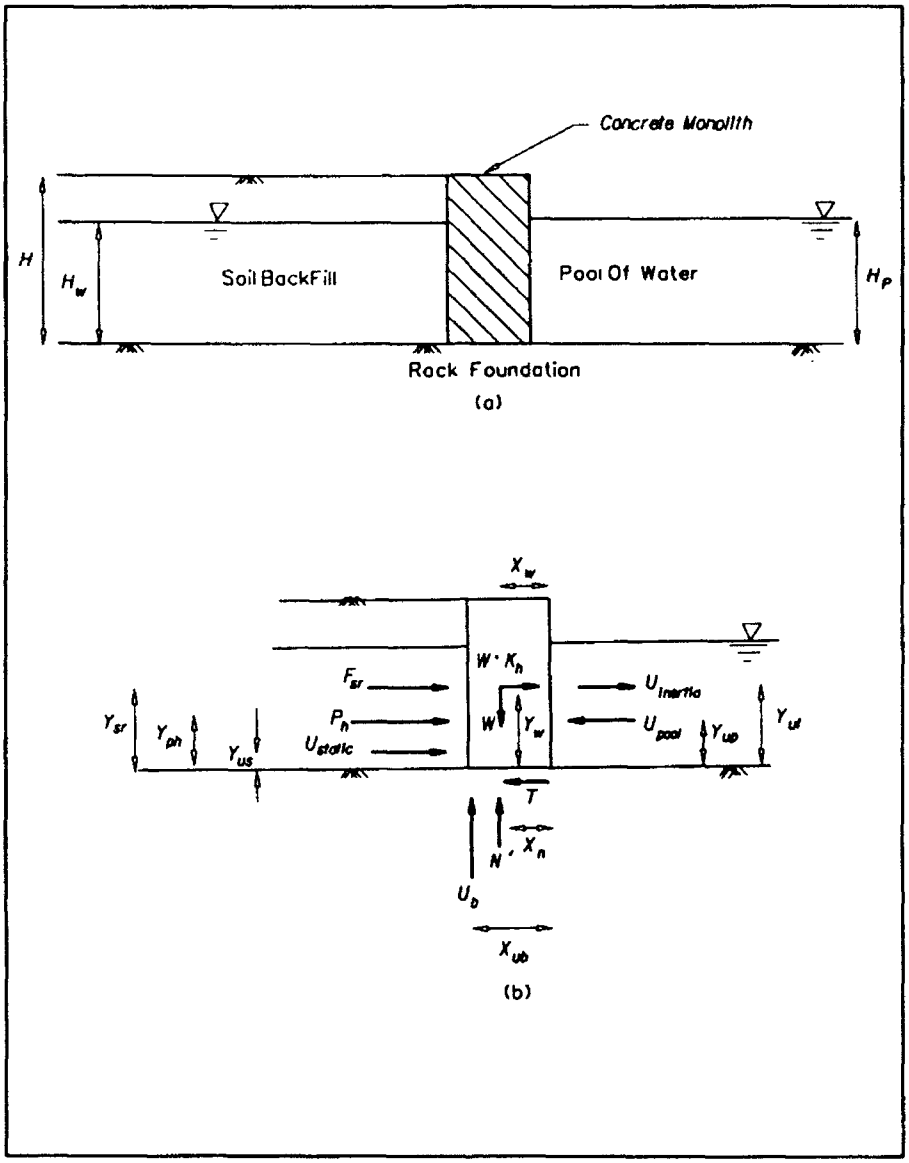

Figure 8.1 Simplified procedure for dynamic analysis of a wall retaining nonyielding backfill

increment based upon the total unit weight of the soil. However, in such a situation the lateral pressures on a wall can be very high. Unless there are structures (including cranes) adjacent to the wall, it might be possible to allow values of r_u in excess of 40 percent. If so, a check should be made for post-seismic stability, using the residual strength of the backfill soil.

8.2 An Example

The application of the simplified procedure to the dynamic analysis is demonstrated for a wall retaining nonyielding backfill founded on rock as shown in Figure 8.1a. A pool of water is included in front, of the wall in this problem. The forces acting along the back, front, and base of the wall include both static and dynamic incremental forces (Figure 8.1b). With negligible wall movements, the value for the static effective earth pressure,

P_h, corresponds to at-rest earth pressures. For gravity earth retaining structures founded on rock, K_o usually ranges in value from 0.45 for compacted granular backfills to 0.55 for uncompacted granular backfills (Duncan, Clough, and Ebeling 1990). U_{static} and U_b are determined from the steady state flow net for the problem. U_{pool} is equal to the hydrostatic water pressure force along the front of the wall. $U_{inertia}$ is the hydrodynamic water pressure force for the pool computed using the Westergaard procedure that is described in Appendix B. Given the horizontal base acceleration value, $k_h \cdot g$, the dynamic earth pressure force F_{sr} is computed using Equation 68, acting at Y_{sr} equal to $0.63 \cdot H$ above the base of the wall. The horizontal force T is the shear force required for equilibrium of the wall and is equal to

$$T = P_h + F_{sr} + W \cdot k_h + U_{static} - U_{pool} + U_{inertia}. \tag{111}$$

The effective normal force between the base of the wall and the rock foundation is equal to

$$N' = W - U_b. \tag{112}$$

The ultimate shear force along the base, T_{ult}, is given by

$$T_{ult} = N' \tan\delta_b \tag{113}$$

where

δ_b = the effective base interface friction angle.

The factor of safety against sliding along the base, F_s, is given by

$$F_s = \frac{\text{ultimate shear force}}{\text{shear force required for equilibrium}} \tag{114}$$

and compared to the minimum value of 1.1 or 1.2 for temporary loading cases. The point of action of the force N', $x_{N'}$, is computed by summing moments about the toe of the wall.

$$x_{N'} = \frac{W \cdot x_W - P_h \cdot Y_{Ph} - F_{sr} \cdot Y_{sr} - U_{static} Y_{ust} - W \cdot k_h \cdot Y_W - U_b X_{ub} + M_{pool}}{N'} \tag{115}$$

where

$$M_{pool} = U_{pool} Y_{up} - U_{inertia} Y_{ui}$$

Y_{Ph} = point of action of P_h. $Y_{Ph} = 0.4 \cdot H$ for a completely dry or completely submerged backfill with a hydrostatic water table (Duncan, Clough, and Ebeling 1990)

The overturning criterion is expressed in terms of the percentage of base contact area B_e/B, where B_e is the width of the area of effective base contact. Assuming that the bearing pressure varies linearly between the base of the wall and the foundation, the normal stress is a maximum at the toe ($q = q_{max}$) and a minimum at the inner edge ($q = 0$) as shown in Figure 8.2.

$$B_e = 3 \cdot x_N \tag{116}$$

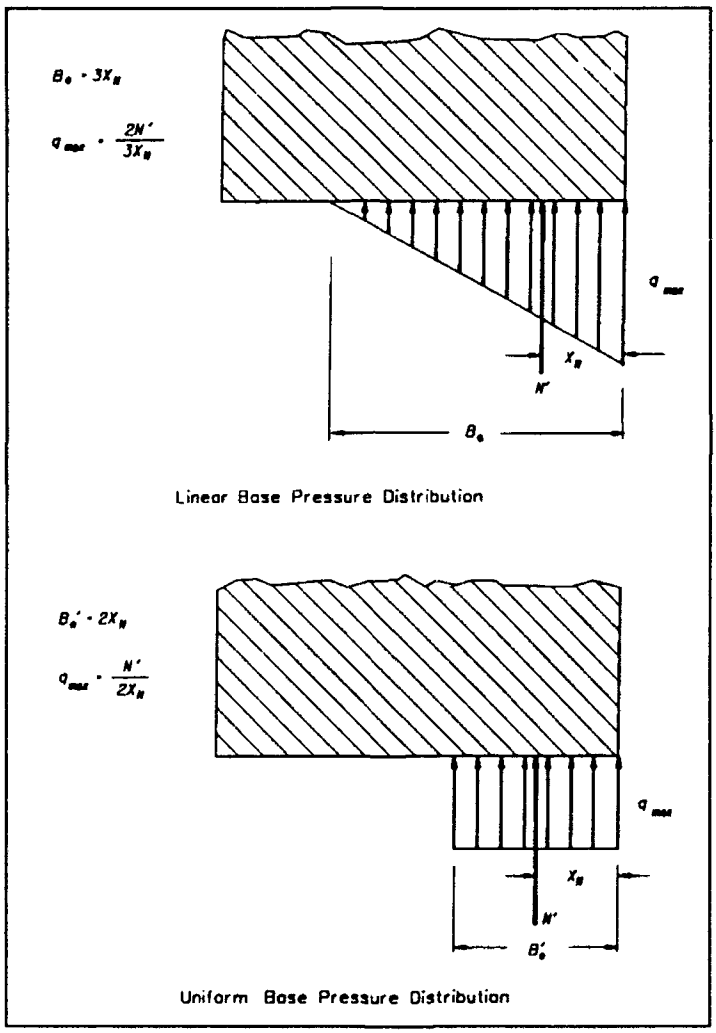

Figure 8.2 Linear and uniform base pressure distributions

An alternative assumption regarding base pressure distribution and contact area was suggested by Meyerhof (1953). Meyerhof assumed a uniform distribution of pressure along the base, resulting in the effective base contact equal to

$$B'_e = 2 \cdot x_N. \tag{117}$$

Meyerhof's pressure distribution has been used widely for foundations on soil, and is most appropriate for foundation materials that exhibit ductile mechanisms of failure. The assumption is less appropriate for brittle materials.

Many retaining walls are designed using static active earth pressures with full contact along the base, B_e/B (or B'_e/B), equal to 100 percent. For temporary loading cases, such as earthquakes, this criteria is relaxed to a minimum value of 75 percent (50 percent for rock foundations, Table 5).

For those structures founded on rock, the factor of safety against bearing capacity failure, or crushing of the concrete or the rock at the toe can be expressed as

$$F_b = \frac{q_{ult}}{q_{max}} \tag{118}$$

where q_{ult} is the ultimate bearing capacity or compressive strength of the concrete or the rock at the toe, and q_{max} is the maximum bearing pressure at the toe. For brittle materials like unconfined concrete, the ultimate bearing capacity is equal to the compressive strength of the material. Building codes are commonly used to obtain values for the allowable bearing stress on rock, q_{all}. Alternately, a large factor of safety is applied to the unconfined compressive strength of intact samples. The maximum bearing pressure q_{max} is restricted to an allowable bearing capacity q_{all}. For ductile foundation materials that undergo plastic failure, the ultimate bearing capacity is larger than the compressive strength of the material, excluding those foundation materials exhibiting a loss in shear resistance due to earthquake induced deformations or due to the development of residual excess pore water pressures. In these cases, a conventional bearing capacity evaluation is conducted to establish the post-earthquake stability of the structure.

In those stability analyses where the vertical accelerations are considered, the force acting downward through the center of mass of the wall that represents the weight of the wall, W, in Figure 8.1, is replaced by the force $(1-k_v) \cdot W$ acting downward. The first term in equations 112 and 115, W and $W \cdot x_w$, are replaced by $(1-k_v) \cdot W$ and $(1-k_v) \cdot W \cdot x_w$, respectively. The direction in which the vertical inertia force, $k_v \cdot W$, acts is counter to the direction assigned to the effective vertical acceleration, $k_v \cdot g$. A $k_v \cdot W$ force acting upward destabilizes the wall, while a $k_v \cdot W$ acting downward increases the stability of the wall.

This procedure is illustrated in example 32 at the end of this chapter.

CHAPTER 8 - EXAMPLE

Content

Example Problem 32.

Commentary

The following example illustrates the procedures described in Chapter 8. The results of the computations shown are rounded for ease of checking calculations and not to the appropriate number of significant figures. Additionally, the wall geometry and values for the material properties were selected for ease of computations.

Example No. 32 Reference Section: 8.2

Design an "nonyielding" rectangular wall (i.e. no wall displacements) of height H = 20 ft to be founded on rock and retaining a dense sand backfill for a peak horizontal acceleration at the ground surface equal to 0.2 g. Assume a frictional contact surface between the wall and the foundation rock (i.e. with no bond).

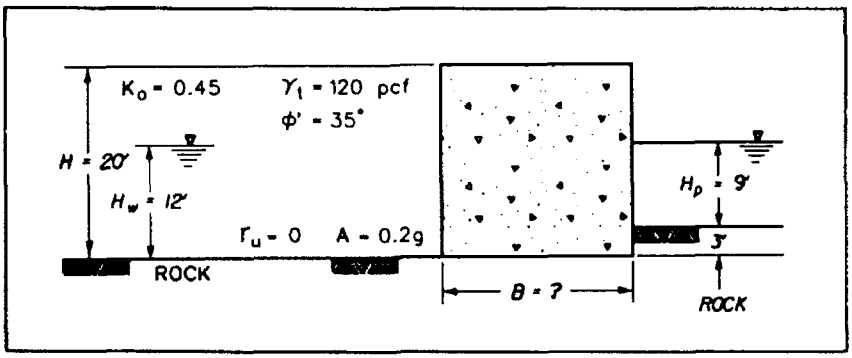

Determine the horizontal acceleration

For Wood's procedure:

$$k_h = A = 0.2$$ (where A is peak ground surface acceleration)

Determine the vertical acceleration

$$k_v = 0$$

Determine P_h (at rest horizontal effective earth pressure) and the point of application.

Find the vertical effective stresses at the ground surface $(\sigma'_y)^{TOP}$, at the water table $(\sigma'_y)^{WT}$, and at the base of the wall $(\sigma'_y)^{BOT}$.

Vertical Effective Stresses at the Top of the Wall

$(\sigma'_y)^{TOP} = 0$

Vertical Effective Stress at the Water Table

$$(\sigma_y)^{WT} = \gamma_t\ (H - H_w) = (120\ \text{pcf})\ (20' - 12') = 960\ \text{psf}$$

$$u = u_{static} + u_{shear} = 0 + 0 = 0$$

$$(\sigma'_y)^{WT} = \sigma_y - u = 960\ \text{psf} - 0 = 960\ \text{psf}$$

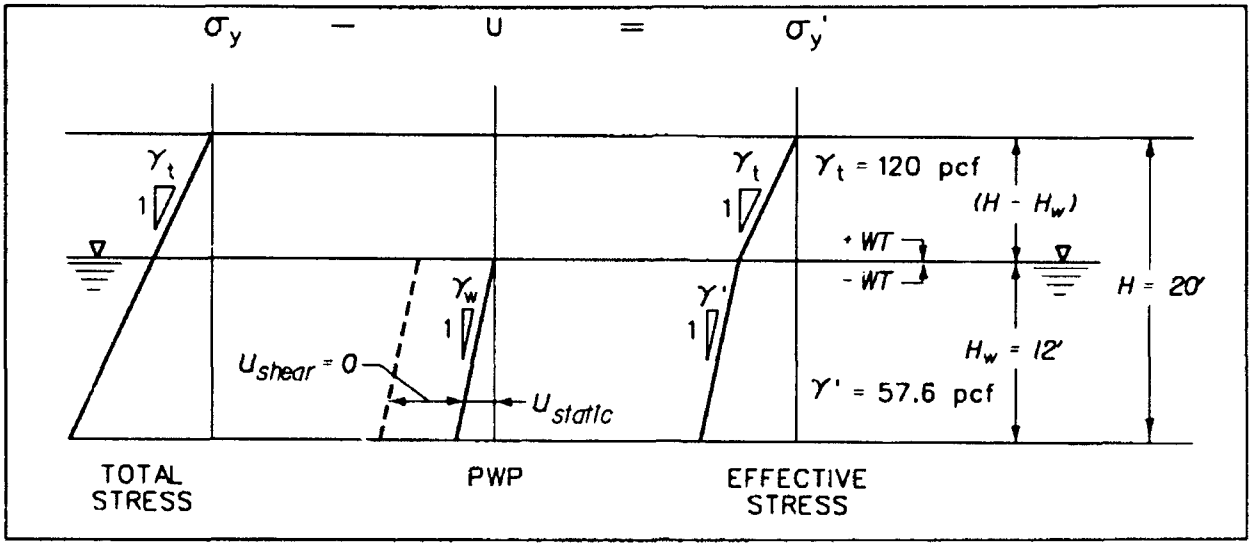

Vertical Effective Stress at the Base of the Wall

$$(\sigma_y')^{BOT} = (\sigma_y')^{WT} + \left[\gamma_t\ (H_w) - u^{BOT}_{static} - u^{BOT}_{shear}\right]$$

$$(\sigma_y')^{BOT} = 960\ \text{psf} + [(120\ \text{pcf})\ (12')\ -\ (12')\ (62.4\ \text{pcf})\ -\ 0]$$

$$(\sigma_y')^{BOT} = 960\ \text{psf} + (120\ \text{pcf} - 62.4\ \text{pcf})\ (12')$$

$$(\sigma_y')^{BOT} = 1{,}651.2\ \text{psf}$$

Determine the horizontal at rest effective stress at the top of the wall σ_h^{TOP}, at the water table σ_h^{WT}, and at the bottom of the wall σ_h^{BOT}.

$$\sigma_h^{TOP} = 0$$

$$\sigma_h^{WT} = K_o(\sigma_y')^{WT} = 0.45\ (960\ \text{psf}) = 432\ \text{psf}$$

$$\sigma_h^{BOT} = K_o(\sigma_y')^{BOT} = 0.45\ (1{,}651.2\ \text{psf}) = 743\ \text{psf}$$

Break the stress distribution diagram into rectangles and triangles to find the magnitude of the resultant force (P_h) and its point of application (Y_{Ph}).

$$E_1 = 1/2\ \sigma_h^{WT}\ (H - H_w) = 1/2\ (432\ \text{psf})\ (20' - 12')$$

$$E_1 = 1{,}728\ \text{lb per ft of wall}$$

$$Y_{E1} = H_w + 1/3\ (H - H_w) = 12' + 1/3\ (20' - 12') = 14.67\ \text{ft}$$

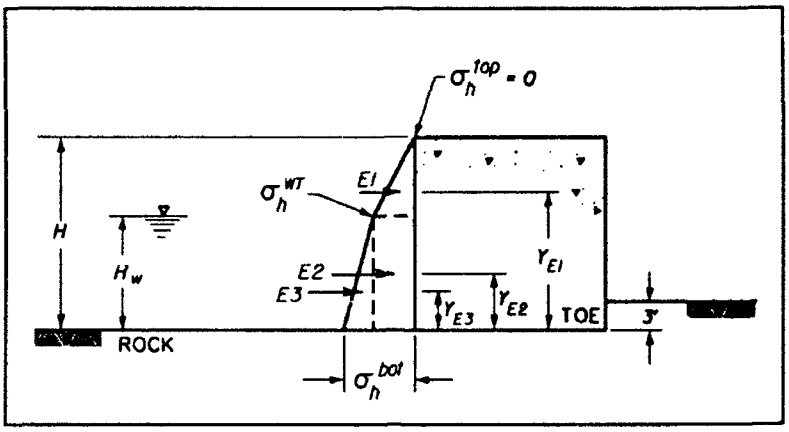

$E_2 = (\sigma_h^{WT})\ (H_w) = (432\ psf)\ (12')$

$E_2 = 5{,}184$ lb per ft of wall

$Y_{E2} = 1/2\ (H_w) = 1/2\ (12') = 6$ ft

$E_3 = 1/2\ (\sigma_h^{BOT} - \sigma_h^{WT})\ (H_w) = 1/2\ (743\ psf - 432\ psf)\ (12')$

$E_3 = 1{,}866$ lb per ft of wall

$Y_{E3} = 1/3\ (H_w) = 1/3\ (12\ ft) = 4$ ft

$P_h = E_1 + E_2 + E_3 = 1{,}728 + 5{,}184 + 1{,}866$

$P_h = 8{,}778$ lb per ft of wall

Sum moments about the base of the wall and solve for:

$$Y_{Ph} = \frac{E_1\ (Y_{E1}) + E_2\ (Y_{E2}) + E_3\ (Y_{E3})}{P_h}$$

$$Y_{Ph} = \frac{(1{,}728)\ (14.67') + (5184)(6') + (1866)\ (4')}{8778}$$

$Y_{Ph} = 7.28$ ft above the base of the wall

Determine water pressure forces acting against the wall

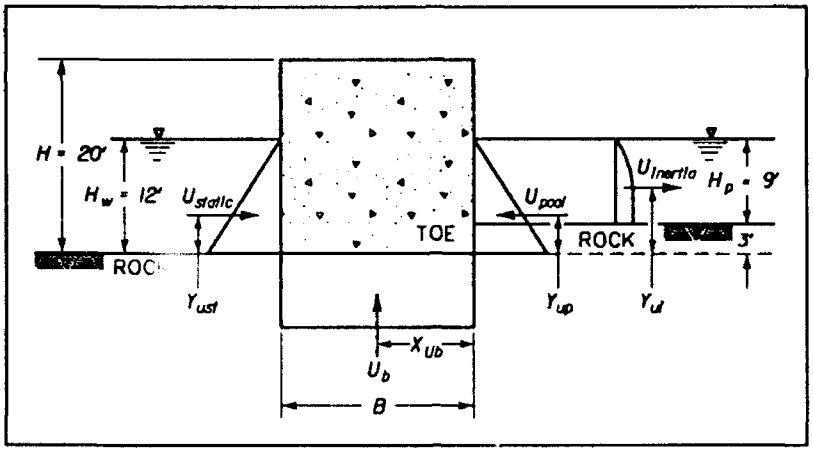

Determine the hydrostatic water pressure force acting against the back of the wall

U_{static} = 4,493 lb per ft of the wall (see ex 19)

Y_{ust} = 4 ft from the base of the wall (see ex 19)

Determine the hydrostatic water pressure force acting against the front of the wall

$U_{pool} = U_{static}$ = 4,493 lb per ft of wall

$Y_{up} = Y_{ust}$ = 4' from the base of the wall

Determine the hydrodynamic water pressure force acting on the front of the wall

(see Appendix B)

$$P_{wd} = \frac{7}{12} k_h \gamma_w H_p^2 \qquad \text{(eq B-5)}$$

P_{wd} = 7/12 (0.2) (62.4 pcf) $(9')^2$ (by eq B-5)

$U_{inertia} = P_{wd}$ = 589.7 lb per ft of wall

Y_{Ui} = 0.4 Hp + 3' = 0.49 (9') + 3'

Y_{Ui} = 6.6 ft above the base of the wall

Determine the hydrostatic water pressure force acting on the base of the wall

Assume full hydrostatic pressure beneath the base of the wall.

$U_b = H_w (\gamma_w) B$

$U_b = (12') (62.4 \text{ pcf}) B = 748.8 (B)$

$X_{Ub} = B/2 = 0.5 B$

Determine the dynamic incremental earth pressures (total stress based calculation)

$F_{sr} = (120 \text{ pcf}) (20')^2 (0.2)$ (by eq 68)

$F_{sr} = 9{,}600$ lb per ft of wall

$Y_{sr} = 0.63 H = 0.63 (20')$

$Y_{sr} = 12.6$ above the base of the wall, acting horizontally

Determine the weight of the wall

$W = (H) (B) (\gamma_{conc}) = (20') (B) (150 \text{ pcf})$

$W = 3{,}000 B$

$X_w = B/2 = 0.5 B$

$Y_w = H/2 = 20'/2 = 10'$

Determine the effective normal force between the base of the wall and the foundation

$N' = 3{,}000 B - 748.8 B = 2{,}251.2 B$ (by eq 112)

Determine the ultimate shear force along the base

$\delta_b = 35°$ (from Table 2)

$T_{ult} = (2{,}251.2 B) \tan (35) = 1{,}576.3 B$

Determine the shear force required for equilibrium

Let $F_s = 1.2$

Solving Equation 114 for T,

$$T = \frac{T_{ult}}{F_s} = \frac{1,576.3\ B}{1.2} = 1,313.6\ B$$

Solve Equation 111 for B required for shear force equilibrium

$$1,313.6\ B = 8,778 + 9,600 + 3,000\ B\ (0.2) + 4,493 - 4,493 + 589.7$$

$$B = \frac{18,968}{1,913.6} = 9.9'$$

Let B = 10′ for $F_s = 1.2$.

Solve Equation 115 such that overturning criteria are met

$$\frac{B_e}{B} = 0.5 \qquad \text{(from Table 5)}$$

$$B_e = 3\ X_{N'} \qquad \text{(adapted from eq 116)}$$

$$\frac{3\ X_{N'}}{B} = 0.5$$

$$X_{N'} = \frac{0.5\ B}{3} = \frac{1}{6}\ B$$

$$M_1 = W\ X_W - W\ k_h\ Y_w = 1,500\ B\ (B - 4) \qquad \text{(see ex 31)}$$

$$M_2 = M_{pool} - U_{static}\ (Y_{ust}) = U_{pool}\ (Y_{Up}) - U_{inertia}\ (Y_{ui}) - U_{static}\ (Y_{ust})$$

$$M_2 = -U_{inertia}\ (Y_{ui}) = -589.7\ (6.6') = -3,892$$

$$M_3 = -P_h\ (Y_{Ph}) = -8,778\ (7.28') = -63,904$$

$$M_4 = -F_{sr}\ (Y_{sr}) = -(9,600)\ (12.6') = -120,960$$

$$M_5 = -U_b\ (X_{Ub}) = -(748.8\ B)\ (0.5\ B) = -374.4\ B^2$$

$$X_{N'} = \frac{M_1 + M_2 + M_3 + M_4 + M_5}{N'}$$

$$X_{N'} = \frac{1{,}500\ B\ (B - 4) - 3{,}892 - 63{,}904 - 120{,}960 - 374.4\ B^2}{2{,}251.2\ B}$$

$$X_{N'} = \frac{1{,}125.6\ B^2 - 6{,}000\ B - 188{,}756}{2{,}251.2\ B}$$

B	1/6 B	$1{,}125.6B^2$	-6,000 B	-188,756	N′ / 2,251.2 B	CALC, $X_{N'}$	$\frac{B_e}{B}$
20′	3.333	450,240	-120,000	-188,756	45,024	3.14	0.471
20.5	3.417	473,033	-123,000	-188,756	46,150	3.50	0.512

Since $\left(\frac{B_e}{B}\right)_{actual} = 0.512 \approx \left(\frac{B_e}{B}\right)_{assumed} = 0.500.$

Therefore select B = 20.5 ft

Check F_b

Compute q_{max}

q_{max} = 2/3 (46,150/3.5) = 8,791 lb/ft (see Figure 8.2)

Check F_b for concrete

Assume for concrete: q_{ult} = 576,000 lb/ft (see Ex 27)

$$(F_b)\ \text{concrete} = \frac{q_{ult}}{q_{max}} = \frac{576{,}000}{8{,}791} = 65.5$$ (by eq 118)

Value for F_b for concrete is adequate.

Check F_b for rock

Calculations omitted.

REFERENCES

Al Homound, A. 1990. "Evaluating Tilt of Gravity Retaining Wall During Earthquakes," ScD Thesis, Department of Civil Engineering, Massachusetts Institute of Technology, Cambridge, MA.

American Association of State Highway and Transportation Officials. 1983. "Guide Specifications for Seismic Design of Highway Bridges," AASHTO, Washington, DC.

Anderson, G., Whitman, R., and Germaine, J. 1987. "Tilting Response of Centrifuge-Modeled Gravity Retaining Wall to Seismic Shaking: Description of Tests and Initial Analysis of Results," Report No. R87-14, Department of Civil Engineering, Massachusetts Institute of Technology, Cambridge, MA.

Agbabian Associates. 1980. "Seismic Response of Port and Harbor Facilities," Report P80-109-499, El Segundo, CA.

Ambraseys, N. N., and Menu, J. M. 1988. Earthquake-Induced Ground Displacements, Earthquake Engineering and Structural Dynamics, Vol. 16, pp. 985-1006.

Amono, R., Azuma, H., and Ishii, Y. 1956. "A Seismic Design of Walls in Japan." Proceedings 1st World Conference on Earthquake Engineering, pp. 32-1 to 32-17.

ASCE Report by the Ad Hoc Group on Soil-Structure Interaction of the Committee on Nuclear Structures and Materials of the Structural Division. 1979. "Analysis for Soil-Structure Interaction Effects for Nuclear Power Plants."

ASCE-Standard. 1986 (Sep). "Seismic Analysis of Safety Related Nuclear Structures and Commentary on Standard for Seismic Analysis of Safety Related Nuclear Structures, 91 p.

Bakeer, R., Bhatia, S., and Ishibashi, S. 1990. "Dynamic Earth Pressure with Various Gravity Wall Movements," Proceedings of ASCE Specialty Conference on Design and Performance of Earth Retaining Structures, Geotechnical Special Publication No. 25., pp.887-899.

Booker, J., Rahman, M., and Seed, H.B. 1976 (Oct). "GADFLEA - A Computer Program for the Analysis of Pore Pressure Generation and Dissipation During Cyclic or Earthquake Loading," Report No. EERC 76-24, Earthquake Engineering Research Center, University of California-Berkeley, Berkeley, CA.

Caquot, A., and Kerisel, F. 1948. "Tables for the Calculation of Passive Pressure, Active Pressure and Bearing Capacity of Foundations," Gauthier-Villars, Paris.

Chang, M., and Chen, W. 1982. "Lateral Earth Pressures on Rigid Retaining Walls Subjected to Earthquake Forces," Solid Mechanics Archives, Vol. 7, No. 4, pp. 315-362.

Chang, C., Power, M., Mok, C., Tang, Y., and Tang, H. 1990 (May). "Analysis of Dynamic Lateral Earth Pressures Recorded on Lotung Reactor Containment Model Structure," Proceedings 4th US National Conference on Earthquake Engineering, EERI, Vol. 3, Palm Springs, CA.

Chopra, A. K. 1967 (Dec). "Hydrodynamic Pressures on Dams During Earthquakes," ASCE, Journal of Engineering Mechanics Division, Vol. 93, No. EM6, pp 205-223.

Clough, G. W. and Duncan, J. M. 1991. Chapter 6: Earth Pressures, in Foundation Engineering Handbook, Second Edition, edited by H. Y. Fang, Van Nostrand Reinhold, NY, pp. 223-235.

Committee on Earthquake Engineering, Commission on Engineering and Technical Systems, National Research Council. 1985. Liquefaction of Soils During Earthquakes, National Academy Press, WA.

Coulomb, C. A. 1776. Essai sur une application des règles des maximis et mininis à quelques problèmes de statique relatifs à l'architecture, *Mem. acad. roy. près divers savants*, Vol. 7, Paris.

Dawkins, W. P. 1991 (Mar). "User's Guide: Computer Program for Design and Analysis of Sheet-Pile Walls by Classical Methods (CWALSHT) with Rowe's Moment Reduction," Instruction Report ITL 91-1, Information Technology Laboratory, US Army Engineer Waterways Experiment Station, Vicksburg, MS.

_____. 1982 (May). "NAVFAC DM-7.2, Foundations And Earth Structures, Design Manual 7.2," Department of the Navy, Naval Facilities Engineering Command, 200 Stovall Street, Alexandria, VA.

Department of the Navy. 1983 (Apr). "NAVFAC DM-7.3, Soil Dynamics, Deep Stabilization, and Special Geotechnical Construction, Design Manual 7.3," Department of the Navy, Naval Facilities Engineering Command, 200 Stovall Street, Alexandria, VA.

Dismuke, T. 1991. Chapter 12: Retaining Structures And Excavations, Foundation Engineering Handbook, Second Edition, edited by H.Y. Fang, Van Nostrand Reinhold, NY, pp. 447-510.

Duncan, J. M. 1985. Lecture Notes Regarding the Design of Anchored Bulkheads.

Duncan, J. M., Clough, G. W., and Ebeling, R. M. 1990. "Behavior and Design of Gravity Earth Retaining Structures," ASCE Specialty Conference on Design and Performance of Earth Retaining Structures, Geotechnical Special Publication 25, pp. 251-277.

Earthquake Engineering Technology, Inc. 1983. "Super FLUSH - Computer Response Analysis Of Soil-Structure Systems Under Various Input Environments."

Ebeling, R. 1990 (Dec). "Review Of Finite Element Procedures for Earth Retaining Structures," Miscellaneous Paper ITL-90-5, Information Technology Laboratory, US Army Engineer Waterways Experiment Station, Vicksburg, MS.

Ebeling, R. M., Duncan, J. M., and Clough, G. W. 1990 (Oct). "Methods of Evaluating the Stability and Safety of Gravity Earth - Retaining Structures Founded on Rock, Phase 2 Study," Technical Report ITL-90-7, Information Technology Laboratory, US Army Engineer Waterways Experiment Station, Vicksburg, MS.

Ebeling, R. M., Clough, G. W., Duncan, J. M., and Brandon, T. L. 1992 (May). "Methods of Evaluating the Stability and Safety of Gravity Earth Retaining Structures Founded on Rock," Technical Report REMR-CS-29, Information Technology Laboratory, US Army Engineer Waterways Experiment Station, Vicksburg, MS.

Edris, E. V., and Wright, S.G. 1987 (Aug). "User's Guide: UTEXAS2 Slope-Stability Package, Volume 1: User's Manual," Instruction Report GL-87-1, Geotechnical Laboratory, US Army Engineer Waterways Experiment Station, Vicksburg, MS.

Elms, D., and Richards, R. 1990. "Seismic Design of Retaining Walls," Proceeding of ASCE Specialty Conference on Design and Performance of Earth Retaining Structures, Geotechnical Special Publication No. 25., pp.854-871.

Finn, W., and Liam, D. 1987. Chapter 3: Geomechanics of Part 3 Finite Element Method Applications in Finite Element Handbook, edited by H. Kardestuncer and D. Norrie, McGraw-Hill, Inc., pp 3.157-3.216.

Finn, W., Liam, D., Yogendrakumar, M., Otsu, H., and Steedman, R.S. 1989. "Seismic Response of a Cantilever Retaining Wall: Centrifuge Model Tests and Dynamic Analysis". Proceedings, 4th International Conference on Soil Dynamics and Earthquake Engineering, Mexico City, Structural Dynamics and Soil Structure Interaction, Editors A.S. Cakmak and I. Herrera, Computational Mechanics Publications, Boston, MA, pp. 39-52.

Finn, W., Liam, D., Yogendrakumar, M., Yoshida, N., and Yoshida, H. 1986. "TARA-3: A Program for Non-Linear Static and Dynamic Effective Stress Analysis," Soil Dynamics Group, University of British Columbia, Vancouver, B.C.

Franklin, G. and Chang, F. 1977 (Nov). "Earthquake Resistance of Earth and Rockfill Dams: Report 5: Permanent Displacement of Earth Embankments by Newmark Sliding Block Analysis," Miscellaneous Paper S-71-17, Soils And Pavements Laboratory, US Army Engineer Waterways Experiment Station, Vicksburg, MS.

Gazetas, G., Dakoulas, P., and Dennehy, K. 1990. "Emperical Seismic Design Method for Waterfront Anchored Sheetpile Walls," Proceedings of ASCE Specialty Conference on Design and Performance of Earth Retaining Structures, Geotechnical Special Publication No. 25., pp. 232-250.

Green, R. 1992. "Selection of Ground Motions for the Seismic Evaluation of Embankments," ASCE Specialty Conference on Stability and Performance of Slopes and Embankments II, A 25-Year Perspective, Geotechnical Special Publication No. 31, Vol. I, pp. 593-607.

Hallquist, J. 1982. "User's Manual for DYNA2D - An Explicit Two-Dimensional Hydrodynamic Finite Element Code With Interactive Rezoning," University of California, Lawrence Livermore National Laboratory, Report UCID-18756, Rev. 1.

Headquarters, Department of the Army. 1989. "Retaining and Flood Walls," Engineer Manual 1110-2-2502, Washington, DC.

_____. 1991. "Design of Pile Foundations," Engineer Manual 1110-2-2906, Washington, DC.

Hung, S., and Werner, S. 1982. "An Assessment of Earthquake Response Characteristics and Design Procedures for Port and Harbor Facilities," Proceeding 3rd International Earthquake Microzonation Conference, Report No. SF/CEE-82070 Seattle, WA, pp. 15.

Hynes-Griffin, M. E., and Franklin, A. G. 1984. "Rationalizing the Seismic Coefficient Method," Miscellaneous Paper S-84-13, US Army Engineer Waterways Experiment Station, Vicksburg, MS.

Iai, S., and Kameoka, T. 1991. "Effective Stress Analysis of a Sheet Pile Quaywall," Proceeding of Second International Conference on Recent Advances in Geotechnical Earthquake Engineering and Soil Dynamics, Paper No. 4.14, Vol. 1, St. Louis, MO, pp. 649-656.

Ichihara, M., and Matsuzawa, H. 1973 (Dec). "Earth Pressure During Earthquake," Soils and Foundations, Vol. 13, No. 4, pp.75-86.

Idriss, I. M. 1985. Evaluating Seismic Risk in Engineering Practice, Proceeding 11th International Conference on Soil Mechanics and Foundation Engineering, Vol. 1, pp.255-320.

Ishibashi, I., and Fang, Y. 1987 (Dec). "Dynamic Earth Pressures with Different Wall Modes," Soils and Foundations, Vol. 27, No. 4, pp. 11-22.

Ishibashi, I., and Madi, L. 1990 (May). "Case Studies On Quaywall's Stability With Liquefied Backfills," Proceeding of 4th U.S. Conference on Earthquake Engineering, EERI, Vol. 3, Palm Springs, CA, pp. 725-734.

Ishibashi, I., Matsuzawa, H., and Kawamura, M. 1985. "Generalized Apparent Seismic Coefficient for Dynamic Lateral Earth Pressure Determination," Proceeding of 2nd International Conference on Soil Dynamics and Earthquake Engineering, edited by C. Brebbia, A. Cakmak, and A. Ghaffer, QE2, pp. 6-33 to 6-42.

Johnson, E. 1953 (Apr). "The Effects of Restraining Boundries on the Passive Resistance of Sand, Results of a Series of Tests with a Medium-Scale Testing Apparatus," Masters of Science Thesis In Engineering, Princeton University.

Joyner, W. B., and Boore, D. M. 1988. "Measurement, Charactization and Prediction of Strong Ground Motion," Earthquake Engineering and Soil Dynamics II - Recent Advances in Ground Motion Evaluation, ASCE Geotechnical Special Publication No. 20, pp. 43-102.

Kerisel, J., and Absi, E. 1990 (May). Active and Passive Earth Pressure Tables," A. A. Balkema International Publishers, pp. 234.

Kitajima, S., and Uwabe, T. 1979 (Mar). "Analysis on Seismic Damage in Anchored Sheet-Piling Bulkheads," Report of the Japanese Port and Harbor Research Institute, Vol. 18, No. 1, pp. 67-130. (in Japanese).

Kurata, S., Arai, H. and Yokoi, T. (1965). "On the Earthquake Resistance of Anchored Sheet Pile Bulkheads," Proceedings, 3rd World Conference On Earthquake Engineering, New Zealand.

Ladd, C. 1991 (Apr). "Stability Evaluation During Staged Construction," ASCE, Journal of Geotechnical Engineering, Vol. 117, No. 4, pp. 540-615.

Lambe, T. and Whitman, R. 1969. "Soil Mechanics," John Wiley & Sons, Inc., New York, Chapters 13 and 23.

Lee, M., and Finn, W. D. Liam. 1975. "DESRA-1: Program for the Dynamic Effective Stress Response Analysis of Soil Deposits including Liquefaction Evaluation," Report No. 36, Soil Mechanic Service, Department of Civil Engineering, University of British Columbia, Vancouver, B.C.

_____. 1978. "DESRA-2: Dynamic Effective Stress Response Analysis of Soil Deposits with Energy Transmitting Boundary Including Assessment of Liquefaction Potential," Report No. 38, Soil Mechanic Service, Department Of Civil Engineering, University of British Columbia, Vancouver, B.C.

Li, X. 1990. "Free-Field Soil Response under Multi-Directional Earthquake Loading, Ph.D. Thesis, Department of Civil Engineering, University of California, Davis, CA.

Lysmer, J., Udaka, T., Tsai, C., and Seed, H. B. 1975. "FLUSH: A Computer Program For Approximate 3-D Analysis of Soil-Structure Interaction Programs," Report No. EERC 75-30, Earthquake Engineering Research Center, University of California, Berkeley, CA.

Makdisi, F. I., and Seed, H. B. 1979. "Simplified Procedure for Estimating Dam and Embankment Earthquake-Induced Deformations," ASCE, Journal of the Geotechnical Engineering Division, Vol. 104, No. GT7, pp. 849-867.

Marcuson, W., Hynes, M., and Franklin, A. 1990 (Aug). "Evaluation and Use of Residual Strength in Seismic Safety Analysis of Embankments," Earthquake Spectra, pp. 529-572.

Matsuo, H., and Ohara, S. 1965. "Dynamic Pore Water Pressure Acting on Quay Walls During Earthquakes," Proceedings of the Third World Conference on Earthquake Engineering, Vol 1, New Zealand, pp. 130-140.

Matsuzawa, H., Ishibashi, I., and Kawamura, M. 1985 (Oct). "Dynamic Soil and Water Pressures of Submerged Soils," ASCE, Journal of Geotechnical Engineering, Vol. 111, No. 10, pp. 1161-1176.

McMahon, D. 1986. Tiebacks for Bulkheads, Collection of Five Papers, Proceeding of a Session Sponsored by the Geotechnical Engineering Division of the ASCE in Conjunction with the ASCE Convention in Seattle, WA., Geotechnical Special Publication No. 4., 90 p.

Meyerhof, G. 1953. "The Bearing Capacity of Foundation Under Inclined and Eccentric Loads," 3rd International Conference Of Soil Mechanics And Foundation Engineering, Vol. 1, pp 440-445.

Mononobe, N., and Matsuo, H. 1929. "On the Determination of Earth Pressures During Earthquakes," Proceedings, World Engineering Congress, 9.

National Earthquake Hazards Reduction Program (NEHRP). 1988. Recommended Provisions for the Development of Seismic Regulations for New Buildings: Building Seismic Safety Council.

National Research Council. 1988. Probabilistic Seismic Hazard Analysis: National Academy Press, Washington, DC, 97 p.

_____. 1985. Liquefaction of Soils During Earthquakes: National Academy Press, Washington, DC, 240 p.

Nadiem, F., and Whitman, R. 1983 (May). "Seismically Induced Movement of Retaining Walls," ASCE, Journal of Geotechnical Engineering, Vol. 109, No. 7, pp. 915-931.

Newmark, N. 1965. Effects of Earthquakes on Dams and Embankments," Geotechnique, Vol. 15., No. 2, pp. 139-160.

Newmark, N. N., and Hall, W. J. 1983. Earthquake Spectra and Design, Earthquake Engineering Research Institute, 499 14th Street, Oakland, CA, 103 p.

Okabe, S. 1926. "General Theory of Earth Pressures," Journal Japan Society of Civil Engineering, Vol. 12, No. 1.

Okamoto, S. 1984. "Introduction to Earthquake Engineering," second edition, University of Tokyo Press, 629 p.

Peterson, M. S., Kulhawy, F. H., Nucci, L. R., and Wasil, B. A. 1976. "Stress-Deformation Behavior of Soil-Concrete Interfaces," Contract Report B-49, Department of Civil Engineering, Syracuse University, Syracuse, NY.

Potyondy, J. G. 1961 (Dec). "Skin Friction Between Various Soils and Construction Materials," Geotechnique, Vol II, No. 4, pp 339-353.

Poulos, S. J., Castro, G., and France, W. (1985). "Liquefaction Evaluation Procedure." ASCE Journal of Geotechnical Engineering Division, Vol. 111, No. 6, pp. 772-792.

Prakash, S., and Basavanna, B. 1969. "Earth Pressure Distribution Behind Retaining Wall During Earthquake," Proceeding, 4th World Conference on Earthquake Engineering, Santiago, Chile.

Provost, J. 1981 (Jan). "DYNAFLOW - A Nonlinear Transient Finite Element Analysis Program, Report No. 81-SM-1, Princeton University, Princeton, NJ.

Provost, J. 1989. "DYNA1D - A Computer Program For Nonlinear Seismic Site Response Analysis, Technical Report NCEER-89-0025, National Center for Earthquake Engineering Research, University of Buffalo.

Rankine, W. (1857). On the Stability of Loose Earth, Phil. Trans. Roy. Soc. London, Vol. 147.

Roth, W. H., Scott, F. F., and Cundall, P. A. 1986. "Nonlinear Dynamic Analysis of a Centrifuge Model Embankment," Proceedings of the Third US National Conference on Earthquake Engineering, Vol. I, Charleston, SC, pp. 505-516.

Richards, R., and Elms, D. 1979 (April). "Seismic Behavior of Gravity Retaining Walls," ASCE, Journal of the Geotechnical Engineering Division, Vol. 105, No. GT4, pp. 449-464.

Richards, R., and Elms, D. 1990. "Seismic Design of Retaining Walls," Proceedings of ASCE Specialty Conference on Design and Performance of Earth Retaining Structures, Geotechnical Special Publication No. 25., pp. 854-871.

Rowe, P. W. 1952. "Anchored Sheet Pile Walls," Proceedings of Institution of Civil Engineers, Vol 1, Part 1, pp 27-70.

Rowe, P. W. 1956. "Sheet Pile Walls at Failure," Proceedings Instruction Civil Engineers London, Vol. 5, Part I, pp. 276-315.

Rowe, P. W. 1957 (Feb). "Limit Design of Flexible Walls," Proceedings Midland Soil Mechanic and Foundation Engineering Society, Vol. 1, pp. 29-40.

Sadigh, K. 1983. "Considerations in the development of site-specific spectra," in proceedings of Conference XXII, site-specific effects of soil and rock on ground motion and the implications for earthquake resistant design: U.S. Geological Survey Open File Report 83-845.

Sarma, S. K. 1979. "Response and Stability of Earth Dams During Strong Earthquakes," Miscellaneous Paper GL-79-13, US Army Engineer Waterways Experiment Station, Vicksburg, MS.

Schnabel, P., Lysmer, J., and Seed, H. B. 1972 (Dec). "SHAKE: A Computer Program for Earthquake Response Analysis of Horizontally Layered Sites," Report No. EERC 72-12, Earthquake Engineering Research Center, University Of California, Berkeley, CA.

Seed, H. B. 1987 (Aug). "Design Problems in Soil Liquefaction," ASCE, Journal of the Geotechnical Engineering Division, Vol. 113, No. 8, pp. 827-845.

_____. 1971. "Simplified Procedure for Evaluating Soil Liquefaction Potential," ASCE, Journal of the Soil Mechanics and Foundations Division, Vol. 97, No. SM9, pp. 1249-1273.

Seed, H. B. and Idriss, I. M. 1982. Ground Motions and Soil Liquefaction During Earthquakes, Earthquake Engineering Research Institute, 499 14th Street, Oakland, CA, pp 134.

Seed, H. B., Idriss, I. M., Arango, I. 1983. "Evaluation of Liquefaction Potential Using Field Performance Data," ASCE, Journal of the Geotechnical Engineering Division, Vol. 109, No. GT3, pp 458-482.

Seed, H. B., Tokimatsu, K. Harder, L. F., and Chung, R. M. 1985 (Dec). "Influence of SPT Procedures in Soil Liquefaction Resistance Evaluations," ASCE, Journal of the Geotechnical Engineering Division, Vol. 111, No. 12, pp. 1425-1445.

Seed, H., and Whitman, R. 1970. "Design of Earth Retaining Structures for Dynamic Loads," ASCE Specialty Conference on Lateral Stresses in the Ground and Design of Earth Retaining Structures, pp. 103-147.

Seed, R. B. and Harder, L. F. (1990). "SPT-Based Analysis of Cyclic Pore Pressure Generation and Undrained Strength," Proceedings of the H. B. Seed Memorial Symposium, Bi Tech Publishing, Vol. II, pp. 351-376.

Sharma, N. (1989). "Refinement of Newmark Sliding Block Model and Application to New Zealand Conditions," Master Thesis, Department of Civil Engineering, University of Canterbury, NZ, 237p.

Sherif, M., Ishibashi, I., and Lee, C. 1982. "Earth Pressure Against Rigid Retaining Walls," ASCE, Journal of the Geotechnical Engineering Division, Vol. 108, No. GT5, pp. 679-695.

Sherif, M., and Fang, Y. 1983 (Nov). "Dynamic Earth Pressures Against Rotating and Non-Yielding Retaining Walls", Soil Engineering Research Report No. 23, Department of Civil Engineering, University of Washington, Seattle, WA, pp. 45-47.

_____. 1984a. "Dynamic Earth Pressures on Rigid Walls Rotating About the Base," Proceedings, Eighth World Conference on Earthquake Engineering, Vol. 6, San Francisco, CA, pp. 993-100.

_____. 1984b. "Dynamic Earth Pressures on Walls Rotating About the Top," Soils and Foundations, Vol. 24, No. 4, pp.109-117.

Spangler, M. 1938. "Lateral Earth Pressures on Retaining Walls Caused by Superimposed Loads," Proceedings of the 18th Annual Meeting of the Highway Research Board, Part II, pp. 57-65.

Stark, T. D., and Mesri, G. 1992 (Nov). "Undrained Shear Strength of Liquefied Sands for Stability Analysis," ASCE, Journal of the Geotechnical Engineering Division, Vol. 118, No. 11.

Steedman, R., and Zeng, X. 1988. "Flexible Anchored Walls Subject to Base Shaking," Report CUED/D-soils TR 217, Engineering Department Cambridge University, UK

Steedman, R., and Zeng, X. 1990. "The Influence of Phase on the Calculation of Pseudo-Static Earth Pressure on a Retaining Wall," Geotechnique, Vol. 40, No. 1, pp. 103-112.

Steedman, R., and Zeng, X. 1990. "Hydrodynamic Pressures on a Flexible Quay Wall," Report CUED/D-soils TR 233, Engineering Department, Cambridge University, UK.

Steedman, R., and Zeng, X. 1990. "The Response of Waterfront Retaining Walls," Proceedings of ASCE Specialty Conference on Design and Performance of Earth Retaining Structures, Geotechnical Special Publication No. 25., pp. 872-886.

Streeter, V., Wylie, and Richart, F. 1974. "Soil Motion Computations by Characteristics Method," Journal of the Geotechnical Engineering Division, ASCE, Vol. 100, No. GT3, pp. 247-263.

Taylor, D. 1948. "Fundamentals of Soil Mechanics," John Wiley & Sons, Inc., New York, pp. 488-491.

Terzaghi, K. 1934 (Feb). "Large Retaining Wall Tests. I. Pressure of Dry Sand," Engineering News Record, Vol. III, pp. 136-140.

_____. 1936 (Apr). "A Fundamental Fallacy in Earth Pressure Calculations," Boston Society of Civil Engineers, pp. 71-88.

_____. 1943. "Theoretical Soil Mechanics", John Wiley & Sons, New York.

_____. 1954. "Anchored Bulkheads," Transactions of the American Society of Civil Engineers, Vol. 119, pp. 1243-1324.

Terzaghi, K., and Peck, R. 1967. "Soil Mechanics in Engineering Practice," Second Edition, John Wiley & Sons, Inc., New York.

Tokimatsu, A. M., and Seed, H. B. 1987 (Aug). "Evaluation of Settlements In Sands Due to Earthquake Shaking," ASCE, Journal of the Geotechnical Division, Vol. 113, No. 8, pp. 861-878.

Tokimatsu, K., and Yoshimi, Y. 1983. "Emperical Correlation of Soil Liquefaction Based on SPT N-Value and Fines Content," Soils and Foundations, Vol. 23, No. 4, pp 56-74.

Towhata, I., and Islam, S. 1987 (Dec.). "Prediction of Lateral Movement of Anchored Bulkheads Induced by Seismic Liquefaction," Soils and Foundations, Vol. 27, No. 4, pp. 137-147.

Tschebotarioff, G. P. 1973. Foundations, Retaining and Earth Structures, McGraw-Hill, Second Edition, 642 p.

USS Steel Sheet Piling Design Manual 1969, 132p.

Vasquez-Herrera, A., and Dobry, R. 1988. "The Behavior of Undrained Contractive Sand and Its Effect on Seismic Liquefaction Flow Failures of Earth Structures," Rensselaer Polytechnic Institute, Troy, NY.

Westergaard, H. 1931. "Water Pressure on Dams During Earthquakes," Transactions of ASCE, Paper No. 1835, pp. 418-433.

Whitman, R. 1979 (Dec). "Dynamic Behavior of Soils and Its Application to Civil Engineering Projects," State of the Art Reports and Special Lectures, 6th Panamerican Conference on Soil Mechanics and Foundation Engineering, Lima, Peru, pp. 59-105.

_____. 1985. "On Liquefaction," Proceedings, 11th International Conference on Soil Mechanism and Foundation Engineering, Vol. 7, San Francisco, CA. pp. 1923-1926.

_____. 1990. "Seismic Design Behavior of Gravity Retaining Walls," Proceedings of ASCE Specialty Conference on Design and Performance of Earth Retaining Structures, Geotechnical Special Publication No. 25., pp. 817-842.

Whitman, R. V. 1992 (Jul). Predicting Earthquake - Caused Permanent Deformations of Earth Structures, Proceedings Wroth Memorial Symposium on Predictive Soil Mechanics, Oxford University (in press).

Whitman, J., and Christian, J. 1990. "Seismic Response of Retaining Structures," Symposium Seismic Design for World Port 2020, Port of Los Angeles, Los Angeles, CA.

Whitman, R., and Liao, S. 1985. "Seismic Design of Retaining Walls," Miscellaneous Paper GL-85-1, US Army Engineer Waterways Experiment Station, Vicksburg, MS.

Wong, C. 1982. "Seismic Analysis and Improved Seismic Design Procedure for Gravity Retaining Walls," Research Report 82-32, Department Of Civil Engineering, Massachusetts Institute of Technology, Cambridge, MA.

Wood, J. 1973. "Earthquake-Induced Soil Pressures on Structures, Report No. EERL 73-05, California Institute of Technology, Pasadena, CA, pp. 311.

Yong, P. M. F. 1985. "Dynamic Earth Pressures Against A Rigid Earth Retaining Wall, Central Laboratories Report 5-8515, Ministry of Works and Development, Lower Hutt, New Zealand.

Zarrabi, K. 1973. "Sliding of Gravity Retaining Wall During Earthquakes Considering Vertical Acceleration and Changing Inclination of Failure Surface, SM Thesis, Department of Civil Engineering, MIT, Cambridge, MA, pp. 140.

Zienkiewicz, O. C., and Xie, Y. M. 1991 (Nov.) "Analysis of the Lower San Fernando Dam Failure Under Earthquake," Dam Engineering, Vol. II, Issue 4, pp. 307-322.

APPENDIX A: COMPUTATION OF THE DYNAMIC ACTIVE AND PASSIVE EARTH PRESSURE FORCES FOR PARTIALLY SUBMERGED BACKFILLS USING THE WEDGE METHOD

A.1 Introduction

This appendix describes the derivation of the dynamic active and passive earth pressure forces for partially submerged backfills using the wedge method. The effect of earthquakes is incorporated through the use of a constant horizontal acceleration, $a_h = k_h \cdot g$, and a constant vertical acceleration, $a_v = k_v \cdot g$, acting on the soil mass comprising the active wedge (or passive wedge) within the backfill, as shown in Figure A.1 (and Figure A.3).

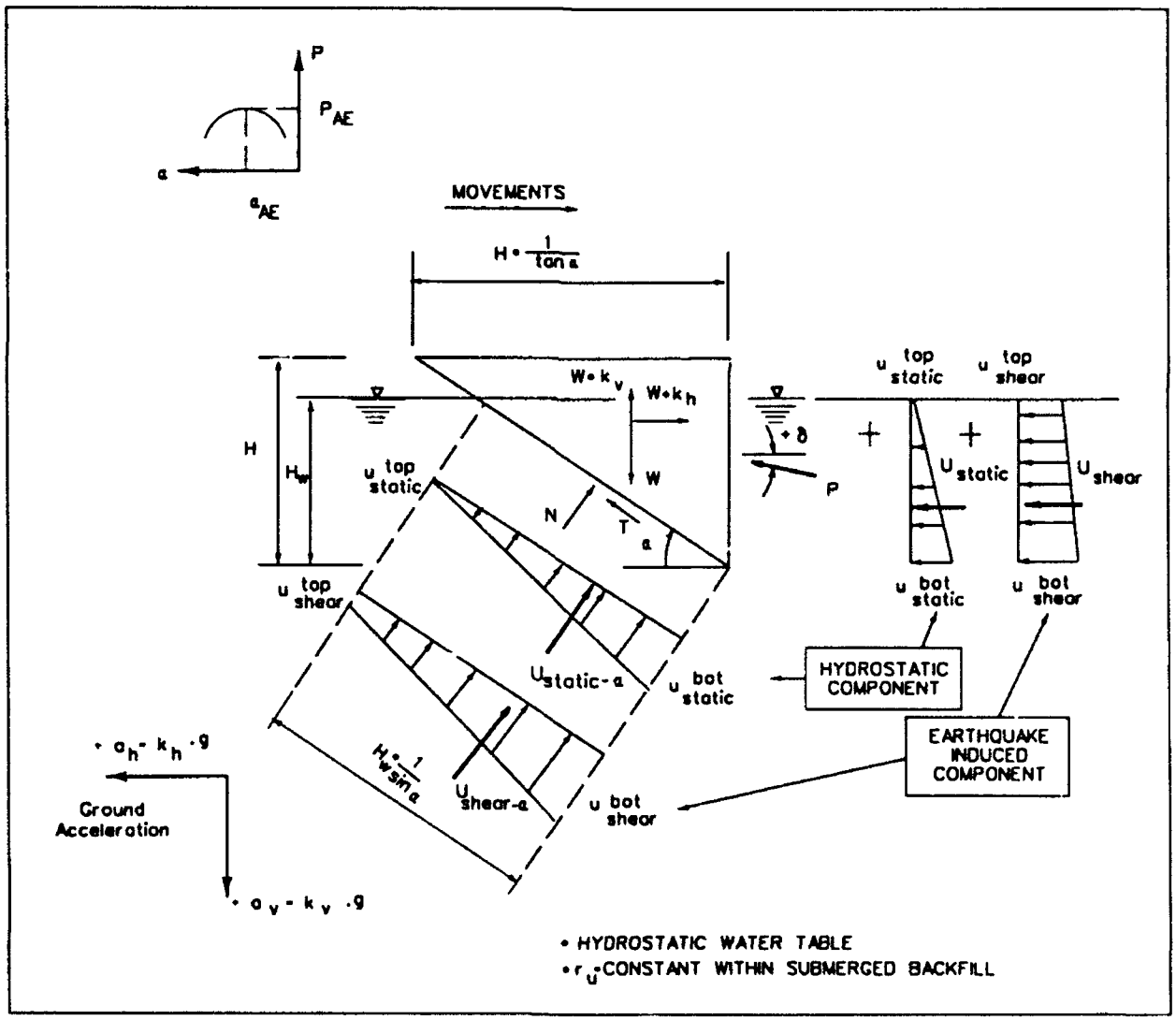

Figure A.1 Dynamic active wedge analysis with excess pore water pressures

The earth and water pressure forces acting on the wedge are derived for the case of restrained water within the backfill and a hydrostatic water table. Any increase in the pore water pressures above their steady state values in response to the shear strains induced within the saturated portion of the backfill during earthquake shaking is reflected in a value of $r_u > 0$. A constant r_u value is used throughout the submerged portion of the backfill in this derivation.

A.2 Active Earth Pressures

Figure A.1 represents a free body diagram for the derivation which follows. The base of the wedge is the trial planar slip surface representing the active failure plane, which is inclined at angle alpha to the horizontal. The top of the wedge is bounded by a horizontal ground surface, and a vertical face along the interface between the backfill and the retaining wall.

The weight of the wedge acts at the center of mass and is computed as

$$W = \frac{1}{2} \gamma_t H^2 \frac{1}{\tan\alpha} \tag{A-1}$$

The three forces acting along the planar slip surface are represented by an effective normal force N', a shear force T and the pore water pressure force. Assuming a cohesionless backfill and full mobilization of shear resistance along the slip surface, the shear force may be computed utilizing the Mohr-Coulomb failure criteria as

$$T = N' \tan\phi' \tag{A-2}$$

The total pore water pressures acting along the submerged faces of the soil wedge are described in terms of the steady state pore water pressure component and the excess pore water pressure component attributed to earthquake shaking.

A.2.1 Calculation of Water Pressure Forces for a Hydrostatic Water Table

The pore water pressure at the ground water table (Figure A.2) is

$$u^{top}_{static} = 0 \tag{A-3}$$

For a hydrostatic water table the pore water pressure distribution is linear with depth, and at the bottom of the wedge is computed as

$$u^{bot}_{static} = \gamma_w H_w \tag{A-4}$$

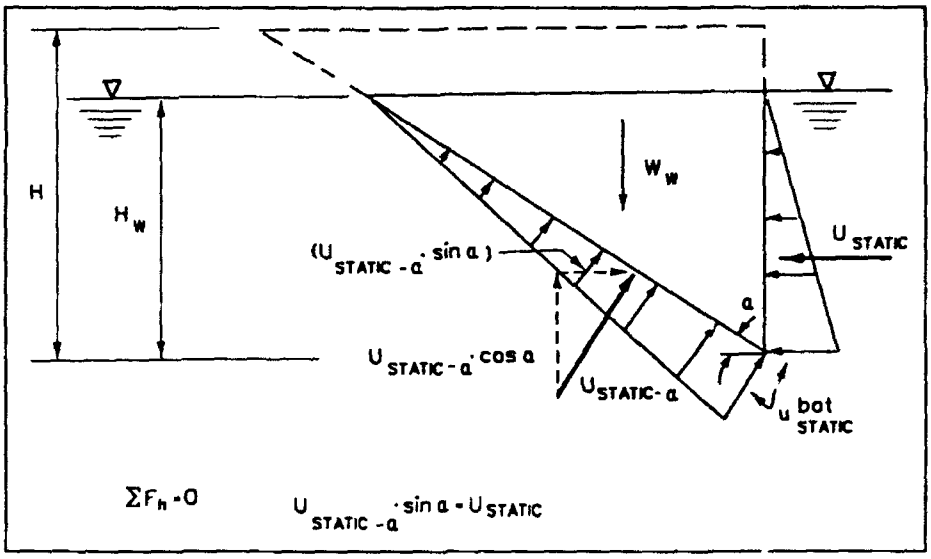

Figure A.2 Equilibrium of horizontal hydrostatic water pressure forces acting on backfill wedge

A.2.2 Static Water Pressure Forces Acting on the Wedge

The static pore pressure distribution immediately behind the wall is triangular and the resultant force may be calculated as

$$U_{static} = \frac{1}{2} \gamma_w H_w^2 \tag{A-5}$$

The static pore pressure force acting along the planar slip surface is also triangular and the resultant force may be computed as

$$U_{static-\alpha} = \frac{1}{2} \gamma_w H_w^2 \frac{1}{\sin\alpha} \tag{A-6}$$

A.2.3 Excess Pore Water Pressures Due to Earthquake Shaking with Constant r_u

Excess pore water pressures due to earthquake shaking are computed assuming the restrained water case as described in section 4.3.2. With r_u constant throughout the submerged portion of the backfill the pressure distribution is linear. The excess pore water pressure at the ground water table is computed as

$$u^{top}_{shear} = \gamma_t (H - H_w) r_u \tag{A-7}$$

Note that when the water table is below the surface of the backfill $u^{top}_{shear} > 0$. The excess pore water pressure at the bottom of the wedge is computed as

$$u^{bot}_{shear} = [\gamma_t (H - H_w) + (\gamma_t - \gamma_w) H_w] r_u \tag{A-8}$$

The total pore water pressures are equal to the sum of the hydrostatic pore water pressures plus the excess pore water pressures.

A.2.4 Excess Pore Water Pressure Forces Acting on the Wedge.

The resultant excess pore water pressure force of a trapezoidal pressure distribution acting normal to the back of the wall is equal to

$$U_{shear} = \frac{1}{2}\left[u^{top}_{shear} + u^{bot}_{shear} \right] H_w \qquad \text{(A-9)}$$

The resultant excess pore water pressure force of the trapezoidal pressure distribution acting normal to the planar slip surface is equal to

$$U_{shear-\alpha} = \frac{1}{2}\left[u^{top}_{shear} + u^{bot}_{shear} \right] H_w \frac{1}{\sin\alpha} \qquad \text{(A-10)}$$

A.2.5 Equilibrium of Vertical Forces

Equilibrium of vertical forces acting on the Figure A.1 soil wedge results in the relationship

$$- P \sin\delta + W(1 - k_v) - T \sin\alpha - N' \cos\alpha$$

$$- (U_{static-\alpha} + U_{shear-\alpha})\cos\alpha = 0 \qquad \text{(A-11)}$$

Introducing Equation A-2 into A-11 results in

$$- P \sin\delta + W(1 - k_v) - N' \tan\phi' \sin\alpha$$

$$- N' \cos\alpha - (U_{static-\alpha} + U_{shear-\alpha})\cos\alpha = 0 \qquad \text{(A-12)}$$

and solving for the normal effective force, N′, becomes

$$N' = -P\frac{\sin\delta}{\tan\phi' \sin\alpha + \cos\alpha} + W\frac{(1- k_v)}{\tan\phi' \sin\alpha + \cos\alpha}$$

$$- (U_{static-\alpha} + U_{shear-\alpha})\frac{\cos\alpha}{\tan\phi' \sin\alpha + \cos\alpha} \qquad \text{(A-13)}$$

A.2.6 Equilibrium of Forces in the Horizonal Direction

Equilibrium of horizontal forces acting on the Figure A.1 soil wedge results in the relationship

$$P\cos\delta - N'\sin\alpha - \left(U_{static-\alpha} + U_{shear-\alpha} \right)\sin\alpha$$

$$+ T\cos\alpha - Wk_h + \left(U_{static} + U_{shear} \right) = 0 \qquad \text{(A-14)}$$

Substituting Equation A-2 into A-14, and with the horizontal components of water pressure forces of equal magnitude and opposite direction, (refer to Figure A.2), Equation A-14 simplifies to

$$P\cos\delta - N'\sin\alpha + N'\tan\phi'\cos\alpha - Wk_h = 0 \qquad \text{(A-15)}$$

Combining the N′ terms results in

$$P\cos\delta - N'\left(\sin\alpha - \tan\phi'\cos\alpha \right) - Wk_h = 0 \qquad \text{(A-16)}$$

Multiplying Equation A-13 (for N′) by $[- (\sin\alpha - \tan\phi'\cos\alpha)]$ and simplifying becomes

$$- N \left(- \tan\phi'\cos\alpha + \sin\alpha \right) = + P\sin\delta\tan(\alpha - \phi')$$

$$- W(1 - k_v)\tan(\alpha - \phi')$$

$$+ \left(U_{static-\alpha} + U_{shear-\alpha} \right)\cos\alpha\tan(\alpha - \phi') \qquad \text{(A-17)}$$

Substituting Equation A-17 into A-16 gives

$$P\cos\delta + P\sin\delta\tan(\alpha - \phi')$$

$$- W(1 - k_v)\tan(\alpha - \phi')$$

$$+ \left(U_{static-\alpha} + U_{shear-\alpha} \right)\cos\alpha\tan(\alpha - \phi') - Wk_h = 0 \qquad \text{(A-18)}$$

Combining terms results in

$$P \left\{ \cos\delta + \sin\delta\tan(\alpha - \phi') \right\} =$$

$$W\left[(1 - k_v)\tan(\alpha - \phi') + k_h \right]$$

$$- \left(U_{static-\alpha} + U_{shear-\alpha} \right)\cos\alpha\tan(\alpha - \phi') \qquad \text{(A-19)}$$

Solving for the resultant force P which acts at angle δ

$$P = \frac{CONSTANT_{A1} - CONSTANT_{A2}}{\cos\delta + \sin\delta\tan(\alpha - \phi')} \tag{A-20}$$

where

$$CONSTANT_{A1} = W\left[(1 - k_v)\tan(\alpha - \phi') + k_h \right]$$

and

$$CONSTANT_{A2} = (U_{static-\alpha} + U_{shear-\alpha})\cos\alpha\tan(\alpha - \phi')$$

The dynamic active earth pressure force P_{AE} is equal to the maximum value of P for the trial wedges analyzed and $\alpha_A = \alpha$ for this critical wedge, as discussed in Section 3.4 and shown in Figure 3.10.

A.2.7 Surcharge Loading

The presence of an additional mass located on top of the backfill during earthquake shaking can increase the magnitude of the dynamic active earth pressures acting on the wall. The effects of an additional surcharge mass idealized in Figure A.3, or a surcharge loading idealized in Figure A.4, may be incorporated within the dynamic active wedge analysis of Section A.2.6 by expanding Equation A-20. For each slip surface analyzed, that portion of the surcharge loading contained within the wedge is included within the equations of equilibrium of forces acting on the wedge. When the surcharge is represented as a uniform pressure distribution q_s, that portion of the surcharge loading contained above the wedge is replaced by an equivalent force W_s acting at its center of mass. The uniformly distributed surcharge pressure q_s shown in Figure A.4 is replaced by the equivalent force (per foot of wall)

$$W_s = q_s\, l_e \tag{A-21}$$

where

$$l_e = l = ((H/\tan\alpha) - x) \text{ for } l_q > l \text{ (refer to Figure A-4)},$$

otherwise

$$l_e = l_q$$

The variable l_e represents the effective length of the surcharge load. Equation A-20 becomes

$$P = \frac{CONSTANT_{A1} + CONSTANT_{AS1} - CONSTANT_{A2}}{\cos\delta + \sin\delta\tan(\alpha - \phi')} \tag{A-22}$$

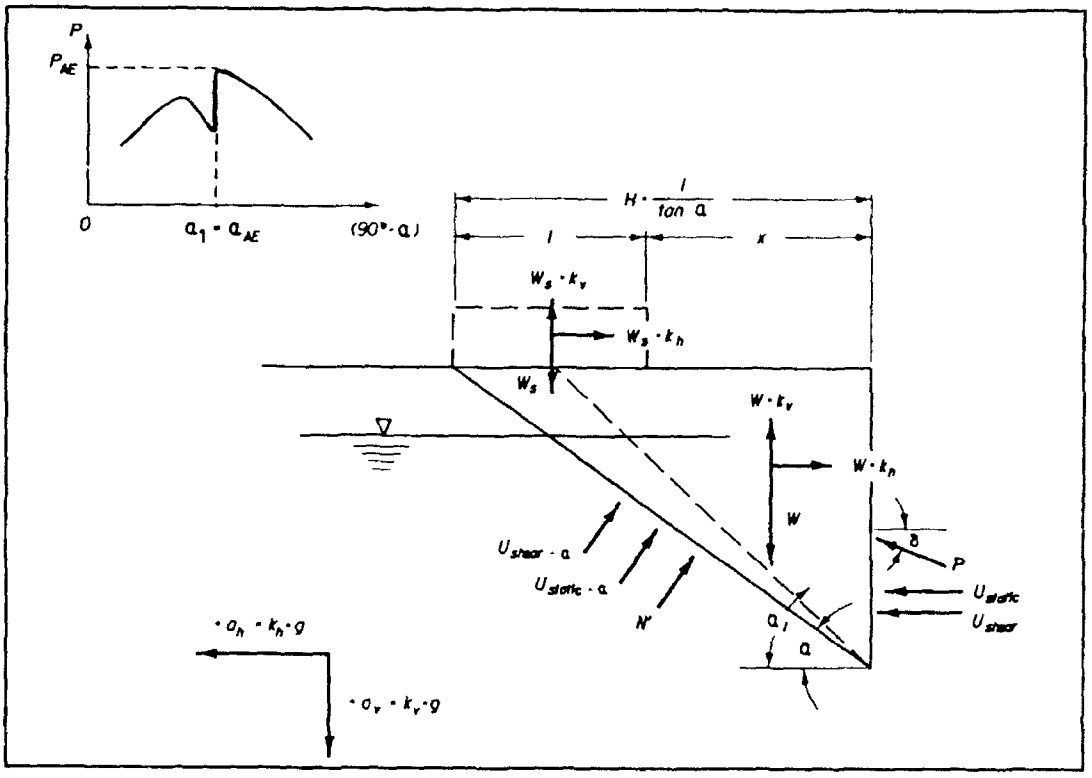

Figure A.3 Dynamic active wedge analysis including a surcharge loading

where

$$CONSTANT_{AS1} = W_S \left[(1 - k_v) \tan(\alpha - \phi') + k_h \right]$$

and $CONSTANT_{A1}$ and $CONSTANT_{A2}$ are computed as in Section A.2.6 for Equation A-20.

For surcharge loadings of finite length, a wide range of slip surfaces must be investigated to ensure that the maximum value for P is calculated and equal to P_{AE}, corresponding to the critical slip surface α_{AE} as shown in Figures A.3 and A.4.

A.2.8 Static Active Wedge Analysis

In the case of a static wedge analysis with $k_v = k_h = U_{shear-\alpha} = 0$, Equation A-20 simplifies to

$$P = \frac{[W - U_{static-\alpha} \cos\alpha] \tan(\alpha - \phi')}{\cos\delta + \sin\delta \tan(\alpha - \phi')} \qquad \text{(A-23)}$$

with α restricted to values of $\alpha > \phi$, since $P > 0$.

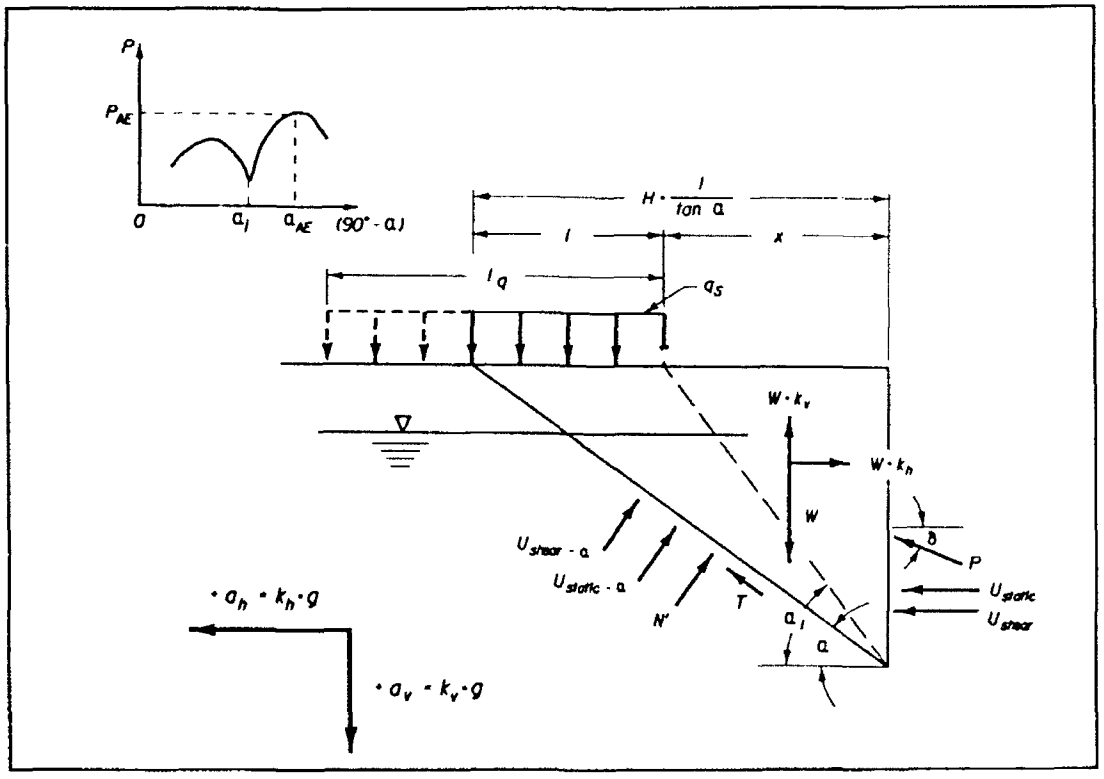

Figure A.4 Dynamic active wedge analysis including a surcharge loading

$P_A = P$ and $\alpha_A = \alpha$ for the static critical wedge as well. For a surcharge loading, Equation A-22 simplifies to

$$P = \frac{\left[W + W_s - U_{static-\alpha} \cos\alpha \right] \tan(\alpha - \phi')}{\cos\delta + \sin\delta \tan(\alpha - \phi')} \qquad \text{(A-24)}$$

where W_s is computed using Equation A-21.

A.3 Passive Earth Pressures

Figure A.5 represents a free body diagram that is used in the derivation of the wedge procedure for computing the value of the dynamic passive earth pressure force P_{PE}. The base of the wedge represents the trial planar slip surface and is inclined at angle α to the horizontal. The top of the wedge is defined by a horizontal ground surface, and the vertical face is located along the interface between the backfill and the retaining wall.

The weight of the wedge acts at the center of mass and is computed using Equation A-1. The three forces acting along the planar slip surface are the normal force N', the shear force T, and the pore water pressure force. The shear force T shown in Figure A.3 for the passive case acts opposite to the shear force shown in Figure A.1 for the active case. Assuming a cohesionless

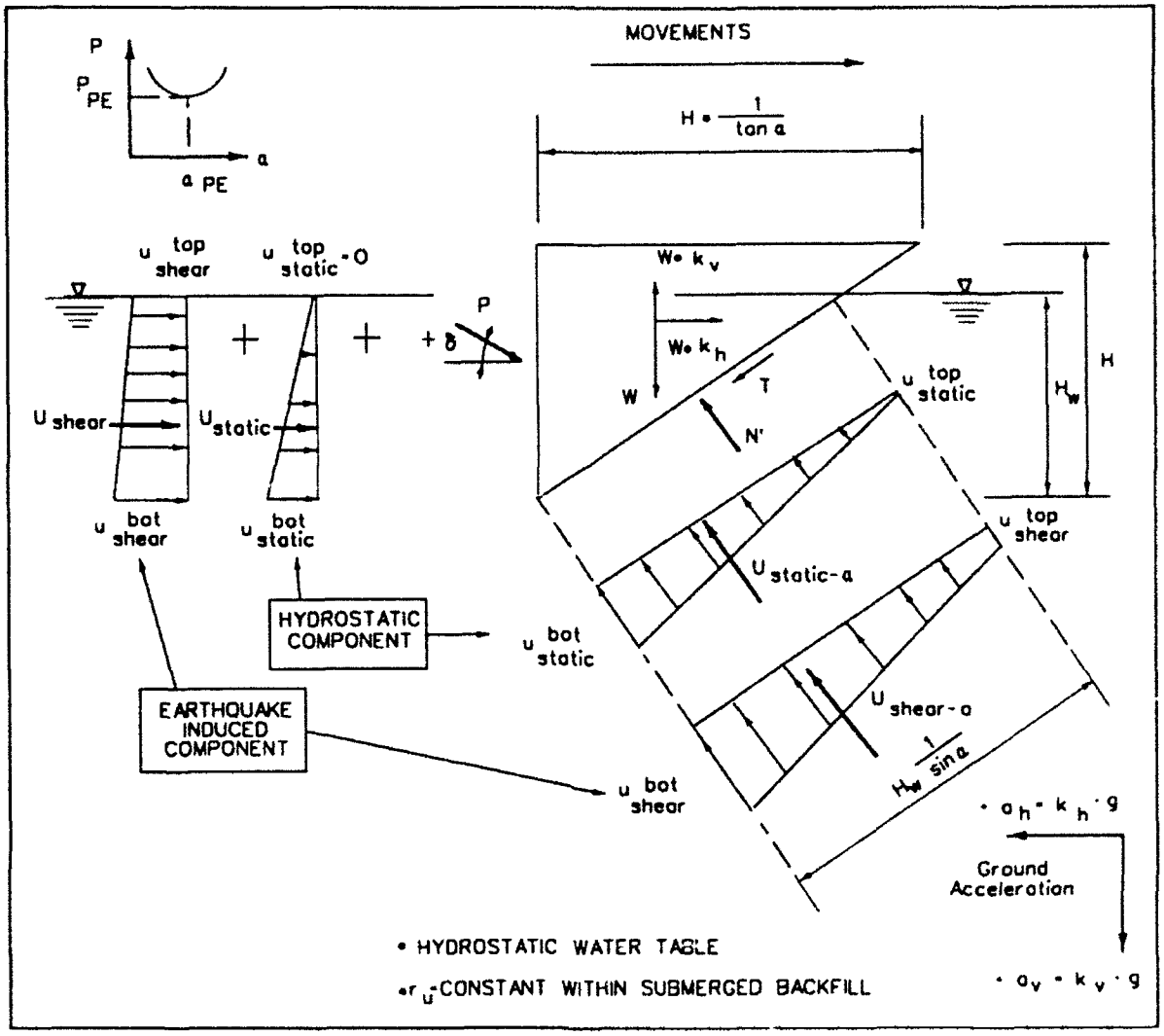

Figure A.5 Dynamic passive wedge analysis with excess pore water pressures

backfill and full mobilization of shear resistance along the slip surface, the shear force may be computed utilizing the Mohr-Coulomb failure criteria as given by Equation A-2.

A.3.1 Calculation of Water Pressure Forces for a Hydrostatic Water Table

The total water pressure forces are equal to the sum of the steady state water pressures plus the excess water pressures due to earthquake shaking. Steady state water pressure forces for a hydrostatic water table are computed using the procedures described in Sections A.2.1 and A.2.2. Excess pore water pressures due to earthquake loads with constant r_u throughout the submerged portion of the backfill are computed using the procedures described in Sections A.2.3 and A.2.4.

A.3.2 Equilibrium of Vertical Forces

Equilibrium of vertical forces acting on Figure A.3 wedge results in the relationship

$$P \sin\delta + W(1 - k_v) + T \sin\alpha - N' \cos\alpha$$

$$- (U_{static-\alpha} + U_{shear-\alpha}) \cos\alpha = 0 \qquad \text{(A-25)}$$

Introducing Equation A-2 into A-25 results in

$$P \sin\delta + W(1 - k_v) + N' \tan\phi' \sin\alpha$$

$$- N' \cos\alpha - (U_{static-\alpha} + U_{shear-\alpha}) \cos\alpha = 0 \qquad \text{(A-26)}$$

and solving for the normal effective force becomes

$$N' = P \frac{\sin\delta}{- \tan\phi' \sin\alpha + \cos\alpha} + W \frac{(1 - k_v)}{- \tan\phi' \sin\alpha + \cos\alpha}$$

$$- (U_{static-\alpha} + U_{shear-\alpha}) \frac{\cos\alpha}{- \tan\phi' \sin\alpha + \cos\alpha} \qquad \text{(A-27)}$$

A.3.3 Equilibrium of Forces in the Horizonal Direction

Equilibrium of horizontal forces acting on Figure A.5 soil wedge results in the relationship

$$P\cos\delta - N' \sin\alpha - (U_{static-\alpha} + U_{shear-\alpha}) \sin\alpha$$

$$- T\cos\alpha + Wk_h + (U_{static} + U_{shear}) = 0 \qquad \text{(A-28)}$$

Substituting Equation A-2 into A-28 and with the horizontal components of the water pressure forces of equal magnitude and opposite direction (refer to Figure A.2), Equation A-28 simplifies to

$$P\cos\delta - N' \sin\alpha - N' \tan\phi' \cos\alpha + Wk_h = 0 \qquad \text{(A-29)}$$

combining the N' terms results in

$$P\cos\delta - N' (\sin\alpha + \tan\phi' \cos\alpha) + Wk_h = 0 \qquad \text{(A-30)}$$

Multiplying Equation A-27 (for N′) by $[- (\sin\alpha + \tan\phi' \cos\alpha)]$ and simplifying becomes

$$- N'(\tan\phi' \cos\alpha + \sin\alpha) = - P\sin\delta \tan(\alpha + \phi')$$

$$- W(1 - k_v)\tan(\alpha + \phi')$$

$$+ (U_{static-\alpha} + U_{shear-\alpha})\cos\alpha \tan(\alpha + \phi') \qquad \text{(A-31)}$$

Substituting Equation A-31 into A-30 gives

$$P\cos\delta - P\sin\delta \tan(\alpha + \phi')$$

$$- W(1 - k_v)\tan(\alpha + \phi')$$

$$+ (U_{static-\alpha} + U_{shear-\alpha})\cos\alpha \tan(\alpha + \phi') + Wk_h = 0 \qquad \text{(A-32)}$$

Combining terms result in

$$P [\cos\delta - \sin\delta \tan(\alpha + \phi')] =$$

$$W \left[(1 - k_v)\tan(\alpha + \phi') - k_h \right]$$

$$- (U_{static-\alpha} + U_{shear-\alpha}) \cos\alpha \tan (\alpha + \phi') \qquad \text{(A-33)}$$

Solving for the resultant force P which acts at angle δ

$$P = \frac{CONSTANT_{P1} - CONSTANT_{P2}}{\cos\delta - \sin\delta \tan(\alpha + \phi')} \qquad \text{(A-34)}$$

where

$$CONSTANT_{P1} = W \left[(1 - k_v)\tan(\alpha + \phi') - k_h \right]$$

and

$$CONSTANT_{P2} = (U_{static-\alpha} + U_{shear-\alpha}) \cos\alpha \tan (\alpha + \phi')$$

The dynamic passive earth pressure force P_{PE} is equal to the minimum value of P for the trial wedges analyzed and $\alpha_P = \alpha$ for this critical wedge.

A.3.4 Surcharge Loading

The presence of an additional mass located on top of the backfill during earthquake shaking can decrease the magnitude of the dynamic passive earth pressures acting on the wall. The effects of an additional surcharge mass idealized in Figure A.6, or a surcharge loading idealyzed in Figure A.7, may be incorporated within the dynamic passive wedge analysis of Section A.3.3 by expanding Equation A-34. For each slip surface analized, that portion of the

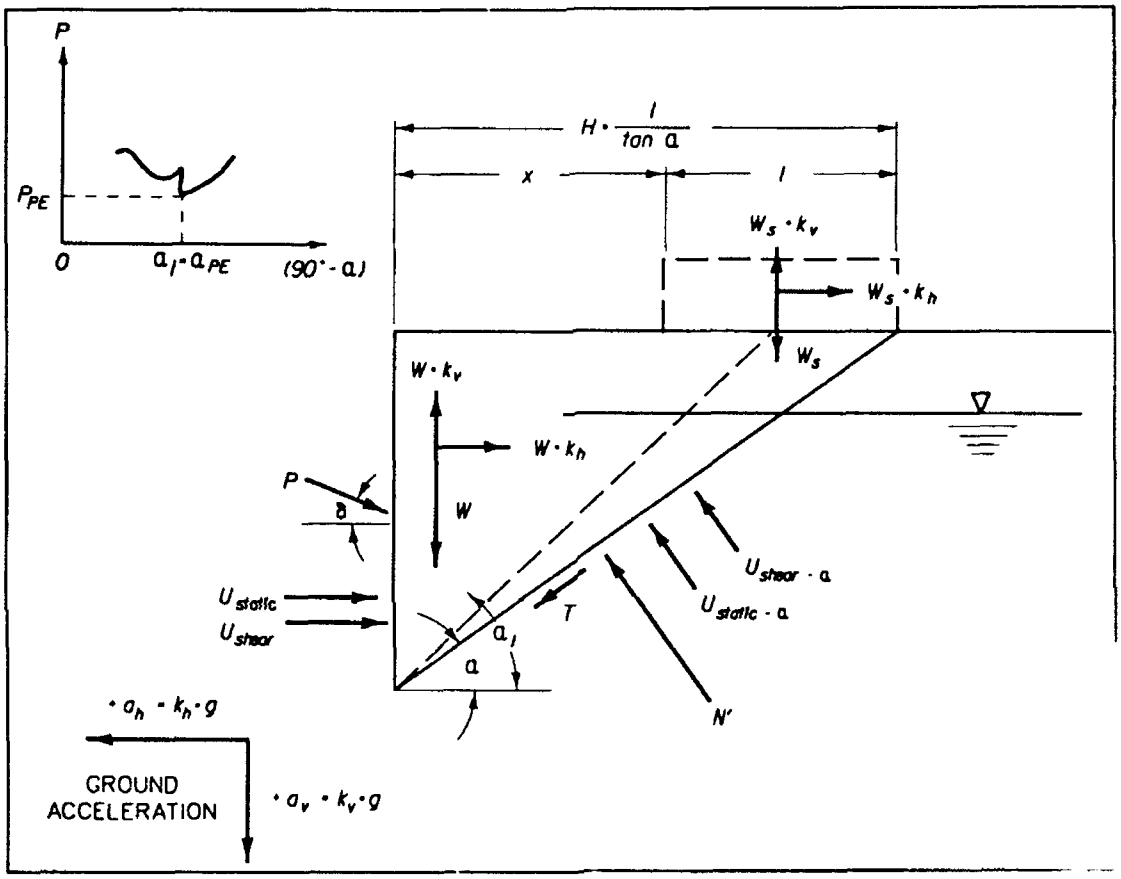

Figure A.6 Dynamic passive wedge analysis including a surcharge load

surcharge loading contained within the wedge is included within the equations of equilibrium of forces acting on the wedge. When the surcharge is represented as a uniform pressure distribution q_s, that portion of the surcharge loading contained above the wedge is replaced by an equivalent force W_s acting at its center of mass. The uniformly distributed surcharge pressure q_s shown in Figure A.7 is replaced by the equivalent force (per foot of wall) W_s, computed using Equation A-21 in Section A.2.7. Figure A.7 surcharge pressure q_s is equivalent to Figure A.6 case of a surcharge of weight W_s, and Equation A-34 becomes

$$P = \frac{CONSTANT_{P1} + CONSTANT_{PS1} - CONSTANT_{P2}}{\cos\delta - \sin\delta \tan(\alpha + \phi')} \qquad \text{(A-35)}$$

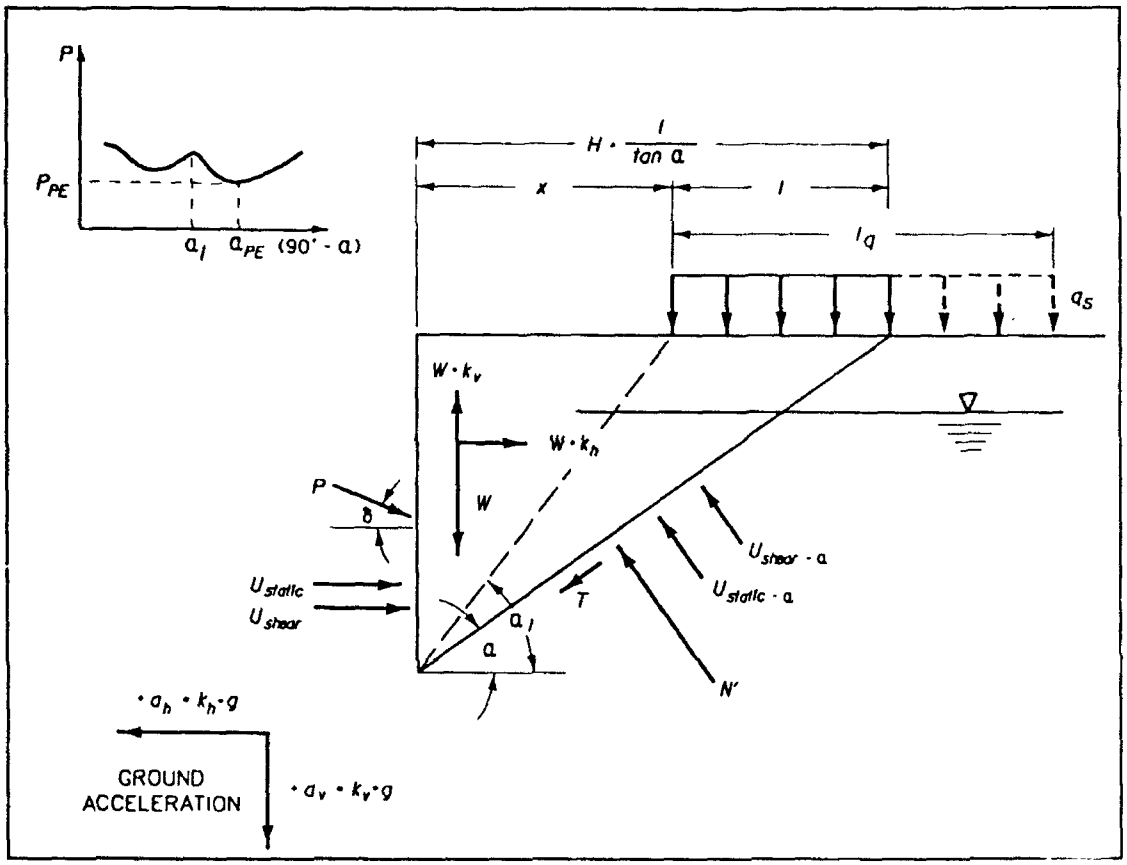

Figure A.7 Dynamic passive wedge analysis including a surcharge load

where

$$CONSTANT_{PS1} = W_S[\ (\ 1 - k_v\ )\tan(\ \alpha + \phi'\ ) - k_h\ ]$$

and $CONSTANT_{P1}$ and $CONSTANT_{P2}$ are computed as in Section A.3.3 for Equation A-34.

For surcharge loads of finite length, a wide range of slip surfaces must be investigated to ensure that the minimum value for P is calculated and equal to P_{PE}, corresponding to the critical slip surface α_{PE} as shown in Figures A.6 and A.7.

A.3.5 Static Passive Wedge Analysis

Note that for static problems with $k_v = k_h = U_{shear-\alpha} = 0$ Equation A-34 simplifies to

$$P = \frac{\left[\ W - U_{static-\alpha}\cos\alpha\ \right]\tan(\ \alpha + \phi'\ )}{\cos\delta - \sin\delta\tan\ (\ \alpha + \phi'\ )} \qquad \text{(A-36)}$$

with α restricted to values of $\alpha > 0$ and $\delta < \phi/2$.

$P_P = P$ and $\alpha_P = \alpha$ for this critical wedge. For a surcharge loading, Equation A-35 simplifies to

$$P = \frac{\left[W + W_s - U_{static-\alpha} \cos\alpha \right] \tan(\alpha + \phi')}{\cos\delta - \sin\delta \tan (\alpha + \phi')} \qquad \text{(A-37)}$$

APPENDIX B: THE WESTERGAARD PROCEDURE FOR COMPUTING HYDRODYNAMIC WATER PRESSURES ALONG VERTICAL WALLS DURING EARTHQUAKES

This section describes the Westergaard procedure for computing the magnitude of the hydrodynamic water pressures along rigid vertical walls during earthquake shaking. The solution developed by Westergaard (1931) is for the case of a semi-infinite long water reservoir retained by a concrete dam and subjected to a horizontal earthquake motion. The fundamental period of the concrete dam is assumed to be much smaller than the fundamental period of the earthquake so that the acceleration for the massive structure is approximated as the acceleration of the earthquake motion along the rigid base. This allows the problem of a very stiff concrete dam to be simplified to the case of a rigid vertical face moving at the same horizontal acceleration as the base horizontal acceleration. Using the equations of elasticity of a solid to describe the propagation of sounds in liquids (waves which propagate without shear distortions) and with the water considered to be compressible, a solution to the equation of motion of the water was developed for a harmonic motion applied along the base of the reservoir. This solution ignores the effects of surface waves and is valid only when the period of the harmonic excitation is greater than the fundamental natural period of the reservoir (Chopra 1967). The fundamental period for the reservoir, T_w, is equal to

$$T_w = \frac{4H_p}{C} \tag{B-1}$$

where the velocity of sound in water, C, is given by

$$C = \sqrt{\frac{K}{\rho}} \tag{B-2}$$

and the mass density of water, ρ, is given by

$$\rho = \frac{\gamma_w}{g} \tag{B-3}$$

With the bulk modulus of elasticity of water, K, equal to 4.32×10^7 lb per ft^2, the unit weight for water, γ_w, equal to 62.4 lb per ft^3 and the acceleration due to gravity, g, equal to 32.17 ft per sec^2, C is equal to 4,720 ft per sec. For example, with a depth of pool of water, H_p, equal to 25 ft, T_w is equal to 0.02 seconds (47 Hz) by Equation B-1.

The resulting relationship for hydrodynamic pressure on the face of the dam is a function of the horizontal seismic coefficient, k_h, the depth of water, Y_w, the total depth of the pool of water, H_p, the fundamental period of the earthquake, and the compressibility of the water, K. The hydrodynamic pressure is opposite in phase to the base acceleration and for positive base accelerations the hydrodynamic pressure is a tensile. Westergaard proposed the following approximate solution for the hydrodynamic water pressure distribution: a parabolic dynamic pressure distribution, p_{wd}, described by the relationship

$$P_{wd} = \frac{7}{8} K_h \gamma_w \sqrt{y_w H_{p2}} \qquad \text{(B-4)}$$

The resultant dynamic water pressure force, P_{wd}, is equal to

$$P_{wd} = \frac{7}{12} K_h \gamma_w H_p^2 \qquad \text{(B-5)}$$

acting at an elevation equal to 0.4 H_p above the base of the pool as shown in Figure B.1. This dynamic force does not include the hydrostatic water pressure force acting along the face of the dam.

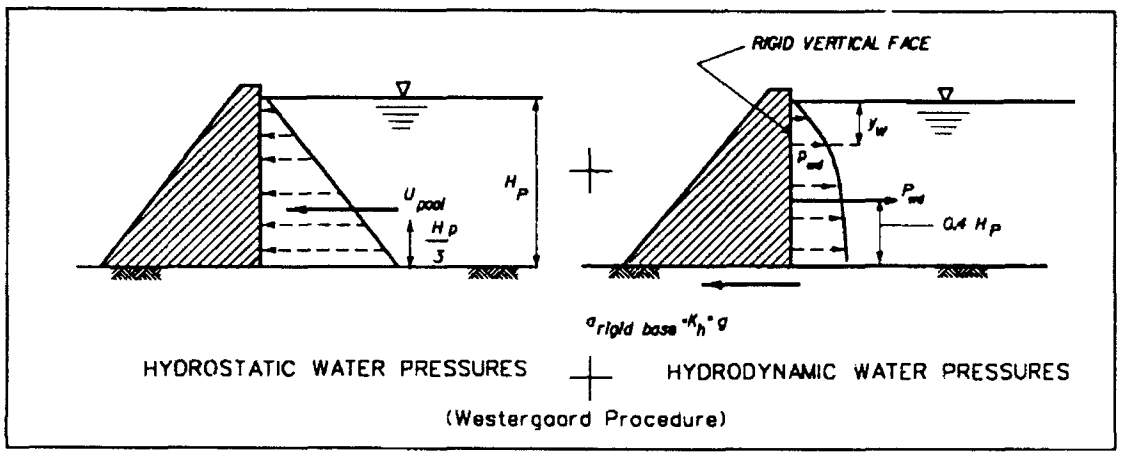

Figure B.1 Hydrostatic and Westergaard hydrodynamic water pressures acting along vertical wall during earthquakes

B.1 The Westergaard Added Mass Procedure

A complete dynamic analysis of a structure that is in contact with a pool of water requires that the hydrodynamic effects be accounted for during the dynamic analysis. This requires that the pool of water must be incorporated within the idealized model for the problem. Most dynamic finite element computer code formulations that are used for soil-structure interaction analyses do not include a fluid element in their catalog of elements. The Westergaard added mass procedure is one method that is used to incorporate the hydrodynamic effects in the analysis for computer codes without a fluid element formulation. With the hydrodynamic water pressure on the vertical face of a rigid structure opposite in phase to the ground acceleration, these hydrodynamic pressures are equivalent to the inertia force of an added mass moving with the dam (Chopra 1967). The Westergaard (1931) added water mass procedure adds an additional water mass to the mass matrix along the front face of the structure. For pools that are wider than three times the depth of the pool, this additional mass of water is enveloped within the parabolic pressure distribution given by Equation B-4 and the front of the wall. This procedure is applicable when the period of harmonic excitation (i.e. the earthquake) is greater than the fundamental natural period of the earthquake (Chopra 1967), which is the case for shallow pools.

APPENDIX C: DESIGN EXAMPLE FOR AN ANCHORED SHEET PILE WALL

The calculations involved in the design of Figure C.1 anchored sheet pile wall and its anchorage is described in this appendix for both static and seismic loadings using the procedures described in Chapter 7. Assume k_h = 0.2, k_v = 0.1 and no excess pore water pressures are generated during earthquake shaking (r_u = 0). The results of the computations shown are rounded for ease of checking calculations and not to the appropriate number of significant figures.

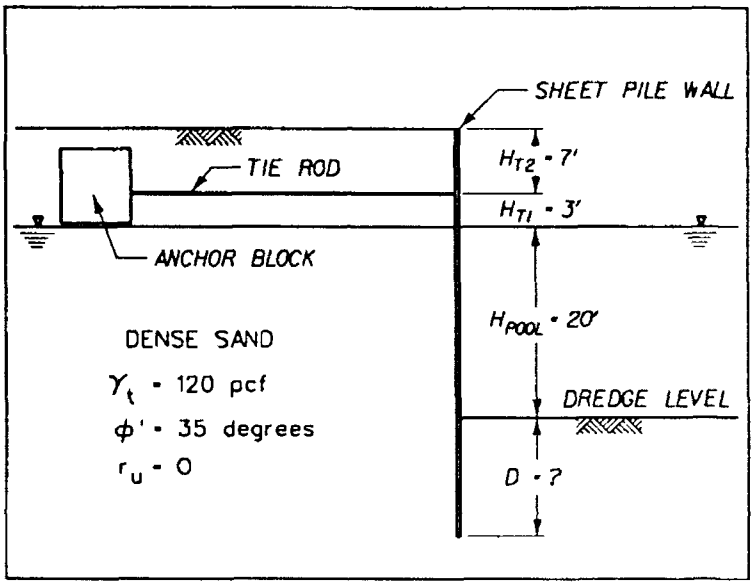

Figure C.1 Anchored sheet pile wall design problem

Section C.1 describes the design of anchored sheet pile wall for static loading and Section C.2 the design for earthquake loading.

Section C.1 Design of An Anchored Sheet Pile Wall for Static Loading

This section describes the design of Figure C.1 anchored sheet pile wall for static loads using the free earth support method of analysis.

C.1.1 Active Earth Pressures Coefficients K_A

Factor of Safety on shear strength = 1.0

Assume $\delta = \frac{\phi}{2}$,

δ = 17.5 degrees

By Equation 16, $K_A = 0.246$

Say $K_A = 0.25$

$K_A \cdot \cos\delta = 0.24$

C.1.2 "Factored" Passive Earth Pressure Coefficient K_p

Factor of Safety on shear strength = 1.5

By Equation 95,

$$\tan\phi_t' = \frac{\tan 35°}{1.5}$$

$$\phi_t' = 25 \text{ degrees}$$

By Equation 96 with $\delta = \phi/2$ and $\delta = 17.5°$,

$$\tan\delta_t = \frac{\tan(17.5)}{1.5}$$

$$\delta_t = 11.9$$

$$\text{say } \delta_t = 12 \text{ degrees}$$

$$\text{and } \frac{\delta_t}{\phi_t} \approx 0.5$$

Using the Log-spiral solutions in Figure 3.11 for K_p with

$$\delta/\phi = -0.5,\ R_d = 0.808$$

$$K_p\ (\delta/\phi = -1.0, \phi = 25 \text{ degrees}) = 4.4$$

$$K_p\ (\delta/\phi = -0.5) = 0.808 \cdot 4.4 = 3.56$$

$$K_p \cos\delta_t = 3.56 \cdot \cos 12° = 3.48$$

C.1.3 Depth of Penetration

Table C.1 summarizes the horizontal force components acting on Figure C.2 sheet pile wall and are expressed in terms of the generalized dimensions H_{T1}, H_{T2}, H_{pool}, and D. The horizontal force components and their moment about the elevation of the tie rod are summarized in Tables C.2 and C.3. The forces and moments are expressed in terms of the unknown depth of penetration, D.

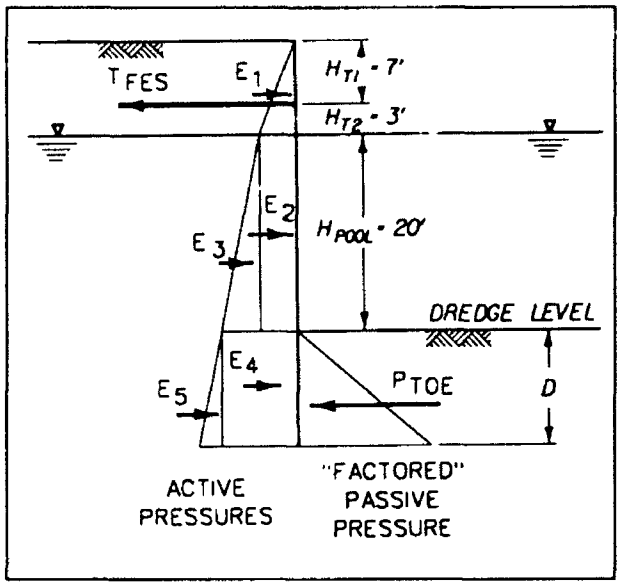

Figure C.2 Horizontal earth pressure components in free earth support design

Table C.1 Horizontal Force Components

Horizontal Force Designation	Horizontal Force	Distance to Tie Rod
E_1	$K_A \cos\delta \cdot \frac{1}{2}\gamma_t (H_{T1} + H_{T2})^2$	$\frac{1}{3}(2\ H_{T2} - H_{T1})$
E_2	$K_A \cos\delta \cdot \frac{1}{2}\gamma_t (H_{T1} + H_{T2})\ H_{pool}$	$H_{T2} + \frac{1}{2}\ H_{pool}$
E_3	$K_A \cos\delta \cdot \frac{1}{2}\gamma_b (H_{pool})^2$	$H_{T2} + \frac{2}{3}\ H_{pool}$
E_4	$K_A \cos\delta \cdot \left[\gamma_t (H_{T1} + H_{T2}) + \gamma_b \cdot H_{pool}\right] \cdot D$	$H_{T2} + H_{pool} + \frac{1}{2}D$
E_5	$K_A \cos\delta \cdot \frac{1}{2}\gamma_b (D)^2$	$H_{T2} + H_{pool} + \frac{2}{3}D$
P_{TOE}	$K_p \cos\delta_t \cdot \frac{1}{2}\gamma_b \cdot (D)^2$	$H_{T2} + H_{pool} + \frac{2}{3}D$

Table C.2 Moments About Tie Rod Due to Active Earth Pressures

Horizontal Force Designation	Horizontal Force (lb per ft wall)	Distance to Tie Rod (ft)	Moment About Tie Rod -CCW Moment +'ve- (ft-lb per ft wall)
E_1	1,440	-0.33	-475
E_2	5,760	13	74,880
E_3	2,765	16.33	45,149
E_4	564.5D	$23 + \frac{1}{2} D$	$12,983.5 D + 282.3 D^2$
E_5	$6.91 (D)^2$	$23 + \frac{2}{3} D$	$159.0 D^2 + 4.6 D^3$
		$M_{Active} = 4.6 D^3 + 441.3 D^2 + 12,983.5 D + 119,554$	

Table C.3 Moments About Tie Rod Due to Passive Earth Pressures

Horizontal Force Designation	Horizontal Force (lb per ft wall)	Distance to Tie Rod (ft)	Moment About Tie Rod -CCW Moment +'ve- (ft-lb per ft wall)
P_{TOE}	$100.2 (D)^2$	$23 + \frac{2}{3} D$	$-66.8 D^3 - 2,304.6 D^2$
		$M_{Passive} = -66.8 D^3 - 2,304.6 D^2$	

Equilibrium of moments about the elevation of the tie rod (CCW moment +'ve) requires

$$\Sigma M_{tie\ rod} = 0$$

$$0 = M_{Active} + M_{Passive}$$

$$0 = -62.2 D^3 - 1,863.3 D^2 + 12,983.5 D + 119,554$$

From the calculations summarized in Table C.4, D = 10.02 ft for calculation purposes (D = 10 ft for construction).

Table C.4 Calculation of the Depth of Penetration

Trial D (ft)	Moment Imbalance (ft-lb per ft wall)	Comment
9	40,134	shallow
10	859	shallow
10.1	-3,473	deep
10.02	-1	exact

C.1.4 Tie Rod Force T_{FES}

Horizontal force equilibrium (refer to Figure C.2).

$\Sigma F_h = 0$

$E_1 + E_2 + E_3 + E_4 + E_5 - P_{TOE} - T_{FES} = 0$

From the calculations summarized in Table C.5,

$16,315 - 10,060 - T_{FES} = 0$

$T_{FES} = 6,255$ lb per ft of wall

Table C.5 Horizontal Force Components for D = 10 Feet

Horizontal Force Designation	Horizontal Force (lb per ft wall)
E_1	1,440
E_2	5,760
E_3	2,765
E_4	5,656
E_5	694
P_{TOE}	10,060

C.1.5 Maximum Moment M_{FES}

The maximum value of moment, M_{FES}, occurs at the elevation of zero shear within the sheet pile. First, determine the elevation of zero shear and then compute the moment internal to the sheet pile by computing the moments of the earth pressures and water pressures about the elevation of the tie rod (refer to Step 8 discussion in Section 7.4.1). This usually occurs at an elevation above the dredge level. By modifying the relationships given in Table C.1, the equilibrium of horizontal forces at a depth, y, below the water table is expressed as

$$E_1 + E_{2x} + E_{3x} - T_{FES} = 0$$

$$1{,}440 + 288 \cdot y + 6.912 \cdot y^2 - 6{,}255 = 0$$

$$6.912 \cdot y^2 + 288y - 4.815 = 0$$

$$y = \frac{-(288) \pm \sqrt{(288)^2 - 4(6.912)(-4815)}}{2(6.912)}$$

$$y = 12.79 \text{ ft below the water table}$$

From the calculations summarized in Table C.6, the maximum moment internal to the sheet pile at y = 12.79 ft below the water table is equal to M_{FES} = 47,165 ft-lb per ft of wall.

Table C.6 Moment Internal to the Sheet Pile at y = 12.79 Feet Below the Water Table and About the Elevation of the Tie Rod

Horizontal Force Designation	Horizontal Force (lb per ft wall)	Lever Arm (ft)	Moment (ft-lb per ft wall)
E_1	1,440	-0.33	-475
E_{2X}	3,683.5	$3 + \frac{1}{2}(12.79)$	34,607
E_{3X}	1,130.7	$3 + \frac{2}{3}(12.79)$	13,033
M_{FES} = 47,165 ft - lb per ft wall			

Refined Procedure for Computing M_{FES}:

The computed value for maximum moment M_{FES} equal to 47,165 ft-lb per ft of wall is greater than would be obtained using the US Army Corps of Engineers (Corps) design procedure for static loading, as described in the U.S. Army Engineers Manual EM 1110-2-2504 (Headquarters, Department of the Army 1992). The Corps design procedure is a refinement to the procedure described in this section with the value for the maximum moment M_{FES} computed using a depth of penetration with FS_P in Equations 95 and 96 set equal to unity. The Corps procedure avoids compounding factors of safety in the selection of the sheet pile section. The value specified for depth of penetration for sheet pile wall construction would be unchanged, equal to 10 ft in this example (Section C.1.4).

Section C.1.6 Design Moment M_{design}

The design moment, M_{design}, is obtained through application of Rowe's moment reduction procedure that is outlined in Figure 7.2.

$$H = H_{T1} + H_{T2} + H_{pool} + D$$

$$H = 7 + 3 + 20 + 10 = 40 \text{ ft } (480.24 \text{ in.})$$

$$E = 30 \times 10^6 \text{ psi}$$

$$\text{Flexibility number, } \rho = \frac{H^4}{EI}$$

where

$$I = \text{moment of inertia } \underline{\text{per ft of wall}}$$

$$\rho = \frac{(480.24 \text{ in.})^4}{(30 \times 10^6 \text{ psi}) \cdot I}$$

$$\rho = \frac{1{,}773.0}{I}$$

The values of M_{design} are given in Table C.7 for four sheet pile sections.

Table C.7 Design Moment for Sheet Pile Wall in Dense Sand

Section Designation	I (in.^{4} per ft of wall)	ρ (in.^{2}/lb per ft of wall)	r_d (Figure 7.2)	M_{design} (ft-lb per ft of wall)
PZ22	84.4	21.0	0.45	21,224
PZ27	184.2	9.62	0.68	32,072
PZ35	361.2	4.91	1.0	47,165
PZ40	490.8	3.61	1.0	47,165

where $M_{design} = r_d \cdot M_{FES}$ (by eq 100)

Section C.1.7 Selection of the Sheet Pile Section

In this design example of sheet pile walls for static loadings, assume the maximum allowable stress within the sheet pile is restricted to

$\sigma_{allowable} = 0.65 \cdot \sigma_{yield}$

for ASTM A328 steel sheet piling,

$\sigma_{yield} = 39{,}000$ psi

$\sigma_{allowable} = 0.65 \cdot 39{,}000 \text{ psi} \approx 25{,}000 \text{ psi}$

The allowable bending moment (Table C.8), $M_{allowable}$, is given by

$M_{allowable} = S \cdot \sigma_{allowable}$ per ft run of wall

where

S = section modulus (in.^{3} per ft run of wall)

Table C.8 Allowable Bending Moment for Four ASTM A328 Grade Sheet Pile Sections ($\sigma_{allowable} = 0.65 \cdot \sigma_{yield}$)

Section Designation	S (in.^{3} per ft of wall)	$M_{allowable}$ (ft-kips per ft run of wall)
PZ22	18.1	38
PZ27	30.2	64
PZ35	48.5	102
PZ40	60.7	128

Comparison of the design moment values (M_{design} in Table C.7) to the allowable bending moments ($M_{allowable}$ in Table C.8) indicates that all four pile sections would be adequate. The lightest section, PZ22, would be selected for this design based upon static loading. Corrosion must also be addressed during the course of the sheet pile wall design. Additionally, the deflection of the anchored sheet pile wall would be checked (Dawkins 1991).

C.1.8 Design Tie Rod

$T_{design} = 1.3\ T_{FES}$

$T_{FES} = 6{,}255$ lb per ft of wall (from Section C.1.4)

$T_{design} = 8{,}132$ lb per ft of wall

Assume

(a) 6 ft spacing of anchors

(b) σ_{yield} = 36,000 psi

$\sigma_{allowable} = 0.4\ \sigma_{yield}$ (40 % of yield)

$$\text{Minimum area of rod} = \frac{6\ \text{ft} \cdot 8{,}132\ \text{lb per ft of wall}}{0.4 \cdot 36{,}000\ \text{psi}}$$

$$\text{Gross Area} = 3.39\ \text{in.}^2$$

$$\text{Diameter} = \sqrt{\frac{4 \cdot \text{Area}}{\pi}} = 2.08\ \text{in.}$$

C.1.9 Design Anchorage

$$T_{ult\text{-}a} = 2.5 \cdot T_{FES} \qquad \text{(by eq 102)}$$

with

$$T_{FES} = 6{,}255\ \text{lb per ft of wall} \qquad \text{(from Section C.1.4)}$$

$T_{ult\text{-}a}$ = 15,638 lb per ft of wall

Details regarding the design of anchorage are provided in numerous references including Dismuke (1991) and the USS Steel Sheet Piling Design Manual (1969). If the overall height of the anchor, h_a, is not less than about 0.6 times the depth from the ground surface to the bottom of anchorage, designated d_a in Figure C.3, the anchor behaves as if it extended to the ground surface.

$$h_a > 0.6 \cdot d_a$$

The full angle of interface friction, δ, used in computing K_p can only be mobilized if the anchor has <u>sufficient dead weight</u> or, in general, is <u>restrained against upward movement</u> (Dismuke 1991). For a slender anchor the <u>ultimate</u> capacity for a <u>continuous</u> anchor is required to satisfy the expression

$$T_{ult\text{-}a} \leq P_P - P_A$$

with δ = 0 degrees (refer to Figure C.3).

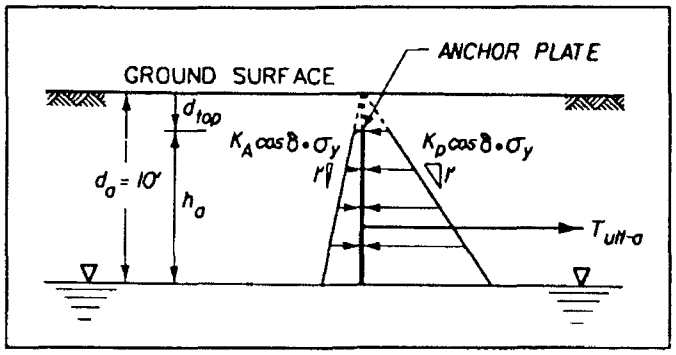

Figure C.3 Horizontal active and passive earth pressure components acting on a continuous slender anchor

For anchorage above the water table

$$T_{ult-a} \leq \frac{1}{2}\gamma_t (h_a)^2 \cdot (K_P - K_A)$$

For $\phi' = 35$ degrees and $\delta = 0$ degrees,

$$K_p = 3.69 \qquad \text{(by eq 11)}$$

$$K_A = 0.27 \qquad \text{(by eq 5)}$$

$$T_{ult-a} \leq \frac{1}{2} \cdot 120 \text{ pcf } (10')^2 \cdot (3.69 - 0.27)$$

15,638 lb per ft of wall < 20,520 lb per ft run of <u>continuous</u> anchor

$h_a \geq 0.6 \cdot 10'$

$h_a \geq 6$ ft.

Because the value of T_{ult-a} is significantly less than the capacity of a continuous wall, a series of separate anchorages would be investigated (refer to the procedures described in the USS Steel Sheet Piling Design manual, 1969).

C.1.10 Site Anchorage

To be effective, the anchorage must be located such that the potential active failure zone behind the sheet pile wall and the potential passive failure zone in front of the anchorage does not intersect. Design criteria for deadman anchorage is shown in Figure C.4. The use of the estimated point of zero moment in the wall (at $\approx \frac{1}{4}$ D) accounts for the increased depth of penetration due to the use of FS_p = 1.5 used in the calculation of the passive earth pressure force provided by the soil below the dredge level (Duncan 1985).

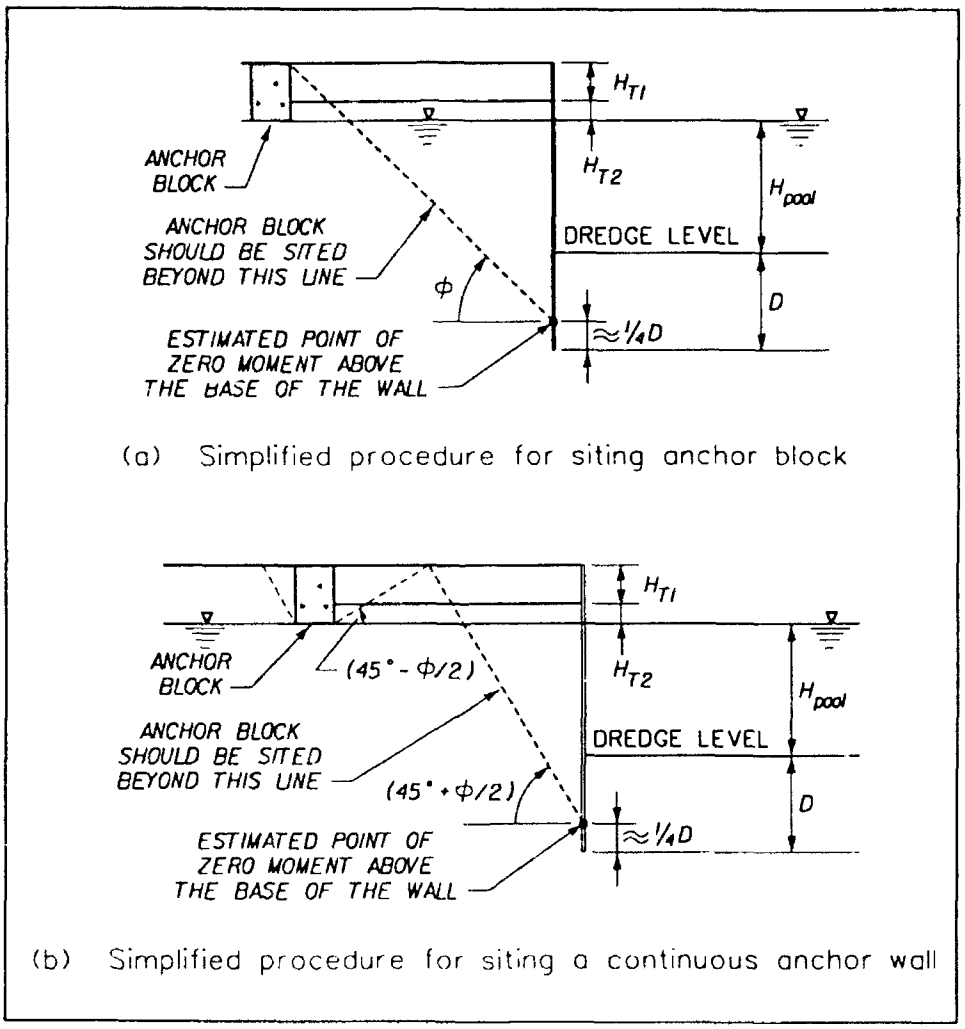

From NAVFAC DM 7.2

Figure C.4 Design criteria for deadman anchorage

C.2 Design of an Anchored Sheet Pile Wall for Seismic Loading

This section describes the calculations involved in the design of Figure C.1 anchored sheet pile wall for earthquake loading using the free earth support method of analysis (13 steps) described in Section 7.4.1 with $r_u = 0$.

C.2.1 Static Design (Step 1)

The static loading design of Figure C.1 anchored sheet pile wall is described in Section C.1. The calculated depth of penetration D equals 10.02 ft (Section C.1.3).

C.2.2 Horizontal Seismic Coefficient, k_h (Step 2)

$$k_h = 0.2$$

C.2.3 Vertical Seismic Coefficient, k_v (Step 3)

k_v = +0.1, 0 and -0.1

according to Section 1.4.3. This appendix contains details regarding the case for k_v = +0.1 only due to the length of the calculations involved.

C.2.4 Depth of Penetration (Steps 4 to 6)

The depth of penetration, D, equal to 10 ft was found not to be stable under earthquake loading. The required minimum depth of penetration is best determined by the trial and error procedure of first assuming a value for D and checking if moment equilibrium of the earth and water pressure forces about the elevation of the tie rod is satisfied (steps 4 through 6).

This iterative procedure results in a minimum required depth of penetration equal to 20.24 ft. The calculations involved in Steps 4 through 6 are summarized in the following paragraphs for the case of D set equal to 20.24 ft.

Backfill

Effective Unit Weight for the Partially Submerged Backfill

According to Figure 4.13,

$$\gamma_e = \left(\frac{h_1}{h}\right)^2 \cdot (\gamma_t - \gamma_w) + \left[1 - \left(\frac{h_1}{h}\right)^2\right] \cdot \gamma_t$$

with D = 20.24 ft

h_1 = 40.24 ft

h = 50.24 ft

$$\gamma_e = \left(\frac{40.24}{50.24}\right)^2 \cdot (120 \text{ pcf} - 62.4 \text{ pcf}) + \left[1 - \left(\frac{40.24}{50.24}\right)^2\right] \cdot 120$$

γ_e = 79.97 pcf

Equivalent Horizontal Seismic Coefficient, k_{hel}, for the backfill

For the restrained water case with $r_u = 0$

$$k_{hel} = \frac{\gamma_t}{\gamma_e} \cdot k_h \qquad \text{(adapted from eq 47)}$$

$$k_{hel} = \frac{120 \text{ pcf}}{79.97 \text{ pcf}} \cdot 0.2 = 0.3001$$

Seismic Inertia Angle, ψ_{el}, for the Backfill

$$\psi_{el} = \tan^{-1}\left[\frac{k_{hel}}{1 - k_v}\right] \qquad \text{(adapted from eq 48)}$$

$$\psi_{el} = \tan^{-1}\left[\frac{0.3001}{1 - 0.1}\right]$$

$$\psi_{el} = 18.44°$$

Dynamic Active Earth Pressure, P_{AE}

with $\phi' = 35°$*, $\delta = \phi/2 = 17.5°$* and $\psi_{el} = 18.44°$, $K_{AE} = 0.512$ (by eq 36)

---

* Strength parameters to be assigned in accordance with the criteria in Section 2.3.

$P_{AE} = K_{AE} \cdot \frac{1}{2} [\gamma_e (1 - k_v)] H^2$ (adapted from eq 33)

$P_{AE} = 0.512 \cdot \frac{1}{2} [79.97 \text{ psf} \cdot (1 - 0.1)] (50.24')^2$

$P_{AE} = 46,506$ lb per ft of wall

$(P_{AE})_x = P_{AE} \cdot \cos\delta = \underline{44,354}$ lb per ft of wall

Horizontal Static Active Earth Pressure Component of P_{AE}

With a hydrostatic water table and $r_u = 0$, the horizontal static active earth pressure force components of P_{AE} are computed using the relationships in Table C.1.

With $\phi' = 35°$ and $\delta = \phi/2 = 17.5°$,

$K_A = 0.246$ (by eq 16)

$K_A \cdot \cos \delta = 0.235$

Above the water table $\gamma_t = 120$ pcf is used to calculate the effective overburden pressure while below the water table $\gamma' = \gamma_t - \gamma_w$ (= 57.6 pcf) is used to calculate the effective overburden pressure with $r_u = 0$. The resulting values for the five horizontal static force components E_1 through E_5 of P_{AE} are given in Table C.9 (forces shown in Figure C.2).

Table C.9. Five Horizontal Static Active Earth Pressure Force Components of P_{AE} with D = 20.24 feet

Horizontal Force Designation	Horizontal Force (lb per ft wall)	Distance to Pile Tip (ft)
E_1	1,410	43.57
E_2	5,640	30.24
E_3	2,707	26.91
E_4	11,187	10.12
E_5	2,772	6.75

$(P_A)_x = E_1 + E_2 + E_3 + E_4 + E_5$

$(P_A)_x = 23,716$ lb per ft of wall

$$Y_{PA} = \frac{1,410 \cdot 43.57 + 5,640 \cdot 30.24 + 2,707 \cdot 26.91 + 11,187 \cdot 10.12 + 2,772 \cdot 6.75}{23,716}$$

$Y_{PA} = 18.42$ ft above the pile tip.

Horizontal Component of the Incremental Dynamic Active Earth Pressure Force, $(\Delta P_{AE})_x$

$(\Delta P_{AE})_x = (P_{AE})_x - (P_A)_x$ (adapted from eq 40)

$(\Delta P_{AE})_x = 44,354 - 23,716 = \underline{20,638}$ lb per ft of wall

$Y_{\Delta PAE} = 0.6 \cdot H = 0.6 \cdot 50.24' = 30.14$ ft above the pile tip.

$$Y_{PAE} = \frac{(P_A)_x \cdot Y_{PA} + (\Delta P_{AE})_x \cdot Y_{\Delta PAE}}{(P_{AE})_x}$$ (adapted from eq 44)

$$Y_{PAE} = \frac{23,716 \cdot 18.42 + 20,638 \cdot 30.14}{44,354}$$

$Y_{PAE} = 23.87$ ft above the pile tip.

Below Dredge Level

Equivalent Horizontal Seismic Coefficient, k_{hel}, Used in Front of Wall

For the restrained water case with $r_u = 0$

$$k_{hel} = \frac{\gamma_t}{\gamma_b} \cdot k_h$$ (by eq 47)

$$k_{hel} = \frac{120 \text{ pcf}}{(120 \text{ pcf} - 62.4 \text{ pcf})} \cdot 0.2$$

$k_{hel} = 0.4167$

Seismic Inertia Angle, ψ_{el}, Used in Front of Wall

$$\psi_{el} = \tan^{-1}\left[\frac{k_{hel}}{1 - k_v}\right]$$ (adapted from eq 48)

$$\psi_{el} = \tan^{-1}\left[\frac{0.4167}{1 - 0.1}\right]$$

$\psi_{el} = 24.84°$

"Factored" Strengths Used in Front of Wall

By equation 95 with $FS_p = 1.2$,*

$$\tan\phi_t' = \frac{\tan 35°}{1.2}$$

$$\phi_t' = 30.3°$$

By equation 96 with $\delta = \phi/2$

---

* $FS_p = 1.2$ for illustration purposes only. See discussion in footnote to step 5.

$$\tan\delta_t = \frac{\tan 17.5°}{1.2}$$

$$\delta_t = 14.7°$$

"Factored" Dynamic Passive Earth Pressure Coefficient K_{PE}

Method 1: Using the equivalent static formulation with K_p by Log-Spiral method (Section 4.4).

$$\beta^* = \beta - \psi_{el} = -24.84°$$

$$\theta^* = \theta - \psi_{el} = -24.84°$$

K_p ($\beta^* = -24.84$, $\theta^* = -24.84$, $\phi = 30.3$, $\delta = -\phi$) = 3.56 and R = 0.746 from Caquot and Kerisel (1948). For $\phi = 30.3°$ and $\delta = -\phi/2$,

$$K_p\ (\beta^*,\ \theta^*,\ \phi,\ \delta = -\phi/2) = 3.56 \cdot 0.746$$

$$K_p\ ((\beta^*,\ \theta^*,\ \phi,\ \delta = -\phi/2) = 2.66$$

$$F_{PE} = \frac{\cos^2(\theta - \psi_{el})}{\cos\psi_{el}\cos^2\theta} \qquad \text{(eq 63)}$$

$$F_{PE} = \frac{\cos^2[0 - (-24.84)]}{\cos(24.84)\cos^2(0)} = 0.907$$

$$K_{PE} = K_p\ (\beta^*,\ \theta^*,\ \phi,\ \delta = -\phi/2) \cdot F_{PE} \qquad \text{(adapted from eq 62)}$$

$$K_{PE} = 2.66 \cdot 0.907 = 2.41$$

$$K_{PE} \cdot \cos\delta_t = 2.41 \cdot \cos(14.7) = \underline{2.33}$$

----------Reference----------

Method 2: K_{PE} by Mononobe-Okabe.

with $\phi' = 30.3°$, $\delta = 14.7°$, $\psi_{el} = 24.84°$, $\beta = 0°$ and $\theta = 0°$

$$K_{PE} = 2.85 \qquad \text{(by eq 60)}$$

and

$$K_{PE} \cdot \cos\delta_t = 2.76$$

The value of K_{PE} by Mononobe-Okabe is 18 percent larger than the value calculated using the log-spiral method. Use the values computed by the Log-spiral method in the calculations that follow.

----------End Reference----------

"Factored" Horizontal Dynamic Passive Earth Pressure Force P_{PE}

$$(P_{PE})_x = K_{PE} \cdot \cos \delta_t \cdot \frac{1}{2} [\gamma_b \cdot (1 - k_v)] D^2$$ (adapted from eq 58)

$$= 2.33 \cdot \frac{1}{2} [(120 \text{ pcf} - 62.4 \text{ pcf}) \cdot (1 - 0.1)] (20.24)^2$$

$(P_{PE})_x$ = 24,740 lb per ft of wall

$$Y_{PE} \approx \frac{1}{3} \cdot D* = \frac{1}{3} \cdot 20.24 = 6.75 \text{ ft above the pile tip.}$$

Pool In Front of Wall

Hydrodynamic Water Pressure Force P_{wd}

$$P_{wd} = \frac{7}{12} k_h \gamma_w (H_{pool})^2$$ (by eq B-5)

$$= \frac{7}{12} \cdot 0.2 \cdot 62.4 \text{ pcf } (2')^2$$

P_{wd} = 2,912 lb per ft of wall

$Y_{Pwd} = 0.4 \cdot H_{pool} = 8$ ft above the dredge level.

Depth of Penetration

Equilibrium of Moments About The Elevation of the Tie Rod

$$\sum M_{CCW} = (P_{AE})_x \cdot (H_{T2} + H_{pool} + D - Y_{PAE})$$
$$+ P_{wd} \cdot (H_{T2} + H_{pool} - 0.4 \cdot \text{pool})$$
$$= 44,354 \cdot (3' + 20' + 20.24' - 23.87')$$
$$+ 2,912 \cdot (3' + 20' - 8')$$
$$= 859,137 + 43,680$$

---

* $Y_{PE} = \frac{1}{3} \cdot D$ for illustration purposes only. See discussion in footnote to step 5.

$\sum M_{CCW}$ = 902,817 ft. - lb per ft. of wall

$\sum M_{CW} = -(P_{PE})_x \cdot (H_{T2} + H_{pool} + D - Y_{PE})$

$= -24,740 \cdot (3' + 20' + 20.24' - 6.75')$

$\sum M_{CW}$ = -902,763 ft-lb per ft of wall

Moment Imbalance = $\Sigma M_{CCW} + \Sigma M_{CW}$

= 54 ft-lb per ft of wall

Small moment imbalance value so D = <u>20.24</u> ft for the case of $k_h = 0.2$ and $k_v = +0.1$.

The two additional cases of k_v = and $k_v = -0.1$ are summarized in Table C.10. The required minimum depth of penetration is equal to 20.24 ft (20.5 ft for construction).

Table C.10 Summary of Depth of Penetration Calculations

Case	k_h	k_v	D (ft)	$\frac{D}{D_{Static}}$
Static	0	0	10.02	1.0
Dynamic	0.2	-0.1	14.88	1.5
Dynamic	0.2	0	17.1	1.7
Dynamic	0.2	+0.1	20.24	2.0

C.2.5 Tie Rod Force T_{FES} (Step 7)

Horizontal force equilibrium for the case of D = 20.24 ft with $k_h = 0.2$ and $k_v = +0.1$,

$\Sigma F_h = 0$

results in

$$T_{FES} = (P_{AE})_x + P_{Wd} - (P_{PE})_x \qquad \text{(adapted from eq 99)}$$

for a hydrostatic water table with $r_u = 0$.

T_{FES} = 44,354 + 2,912 - 24,740

T_{FES} = 22,526 lb per ft of wall.

The two additional cases of $k_v = 0$ and $k_v = -0.1$ are summarized in Table C.11. The anchorage is designed using T_{FES} = 22,526 lb per ft of wall.

Table C 11 Tie Rod Force T_{FES}

Case	k_h	k_v	D (ft)	T_{FES} lb per ft of wall	$\frac{T_{FES}}{(T_{FES})_{static}}$
Static	0	0	10.02	6,255	1
Dynamic	0.2	-0.1	14.88	20,819	3.3
Dynamic	0.2	0	17.1	21,368	3.4
Dynamic	0.2	+0.1	20.24	22,526	3.6

C.2.6 Maximum Moment M_{FES} (Step 8)

The maximum value of moment internal to the sheet pile wall, M_{FES}, occurs at the elevation of zero shear within the sheet pile. First determine the elevation of zero shear and then compute the moment of earth and water pressure forces about the tie rod (refer to Figure 7.10).

Above the dredge level, at elevation y below the hydrostatic water table

$$(P_{AE})_x + P_{Wd} - T_{FES} = 0$$

with

$$(P_{AE})_x = (P_A)_X + (\Delta P_{AE})_x$$

$(P_A)_x$ above the dredge level (refer to Figure C.2)

$$(P_A)_x = E_1 + E_{2y} + E_{3y}$$

$$\underline{(P_A)_x = 1{,}410 + 282\ y + 6.768\ y_2}$$

With $(\Delta P_{AE})_x$ equal to 20,638 lb per ft of wall, the equivalent stress distribution is given in Figure C.5 (adapted from Figure 7.9).

$$(\Delta P_{AE})_x = \frac{1}{2} \cdot (\sigma_{top} + \sigma_y) \cdot (10' + y)$$

$$= \frac{1}{2} \cdot (657.3 + 559.2 - 9.807y) \cdot (10 + y)$$

$$\underline{\Delta P_{AE} = -4.9035\ y^2 + 559.215\ y + 6{,}082.5}$$

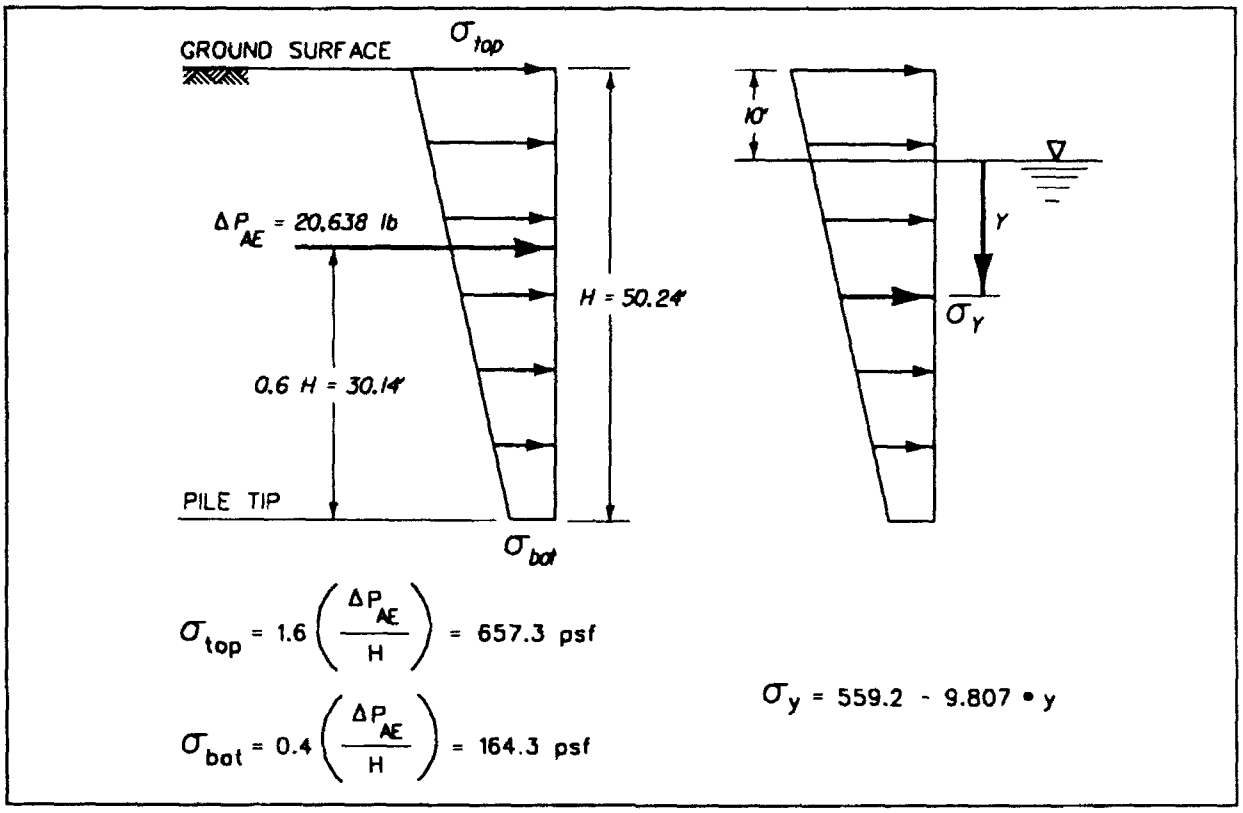

Figure C.5 Distributions of horizontal stresses corresponding to ΔP_{AE}

$$P_{wd} = \frac{7}{12} \cdot k_h \gamma_w (y)^2 \qquad \text{(adapted from eq B-5)}$$

$$\underline{P_{wd} = 7.28\ y^2}$$

$$\underline{T_{FES} = 22{,}526 \text{ lb per ft of wall}}$$

Above the dredge level

$$(P_A)_x + (\Delta P_{AE})_x + P_{Wd} - T_{FES} = 0$$

becomes

$$9.1445\ y^2 + 841.215\ y - 15{,}033.5 = 0$$

$$y = \frac{-(841.215) \pm \sqrt{(841.215)^2 - 4(9.1445)\ (-15{,}033.5)}}{2\ (9.1445)}$$

y = <u>15.32</u> ft below the water table (above dredge level ∴ ok) (Table C.12)

Table C.12 Moment of Forces Acting Above the Point y = 15.32 feet Below the Water Table and About the Tie Rod

Horizontal Force Designation	Horizontal Force (lb per ft wall)	Lever Arm (ft)	Moment About Tie Rod -CCW +'ve - (ft-lb per ft wall)
E_1	1,410	-0.33	-465
E_{2x}	4,320	$3 + \frac{1}{2}(15.32)$	46,051
E_{3x}	1,588	$3 + \frac{2}{3}(15.32)$	20,983
$(\Delta P_{AE})_x$	13,499	4.68*	63,175
P_{Wd}	1,709	$3 + 0.6 \cdot (15.32)$	20,836
M_{FES} = 150,580 ft-lb per ft wall			

* From Figure C.5 pressure distribution for y = 15.32 ft

The maximum moment internal to the sheet pile at y = 15.32 ft below the water table is equal to M_{FES} = 150,580 ft-lb per ft of wall.

Section C.2.7 Design Moment M_{design} (Step 9)

The design moment, M_{design}, is obtained through application of Rowe's (1952) moment reduction procedure that is outlined in Figure 7.2. The ability of the system to develop flexure below the dredge level during earthquake shaking must be carefully evaluated prior to application of Rowe's moment reduction factor or any portion of the reduction factor (refer to the introductory discussion of Section 7.4).

$$H = H_{T1} + H_{T2} + H_{pool} + D$$

$$H = 7' + 3' + 20' + 20.24' = 50.24 \text{ ft} = (602.88 \text{ in.})$$

$$E = 30 \times 10^6 \text{ psi}$$

$$\text{Flexibility number, } \rho = \frac{H^4}{EI}$$

where

$$I = \text{moment of inertia } \underline{\text{per ft of wall}}$$

$$\rho = \frac{(602.88 \text{ in})^4}{(30 \times 10^6 \text{ psi}) \cdot I}$$

$$\rho = \frac{4,403.54}{I}$$

The values of M_{design} are given in Table C.13 for four sheet pile sections.

Table C.13 Design Moment for Sheet Pile Wall in Dense Sand

Section Designation	I (in.^{4} per ft of wall)	ρ (in.^{2}/lb per ft of wall)	r_d (Figure 7.2)	M_{design} (ft-lb per ft of wall)
PZ22	84.4	52.2	0.38	57,220
PZ27	184.2	23.9	0.46	69,267
PZ35	361.2	12.2	0.58	87,336
PZ40	490.8	9.0	0.74	111,429

where $M_{design} = r_d \cdot M_{FES}$ (by eq 100)

In this design example, the maximum allowable stress within the sheet pile for seismic loadings is restricted to

$$\sigma_{allowable} = (1.33) \cdot 0.65 \cdot \sigma_{yield} \approx 0.87 \cdot \sigma_{yield}$$

for ASTM A328 steel sheet piling,

$$\sigma_{yield} = 39{,}000 \text{ psi}$$

$$\sigma_{allowable} = 0.87 \cdot 39{,}000 \text{ psi} \approx 34{,}000 \text{ psi}$$

The allowable bending moment, $M_{allowable}$, is given by

$$M_{allowable} = S \cdot \sigma_{allowable} \text{ per ft run of wall}$$

where

S = section modulus (in.^{3} per ft run of wall)

Comparison of the design moment values (M_{design} in Table C.13) to the allowable bending moments ($M_{allowable}$ in Table C.14) indicates that the pile section would be upgraded from PZ22 to PZ27 due to seismic considerations. Corrosion must also be addressed during the course of sheet pile wall design.

Table C.14. Allowable Bending Moment for Four ASTM A328 Grade Sheet Pile SECTIONS ($\sigma_{allowable} = 0.87 \cdot \sigma_{yield}$)

Section Designation	S (in.^{3} per ft of wall)	$M_{allowable}$ (ft-kips per ft of wall)
PZ22	18.1	51.3
PZ27	30.2	85.6
PZ35	48.5	137.4
PZ40	60.7	172.0

C.2.8 Design Tie Rods (Step 10)

For seismic loadings

$T_{design} = 1.3 \cdot T_{FES}$ (by eq 101)

with $T_{FES} = 22,526$ lb per ft of wall

$T_{design} = 29,284$ lb per ft of wall

Assume

(a) 6 ft spacing of tie rods

(b) $\sigma_{yield} = 36,000$ psi

$\sigma_{allowable} = 0.6 \cdot \sigma_{yield}$ (60% of yield)

$$\text{Minimum area of rod} = \frac{6 \text{ ft.} \cdot 29,284 \text{ lb per ft of wall}}{0.6 \cdot 36,000 \text{ psi}}$$

$$\text{Gross Area} = 8.13 \text{ in.}^2$$

$$\text{Minimum Diameter} = \sqrt{\frac{4 \cdot \text{Area}}{\pi}} = 3.22 \text{ inches}$$

Table C.15 summarizes the required geometry of tie rod for the four load cases.

Table C.15 Required Geometry of Tie Rod*

Case	k_h	k_v	D (ft)	$\frac{\sigma_{allowable}}{\sigma_{yield}}$	T_{design} (lb per ft of wall)	Area (in.^{2})	Rod Diameter (in.)
Static	0	0	10.02	0.4	8,132	3.30	2.08
Dynamic	0.2	-0.1	14.88	0.6	27,065	7.52	3.09
Dynamic	0.2	0	17.1	0.6	27,778	7.72	3.13
Dynamic	0.2	+0.1	20.24	0.6	29,284	8.13	3.22

*Calculated for the case of

(a) 6 ft spacing of tie rods

(b) $\sigma_{yield} = 36,000$ psi

(c) $T_{design} = 1.3 \cdot T_{FES}$

Comparison of the minimum diameter of tie rod (Table C.15) required for seismic loading to the diameter required for static loading indicates that for a 6 ft spacing, the diameter of the tie rods (σ_{yield} = 36,000 psi) would be upgraded from 2.08 in. to 3.22 in.

C.2.9 Design of Anchorage (Step 11)

For seismic loadings

$$T_{ult-a} = T_{FES} \qquad \text{(refer to discussion in step 11)}$$

In the case of k_h = 0.2 and k_v = +0.1,

$$T_{ult-a} = 22{,}526 \text{ lb per ft of wall}$$

The dynamic forces acting on the continuous anchor wall are shown in Figure C.6.

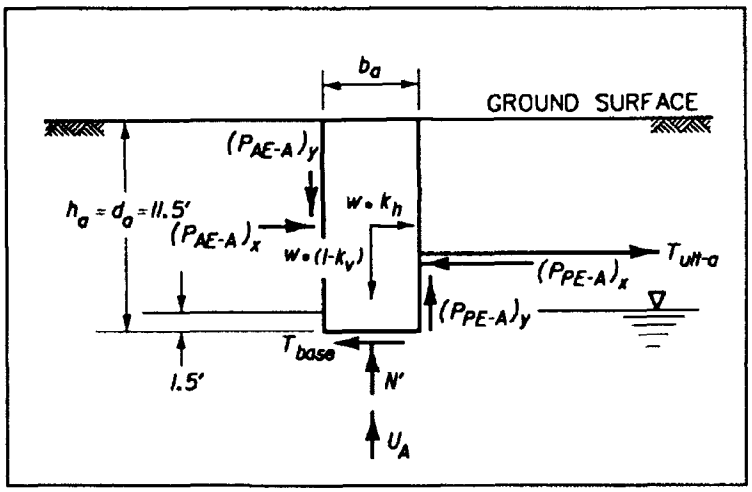

Figure C.6 Seismic design problem for a continuous anchor block

C.2.10 Size Anchor Wall (Step 12)

Assume that a continuous concrete wall is selected to be the anchorage. The "factored" dynamic earth pressures that develop in front of the anchor wall provides nearly all of the lateral resistance to the pull force T_{ult-a}. The anchor wall will be designed using ϕ_t and δ_t (Equations 95 and 96) due to the magnitude of T_{ult-a} for seismic loading (equal to 3.6 times the static value). The required depth and width of anchor wall is best determined by the trial and error procedure of first assuming a value for d_a and checking if equilibrium of horizontal forces acting on the anchor (Equation 103) is

satisfied (step 12). Once the value of d_a is determined, equilibrium of the vertical forces acting on the anchor wall (Equation 104) will dictate the minimum value of wall width b_a. Refer to Section C.1.9 in this appendix for additional discussion of anchorage design.

This iterative procedure results in a minimum required depth of anchorage equal to 11.5 ft and a minimum width of anchor wall equal to 4.5 ft The calculations involved in Step 12 are summarized in the following paragraphs for d_a = 11.5 ft and $(b_a)_{min}$ = 4.5 ft in Figure C.6 .

Dynamic Active Earth Pressure Force P_{AE-A}

For the case of d_a = 11.5 ft (the anchor submerged 1.5 ft below the water table), the effective unit weight is equal to

γ_e = 118.94 pcf

with h_1 = 1.5 ft and h = 11.5 ft in Figure 4.13.

The equivalent horizontal seismic coefficient k_{hel} is equal to 0.2018 (obtained by substituting γ_e for γ_b in Equation 47). A value of k_{hel} equal to 0.2 is used in the subsequent calculations.

For the case of k_{hel} = 0.2 and k_v = +0.1

$$\psi_{el} = \tan^{-1}\left[\frac{k_{hel}}{1 - k_v}\right] \qquad \text{(adapted from eq 48)}$$

$$\psi_{el} = 12.529°$$

With ϕ' = 35°, δ = 17.5° and ψ_{el} = 12.529°

K_{AE} = 0.3987

and

$K_{AE} \cdot \cos\delta$ = 0.38

$K_{AE} \cdot \sin\delta$ = 0.12

With d_a = 11.5 ft in Figure C.6.

(adapted from eq 33)

$$(P_{AE-A})_x = K_{AE} \cdot \cos\delta \cdot \frac{1}{2}\left[\gamma_e(1 - k_v)\right](d_a)^2$$

$$(P_{AE-A})_x = 0.38 \cdot \frac{1}{2}\left[\,118.94 \text{ pcf } (1 - 0.1)\,\right](11.5')^2$$

$$(P_{AE-A})_x = 2{,}690 \text{ lb per ft of wall}$$

by a similar calculation

$$(P_{AE-A})_y = 849 \text{ lb per ft of wall}$$

Dynamic Passive Earth Pressure Force P_{PE-A}

With $\phi' = 35°$ and with FS_p set equal to 1.2 in this example (see step 12 discussion regarding the relationship between anchorage displacement and FS_p)

$$\phi_t' = 30.3° \qquad \text{(by eq 95)}$$

and $\delta = 17.5°$,

$$\delta_t = 14.7°$$

For $\psi = 12.529°$ (refer to P_{AE-A} calculations), $\phi_t' = 30.3°$ and $\delta_t = 14.7°$

$$K_{PE} = 4.06 \qquad \text{(by eq 60)}$$

$$K_{PE} \cdot \cos \delta_t = 3.93$$

and

$$K_{PE} \cdot \sin \delta_t = 1.03$$

With $d_a = 11.5$ ft in Figure C.6

$$(P_{PE-A})_x = K_{PE} \cdot \cos\delta \cdot \frac{1}{2} \left[\gamma_e(1 - k_v)\right] (d_a)^2 \qquad \text{(adapted from eq 58)}$$

$$(P_{PE-A})_x = 3.93 \cdot \frac{1}{2} \left[118.94 \text{ pcf } (1 - 0.1) \right] (11.5')^2$$

$$(P_{PE-A})_x = 27{,}818 \text{ lb per ft of wall}$$

by a similar calculation

$$(P_{PE-A})_y = 7{,}291 \text{ lb per ft of wall}$$

Size Anchor

The depth of the continuous anchor wall is governed by the equilibrium of horizontal forces. Ignoring the contribution of the shear force along the base of the wall, Equation 103

$$T_{ult-a} = (P_{PE-A})_x - (P_{AE-A})_x - W \cdot k_h$$

For Figure C.6 concrete wall, the weight W per foot run of wall with d_a = 11.5 ft and γ_{conc} = 150 pcf is given by

$$W = \gamma_{conc} \cdot b_a \cdot d_a = 1,725 \cdot b_a$$

Introducing this relationship for W and

$k_h = 0.2$

$T_{ult-a} = 22,526$ lb per ft of wall ($k_v = +0.1$)

$(P_{PE-A})_y = 27,818$ lb per ft of wall

$(P_{AE-A})_x = 2,690$ lb per ft of wall

into the modified equation of horizontal equilibrium results in a <u>maximum</u> value of b_a equal to 7.5 ft for $d_a = 11.5$ ft. Larger b_a values would result in excessive horizontal inertia forces acting on the concrete block, requiring revisions of the previous calculations.

Mobilization of friction along interface between the front of the anchor wall and the passive wedge requires that the wall have sufficient dead weight to restrain against upward movement as it displaces the soil in front of the wall (Dismuke 1991). The equation of equilibrium of vertical forces acting on the wall is used to compute the <u>minimum</u> width of anchor wall. With N′ set equal to zero, Equation 104 becomes

$$0 = W(1 - k_v) - U_A - (P_{PE-A})_y + (P_{AE-A})_y$$

with

$W = 1,725 \cdot b_a$

$k_v = 0.1$

$U_A = 62.4$ pcf $\cdot 1.5' \cdot b_a = 93.6 \cdot b_a$

$(P_{PE-A})_y = 7,291$ lb per ft of wall

$(P_{AE-A})_y = 849$ lb per ft of wall

the modified equation of vertical equilibrium results in a <u>minimum</u> value of b_a equal to 4.4 ft or $(b_a)_{min} \approx 4.5$ ft.

Alternative Anchorage:

Other types of anchorages to be considered include slender anchorage, multiple tie rods and anchorage, A-frame anchors, sheet pile anchorage, soil or rock anchors and tension H-piles. Slender anchorage refers to a slender wall designed using the procedure described in this section with δ set equal to 0 degrees.

C.2.11 Site Anchorage (Step 13)

The anchor wall is to be located a sufficient distance behind the sheet pile wall so that the dynamic active failure surface <u>does not intersect</u> the passive failure developing in front of the anchor wall. Figure C.7 outlines the <u>minimum</u> required distances for this design problem.

Dynamic Active Wedge - Sheet Pile Wall

With $\phi' = 35°$, $\delta = 17.5°$ and $\psi_{el} = 18.44°$ (from Section C.2.4, Step 4)

$\alpha_{AE} = 40.695°$ (by eq 37)

$$x_{AE} = \frac{50.24'}{\tan \alpha_{AE}} = 58'$$

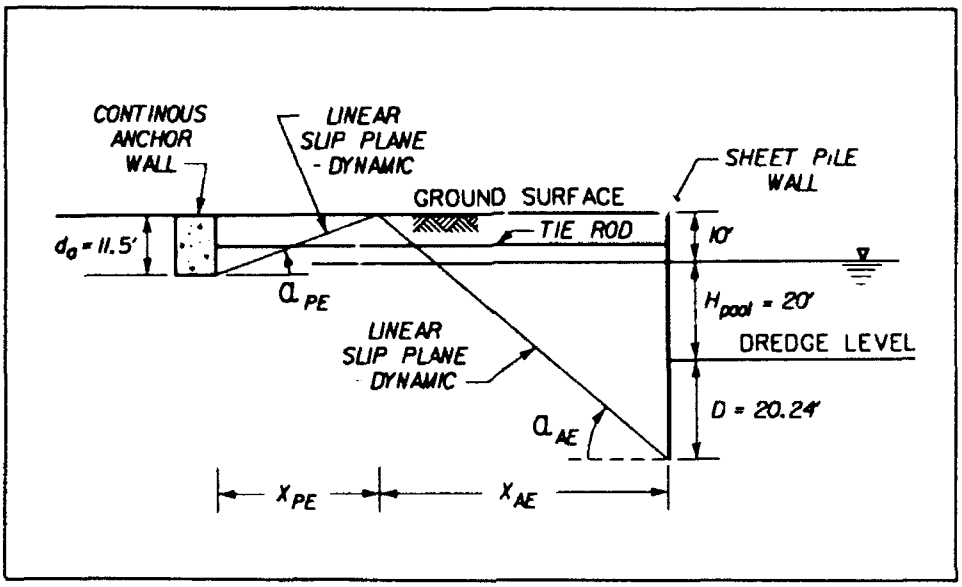

Figure C.7 Simplified procedure for siting a continuous anchor wall

Dynamic Passive Wedge - Anchor Wall

with $\phi'_t = 30.3°$, $\delta_t = 14.7°$ and

$\psi_{el} = 12.529°$ (Section C.2.10, Step 12)

$\alpha_{PE} = 18.27°$ (by eq 61)

$$x_{PE} = \frac{11.5'}{\tan \alpha_{PE}} = 35'$$

Site Anchorage

Site concrete anchor wall at a distance of 93 ft behind the sheet pile wall ($= x_{AE} + x_{PE}$).

APPENDIX D: COMPUTER-BASED NUMERICAL ANALYSES

This appendix is a brief guide to issues that must be faced when making a decision to utilize a computer-based numerical analysis and to the literature concerning such methods. As discussed in the main body of this report, there are circumstances in which analyses carried out by some such method may be appropriate during design of a waterfront structure.

There exists a bewildering array of computer-based methods applicable to analysis of the dynamic response of earthen mosses or soil-structure systems. Table D.1 presents a partial listing of some of the better-known methods. Most, but not all, such methods use a finite element formulation, and hence somewhat incorrectly are referred to collectively as finite element methods. Most methods were developed originally for applications other than waterfront structures - especially problems related to nuclear power plants and earthdams.

Some methods are relatively simple but approximate only one or two aspects of soil behavior. Others, which can be quite complex and difficult to use, simulate a number of different features of soil behavior quite well. All must be used with care and judgment. A key is to select a method no more complex than is required for the problem at hand.

Table D.1 Partial Listing of Computer-Based Codes for Dynamic Analysis of Soil Systems

Reference	Names of Code
Lysmer, Udaka, Tsai and Seed (1975)	FLUSH
Earthquake Engineering Technology, Inc. (1983)	SuperFLUSH
Hallquist (1982)	DYNA2D
Finn, Yogendrakumar, Yoshida, and Yoshida (1986)	TARA
Provost (1981)	DYNA-FLOW
Lee and Finn (1975, 1978)	DESRA
Streeter, Wylie and Richart (1974)	CHARSOIL
Provost (1989)	DYNA1D
Li (1990)	SUMDES
Schnabel, Lysmer, and Seed (1972)	SHAKE
Roth, Scott, and Cundall (1986)	DSAGE
Zienkiewicz and Xie (1990)	SWANDYNE-X
Iai (see Iai and Kameoka 1991)	----
Earth Mechanics, Inc. of Fountain Valley, CA	LINOS

D.1 Some Key References

For dynamic soil-structure interaction analysis related to heavy buildings resting on earth, a concise summary of the various procedures available is reported in the 1979 ASCE report by the Ad Hoc Group on Soil-Structure Interaction of the Committee on Nuclear Structures and Materials of the Structural Division. While in many ways out-of-date, this is still a useful reference concerning basic principles.

Several different finite element formulations are described in detail in Chapter 3, titled Geomechanics and written in part and edited by W. D. L. Finn in the Finite Element Handbook, edited by H. Kardestuncer. The scope and type of laboratory and/or field testing program used to characterize the soil model parameters will vary among the computer codes, as discussed by Finn, the Committee on Earthquake Engineering of the National Research Council (1985), and others.

Whitman (1992) has suggested a scheme for categorizing the various types of methods, and has discussed the status of validation of various methods by comparison to observations during actual earthquakes or to results from model tests.

D.2 Principal Issues

According to the guidelines set forth by the ASCE Ad Hoc Group on Soil-Structure Interaction of the Committee on Nuclear Structures and Materials of the Structural Division 1979 report on the "Analysis For Soil-Structure Interaction Effects For Nuclear Power Plants" and the ASCE Standard (1986), to perform a complete soil-structure interaction analysis the analytical procedure must (1) account for the variation of soil properties with depth, (2) give appropriate consideration to the material nonlinear behavior of soil, (3) consider the three-dimensional nature of the problem, (4) consider the complex nature of wave propagation which produced the ground motions, and (5) consider possible interaction with neighboring structures.

The reference to a "complete" analysis results from the existence of two distinguishable aspects of soil-structure interaction: (1) the relative motion of the foundation of the structure with respect to the surrounding soil as a result of the inertial forces in the structure being transmitted to the compliant soil foundation and backfill and/or (2) the inability of the stiffer structural foundation and walls to conform to the distortions of the soil generated by the ground motion. The former is referred to as inertial interaction and the latter is referred to as kinematic interaction. Both features co-exist in most actual problems. However, several analytical procedures available to perform the soil-structure interaction analysis of earth retaining structures take advantages of this separation of behavior in their numerical formulation.

Specific feature that must be accounted for in some problems include softening the soil stiffness during shaking, the material and geometrical damping and the separation of portions of the backfill from the structure, followed by recontact or "slap," that can occur during shaking. It may be necessary to use special interface elements at boundaries between soil and structure. It also may be necessary to model the actual process of construction as accurately as possible.

D.2.1 Total versus Effective Stress Analysis

Effective stress analyses explicitly predict and take into account the effects of excess pore pressures caused by the cyclic shearing of soil during earthquake shaking. The generation of significant excess pore pressures causes the stiffness of soil to degrade and may lead to a nearly-total loss of shear strength. TARA, DYNAFLOW, DESRA, and DSAGE are examples of effective stress analyses. As a general rule, such analyses should be used if significant excess pore pressures are anticipated.

Total stress analyses do not explicitly account for the effects of excess pore pressures, although some may consider this effect indirectly by adjusting stiffness for the anticipated intensity of cyclic shear strains. FLUSH and SHAKE are examples of total stress analyses. Total stress analyses are appropriate when cohesionless soils are dry or very coarse, with most cohesive soils, and for problems such as analyzing lateral earth pressures caused by surface loadings.

D.2.2 Modeling Nonlinear Behavior

Using an effective stress analysis accounts partially, but not fully, for the nonlinear behavior of soils. In addition, it is necessary to consider the effect of shear strain upon stiffness at a given effective stress.

As somewhat of an oversimplification, three ways of introducing such non-linearity have been utilized. (1) By using a linear analysis in which shear modulus is linked, via an iterative procedure, to a measure of cyclic shear strain during shaking. FLUSH and SHAKE are examples of this approach. (2) By introducing a nonlinear stress-strain law, such as a hyperbolic backbone curve together with Masing rules for strain reversals. DESRA and TARA are examples. (3) By utilizing concepts and principles from the theory of plasticity. DYNAFLOW is an example of this approach.

It is not really possible to say that one way is better than another. All involve some degree of approximation. The choice involves a trade-off between accuracy and convenience/cost, and perhaps the availability of a code.

D.2.3 Time versus Frequency Domain Analysis

Problems involving nonlinear material behavior can be solved in either (1) the time domain or (2) the frequency domain by using equivalent linear material property approximations for the nonlinear material(s). The one-dimensional computer programs DESRA, CHARSOIL, DYNA1D, and SUMDES and the two-dimensional programs TARA, DYNA-FLOW, and DYNA2D are examples of the time domain procedure. The one-dimensional computer program SHAKE and the two-dimensional programs FLUSH and SuperFLUSH are examples of the frequency domain solutions.

Frequency-domain techniques formerly favored owing to greater computational efficiency. However, the growth in the power of relatively inexpensive computers has diminished this advantage.

D.2.4 1-D versus 2-D versus 3-D

Today it is, in principle possible to model the three-dimensional aspects of soil response problems, but seldom is the effort justified. In many cases the responses of a soil profile can be modeled satisfactorily using one-dimensional programs such as SHAKE, CHARSOIL, or DESRA. For most problems involving retaining structures, a 2-D analysis (such as TARA, DYNAFLOW, DYNA2D, or DSAGE) will be necessary. The code FLUSH approximates some aspects of 3-D response.

D.2.5 Nature of Input Ground Motion

Typically analyses use the idealization that the patterns of ground motion are simple mechanisms; the most common procedures use vertically propagating shear waves or dilatation waves. While it is possible to consider more general forms of input with horizontally traveling waves, seldom will such an effort be warranted for waterfront structures.

D.2.6 Effect of Free Water

Consider the problem of a complete soil-structure interaction analysis of the earth retaining structure shown in Figure D.1a. The finite element mesh used to model this problem includes the retaining structure, the soil backfill and the pool of water in front of the wall, as shown in Figure D.1b. The mass and stiffness effects are included within the analysis for both the structure and the soil backfill by incorporating these regimes within the finite element mesh that is used to model the problem. Most computer codes do not include within their formulation a water element among their catalog of finite elements, so the Westergaard (1931) added water mass procedure is used to account for the effect of the hydrodynamic water pressures on the dynamic response of the retaining wall (see Appendix B). One computer code that does include a fluid element within its catalog of elements is SuperFLUSH.

D.3 A Final Perspective

The preparation time for developing the finite element mesh, assigning material properties, selecting the ground motion, performing the analysis, and interpreting the computed results is much greater than the time required for performing a simplified analysis. However, the information provided by a dynamic finite element analysis is much more complete and extensive. The computed results include: the variation in computed accelerations with time and the variation in computed dynamic normal and shear stresses with time throughout the wall and the soil regime(s). Thus, a complete soil-structure interaction analysis, when done properly, provides much more accurate and detailed information regarding the dynamic behavior of the earth retaining structure being analyzed.

In a complete soil-structure interaction analysis, the total earth pressures along the back of the wall at any time during the earthquake are equal to the sum of the computed dynamic earth pressures and the static earth and water pressures. At any elevation along the back of the wall, the effective stress component (static + dynamic) of this total pressure is restricted to range in values between the static active earth pressure value and the static passive earth pressure value. Exceedence of these values may occur where in actuality separation may occur during earthquake shaking.

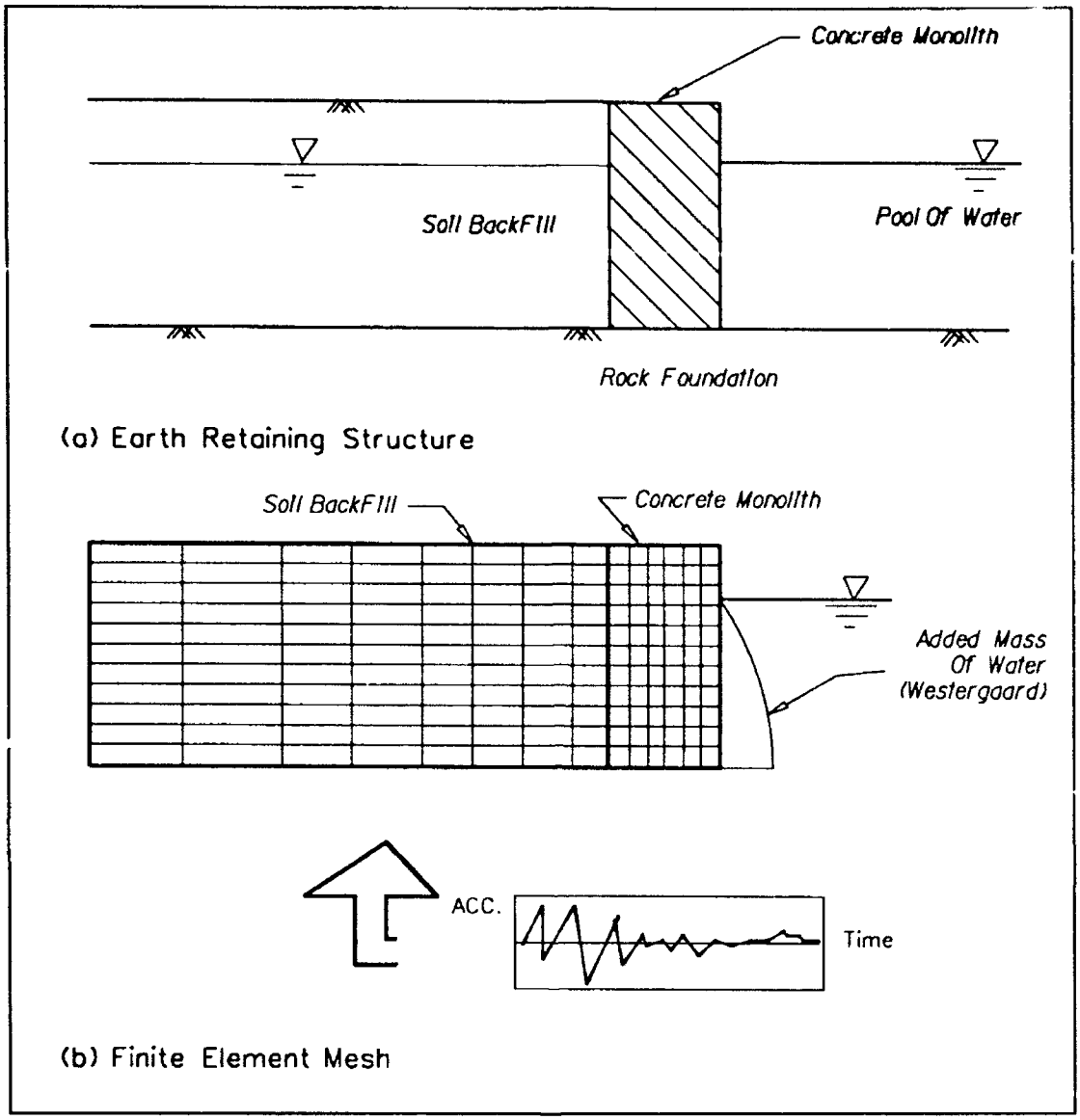

Figure D.1 Earth retaining structure, soil-structure interaction

The potential for liquefaction within the submerged soils comprising the backfill may be computed using the equivalent values for the induced shear stresses form the results of the complete soil-structure interaction analysis. The residual excess pore water pressures are then computed using the procedure described in Seed and Harder (1990) or Marcuson, Hynes, and Franklin (1990).

APPENDIX E: NOTATION

GREEK LETTER SYMBOLS

α	(alpha)	Inclination from horizontal of a planar slip surface extending upward through the backfill
α_A	(alpha)	Inclination from horizontal of a planar slip surface extending upward through the backfill, static active case
α_{AE}	(alpha)	Inclination from horizontal of a planar slip surface extending upward through the backfill, dynamic active case
α_P	(alpha)	Inclination from horizontal of a planar slip surface extending upward through the backfill, static passive case
α_{PE}	(alpha)	Inclination from horizontal of a planar slip surface extending upward through the backfill, dynamic passive case
β	(beta)	Inclination of backfill from horizontal
β^*	(beta)	Inclination of backfill from horizontal, used in the equivalent static procedure for computing K_{AE} and K_{PE}
δ	(delta)	Effective angle of interface friction between the soil and the structure
δ_b	(delta)	Effective angle of interface friction between the base of the wall and its foundation
Δh	(delta)	Change in total head
ΔK_{AE}	(delta)	Incremental dynamic active earth pressure coefficient
ΔK_{PE}	(delta)	Incremental dynamic passive earth pressure coefficient with $\delta = 0$
Δl	(delta)	The length of flow path over which Δh occurs
ΔP_{AE}	(delta)	Incremental dynamic active earth pressure force
ΔP_{PE}	(delta)	Incremental dynamic passive earth pressure force with $\delta = 0$
ΔU	(delta)	Resultant excess pore water pressure force along the base of a wall
Δu	(delta)	Excess pore water pressure due to earthquake shaking
γ'	(gamma)	Effective unit weight of soil
γ_b	(gamma)	Buoyant unit weight of soil
γ_d	(gamma)	Dry unit weight of soil

γ_e	(gamma)	Effective unit weight of a partially submerged backfill for the restrained water case
γ_{e3}	(gamma)	Effective unit weight of soil for the restrained water case with $r_u > 0$
γ_t	(gamma)	Total unit weight of soil
γ_w	(gamma)	Unit weight of water
γ_{w3}	(gamma)	Effective unit weight of water for the restrained water case with $r_u > 0$
ϕ	(phi)	Effective angle of internal friction for soil
ϕ'_{eq}	(phi)	Equivalent angle of internal friction for soil with $r_u > 0$
ψ	(psi)	Seismic inertia angle
ψ_e	(psi)	Seismic inertia angle
ψ_{e1}	(psi)	Equivalent seismic inertia angle for the restrained water case with $r_u = 0$
ψ_{e2}	(psi)	Equivalent seismic inertia angle for the free water case with $r_u = 0$
ψ_{e3}	(psi)	Equivalent seismic inertia angle for the restrained water case with $r_u > 0$
ψ_{e4}	(psi)	Equivalent seismic inertia angle for the free water case with $r_u > 0$
σ	(sigma)	Total normal stress
σ'	(sigma)	Effective normal stress
σ_a	(sigma)	Active earth pressure (effective stress)
σ_p	(sigma)	Passive earth pressure (effective stress)
σ'_v	(sigma)	Vertical effective stress
$\sigma'_{v\text{-initial}}$		Pre-earthquake vertical effective stress
σ'_{wt}	(sigma)	Effective weight of backfill, excluding surcharge
τ	(tau)	Shear stress
τ_f	(tau)	Shear stress at failure
θ	(theta)	Inclination of the back of wall to soil interface from vertical

θ^* (theta) Inclination of the back of the wall to soil interface from vertical, used in the equivalent static procedure for computing K_{AE} and K_{PE}

ROMAN LETTER SYMBOLS

A Maximum ground acceleration as a fraction of g (dimensionless)

a_h Maximum horizontal ground acceleration, equal to $k_h \cdot g$

a_{max} Maximum ground acceleration, equal to $A \cdot g$

a_v Maximum vertical ground acceleration, equal to $k_v \cdot g$

B Width of wall base

B_e Effective base width of the wall in contact with the foundation

c Effective cohesion

c_1 Constant used to compute α_A

c_2 Constant used to compute α_A

c_3 Constant used to compute α_P

c_4 Constant used to compute α_P

c_{1AE} Constant used to compute α_{AE}

c_{2AE} Constant used to compute α_{AE}

c_{3PE} Constant used to compute α_{PE}

c_{4PE} Constant used to compute α_{PE}

d_r Maximum displacement

F_{AE} Factor used in the equivalent static procedure to compute K_{AE}

F_b Factor of safety against bearing capacity failure of a wall

F_{PE} Factor used in the equivalent static procedure to compute K_{PE}

F_s Factor of safety against sliding along the base of a wall

F_{sr} Lateral seismic force component by Woods procedure

FS_p Factor of safety applied to both the shear strength of the soil and the effective angle of friction along the interface when computing P_{PE} for a sheet pile wall and the anchorage.

g Acceleration of gravity

H Height of wall

h	Total head
h_e	Elevation head
h_p	Pressure head
HF_{static}	Static component of heavy fluid force behind a wall retaining liquefied backfill
$HF_{inertia}$	Inertial component of heavy fluid force behind a wall retaining liquefied backfill during shaking
i	Seepage gradient, equal to $\Delta h/\Delta l$
K_A	Static active earth pressure coefficient
K_{AE}	Dynamic active earth pressure coefficient
K_h	Horizontal earth pressure coefficient
k_h	Horizontal seismic coefficient as a fraction of g (dimensionless)
k_h^*	Limiting value for the horizontal seismic coefficient as a fraction of g (dimensionless)
k_{he}	Equivalent horizontal seismic coefficient as a fraction of g (dimensionless)
k_{he1}	Equivalent horizontal seismic coefficient as a fraction of g (dimensionless) for the restrained water case with $r_u = 0$
k_{he2}	Equivalent horizontal seismic coefficient as a fraction of g (dimensionless) for the free water case with $r_u = 0$
k_{he3}	Equivalent horizontal seismic coefficient as a fraction of g (dimensionless) for the restrained water case with $r_u > 0$
k_{he4}	Equivalent horizontal seismic coefficient as a fraction of g (dimensionless) for the free water case with $r_u > 0$
K_P	Static passive earth pressure coefficient
K_{PE}	Dynamic passive earth pressure coefficient
k_v	Vertical seismic coefficient as a fraction of g (dimensionless)
K_o	At-rest horizontal earth pressure coefficient
M_{design}	Design moment for a sheet pile wall
M_{FES}	Maximum moment computed using the Free Earth Support method for a sheet pile wall
N	Total normal force between the wall and the foundation

N'	Effective normal force between the wall and the foundation
N^*	Maximum transmissible acceleration coefficient, as a fraction of g (dimensionless)
P	Resultant earth pressure force acting on a wall
P_A	Active earth pressure force acting on a wall for static loading
P_{AE}	Active earth pressure force acting on a wall for pseudo-static loading
P_P	Passive earth pressure force acting on a wall for static loading
P_{PE}	Passive earth pressure force acting on a wall for pseudo-static loading
P_{wd}	Westergaard hydrodynamic water pressure force
q	Vertical surcharge stress
q_{all}	allowable bearing pressure of rock
q_{max}	maximum bearing pressure below toe of wall
q_{ult}	ultimate bearing capacity or unconfined compressive strength of concrete
r_d	Moment reduction factor due to Rowe
r_u	Excess pore water pressure ratio, equal to $\Delta u/\sigma'_{v\text{-initial}}$
S_u	Undrained shear strength of soil
T	Horizontal shear force along the base of the wall required for equilibrium
T_{design}	Design tie rod force for a sheet pile wall
T_{FES}	Tie rod force computed using the Free Earth Support method for a sheet pile wall
T_{ult}	Ultimate horizontal shear force along the base of the wall
$T_{ult\text{-}a}$	Ultimate force for which the sheet pile wall anchorage is to be designed
U_b	Resultant steady state pore water pressure force normal to the base of the wall
$U_{inertia}$	Hydrodynamic water pressure force for the pool, directed away from the wall
U_{pool}	Resultant hydrostatic water pressure force for the pool

U_{shear} Resultant excess pore water pressure force due to earthquake shaking acting normal to the backfill to wall interface

$U_{shear-b}$ Resultant excess pore water pressure force due to earthquake shaking acting normal to the backfill to sheet pile wall interface

$U_{shear-t}$ Resultant excess pore water pressure force due to earthquake shaking acting normal to the dredge level soil to sheet pile wall interface

$U_{shear-\alpha}$ Resultant excess pore water pressure force due to earthquake shaking acting normal to planar slip surface inclined at α from vertical

U_{static} Resultant steady state pore water pressure force acting normal to the backfill to wall interface

$U_{static-b}$ Resultant steady state pore water pressure force acting normal to the backfill to sheet pile wall interface

$U_{static-t}$ Resultant steady state pore water pressure force acting normal to the dredge level soil to sheet pile wall interface

$U_{static-\alpha}$ Resultant steady state pore water pressure force acting normal to planar slip surface inclined at α from vertical

u Steady-state pore water pressure

V Maximum ground velocity

W Weight of rigid body (e.g. wall or soil wedge)

w Water content of soil

X_N Point of action of normal force N

DISTRIBUTION LIST

1SG/CEEE / LT MARSH, LANGLEY AFB, VA
AF / 438 ABG/DEE (WILSON), MCGUIRE AFB, NJ; CSR 4200 (K. DAVIDSON), PATRICK AFB, FL
AFB / HQ TAC/DEMM (POLLARD), LANGLEY AFB, VA
AFESC / TECH LIB, TYNDALL AFB, FL
AMERICAN CONCRETE / LIB, DETROIT, MI
APPLIED TECHNOLOGY AND MANAGEMENT / C. JONES, CHARLESTON, SC
ARMSTRONG, W. / MYSTIC, CT
ARMY / ENGR CEN, ATSE-DAC-LC, FORT LEONARD WOOD, MO; HQDA (DAEN-ZCM), WASHINGTON, DC; R&D LAB, STRNC-UE, NATICK, MA
ARMY CECOM R&D TECH LIBRARY / ASNC-ELC-I-T, FORT MONMOUTH, NJ
ARMY CERL / CECER-FME (HAYES), CHAMPAIGN, IL; LIB, CHAMPAIGN, IL
ARMY CEWES / (TW RICHARDSON), VICKSBURG, MS
ARMY CRREL / ISKANDAR, HANOVER, NH
ARMY ENGRG DIST / CENPS-ED-SD, SEATTLE, WA; LIB, PORTLAND, OR; LIB, SEATTLE, WA; LIB, PHILADELPHIA, PA
ARMY ENGRG DIV / CEEUD-ED-TA (MCVAY), FRANKFURT, GE, APO AE; CEHND-ED-CS, HUNTSVILLE, AL; ED-SY (LOYD), HUNTSVILLE, AL
ARMY EWES / CEWES-CD-P, VICKSBURG, MS; CEWES-GP-N (CJ SMITH), VICKSBURG, MS; LIB, VICKSBURG, MS; WESCD-P (MELBY), VICKSBURG, MS; WESCW-D, VICKSBURG, MS
ARMY MISSILE R&D CMD / CH, DOCS, SCI INFO CTR, REDSTONE ARSENAL, AL
ARVID GRANT & ASSOC / OLYMPIA, WA
ATLANTIC RICHFIELD CO / RE SMITH, DALLAS, TX
BATTELLE / D. FRINK, COLUMBUS, OH
BATTELLE NEW ENGLAND MARINE RSCH LAB / LIB, DUXBURY, MA
BECHTEL CIVIL, INC / K. MARK, SAN FRANCISCO, CA
BEN C GERWICK INC / FOTINOS, SAN FRANCISCO, CA
BETHLEHEM STEEL CO / ENGRG DEPT, BETHLEHEM, PA
BLAYLOCK ENGINEERING GROUP / T SPENCER, SAN DIEGO, CA
BRITISH EMBASSY / SCI & TECH DEPT (WILKINS), WASHINGTON, DC
BROWN, ROBERT / TUSCALOOSA, AL
BULLOCK, TE / LA CANADA, CA
BUREAU OF RECLAMATION / D-1512 (GS DEPUY), DENVER, CO
CAL STATE UNIV / C.V. CHELAPATI, LONG BEACH, CA
CALIFORNIA / DEPT BOATING AND WATERWAYS (ARMSTRONG), SACRAMENTO, CA
CASE WESTERN RESERVE UNIV / CE DEPT (PERDIKARIS), CLEVELAND, OH
CBC / CODE 155, PORT HUENEME, CA; CODE 82, PORT HUENEME, CA; PWO (CODE 400), GULFPORT, MS
CECOS / CODE C35, PORT HUENEME, CA
CHAO, JC / HOUSTON, TX
CHEE, WINSTON / GRETNA, LA
CHESNAVFACENGCOM / CODE 112.1, WASHINGTON, DC; CODE 402 (FRANCIS), WASHINGTON, DC; CODE 407, WASHINGTON, DC; YACHNIS, WASHINGTON, DC
CHEVRON OIL FLD RSCH CO / ALLENDER, LA HABRA, CA
CHILDS ENGRG CORP / K.M. CHILDS, JR., MEDFIELD, MA
CINCUSNAVEUR / LONDON, UK, FPO AE
CITY OF MONTEREY / CONST MGR (REICHMUTH), MONTEREY, CA
CITY OF SACRAMENTO / GEN SVCS DEPT, SACRAMENTO, CA

CITY OF WINSTON-SALEM / RJ ROGERS, PWD, WINSTON SALEM, NC
CLARK, T. / SAN MATEO, CA
CLARKSON UNIV / CEE DEPT, POTSDAM, NY
CNO / DCNO, LOGS, OP-424C, WASHINGTON, DC
COGUARD / SUPERINTENDENT, NEW LONDON, CT
COLLEGE OF ENGINEERING / CE DEPT (AKINMUSURU), SOUTHFIELD, MI; CE DEPT (GRACE), SOUTHFIELD, MI
COLLINS ENGRG, INC / M GARLICH, CHICAGO, IL
COLORADO STATE UNIV / CE DEPT (CRISWELL), FORT COLLINS, CO
COMDT COGUARD / G-ECV, WASHINGTON, DC
COMFAIR / MED, SCE, NAPLES, ITALY, FPO AE
COMFLEACT / PWO, FPO AP
COMFLEACT / SCE, FPO AP
COMNAVACT / PWO, LONDON, UK, FPO AE
COMNAVSURF / CODE N42A, NORFOLK, VA
COMSUBPAC / CODE 541, SCE, PEARL HARBOR, HI
CONRAD ASSOC / LUISONI, VAN NUYS, CA
CONSOER TOWNSEND & ASSOC / DEBIAK, CHICAGO, IL
CONSTRUCTION TECH LABS, INC / G. CORLEY, SKOKIE, IL
CONTINENTAL OIL CO / O. MAXSON, PONCA CITY, OK
CORNELL UNIV / CIVIL & ENVIRON ENGRG, ITHACA, NY; LIB, ITHACA, NY
DAMES & MOORE / LIB, LOS ANGELES, CA
DAVY DRAVO / WRIGHT, PITTSBURG, PA
DE PALMA, J R / LEBANON, NH
DELAWARE / EMERGENCY MGMT, DELAWARE CITY, DE
DEPT OF BOATING / ARMSTRONG, SACRAMENTO, CA
DEPT OF STATE / FOREIGN BLDGS OPS, BDE-ESB, ARLINGTON, VA
DFSC-F / ALEXANDRIA, VA
DOBROWOLSKI, JA / ALTADENA, CA
DODDS / PAC, FAC, FPO AP
DTRCEN / CODE 172, BETHESDA, MD
EASTPORT INTL, INC / VENTURA, CA
EDWARD K NODA & ASSOC / HONOLULU, HI
ENGINEERING DATA MANAGEMENT / RONALD W. ANTHONY, FORT COLLINS, CO
ESCO SCIENTIFIC PRODUCTS (ASIA) / PTE LTD, CHAI
EWI ENGINEERING ASSOCIATES / JACK COX, MIDDLETON, WI
FAA / ARD 200, WASHINGTON, DC
FACILITIES DEPT / FACILITIES OFFICER, FPO AP
FLORIDA ATLANTIC UNIV / OCEAN ENGRG DEPT (MARTIN), BOCA RATON, FL; OCEAN ENGRG DEPT (MCALLISTER), BOCA RATON, FL; OCEAN ENGRG DEPT (SU), BOCA RATON, FL
FLORIDA INST OF TECH / CE DEPT (KALAJIAN), MELBOURNE, FL
FOWLER, J.W. / VIRGINIA BEACH, VA
GEI CONSULTANTS, INC. / T.C. DUNN, WINCHESTER, MA
GEIGER ENGINEERS / FUNSTON, BELLINGHAM, WA
GEOCON INC / CORLEY, SAN DIEGO, CA
GEORGE WASHINGTON UNIV / ENGRG & APP SCI SCHL (FOX), WASHINGTON, DC
GEORGIA INST OF TECH / CE SCHL (KAHN), ATLANTA, GA; CE SCHL (SWANGER), ATLANTA, GA; CE SCHL (ZURUCK), ATLANTA, GA; DR. J. DAVID FROST, ATLANTA, GA
GEOTECHNICAL ENGRS, INC / MURDOCK, WINCHESTER, MA
GERWICK, BEN / SAN FRANCISCO, CA
GIORDANO, A.J. / SEWELL, NJ

GLIDDEN CO / RSCH LIB, STRONGSVILLE, OH
GRUMMAN AEROSPACE CORP / TECH INFO CENTER, BETHPAGE, NY
GSA / HALL, WASHINGTON, DC
HAN-PADRON ASSOCIATES / DENNIS PADRON, NEW YORK, NY
HANDLEY, DM / GULF BREEZE, FL
HARDY, S.P. / SAN RAMON, CA
HARTFORD STEAM BOILER INSP & INS CO / SPINELLI, HARTFORD, CT
HAYNES & ASSOC / H. HAYNES, PE, OAKLAND, CA
HAYNES, B / LYNDEN, WA
HEUZE, F / ALAMO, CA
HJ DEGENKOLB ASSOC / W. MURDOUGH, SAN FRANCISCO, CA
HOIDRA / NEW YORK, NY
HOPE ARCHTS & ENGRS / SAN DIEGO, CA
HQ AFLC / CAPT SCHMIDT, WRIGHT PATTERSON AFB, OH
HUGHES AIRCRAFT CO / TECH DOC CEN, EL SEGUNDO, CA
INFOTEAM INC / M. ALLEN, PLANTATION, FL
INST OF MARINE SCIENCES / LIB, PORT ARANSAS, TX; LUETTICH, MOREHEAD CITY, NC
INTL MARITIME, INC / D. WALSH, SAN PEDRO, CA
JOHN HOPKINS UNIV / CE DEPT, JONES, BALTIMORE, MD
JOHN J MC MULLEN ASSOC / LIB, NEW YORK, NY
KAISER PERMANENTE MEDCIAL CARE PROGRAM / OAKLAND, CA
KLIEGER, PAUL / CE, NORTHBROOK, IL
KTA-TATOR, INC / PITTSBURG, PA
LAWRENCE LIVERMORE NATL LAB / FJ TOKARZ, LIVERMORE, CA; PLANT ENGRG LIB (L-654), LIVERMORE, CA
LAYTON & SELL, INC, P.S. / REDMOND, WA
LBNSY / CODE 106.3, LONG BEACH, CA
LEHIGH UNIV / CE DEPT, HYDRAULICS LAB, BETHLEHAM, PA; MARINE GEOTECH LAB, BETHLEHAM, PA
LEC A DALY CO / HONOLULU, HI
LIN OFFSHORE ENGRG / P. CHOW, SAN FRANCISCO, CA
LONG BEACH PORT / ENGRG DIR (ALLEN), LONG BEACH, CA; ENGRG DIR (LUZZI), LONG BEACH, CA
MAINE MARITIME ACADEMY / LIB, CASTINE, ME
MARATHON OIL CO / GAMBLE, HOUSTON, TX
MARCORBASE / CODE 4.01, CAMP PENDLETON, CA; CODE 406, CAMP LEJEUNE, NC; PAC, PWO, FPO AP
MARCORPS / FIRST FSSG, ENGR SUPP OFFR, CAMP PENDLETON, CA
MARINE CONCRETE STRUCTURES, INC / W.A. INGRAHAM, METAIRIE, LA
MARITECH ENGRG / DONOGHUE, AUSTIN, TX
MARITIME ADMIN / MAR-840, WASHINGTON, DC; MMA, LIB, KINGS POINT, NY
MCAS / CODE 1JD-31 (HUANG), SANTA ANA, CA; CODE 1JE.50 (ISAACS), SANTA ANA, CA; CODE 6EDD, FPO AP; CODE LE, CHERRY POINT, NC; PWO, KANEOHE BAY, HI
MCRD / PWO, SAN DIEGO, CA
MCRDAC / AROICC, QUANTICO, VA
MERMEL, TW / WASHINGTON, DC
MICHIGAN TECH UNIV / CO DEPT (HAAS), HOUGHTON, MI
MOBIL R&D CORP / OFFSHORE ENGRG LIB, DALLAS, TX
MT DAVISSON / CE, SAVOY, IL
NAF / ENGRG DIV, PWD, FPO AP; PWO, FPO AP
NALF / OIC, SAN DIEGO, CA

NAS / CHASE FLD, PWO, BEEVILLE, TX; CODE 421, SAN DIEGO, CA; CODE 8, PATUXENT RIVER, MD; CODE 83, PATUXENT RIVER, MD; CODE 85GC, GLENVIEW, IL; DIR, ENGRG DIV, PWD, KEFLAVIK, ICELAND, FPO AE; FAC MGMT OFFC, ALAMEDA, CA; MIRAMAR, PWO, SAN DIEGO, CA; NI, SCE, SAN DIEGO, CA; PW ENGRG, PATUXENT RIVER, MD; PWO, KEY WEST, FL; PWO, CECIL FIELD, FL; PWO, MOFFETT FIELD, CA; PWO, SIGONELLA, ITALY, FPO AE; SCE, BARBERS POINT, HI; SCE, FPO AP; WHITING FLD, PWO, MILTON, FL
NAS ADAK / CODE 114, FPO AP
NAS MEMPHIS / CODE N-81, MILLINGTON, TN
NAS NPWC / CODE 102 (J. ARESTO), SAN DIEGO, CA
NAS OCEANA / ADAMETZ, VIRGINIA BEACH, VA
NATL ACADEMY OF ENGRY / ALEXANDRIA, VA
NAVAIRDEVCEN / CODE 832, WARMINSTER, PA
NAVAVNDEPOT / CODE 640, PENSACOLA, FL
NAVCAMS / PWO, NORFOLK, VA
NAVCOASTSYSCEN / CO, PANAMA CITY, FL; CODE 715 (J. MITTLEMAN), PANAMA CITY, FL; PWO (CODE 740), PANAMA CITY, FL
NAVCOMMSTA / PWO, FPO AP
NAVCONSTRACEN / CODE D2A, PORT HUENEME, CA; CODE S24, GULFPORT, MS; TECH LIB, INDIAN HEAD, MD
NAVFACENGCOM / CODE 04A3, ALEXANDRIA, VA; CODE 04A3A, ALEXANDRIA, VA; CODE 07, ALEXANDRIA, VA; CODE 07M (BENDER), ALEXANDRIA, VA; CODE 163, ALEXANDRIA, VA; CODE 1632B, ALEXANDRIA, VA
NAVHOSP / SCE, NEWPORT, RI
NAVMAG / SCE, FPO AP
NAVMEDCOM / NWREG, FAC ENGR, PWD, OAKLAND, CA
NAVOCEANO / CODE 6200 (M PAIGE), NSTL, MS; LIB, NSTL, MS
NAVPGSCOL / CODE 68WY (WYLAND), MONTEREY, CA; PWO, MONTEREY, CA
NAVPHIBASE / PWO, NORFOLK, VA; SCE, SAN DIEGO, CA
NAVSCSCOL / PWO, ATHENS, GA
NAVSEASYSCOM / CODE 56W23, WASHINGTON, DC
NAVSECGRUACT / CODE 31 PWO, FPO AA; PWO, FPO AP
NAVSHIPREPFAC / SCE, FPO AP
NAVSHIPYD / CARR INLET ACOUSTIC RANGE, BREMERTON, WA; CODE 134, PEARL HARBOR, HI; CODE 244.13, LONG BEACH, CA; CODE 308.3, PEARL HARBOR, HI; CODE 380, PORTSMOUTH, VA; CODE 440, PORTSMOUTH, VA; CODE 441, PORTSMOUTH, NH; CODE 903, LONG BEACH, CA; MARE IS, CODE 106.3, VALLEJO, CA; MARE IS, CODE 401, VALLEJO, CA; MARE IS, CODE 421, VALLEJO, CA; MARE IS, CODE 440, VALLEJO, CA; MARE IS, CODE 457, VALLEJO, CA; MARE IS, PWO, VALLEJO, CA; TECH LIB, PORTSMOUTH, NH
NAVSTA / CODE N4214, MAYPORT, FL; CODE ODA, SAN DIEGO, CA; DIR, ENGR DIV, PWD, GUANTANAMO BAY, CUBA, FPO AE; ENGR DIV, PWD, FPO AA; ENGRG DIR, PWD, ROTA, SPAIN, FPO AE; PWO, MAYPORT, FL; PWO, GUANTANAMO BAY, CUBA, FPO AE; PWO, ROTA, SPAIN, FPO AE; SCE PEARL HARBOR, HI
NAVSTA PANAMA CANAL / CODE 54, FPO AA
NAVSUBBASE / AMES, NEW LONDON, CT
NAVSUPACT / CODE 430, NEW ORLEANS, LA
NAVSUPPACT / PWO, NAPLES, ITALY, FPO AE
NAVSUPSYSCOM / CODE 0622, WASHINGTON, DC
NAVSWC / CODE U48, FORT LAUDERDALE, FL; CODE W41C1, DAHLGREN, VA; CODE W42 (GS HAGA), DAHLGREN, VA; DET, WHITE OAK LAB, PWO, SILVER SPRING, MD; PWO, DAHLGREN, VA
NAVWPNCEN / PWO (CODE 266), CHINA LAKE, CA

NAVWPNSTA / CODE 092B (HUNT), YORKTOWN, VA; CODE 093, YORKTOWN, VA; CODE 104, CHARLESTON, SC; PWO, YORKTOWN, VA
NAVWPNSTA EARLE / CODE 092 AND PWO (CODE 09B), COLTS NECK, NJ
NAWC / CODE 1018, POINT MUGU, CA; CODE 5041, POINT MUGU, CA; CODE P4234 (G. NUSSEAR), POINT MUGU, CA
NBS / BLDG MAT DIV, MATHEY, GAITHERSBURG, MD
NCBC / PWO, DAVISVILLE, RI
NCCOSC / CODE 9642, SAN DIEGO, CA
NEESA / CODE 111E (MCCLAINE), PORT HUENEME, CA
NETPMSA / TECH LIB, PENSACOLA, FL
NEW MEXICO SOLAR ENERGY INST / LAS CRUCES, NM
NEW ZEALAND CONCRETE RSCH ASSN / LIB, PORIRUA,
NIEDORODA, AW / GAINESVILLE, FL
NOAA / JOSEPH VADUS, ROCKVILLE, MD
NOARL / CODE 440, NSTL, MS
NORDA / CODE 440, NSTL, MS
NORTHNAVFACENGCOM / CO, LESTER, PA; CODE 164, LESTER, PA; CODE 408AF, LESTER, PA
NORTHWEST ENGRG CO / GRIMM, BELLEVUE, WA
NRL / CODE 4670, WASHINGTON, DC; CODE 6127, WASHINGTON, DC
NSC / SCE, NORFOLK, VA; SCE, CHARLESTON, SC; SCE, PEARL HARBOR, HI
NSWC / CODE 09RA, INDIAN HEAD, MD
NSY / CODE 214.3 (WEBER), PORTSMOUTH, VA
NUHN & ASSOC / A.C. NUHN, WAYZATA, NM
NUSC DET / CODE 2143 (VARLEY), NEW LONDON, CT; CODE 44 (MUNN), NEW LONDON, CT; CODE TA131, NEW LONDON, CT; LIB, NEWPORT, RI; PWO, NEW LONDON, CT
NY CITY COMMUNITY COLLEGE / LIB, BROOKLYN, NY
OCNR / CODE 1121 (EA SILVA), ARLINGTON, VA
OMEGA MARINE, INC. / SCHULZE, LIBRARIAN, HOUSTON, TX
OREGON STATE UNIV / CE DEPT (HICKS), CORVALLIS, OR; CE DEPT (YIM), CORVALLIS, OR; OCEANOGRAPHY SCOL, CORVALLIS, OR
PACIFIC MARINE TECH / M. WAGNER, DUVALL, WA
PACNAVFACENGCOM / CODE 102 AND CODE 2011, PEARL HARBOR, HI
PAULI, DC / SILVER SPRING, MD
PAYE-KOSANOWSKY, S / POND EDDY, NY
PENNSYLVANIA STATE UNIV / GOTOLSKI, UNIVERSITY PARK, PA; RSCH LAB, STATE COLLEGE, PA
PERKOWSKI, MICHAEL T. / TIPPECANOE, OH
PHILADELPHIA ELEC CO / E. D. FREAS, WESTCHESTER, PA
PIKE, L / SAN ANTONIO, TX
PILE BUCK, INC / SMOOT, JUPITER, FL
PMB ENGRG / LUNDBERG, SAN FRANCISCO, CA
PORTLAND CEMENT ASSOC / AE FIORATO, SKOKIE, IL
PORTLAND STATE UNIV / ENGRG DEPT (MIGLIORI), PORTLAND, OR
PUGET SOUND / REUNINE, BREMERTON, WA
PURDUE UNIV / CE SCOL (ALTSCHAEFFL), WEST LAFAYETTE, IN; CE SCOL (CHEN), WEST LAFAYETTE, IN; CE SCOL (LEONARDS), WEST LAFAYETTE, IN

PWC / CO, OAKLAND, CA; CODE 101, GREAT LAKES, IL; CODE 101.5, FPO AP; CODE 102, OAKLAND, CA; CODE 123C, SAN DIEGO, CA; CODE 400, OAKLAND, CA; CODE 400A.3, FPO AP; CODE 420, OAKLAND, CA; CODE 421 (KAYA), PEARL HARBOR, HI; CODE 421 (QUIN), SAN DIEGO, CA; CODE 421 (REYNOLDS), SAN DIEGO, CA; CODE 421, NORFOLK, VA; CODE 422, SAN DIEGO, CA; CODE 423, SAN DIEGO, CA; CODE 430 (KYI), PEARL HARBOR, HI; CODE 500, NORFOLK, VA; CODE 505A, OAKLAND, CA; CODE 590, SAN DIEGO, CA; SAN DIEGO (WAID), SAN DIEGO, CA
Q ASSOCIATES / QUIRK, J PANAMA CITY, FL
SAN DIEGO PORT / PORT FAC, PROJ ENGR, SAN DIEGO, CA
SAN DIEGO STATE UNIV / CE DEPT (KRISHNAMOORTHY), SAN DIEGO, CA
SANDIA LABS / LIB, LIVERMORE, CA
SARGENT & HERKES, INC / JP PIERCE, JR, NEW ORLEANS, LA
SEATECH CORP / PERONI, MIAMI, FL
SEATTLE PORT / DAVE VAN VLEET, SEATTLE, WA; DAVID TORSETH, SEATTLE, WA
SEATTLE UNIV / CE DEPT (SCHWAEGLER), SEATTLE, WA
SHELL OIL CO / E. DOYLE, HOUSTON, TX
SIMPSON, GUMPERTZ & HEGER, INC / HILL, ARLINGTON, MA
SMELSER, D / SEVIERVILLE, TN
SOUTHNAVFACENGCOM / CODE 04A, CHARLESTON, SC; CODE 1622, CHARLESTON, SC
SOUTHWEST RSCH INST / ENERGETIC SYS DEPT (ESPARZA), SAN ANTONIO, TX; KING, SAN ANTONIO, TX; M. POLCYN, SAN ANTONIO, TX; MARCHAND, SAN ANTONIO, TX; THACKER, SAN ANTONIO, TX
SOWESTNAVFACENGCOM / CODE 101.1 AND LANGSTRAAT, SAN DIEGO, CA
SPCC / PWO, MECHANICSBURG, PA
STATE UNIV OF NEW YORK / CE DEPT, BUFFALO, NY; REINHORN, BUFFALO, NY
SUBASE / PWO (CODE 8323), BREMERTON, WA; SCE, PEARL HARBOR, HI
SUPSHIP / CODE 190, NEWPORT, VA; TECH LIB, NEWPORT, VA
TECHNOLOGY UTILIZATION / K WILLINGER, WASHINGTON, DC
TEXAS A&M UNIV / CE DEPT (HERBICH), COLLEGE STATION, TX; CE DEPT (MACHEMEHL), COLLEGE STATION, TX; CE DEPT (NIEDZWECKI), COLLEGE STATION, TX; CE DEPT (SNOW), COLLEGE STATION, TX; OCEAN ENGR PROJ, COLLEGE STATION, TX
THE WORLD BANK / ARMSTRONG, WASHINGTON, DC
TRW INC / ENGR LIB, CLEVELAND, OH
TRW SPACE AND TECHNOLOGY GROUP / CARPENTER, REDONDO BEACH, CA
TUDOR ENGRG CO / ELLEGOOD, PHOENIX, AZ
UNIV OF ALASKA / BIOMED & MARINE SCI LIB, FAIRBANKS, AK
UNIV OF CALIFORNIA / CE DEPT (FENVES), BERKELEY, CA; CE DEPT (FOURNEY), LOS ANGELES, CA; CE DEPT (TAYLOR), DAVIS, CA; CE DEPT (WILLIAMSON), BERKELEY, CA; NAVAL ARCHT DEPT, BERKELEY, CA
UNIV OF HAWAII / CE DEPT (CHIU), HONOLULU, HI; MANOA, LIB, HONOLULU, HI; OCEAN ENGRG DEPT (ERTEKIN), HONOLULU, HI; RIGGS, HONOLULU, HI
UNIV OF ILLINOIS / METZ REF RM, URBANA, IL
UNIV OF MARYLAND / CE DEPT, COLLEGE PARK, MD
UNIV OF MICHIGAN / CE DEPT (RICHART), ANN ARBOR, MI
UNIV OF N CAROLINA / CE DEPT (AHMAD), RALEIGH, NC
UNIV OF NEW MEXICO / NMERI (BEAN), ALBUQUERQUE, NM; NMERI, HL SCHREYER, ALBUQUERQUE, NM
UNIV OF PENNSYLVANIA / DEPT OF ARCH, PHILADELPHIA, PA
UNIV OF RHODE ISLAND / CE DEPT (KARAMANLIDIS), KINGSTON, RI; CE DEPT (KOVACS), KINGSTON, RI; CE DEPT (TSIATAS), KINGSTON, RI; DR. VEYERA, KINGSTON, RI

UNIV OF TEXAS / CONSTRUCTION INDUSTRY INST, AUSTIN, TX; ECJ 4.8 (BREEN), AUSTIN, TX; ECJ 5.402 (TUCKER), AUSTIN, TX
UNIV OF WASHINGTON / APP PHYS LAB (SANDWITH), SEATTLE, WA
UNIV OF WASHINGTON / CE DEPT (HARTZ), SEATTLE, WA
UNIV OF WASHINGTON / CE DEPT (MATTOCK), SEATTLE, WA
UNIV OF WISCONSIN / GREAT LAKES STUDIES CEN, MILWAUKEE, WI
UNIV OF WYOMING / SCHMIDT, LARAMIE, WY
US GEOLOGICAL SURVEY / MARINE GEOLOGICAL OFFC, RESTON, VA
US NUCLEAR REGULATORY COMMISSION / KIM, WASHINGTON, DC
USACOE / CESPD-CO-EQ, SAN FRANCISCO, CA
USAE / CEWES-IM-MI-R, VICKSBURG, MS
USCG / G-ECV-4B, WASHINGTON, DC
USCINCPAC / CODE J44, CAMP HM SMITH, HI
USDA / FOR SVC, REG BRIDGE ENGR, ALOHA, OR; FOREST PROD LAB (DEGROOT), MADISON, WI; FOREST PROD LAB (JOHNSON), MADISON, WI
USN / CAPT COLIN M JONES, HONOLULU, HI
USNA / CH, MECH ENGRG DEPT (C WU), ANNAPOLIS, MD; OCEAN ENGRG DEPT, ANNAPOLIS, MD; PWO, ANNAPOLIS, MD
USPS / BILL POWELL, WASHINGTON, DC
VALLEY FORGE CORPORATE CENTER / FRANKLIN RESEARCH CENTER, NORRISTOWN, PA
VAN ALLEN, B / KINGSTON, NY
VENTURA COUNTY / DEPUTY PW DIR, VENTURA, CA
VIATEUR DE CHAMPLAIN / INST OF MARITIME ENGRG, MATANE, QUEBEC
VSE / OCEAN ENGRG GROUP (MURTON), ALEXANDRIA, VA; LOWER, ALEXANDRIA, VA
VULCAN IRON WORKS, INC / DC WARRINGTON, CLEVELAND, TN
WESCR-P / HALES, VICKSBURG, MS
WESTINGHOUSE ELECTRIC CORP / LIB, PITTSBURG, PA
WESTNAVFACENGCOM / CODE 162, SAN BRUNO, CA; CODE 1833, SAN BRUNO, CA; CODE 401, SAN BRUNO, CA; CODE 407, SAN BRUNO, CA; PAC NW BR OFFC, CODE C/42, SILVERDALE, WA; VALDEMORO, SAN BRUNO, CA
WISS, JANNEY, ELSTNER, & ASSOC / DW PFEIFER, NORTHBROOK, IL
WISWELL, INC. / SOUTHPORT, CT
WOODWARD-CLYDE CONSULTANTS / R. CROSS, OAKLAND, CA; WEST REG, LIB, OAKLAND, CA

DISTRIBUTION QUESTIONNAIRE

The Naval Civil Engineering Laboratory is revising its primary distribution lists.

SUBJECT CATEGORIES

1 **SHORE FACILITIES**
1A Construction methods and materials (including corrosion control, coatings)
1B Waterfront structures (maintenance/deterioration control)
1C Utilities (including power conditioning)
1D Explosives safety
1E Aviation Engineering Test Facilities
1F Fire prevention and control
1G Antenna technology
1H Structural analysis and design (including numerical and computer techniques)
1J Protective construction (including hardened shelters, shock and vibration studies)
1K Soil/rock mechanics
1L Airfields and pavements
1M Physical security
2 **ADVANCED BASE AND AMPHIBIOUS FACILITIES**
2A Base facilities (including shelters, power generation, water supplies)
2B Expedient roads/airfields/bridges
2C Over-the-beach operations (including breakwaters, wave forces)
2D POL storage, transfer, and distribution
2E Polar engineering
3 **ENERGY/POWER GENERATION**
3A Thermal conservation (thermal engineering of buildings, HVAC systems, energy loss measurement, power generation)
3B Controls and electrical conservation (electrical systems, energy monitoring and control systems)
3C Fuel flexibility (liquid fuels, coal utilization, energy from solid waste)
3D Alternate energy source (geothermal power, photovoltaic power systems, solar systems, wind systems, energy storage systems)
3E Site data and systems integration (energy resource data, integrating energy systems)
3F EMCS design
4 **ENVIRONMENTAL PROTECTION**
4A Solid waste management
4B Hazardous/toxic materials management
4C Waterwaste management and sanitary engineering
4D Oil pollution removal and recovery
4E Air pollution
4F Noise abatement
5 **OCEAN ENGINEERING**
5A Seafloor soils and foundations
5B Seafloor construction systems and operations (including diver and manipulator tools)
5C Undersea structures and materials
5D Anchors and moorings
5E Undersea power systems, electromechanical cables, and connectors
5F Pressure vessel facilities
5G Physical environment (including site surveying)
5H Ocean-based concrete structures
5J Hyperbaric chambers
5K Undersea cable dynamics
ARMY FEAP
BDG Shore Facilities
NRG Energy
ENV Environmental/Natural Responses
MGT Management
PRR Pavements/Railroads

TYPES OF DOCUMENTS

D - Techdata Sheets; **R** - Technical Reports and Technical Notes; **G** - NCEL Guides and Abstracts; **I** - Index to TDS; **U** - User Guides; ☐ None - remove my name

Old Address:

_____

_____

_____

_____

Telephone No.: _____

New Address:

_____

_____

_____

_____

Telephone No.: _____

INSTRUCTIONS

The Naval Civil Engineering Laboratory has revised its primary distribution lists. To help us verify our records and update our data base, please do the following:

- Add - circle number on list
- Remove my name from all your lists - check box on list.
- Change my address - line out incorrect line and write in correction **(DO NOT REMOVE LABEL).**
- Number of copies should be entered after the title of the subject categories you select.
- Are we sending you the correct type of document? If not, circle the type(s) of document(s) you want to receive listed on the back of this card.

Fold on line, staple, and drop in mail.

DEPARTMENT OF THE NAVY
Naval Civil Engineering Laboratory
560 Laboratory Drive
Port Hueneme CA 93043-4328

Official Business
Penalty for Private Use, $300

NO POSTAGE NECESSARY IF MAILED IN THE UNITED STATES

BUSINESS REPLY CARD

FIRST CLASS PERMIT NO. 12503 WASH D.C.

POSTAGE WILL BE PAID BY ADDRESSEE

COMMANDING OFFICER
CODE L34
560 LABORATORY DRIVE
NAVAL CIVIL ENGINEERING LABORATORY
PORT HUENEME CA 93043-4328

NCEL DOCUMENT EVALUATION

You are number one with us; how do we rate with you?

We at NCEL want to provide you our customer the best possible reports but we need your help. Therefore, I ask you to please take the time from your busy schedule to fill out this questionnaire. Your response will assist us in providing the best reports possible for our users. I wish to thank you in advance for your assistance. I assure you that the information you provide will help us to be more responsive to your future needs.

R. N. STORER, Ph.D, P.E.
Technical Director

DOCUMENT NO. _____ TITLE OF DOCUMENT: _____

Date: _____ Respondent Organization : _____

Name: _____ Activity Code: _____
Phone: _____ Grade/Rank: _____

Category (*please check*):

Sponsor ____ User ____ Proponent ____ Other (*Specify*) _____

Please answer on your behalf only; not on your organization's. Please check (*use an X*) only the block that most closely describes your attitude or feeling toward that statement:

SA Strongly Agree A Agree O Neutral D Disagree SD Strongly Disagree

	SA	A	N	D	SD
1. The technical quality of the report is comparable to most of my other sources of technical information.	( )	( )	( )	( )	( )
2. The report will make significant improvements in the cost and or performance of my operation.	( )	( )	( )	( )	( )
3. The report acknowledges related work accomplished by others.	( )	( )	( )	( )	( )
4. The report is well formatted.	( )	( )	( )	( )	( )
5. The report is clearly written.	( )	( )	( )	( )	( )
6. The conclusions and recommendations are clear and directly supported by the contents of the report.	( )	( )	( )	( )	( )
7. The graphics, tables, and photographs are well done.	( )	( )	( )	( )	( )

Do you wish to continue getting NCEL reports? ☐ YES ☐ NO

Please add any comments (e.g., in what ways can we improve the quality of our reports?) on the back of this form.

Comments:

Fold on line, staple, and drop in mail.

DEPARTMENT OF THE NAVY
Naval Civil Engineering Laboratory
560 Laboratory Drive
Port Hueneme CA 93043-4328

Official Business
Penalty for Private Use, $300

NO POSTAGE NECESSARY IF MAILED IN THE UNITED STATES

BUSINESS REPLY CARD

FIRST CLASS PERMIT NO. 12503 WASH D.C.

POSTAGE WILL BE PAID BY ADDRESSEE

COMMANDING OFFICER
CODE L03
560 LABORATORY DRIVE
NAVAL CIVIL ENGINEERING LABORATORY
PORT HUENEME CA 93043-4328